

1-1-2012

Investigation of Load Distribution Factors for Two-Span Continuous Composite Multiple Boxgirder Bridges

Manal Ibrahim
Ryerson University

Follow this and additional works at: <http://digitalcommons.ryerson.ca/dissertations>

 Part of the [Civil Engineering Commons](#), and the [Structural Engineering Commons](#)

Recommended Citation

Ibrahim, Manal, "Investigation of Load Distribution Factors for Two-Span Continuous Composite Multiple Boxgirder Bridges" (2012). *Theses and dissertations*. Paper 711.

**INVESTIGATION OF LOAD DISTRIBUTION FACTORS FOR
TWO-SPAN CONTINUOUS COMPOSITE MULTIPLE BOX-
GIRDER BRIDGES**

**by
Manal Ibrahim, B.Sc.
Benha University, Egypt**

**A Thesis
Present to Ryerson University
In partial fulfillment of the
Requirement for the Degree of
Master of Applied Science
In the program of
Civil Engineering
Toronto, Ontario, Canada
© Manal S. S. Ibrahim, 2012**

AUTHOR'S DECLARATION

I hereby declare that I am the sole author of this thesis.

I authorize Ryerson University to lend this document to other institutions or individuals for the purpose of scholarly research. I understand that my thesis may be made electronically available to the public.

Manal Ibrahim

I further authorize Ryerson University to document by photocopying or by other means, in total or part, at the request of other institutions or individuals for the purpose of scholarly research.

Manal Ibrahim

INVESTIGATION OF LOAD DISTRIBUTION FACTORS FOR TWO-SPAN CONTINUOUS COMPOSITE MULTIPLE BOX- GIRDER BRIDGES

By
Manal Ibrahim

A Thesis Present to Ryerson University
In partial fulfillment of the
Requirement for the Degree of
Master of Applied Science
In the program of Civil Engineering
Toronto, Ontario, Canada 2012

ABSTRACT

Bridges formed of concrete deck slab over built-up steel-box girders are frequently used in bridge construction for their economic and structural advantages. Box girder bridges impose structural challenges to get the straining actions for the design of girders. The objective of this study is to determine the load distribution characteristics for continuous composite multiple-box girder bridges under CHBDC truck loading. An extensive parametric study was conducted using the three-dimensional finite element to evaluate the moment and shear distribution factors when bridges subjected to CHBDC truck loading. The parameters considered in this study are the span length, number of lanes and number of boxes. Then, simple empirical formula for the bending moment and shear force were developed for the structural design. Correlation of the developed expressions based on FEA results with available CHBDC and AASHTO-LRFD formula showed that the former allow engineers to design such bridges more economically and reliably.

ACKNOWLEDGEMENTS

I wish to express my deep appreciation to my advisor Dr. K. Sennah, for his continuous support and valuable supervision during the development of this research. Dr. Sennah devoted his time and effort to make this study a success. His most helpful guidance is greatly appreciated.

I wish to thank my friends who provided me with their support.

My sincere thanks and gratitude are due to my family, who helped me and blessed my work during the days of my study and research. I am also very grateful to my family for their great support and encouragement during the course of this study.

TO MY MOTHER

TABLE OF CONTENTS

ABSTRACT	iii
ACKNOWLEDGEMENTS	iv
TABLE OF CONTENTS.....	vi
LIST OF TABLES.....	ix
LIST OF FIGURES.....	x
APPENDICES.....	xv
NOTATIONS.....	xvi
1. INTRODUCTION.....	1
1.1 General.....	1
1.2 The Problem.....	2
1.3 Objectives.....	2
1.4 Scope.....	3
1.5 Arrangement of the thesis.....	4
2. LITERATURE REVIEW.....	5
2.1 General.....	5
2.2 Analytical Methods for Box Girder Bridges.....	5
2.2.1 Grillage Analogy Method.....	6
2.2.2 Orthotropic Plate Theory Method.....	6
2.2.3 Folded Plate Method.....	7
2.2.4 Finite Strip Method	7
2.2.5 Thin –Walled Beam Theory Method.....	8
2.2.6 Finite Element Method	9
2.3 Experimental Studies.....	10
2.4 Available Code Provisions and Related Literature	11
2.4.1 AASHTO Methods.....	11
2.4.2 AASHTO-LRFD Method.....	12
2.4.3 Canadian Highway Bridge Design Code (CHBDC).....	14
3. FINITE ELEMENT ANALYSES	19
3.1 General.....	19
3.2 Finite Element Procedure.....	20
3.3 SAP2000 Computer Program.....	21
3.4 Finite – Element Modeling of Composite Multiple Box Girder Bridges.....	22
3.4.1 Material Modeling.....	23
3.4.2 Geometric Modeling.....	23
3.4.2.1 Modeling of Deck Slab, Webs, Bottom Flange and End-Diaphragms.....	24
3.4.2.2 Modeling of Connections	24
3.4.3 Boundary Conditions.....	24
3.4.4 Aspect Ratio of shell elements.....	25
3.5 Finite Element Analysis of Bridge Models	25

4. PARAMETRIC STUDY.....	27
4.1 General	27
4.2 Composite Bridge Configuration.....	28
4.3 Loading Conditions of Composite Multiple Box Girder Bridges in Service	29
4.4 Parametric Study for Load Distribution Factors	30
4.4.1 Load Distribution Factors for Longitudinal Bending Moment.....	30
4.4.2 Load Distribution Factors for Vertical Shear.....	32
5. RESULTS FROM THE PARAMETRIC STUDY	34
5.1 General.....	34
5.2 Positive Moment Distribution Factors at Ultimate Limit State.....	35
5.2.1 Effect of Span Length	35
5.2.2 Effect of Number of Lanes.....	35
5.2.3 Effect of Number of Boxes.....	36
5.3 Positive Moment Distribution Factors at Fatigue Limit State	36
5.3.1 Effect of Span Length	36
5.3.2 Effect of Number of Lanes.....	36
5.3.3 Effect of Number of Boxes.....	37
5.4 Negative Moment Distribution Factors at Ultimate Limit State.....	37
5.4.1 Effect of Span Length	37
5.4.2 Effect of Number of Lanes.....	37
5.4.3 Effect of Number of Boxes.....	38
5.5 Negative Moment Distribution Factors at Fatigue Limit State.....	38
5.5.1 Effect of Span Length	38
5.5.2 Effect of Number of Lanes.....	38
5.5.3 Effect of Number of Boxes.....	39
5.6 Shear Distribution Factors at Ultimate Limit State	39
5.6.1 Effect of Span Length	39
5.6.2 Effect of Number of Lanes.....	39
5.6.3 Effect of Number of Boxes.....	40
5.7 Vertical Shear Distribution Factors at Fatigue Limit State.....	40
5.7.1 Effect of Span Length	40
5.7.2 Effect of Number of Lanes.....	40
5.7.3 Effect of Number of Boxes.....	41
5.8 Correlation between the Load Distribution Factors from the FEA and CHBDC Equation.....	41
5.8.1 Ultimate Limit State Design.....	41
5.8.2 Fatigue Limit State Design.....	42
5.9 Correlation between the Load Distribution Factors from the FEA and AASHTO Equation.....	42
5.9.1 Ultimate Limit State.....	42
5.9.2 Fatigue Limit State	43
5.10 Empirical Equations for the Load Distribution Factors	44
6. CONCLUSIONS AND RECOMMENDATIONS.....	48
6.1 Summary.....	48

6.2 Conclusions.....	48
6.3 Recommendations for Further Research	49
TABLES.....	50
FIGURES.....	59
APPENDICES.....	128
REFERENCES.....	160

LIST OF TABLES

Table 2.1 Expression for F and C_f for longitudinal moments in multi-box bridges as determined by CHBDC 2006	50
Table 2.2 Expression for F for longitudinal vertical shear in multi-box bridges as determined by CHBDC 2006	50
Table 4.1 Modification Factors for Multilane Loading as Determined by CHBDC 2006	51
Table 4.2 Comparison between truck load and lane load under CL-625-ONT	52
Table 4.3 Number of Design Lanes as Determined by CHBDC 2006.....	53
Table 4.4 Geometries of Bridges used in Parametric Study for Load Distribution Factor.....	54
Table 5.1 Summary of Parameters of Empirical Equation of Positive Moment Distribution Factors at ULS.....	55
Table 5.2 Summary of Parameters of Empirical Equation of Negative Moment Distribution Factors at ULS	55
Table 5.3 Summary of Parameters of Empirical Equation of Positive Moment Distribution Factors at FLS.....	55
Table 5.4 Summary of Parameters of Empirical Equation of Negative Moment Distribution Factors at FLS.....	55
Table 5.5 Summary of Parameters of Empirical Equation of Shear Distribution Factors as function of (L) at ULS at inner support	56
Table 5.6 Summary of Parameters of Empirical Equation of Shear Distribution Factors as Function of (L) at ULS at outer support	56
Table 5.7 Summary of Parameters of Empirical Equation of Shear Distribution Factors as Function of (L) at FLS at inner support.....	56
Table 5.8 Summary of Parameters of Empirical Equation of Shear Distribution Factors as Function of (L) at FLS at outer support.....	56
Table 5.9 Summary of Parameters of Empirical Equation of Shear Distribution Factors as Function of (β) at ULS at inner support.....	57
Table 5.10 Summary of Parameters of Empirical Equation of Shear Distribution Factors as Function of (β) at ULS at outer support.....	57
Table 5.11 Summary of Parameters of Empirical Equation of Shear Distribution Factors as Function of (β) at FLS at inner support.....	57
Table 5.12 Summary of Parameters of Empirical Equation of Shear Distribution Factors as Function of (β) at FLS at outer support.....	57
Table 5.13 Summary of Parameters of Empirical Equation of Shear Distribution Factors as Function of (β^2) at ULS at inner support.....	58
Table 5.14 Summary of Parameters of Empirical Equation of Shear Distribution Factors as Function of (β^2) at ULS at outer support.....	58
Table 5.15 Summary of Parameters of Empirical Equation of Shear Distribution Factors as Function of (β^2) at FLS at inner support.....	58
Table 5.16 Summary of Parameters of Empirical Equation of Shear Distribution Factors as Function of (β^2) at FLS at outer support.....	58

LIST of FIGURES

Figure 1.1 Various box girder cross – sections	59
Figure 1.2 Typical twin-box girder bridge cross section	60
Figure 1.3 Typical of multiple box girder bridge.....	60
Figure 1.4 Organization chart of the research study.....	61
Figure 3.1 Sketch of the four-node shell element used in the analysis, (SAP 2000).....	62
Figure 3.2 Schematic view of the bridge model showing the intermittent connections between steel box- girder and concrete slab.....	63
Figure 3.3 Boundary condition of the bridges used in the parametric studies	64
Figure 3.4 Finite element discretization of a two box girder cross section	65
Figure 3.5 Typical finite element meshes	66
Figure 4.1 CL-625-ONT truck loading and lane load	67
Figure 4.2 Symbols used for cross –section of four-box Girder Bridge	68
Figure 4.3 Cross-section configurations used in the parametric studies.....	69
Figure 4.4 Loading cases for two-design lane, two girders.....	70
Figure 4.5 Loading cases for three- design lane, three-girders.....	71
Figure 4.6 Loading cases for exterior girder for four – design lane, three- girders	72
Figure 4.7 Loading cases for middle girder for four- design lane, three-girders.....	73
Figure 4.8 Loading cases for fatigue load for four-design lane, three-girders.....	74
Figure 4.9 Loading cases for exterior girder for five- design lane, four-girders.....	75
Figure 4.10 Loading cases for middle girder for five- design lane, four-girders.....	76
Figure 4.11 Loading cases for fatigue load for five-design lane, four-girders.....	77
Figure 4.12 idealized four- box bridge cross-section.....	78
Figure 5.1 Effect of span length on positive moment distribution factors at ULS due to CHBDC truck load.....	79
Figure 5.2 Effect of no. of lanes on positive moment distribution factors at ULS due to CHBDC truck load	79
Figure 5.3 Effect of no. of boxes on positive moment distribution factors at ULS due to CHBDC truck load.....	80
Figure 5.4 Effect of span length on positive moment distribution factors at FLS due to CHBDC truck load.....	80
Figure 5.5 Effect of no. of lanes on positive moment distribution factor at FLS due to CHBDC truck load.....	81
Figure 5.6 Effect of no. of boxes on positive moment distribution factor at FLS due to CHBDC truck load.....	81
Figure 5.7 Effect of span length on negative moment distribution factors at ULS due to CHBDC truck load	82
Figure 5.8 Effect of no. of lanes on negative moment distribution factors at ULS due to CHBDC truck load.....	82
Figure 5.9 Effect of no. of boxes on negative moment distribution factor at ULS due to CHBDC truck load	83
Figure 5.10 Effect of span length on negative moment distribution factor at FLS due to CHBDC truck load	83

Figure 5.11 Effect of no. of lanes on negative moment distribution factors at FLS due to CHBDC truck load	84
Figure 5.12 Effect of no. of boxes negative moment distribution factors at FLS due to CHBDC Truck load.....	84
Figure 5.13 Effect of span length on shear distribution factors at ULS due to CHBDC truck load	85
Figure 5.14 Effect of no. of lanes on shear distribution factors at ULS due to CHBDC truck load	85
Figure 5.15 Effect of no. of boxes on shear distribution factors at ULS due to CHBDC truck load	86
Figure 5.16 Effect of span length on shear distribution factors at FLS due to CHBDC truck load	86
Figure 5.17 Effect of no. of lanes on shear distribution factors at FLS due to CHBDC truck load.....	87
Figure 5.18 Effect of no. of boxes on shear distribution factor at FLS due to CHBDC truck load	87
Figure 5.19 Correlation between positive moment distribution factor (F_{m+}) from FEA and CHBDC results at ULS.....	88
Figure 5.20 Correlation between positive moment distribution factor (F_{m-}) from FEA and CHBDC results at ULS.....	88
Figure 5.21 Correlation between Shear Distribution factors (F_v) at internal support from FEA and CHBDC results at ULS.....	89
Figure 5.22 Correlation between shear distribution factors (F_v) at external support from FEA and CHBDC results at ULS.....	89
Figure 5.23 Correlation between positive moment distribution factors (F_{m+}) from FEA and CHBDC results at FLS	90
Figure 5.24 Correlation between negative moment distribution factor (F_{m-}) from FEA and CHBDC results at FLS	90
Figure 5.25 Correlation between shear distribution factors (F_v) at internal support from FEA and CHBDC results at FLS.....	91
Figure 5.26 Correlation between shear distribution factor (F_v) at external support from FEA and CHBDC results at FLS.....	91
Figure 5.27 Correlation between positive moment distribution factors (F_{m+}) from FEA and AASHTO results at ULS.....	92
Figure 5.28 Correlation between negative moment distribution factor (F_{m-}) from FEA and AASHTO results at ULS	92
Figure 5.29 Correlation between shear distribution factor (F_v) at internal support from FEA and AASHTO results at ULS.....	93
Figure 5.30 Correlation between shear distribution factor (F_v) at external support from FEA and AASHTO results at ULS.....	93
Figure 5.31 Correlation between positive moment distribution factors (F_{m+}) from FEA and AASHTO results at FLS	94
Figure 5.32 Correlation between negative moment distribution factor (F_{m-}) from FEA and AASHTO results at FLS.....	94
Figure 5.33 Correlation between shear distribution factor (F_v) at internal support from FEA and AASHTO results at FLS.....	95

Figure 5.34 Correlation between shear distribution factors (F_v) at external support from FEA and AASHTO results at FLS	95
Figure 5.35 Comparison between positive moment distribution factors from the empirical equation and FEA for two lanes bridges at ULS	96
Figure 5.36 Comparison between negative moment distribution factors from the empirical equation and FEA for two lanes bridges at ULS.....	96
Figure 5.37 Comparison between positive moment distribution factors from the empirical equation and FEA for three lanes bridges at ULS.....	97
Figure 5.38 Comparison between negative moment distribution factors from the empirical equation and FEA for three lanes bridges at ULS.....	97
Figure 5.39 Comparison between positive moment distribution factors from the empirical equation and FEA for four lanes bridges at ULS.....	98
Figure 5.40 Comparison between positive moment distribution factors from the empirical equation and FEA for four lanes bridges at ULS.....	98
Figure 5.41 Comparison between positive moment distribution factors from the empirical equation and FEA for five lanes bridges at ULS.....	99
Figure 5.42 Comparison between negative moment distribution factors from the empirical equation and FEA for five lanes bridges at ULS.....	99
Figure 5.43 Comparison between positive moment distribution factors from the empirical equation and FEA for two lanes bridges at FLS	100
Figure 5.44 Comparison between negative moment distribution factors from the empirical equation and FEA for two lanes bridges at FLS.....	100
Figure 5.45 Comparison between positive moment distribution factors from the empirical equation and FEA for three lanes bridges at FLS.....	101
Figure 5.46 Comparison between negative moment distribution factors from the empirical equation and FEA for three lanes bridges at FLS.....	101
Figure 5.47 Comparison between positive moment distribution factors from the empirical equation and those from FEA for four lanes bridges at FLS.....	102
Figure 5.48 Comparison between negative moment distribution factors from the empirical equation and those from FEA for four lanes bridges at FLS.....	102
Figure 5.49 Comparison between positive moment distribution factors from the empirical equation and FEA for five lanes bridges at FLS.....	103
Figure 5.50 Comparison between negative moment distribution factors from the empirical equation and FEA for five lanes bridges at FLS.....	103
Figure 5.51 Comparison between vertical shear at internal support from the empirical equation and FEA for two lanes bridges at ULS as function of (L).....	104
Figure 5.52 Comparison between vertical shear at external support from the empirical equation and FEA for two lanes bridges at ULS as function of (L).....	104
Figure 5.53 Comparison between vertical shear at internal support from the empirical equation and FEA for three lanes bridges at ULS as function of (L).....	105
Figure 5.54 Comparison between vertical shear at external support from the empirical equation and FE A for three lanes bridges at ULS as function of (L).....	105
Figure 5.55 Comparison between vertical shear at internal support from the empirical equation and FEA for four lanes bridges at ULS as function of (L).....	106
Figure 5.56 Comparison between vertical shear at external support from the empirical equation and FEA for four lanes bridges at ULS as function of (L).....	106

Figure 5.57 Comparison between vertical shear at internal support from the empirical equation and FEA for five lanes bridges at ULS as function of (L).....	107
Figure 5.58 Comparison between vertical shear at external support from the empirical equation and FEA for five lanes bridges at ULS as function of (L).....	107
Figure 5.59 Comparison between vertical shear at internal support from the empirical equation and FEA for two lanes bridges at FLS as function of (L).....	108
Figure 5.60 Comparison between vertical shear at external support from the empirical equation and FEA for two lanes bridges at FLS as function of (L).....	108
Figure 5.61 Comparison between vertical shear at internal support from the empirical equation and FEA for three lanes bridges at FLS as function of (L).....	109
Figure 5.62 Comparison between vertical shear at external support from the empirical equation and FEA for three lanes bridges at FLS as function of (L).....	109
Figure 5.63 Comparison between vertical shear at internal support from the empirical equation and FEA for four lanes bridges at FLS as function of (L).....	110
Figure 5.64 Comparison between vertical shear at external support from the empirical equation and FEA for four lanes bridges at FLS as function of (L).....	110
Figure 5.65 Comparison between vertical shear at internal support from the empirical equation and FEA for five lanes bridges at FLS as function of (L).....	111
Figure 5.66 Comparison between vertical shear at external support from the empirical equation and FEA for five lanes bridges at FLS as function of (L).....	111
Figure 5.67 Comparison between vertical shear at internal support from the empirical equation and FEA for two lanes bridges at ULS as function of (β).....	112
Figure 5.68 Comparison between vertical shear at external support from the empirical equation and FEA for two lanes bridges at ULS as function of (β).....	112
Figure 5.69 Comparison between vertical shear at internal support from the empirical equation and FEA for three lanes bridges at ULS as function of (β).....	113
Figure 5.70 Comparison between vertical shear at external support from the empirical equation and FEA for three lanes bridges at ULS as function of (β).....	113
Figure 5.71 Comparison between vertical shear at internal support from the empirical equation and FEA for four lanes bridges at ULS as function of (β).....	114
Figure 5.72 Comparison between vertical shear at external support from the empirical equation and FEA for four lanes bridges at ULS as function of (β).....	114
Figure 5.73 Comparison between vertical shear at internal support from the empirical equation and FEA for five lanes bridges at ULS as function of (β).....	115
Figure 5.74 Comparison between vertical shear at external support from the empirical equation and FEA for five lanes bridges at ULS as function of (β).....	115
Figure 5.75 Comparison between vertical shear at internal support from the empirical equation and FEA for two lanes bridges at FLS as function of (β).....	116
Figure 5.76 Comparison between vertical shear at external support from the empirical equation and FEA for two lanes bridges at FLS as function of (β).....	116
Figure 5.77 Comparison between vertical shear at internal support from the empirical equation and FEA for three lanes bridges at FLS as function of (β).....	117
Figure 5.78 Comparison between vertical shear at external support from the empirical equation and FEA for three lanes bridges at FLS as function of (β).....	117
Figure 5.79 Comparison between vertical shear at internal support from the empirical equation and FEA for four lanes bridges at FLS as function of (β).....	118

Figure 5.80 Comparison between vertical shear at external support from the empirical equation and FEA for four lanes bridges at FLS as function of (β)	118
Figure 5.81 Comparison between vertical shear at internal support from the empirical equation and FEA for five lanes bridges at FLS as function of (β)	119
Figure 5.82 Comparison between vertical shear at external support from the empirical equation and FEA for five lanes bridges at FLS as function of (β)	119
Figure 5.83 Comparison between vertical shear at internal support from the empirical equation and FEA for two lanes bridges at ULS as function of (β^2)	120
Figure 5.84 Comparison between vertical shear at external support from the empirical equation and FEA for two lanes bridges at ULS as function of (β^2)	120
Figure 5.85 Comparison between vertical shear at internal support from the empirical equation and FEA for three lanes bridges at ULS as function of (β^2)	121
Figure 5.86 Comparison between vertical shear at external support from the empirical equation and FEA for three lanes bridges at ULS as function of (β^2)	121
Figure 5.87 Comparison between vertical shear at internal support from the empirical equation and FEA for four lanes bridges at ULS as function of (β^2)	122
Figure 5.88 Comparison between vertical shear at external support from the empirical equation and FEA for four lanes bridges at ULS as function of (β^2)	122
Figure 5.89 Comparison between vertical shear at internal support from the empirical equation and FEA for five lanes bridges at ULS as function of (β^2)	123
Figure 5.90 Comparison between vertical shear at external support from the empirical equation and FEA for five lanes bridges at ULS as function of (β^2)	123
Figure 5.91 Comparison between vertical shear at internal support from the empirical equation and FEA for two lanes bridges at FLS as function of (β^2)	124
Figure 5.92 Comparison between vertical shear at external support from the empirical equation and FEA for two lanes bridges at FLS as function of (β^2)	124
Figure 5.93 Comparison between vertical shear at internal support from the empirical equation and FEA for three lanes bridges at FLS as function of (β^2)	125
Figure 5.94 Comparison between vertical shear at external support from the empirical equation and FEA for three lanes bridges at FLS as function of (β^2)	125
Figure 5.95 Comparison between vertical shear at internal support from the empirical equation and FEA for four lanes bridges at FLS as function of (β^2)	126
Figure 5.96 Comparison between vertical shear at external support from the empirical equation and FEA for four lanes bridges at FLS as function of (β^2)	126
Figure 5.97 Comparison between vertical shear at internal support from the empirical equation and FEA for five lanes bridges at FLS as function of (β^2)	127
Figure 5.98 Comparison between vertical shear at external support from the empirical equation and FEA for five lanes bridges at FLS as function of (β^2)	127

APPENDICES

Appendix A.1 Parameters of empirical equation of moment distribution factors at ULS.....	128
Appendix A.2 Parameters of empirical equation of moment distribution factors at FLS.....	131
Appendix A.3 Parameters of empirical equation of shear distribution factors as function of (L) span length at ULS.....	134
Appendix A.4 Parameters of empirical equation of shear distribution factors as function of (L) span length at FLS.....	137
Appendix A.5 Parameters of empirical equation of shear distribution factors as function of (β) at ULS	140
Appendix A.6 Parameters of empirical equation of shear distribution factors as function of (β) at FLS.....	143
Appendix A.7 Parameters of empirical equation of shear distribution factors as function of (β^2) at ULS.....	146
Appendix A.8 Parameters of empirical equation of shear distribution factors as function of (β^2) at FLS.....	149
Appendix A.9 Comparison between the load distribution factor from the FEA and CHBDC equation in ULS	152
Appendix A.10 Comparison between the load distribution factor from the FEA and CHBDC equation in FLS	154
Appendix A.11 Comparison between the load distribution factor from the FEA and AASHTO-LRFD equation in ULS.....	156
Appendix A.12 Comparison between the load distribution factor from the FEA and AASHTO-LRFD equation in FLS	158

NOTATIONS

B	= Bridge width
B_1	= Box girder width
B_2	= Shoulder width
B_3	= Barrier width
C_f	= percentage correction factor as per CHBDC
D_X	= total bending stiffness, EI, of the bridge cross-section divided by the width of the bridge.
D_{XY}	= total torsional stiffness, GJ, of the bridge cross – section divided by the width of the bridge.
E	= Young’s modulus
E_c	= the modulus of elasticity of concrete
E_s	= the modulus of elasticity of steel
F	= the width dimension that characterizes the load distribution for the bridge
F_m	= load distribution factor for longitudinal bending moment
$(F_m)^{+ve}$	= the distribution factor for positive moment
$(F_m)^{-ve}$	= the distribution factor for negative moment
$(F_V)_{internal}$	= load distribution factor for vertical shear at internal support of two-equal- span bridge
$(F_V)_{external}$	= load distribution factor for vertical shear at external support of two-equal- span bridge
G	= the shear modulus
I	= the moment of inertia of the box girder
[K]	= global stiffness matrix;
L	= Span length
M_g^{avg}	= the average moment per box girder
M^+	= the maximum positive moment near the mid-span for a straight continuous span due to the CHBDC truck loading
M^-	= the maximum negative moment at the interior support for a straight continuous span due to the CHBDC truck loading
M_T	= the maximum moment per design lane
n	= number of design lanes
N	= number of Girder
[P]	= nodal load vector;
R_L	= modification factor for multi-design lanes based on the number of the design lanes,
R'_L	= modification factor for multilane loading
S	= centre- to-centre spacing of longitudinal girders of a deck-on-girder bridge.
t_1	= thickness of concrete slab
t_2	= thickness web and bottom flange of box girder
[U]	= nodal displacement vector
$(V_{FEA})_{pier}$	= vertical shear at internal support from finite element analysis
$(V_{FEA})_{end}$	= vertical shear at external support from finite element analysis
$(V_{beam})_{pier}$	= vertical shear at internal support from simple beam or idealize girder

$(V_{\text{beam}})_{\text{end}}$ = vertical shear at external support from simple beam or idealize girder
 W_c = Deck width
 W_e = width of design lane
 W_L = is the live load distribution factor for each box –girder
 Y = the distance from the neutral axis to the bottom flange
 ν =Poisson's ratio
 σ = the stresses in equilibrium with applied loads
 $(\sigma)_{\text{FEA}}$ = the maximum stresses obtain from the finite element analysis
 $(\sigma)_{\text{beam}}$ = the maximum stresses obtain from simple beam or idealize girder
 μ = lane width modification factor
 φ = rotation (degree of freedom)

CHAPTER 1

INTRODUCTION

1.1 General

In recent years, box girder bridges became a popular solution for medium-and long-span bridges in modern highways and even in railway bridges. This type of bridges is aesthetically pleasing and less vulnerable to environmental conditions compared to open-section Bridge. Accordingly, maintenance costs could be significantly reduced throughout the life of the structure.

Box girders are more advantageous than the I-girders due to (i) its high bending stiffness combined with a low dead load, yielding a favorable ratio of dead load to live load, (ii) its high torsional stiffness which allows freedom in the selection of both the supports and bridge alignment, (iii) the possibility of utilizing the space inside the box girder.

Box girder bridges may be made of reinforced concrete, prestressed concrete or steel. Steel box girders may be used to support orthotropic steel decks, or concrete deck slab.

A composite steel box girder is a tub girder that consists of independent top flanges and cast-in-place reinforced concrete decks. Box girder bridges have single or multiple boxes as shown in Figure 1.1. The composite box section has a superb torsional rigidity. On the other hand, the non-composite steel section becomes critical when subjected to large torsional demand. The naked steel girder usually supports only the loading during the early stages of bridge construction prior to hardening of the concrete deck. The non-composite dead load stress may account for up to 60 – 70 % of the total stress for typical box Girder Bridge (Topkaya and Williamson 2003).

The use of multiple box girders, shown in Figure 1.2 in bridge deck construction can lead to considerable economy due to their superb torsional stiffness that may be 100 to more than 1000 times that of comparable I-girders (Heins and Hall 1981). Figure 1.3 shows view of a twin-box girder bridge built in USA.

1.2 The Problem

The live load distribution factor equations are among the most important bridge design parameters because they assist in providing accurate distributed moment and shear forces, for the design of girders. The current practice in North America has adopted the load distribution factors for the design of multiple box-girder bridges due to their simple use and cost efficiency in the design process. In addition, there is neither need for any complex analysis nor for computer software programs to obtain the straining actions on the bridge girders. However, the equations' ease of use should not compromise the accuracy and reliability of the design.

Simplified methods of analysis specified in the Canadian Highway Bridge Design Code (CHBDC, 2006) for live load distribution factors are based upon the results obtained from some bridge structures using grillage, semi-continuum method for which the idealized structure was essentially an orthotropic plate theory. One major problem with the orthotropic plate method is the evaluation of the flexural and torsional stiffnesses of the flanges and girders of the bridge. AASHTO LRFD (2007) specifies empirical studies revealed that for shorter or longer bridges the load distribution factor expressions lose accuracy (Zokaie, 2000). Investigations for the load distribution factors calculated based on North American bridge codes have shown that these values may be very conservative in some cases and in others they may be unconservative (Yousif, 2007; Samaan, 2004; Nour, 2003). Accordingly, more precise expressions for load distribution factors are required to be developed in the bridge codes. Therefore, detailed parametric study is undertaken to evaluate the load distribution factors for multiple box girder bridges by utilizing the finite element method.

1.3 Objectives

The objectives of this study are:

- 1- Conduct a parametric study, using the finite element modeling, two-span continuous box girders under different CHBDC truck loading conditions to determine their load distribution factors. The results are correlated with the available CHBDC and AASHTO-LRFD equation to determine their level of accuracy.

- 2- Develop more reliable expressions for the moment and shear distribution factors for such bridges based on the data generated from the parametric study.

1.4 Scope

In order to achieve the above mentioned objectives for this type of bridges, the scope of this study is as follows:

- 1- A literature review of previous research work and codes of practice related to the structural behavior and load distribution of straight multiple box girder bridges.
- 2- Development of the finite element modeling for this type of bridges using the 3D finite element analysis.
- 3- A parametric study on different parameters governing the bending moments and shear forces distributions among girders due to the CHBDC moving truck for both ultimate and fatigue limit states. In order to get the load distribution factors, the maximum and minimum flexural stresses in the bottom steel flanges near the mid-span and at the pier location were determined, respectively. The maximum shear forces at the external and internal support locations were obtained. The technique of 3D finite element modeling was utilized to obtain these results. The maximum stresses and shear forces for the 2D-idealized girder were calculated. Then the load distribution factors for moments and shear forces were calculated for all bridges considered in the study. The effect of the span length, number of lanes and number of boxes on the load distribution factors are also investigated and compared for different bridge prototypes.
- 4- Deducing of simplified live load distribution factors formulas for multiple box girder bridges that can be utilized for the design of the steel box girders. Using the fit curve regression method, simplified formulas for shear and moment distribution factors for all bridges considered in this study were developed and compared with the existing ones available in the CHBDC. The equations induced in this study were function of the span length, number of lanes and number of boxes.
- 5- Comparison between the available CHBDC code equations, AASHTO code equations and the results obtained from finite element analysis results for straight bridges to

determine the accuracy of the available equations in the North American bridge codes. Figure 1.4 shows the organization chart of the research work.

1.5 Arrangement of the thesis

In Chapter 2, some previous work and literature review on multiple box girder bridges are presented. Chapter 3 includes a description of the finite-element procedure and the commercial available software program “SAP2000”, the linear static analysis method used in the study and the finite-element modeling of composite multiple box-girder bridges. Chapter 4 presents the configurations of the composite box-girder bridges considered in the analyses, Truck loading conditions and parametric study for load distribution factors. Results obtained from the parametric study for all bridge prototypes are presented in Chapter 5. In addition, Chapter 5 presents correlations between the results obtained from the finite-element analysis and those calculated based on the expressions specified in the CHBDC simplified methods of analysis as well as AASHTO-LRFD for bending moment and shear force distribution factors at ULS and FLS. The results calculated based on the proposed empirical equations for load distribution factors are also included in the correlations. Finally, Chapter 6 summarizes the findings of this research, outlines conclusions reached and provides recommendations for future researches.

CHAPTER 2

LITERATURE REVIEW

2.1 General

In the past, a significant amount of research was conducted to predict the behavior of different types of box girder bridges in the elastic range. The connection between the concrete deck and steel box girder, torsional warping, distortional warping and interaction between different kinds of cross-sectional forces make it difficult to accurately predict the behavior of all types of composite box-girder bridges. Bridge continuity added to the difficulty of the prediction of the behavior of this type of bridges. In the digital computer age, that difficulty in the analysis and design of continuous box girder bridges has been overcome by the use of the various software programs in the design. Since the overall behavior of continuous box girder bridges is always elastic under service loads, methods of linear structural analysis, such as orthotropic plate theory, folded plate and finite element, may be applied. The goal of work in this study is to develop a simplified method to design such bridges, enhance the available design specifications and to better understand the structural behavior of box-girder bridges.

2.2 Analytical Methods for Box Girder Bridges

Several methods are available for the design and analysis of box girder bridges. Each method is usually simplified by mean of assumptions in the geometry, material, boundary conditions and the relationship between its components. The accuracy of such solutions depends on the validity of the assumptions made. The Canadian Highway Bridge Design Code (CHBDC 2006) as well as the American Association of State Highway Transportation Officials (AASHTO-LRFD 2007) has recommended several methods of analysis of box-girder bridges. The following subsections present a brief review of these methods includes: Grillage Analogy, Orthotropic Plate, Folded Plate, Finite Strip, Finite Element and Thin-walled beam.

2.2.1 Grillage Analogy Method

Grillage analysis has been applied to multiple boxes with vertical and sloping webs and voided slabs, based on stiffness matrix approach. In this method, the bridge deck is idealized as a series of “beam” elements in the transverse direction (or grillages) connected and restrained at their joints. The continuous straight bridge is modeled as a system of discrete straight longitudinal beam members, representing the longitudinal beams at the web locations, intersecting orthogonally with transverse grillage members. As a result of the fall-off in stress at points remote from webs due to shear lag, the slab width is replaced by a reduced effective width over which the stress is assumed to be uniform. The equivalent stiffness of the continuum is lumped orthogonally along the grillage members. The main advantage of this method is the entire bridge superstructure can be modeled using beam elements which did not require high demand calculations. However, grillage analysis cannot be used to determine the effect of distortion and warping. Moreover, the effect of shear lag can hardly be assessed by using grillage analysis. The effect of the continuity of the slab in the longitudinal direction is ignored in this method. By using fine mesh of elements, local effects can be determined with a grillage. Alternatively, the local effects can be assessed separately and put in the results of grillage analysis.

2.2.2 Orthotropic Plate Theory Method

An orthotropic system is defined as a plate that exhibit significant different bending stiffness in two orthogonal directions and is presented for use in bridge analysis. Structural continuity between all supporting members and their flexibilities may be considered. The stiffness of the diaphragms is distributed over the girder length. The stiffness of the flanges and girders are lumped into an orthotropic plate of equivalent stiffness. Few researchers, (a many thesis Baker, T.H. 1991; Gangarao et al. 1992 ; Mangelsdorf et al. 2002 ; Huang et al. 2002 ; Higgins, 2004 ; and Huang et al. 2007 have utilized orthotropic thin plate theory for analyzing orthotropic bridge decks. However, the estimation of the flexural and torsional stiffnesses is considered to be one major problem in this method. The Canadian Highway Bridge Design Code (CHBDC) has recommended using this method mainly for the analysis

of straight box girder bridges. The accuracy of the method is reduced significantly for systems consisting of a small number of components under vehicular loadings.

2.2.3 Folded Plate Method

Spatial structures with large flat panels are common in engineering design, such as welded girders span of bridges. A folded plate structure or sometimes called prismatic shell is composed of a series of individual plane surfaces, jointed together to produce a stable construction capable of carrying loads. The lines of intersection between the individual plates are usually termed “fold lines or “joints”. The method can be used for simple and continuous spans, with considering the end diaphragms infinitely stiff in their plane. The prismatic folded plate theory by Goldberg and Leve, 1975 considers the box girder to be made up of an assemblage of folded plates. This method uses two-dimensional elasticity theory for determining membrane stresses and classical plate theory for analyzing bending and twisting of the component plates. The analysis is limited to straight, prismatic box girder composed of isotropic plates with no interior diaphragms and with simply supported end conditions. Meyer and Scordelis (1971) later presented a folded plate analysis for simply supported, single-span box girder bridges with or without intermediate diaphragms. Canadian Highway Bridge Design Code restricts the use of this method to bridges with support conditions closely equivalent to a line support.

2.2.4 Finite Strip Method

The finite-strip method (FSM) is one of the most efficient methods for structural analysis of bridges, reducing the time required for analysis without largely affecting the degree of accuracy. FSM is therefore an ideal platform for traditional time-consuming fracture analysis. The finite strip method may be regarded as a special form of the displacement formulation of the finite element method. The finite strip method discretizes the bridge into a longitudinal number of rectangular strips, running from one end support to the other and connected transversely along their edges by longitudinal nodal lines. The stiffness matrix is then calculated for each strip based upon a displacement function in terms of Fourier series. The displacement functions of the finite strips are assumed as a combination of harmonic

varying longitudinally and polynomials varying in the transverse direction. Therefore, the strip method is considered as a transition between the folded plate method and the finite element method. In 1968, the finite strip method was first introduced by Cheung in 1971; Cheung and Cheung applied the finite strip method for curved box girder bridges. In 1974, Kabir, and Scordelis, developed a finite strip computer program to analyze curved continuous span cellular bridges, with interior radial diaphragms, on supporting planar frame bents. Free vibration of curved and straight beam-slab and box-girder bridges was conducted by Cheung, and Cheung, 1972 using the finite strip method. In 1978, the method was adopted by Cheung and Chaung, to determine the effective width of the compression flange of straight multi-box and multi-cell box girder bridges. In 1984, Cheung, used a numerical technique based on the finite strip method and the force method for the analysis of continuous curved box girder bridges. In 1989, Ho et al. used the finite strip to analyze three different types of simply supported highway bridges, slab-on-girder, two-cell box girder, and rectangular voided slab bridges. Sennah and Kennedy (2002) and Ozakca et al. (2003) stated that the shape optimization of folded plates can be carried out on box girders by integrating finite strip method.

The advantage of the finite strip method is that it requires small computer storage and relatively little computation time. Although the finite strip method has broader applicability as compared to folded plate method, the method is still limited to simply support prismatic structures. For multi- span bridges, Canadian Highway Bridge Design Code restricts the method to those with interior supports closely equivalent to line supports and isolated columns supports. Any plate or shell structure subjected to translational displacement along the transverse edges of the strips cannot be analyzed by this method.

2.2.5 Thin-Walled Beam Theory Method

Thin-walled beam theory was established by Vlasov (1965) and then extended by Dabrowski (1968). The theory is based on the usual beam assumptions. The theory assumes non-distortional cross-section and, hence, does not account for all warping, distortion or bending stress. The theory cannot predict shear lag or the response of deck slabs due to local wheel loads. In 1985, Maisel extended Vlasov's thin-walled beam theory to account for torsional, distortional, and shear lag effects of straight, thin-walled cellular box beams. Li (1992) and

Razaqpur and Li (1997) developed a box girder finite element, which includes extension, torsion, flexure, distortion and shear lag analysis of straight and curved multi-cell box girders using thin-walled finite element based on Vlasov's theory. Razaqpur et al. (2000) used the straight thin-walled box beam element, along with exact shape functions were used to eliminate the need for dividing the box into many elements in the longitudinal direction. The results of the proposed element agreed well with those results obtained from full three-dimensional shell finite element analysis. The theory was incorporated into a computer program to solve linear elastic analysis and nonlinear material analysis. For both static and dynamic analyses of multi-cell box girder bridges, Vlasov's thin-walled beam theory was cast in a finite element formulation and exact shape function was used by El-Azab (1999) to derive the stiffness matrix.

2.2.6 Finite Element Method

The finite-element method of analysis has rapidly become a very popular technique for the computer solution of complex problems. In the finite element analysis the structure is represented as an assemblage of discrete elements interconnected at a finite number of nodal points, the individual element stiffness matrix, which approximates the behavior or stress patterns. Then, the nodal displacements and hence the internal stresses in the finite element are obtained by the overall equilibrium equations. The finite elements may be one-dimensional beam-type elements, two-dimensional plate or shell elements or even three-dimensional solid elements.

In 1971, Chu and Pinjarkar developed a finite-element formulation of curved box-girder bridges, consisting of horizontal sector plates and vertical cylindrical shell elements. The method can be applied only to simply supported bridges without intermediate diaphragms. In 1972, William and Scordelis presented an elastic analysis of cellular structures of constant depth with arbitrary geometry in plan using quadrilateral elements. In 1974, Bazant and El Nimeiri attributed the problems associated with the neglect of curvilinear boundaries in the elements used to model curved box beams by the loss of continuity at the end cross-section of two adjacent elements meet at an angle. Fam and Turkstra (1975) described a finite-element scheme for static and free-vibration analysis of box girders with orthogonal

boundaries and arbitrary combinations of straight and horizontally curved sections using a four- node plate bending annular element with two straight radial boundaries, for the top and bottom flanges. In 1976, Moffatt and Lim presented a finite-element technique to analyze straight composite box- girder bridges with complete or incomplete interaction with respect to the distribution of the shear connectors. Chang and Zheng (1987) used a finite–element technique to analyze the shear lag and negative shear lag effects in cantilever box girders. Shush-kewich (1988) showed the three–dimensional behavior of a straight box girder bridge, as predicted by a folded plate, finite-strip, or finite-element analysis, can be approximated by using some simple membrane equations in conjunction with a plane frame analysis. In 1995, Galuta and Cheung combined the boundary element with the conventional finite element method to analyze box girder bridges. The bending moments and vertical deflection were found to be in good agreement when compared with the finite strip solution. Elbadry and Debaiky (1998) presented a numerical procedure and a computer program for the analysis of the time dependent stresses and deformations induced in curved, pre-stressed, concrete cellular bridges due to changes in geometry, in the static system, and in the loading conditional during construction. In 1998 Sennah and Kennedy conducted an extensive parametric study on composite multi-cell box girder bridges using the finite element analysis to study their vibration characteristics. In 2009, Fang-LI applied a 3D finite element technique in web cracking analysis of concrete box–girder bridges. The results obtained from the finite-element method were in good agreement with the experimental findings. Therefore, many investigators have been attracted to adopt the finite-element method to analysis the complex mechanics of arbitrary box girder bridges. Canadian Highway Bridge Design Code has recommended the finite-element method for all type of bridges.

2.3 Experimental Studies

In order to verify the results obtained from the analytical solutions and the developed computer programs few experimental studies were conducted on box girder bridges. In some cases, experimental studies were conducted on field testing of existing box girders. However, the majority of experimental tests have conducted in the laboratories on small scale bridge models. In 1993, Ng et al. tested on two- span, continuous composite concrete, deck-aluminum, four-cell model, under OHBDC, truck loading conditions. The prototype bridge

was a two-lane, concrete curved, four-cell, box-girder structure and continuous over two spans. The experimental results reported were in good agreement with the elastic behavior results predicted by a 3D finite-element modeling. In 1998, Sennah tested five straight and curved deck steel three-cell bridge models under various static loading conditions and free vibration tests. Four models were simply-supported and the fifth was a two-equal-span continuous bridge model. The results obtained from the experimental work were utilized to verify the finite element model. In 2003, Androus performed experiments on a curved and straight composite multiple box girder bridge models up-to-complete collapse. Results obtained from these tests good trend agreement between the experimental and theoretical results supports the reliability of using the finite element modeling and the cross-bracing did not have a significant effect on the bridge natural frequencies. In 2004, Samaan tested four loading stages on continuous curved concrete deck on steel multiple box girder bridges namely: at construction phase' under elastic loading of the composite bridge model, free-vibration of the composite bridge model, elastic loading of the composite bridge model, and loading of the bridge up-to-collapse. The results obtained from the experimental work were used to verify the elastic response and finite element model. In 2007, Sennah et al. conducted an experimental study on two continuous twin-box girder bridge models of different curvatures .The first model was straight while the second one was curved in plan. The experimental finding was used to verify and substantiate the finite–element model.

2.4 Available Code Provisions and Related Literature

2.4.1 AASHTO Methods

AASHTO specifications introduced simplified empirical methods for load distribution factors which are more convenient and cost efficient to use as compared with the theoretical methods. AASHTO defines the load distribution factor as the ration of the moment or shear obtained from the bridge system to the moment or shear obtained from a single girder loaded by one truck wheel line (AASHTO,1996) or the axle loads (AASHTO LRFD, 2007). It should be noted that AASHTO Standard specifications consists of a HS-20 Truck or a Lane load. While, the live load in the LRFD specifications consists of a HS-20 Truck in conjunction with a Lane load.

AASHTO Standard specifications contain simple procedure used in the analysis and design of highway bridges. AASHTO adopted the simplified formulas for distribution factors based on the work done in the 1940 by Newmark et al. (1948). AASHTO simple formula, S/D , has been used for live load distribution factors in most common cases to calculate the bending moment and shear in bridge design, where S is the girder spacing and D is a constant that depends on the type of the bridge superstructure and bridge geometry. This formula allows the designer to simply calculate the part of live load to be transferred to the girders without any consideration for the bridge deck, girder stiffness, and span. Further, some bridge designers apply the above-mentioned formula even to more complicated bridges such as skewed, curved, continuous, and large spans with wide and different girder spacing, even though, the formula is developed for simple bridges with typical geometry. A major shortcoming of the AASHTO Standard Specifications is that the changes in bridge structures that have taken place over the last 55 years led to inconsistencies in the load distribution criteria. Upon review of these formulas, it was found that these formulas were generating valid results for bridges of a typical geometry (i.e. beam spacing near 1.83 m and span length of about 18.29 m). The formulas could result in highly unconservative shear distribution factors (more than 40%) in some cases and highly conservative results (more than 50%) in some other cases. The unconservative distribution factors may lead to unsafe bridge designs (Zokaie and Imbsen, 1993).

Nour (2003) used the commercially available finite element program “ABAQUS” to determine the load distribution factors in straight and curved concrete deck-on-steel multiple box girder bridges. He examined the AASHTO distribution factors by conducting theoretically investigation based on AASHTO standard of 1996. He concluded that the load distribution factors decrease with increase the number of boxes. Also, he observed that cross bracing with a maximum spacing of 7.5m enhances the transverse load distribution factors. It was concluded in his study that the curvature of the bridge is one of the most critical parameter that influences the design of girders and bracing members in curved multiple-box girder bridges.

Most of the formulas of the AASHTO standard are based only on the beam spacing and do not take into account any other parameters such as span length, lateral stiffness and lane

width. Later editions of the standard specifications included more accurate equations that take into account more bridge parameters for calculating distributions factors for few bridge types.

2.4.2 AASHTO-LRFD Method

The live load distribution formulas in AASHTO-LRFD (2007) have resulted from the National Cooperative Highway Research Program (NCHRP) 12-26 project, entitled “Distribution of Live Loads on Highway Bridges” (Zokaie et al. 1991). This project was initiated in 1985, long before the LRFD specifications were developed, to improve the accuracy of the S/D formulas contained in the AASHTO specifications (AASHTO Standard 1996). The equation for live load distribution factors contained in the AASHTO-LRFD Specifications present a major change to the AASHTO Standard Specifications. The equations are more accurate but vastly more complex than the Standard method. In case composite steel box girders, the live load distribution factor for each box girder is specified to be determined by applying to the girder the fraction W_L of a wheel load according to the following:

$$W_L = 0.1 + 1.7 \frac{N_L}{N_B} + \frac{0.85}{N_L} \quad (2.1)$$

Where:

W_L is the live load distribution factor for each box-girder

N_b is the number of box girder; and

N_L is the number of lanes taken as the integral part of the ratio $\frac{W_c}{3.6}$, as W_c is the clear roadway width in m.

The drawback of this equation is that it was developed for number of lanes equal to the number of boxes. Also, the equation, dated back to 1968, was developed using the finite-difference method that does not capture all the 3D effects of the bridge superstructure.

When the parameters of a bridge exceed the ranges of applicability of the equations, the AASHTO LRFD Specifications mandate that a refined analysis such as grillage analysis or finite element analysis should be performed for the distribution factors of bridge beams. In

such cases, designers have to work on a case by case basis. Therefore, the design community would welcome simpler and less complex live load distribution factor equations.

Samaan, (2004) used the AASHTO-LRFD to conduct dynamic and static analyses of continuous curved composite multiple-box girder bridges as well as CHBDC. The finite element program “ABAQUS” was adopted in that study. Expressions for load distribution factors for curved bridges were proposed. Experimental program was also conducted to verify the results obtained from the finite element analysis. It was recommended to use cross-bracing with spacing less than 10 m to enhance the distribution of loads among bridge girders. It was shown in his study that load distribution factors are not affected by using either vertical or inclined webs in the finite element modeling of box girders. It was concluded that the bridge span length, number of lanes, number of boxes and span-to-radius of curvature ratio are the most crucial parameters that affect the load distribution factors. Expressions for fundamental frequency and impact factors of multiple box girder bridges were also proposed.

AASHTO-LRFD formulas were evaluated by Zaher Yousif et al. (2007). They made comparison between the distribution factors of simple span concrete bridges due to live load calculated in accordance with the AASHTO-LRFD formulas and the finite-element analysis. Their evaluation showed that AASHTO-LRFD formula seem to give very comparable results to the finite elements for bridges with parameters within the intermediate ranges and tends to deviate within the extreme ranges of these limitations.

2.4.3 Canadian Highway Bridge Design Code (CHBDC)

The Canadian code proposed a simplified analysis method using the load distribution factors to determine the shear and bending moments for steel box girder bridges. The method was developed based upon the results obtained from some bridges analyzed using grillage, semi-continuum and orthotropic plate methods (CHBDC commentary, 2006). The method was created based on the assumption that the steel box girders are sufficiently braced against any distortion through the cross bracing placed inside the boxes.

In 2003, Androus applied the CHBDC truck loading to examine the behavior and load distribution characteristics of straight and curved composite multiple box-girder bridges. His experimental tests proved that the presence of external cross bracing ensured better

distribution of the stresses under ultimate loading conditions. Results from his work showed that bridge curvature is the most critical parameter that influences the design of girders and bracing members in multiple-box bridges. Also, the study showed that bending stress distribution factors decrease with the increase in number of box girders. On the other hand, the bending stress distribution factors for the outer and inner girders increase with increase in the span length of the bridge.

In 2005, Hassan used CHBDC truck load to investigate the shear distribution in straight and curved composite multiple box-girder bridges by using the finite-element modeling. It was observed that the bridge span length slightly affects the shear distribution factor of straight bridges. However, its effect significantly increases with increase in bridge curvature. On the other hand, the shear distribution factor is significantly affected by the change in number of boxes.

The Canadian Highway Bridge Design Code specifies equations for the simplified method of analysis to determine the longitudinal bending moments and vertical shear in composite steel multiple-box girder bridges due to live load for ultimate, serviceability and fatigue limit states using load distribution factors. The CHBDC distribution factor equations used to evaluate the maximum longitudinal moments and shear forces for multi-box girder bridges are as follows:

The longitudinal bending moment per girder, M_g , for ultimate and serviceability limit states is specified as:

$$M_g = F_m M_{g \text{ avg}} \quad (2.2)$$

Where:

$M_{g \text{ avg}}$ = the average moment per box girder determined by sharing equally the total moment on the bridge cross section among all box girders in the cross section

F_m = an amplification factor for the transverse variation in maximum longitudinal moment intensity

$$M_{g \text{ avg}} = \frac{nM_\tau R_L}{N} \quad (2.3)$$

$$F_m = \frac{SN}{F(1 + \frac{\mu C_f}{100})} \geq 1.05 \quad (2.4)$$

$$\mu = \frac{w_e - 3.3}{0.6} \leq 1.0 \quad (2.5)$$

$$W_e = \frac{W_c}{n} \quad (2.6)$$

- Where
- M_T = the maximum moment per design lane
 - n = the number of design lanes
 - R_L = a modification factor for multilane loading
 - N = the number of longitudinal box girders
 - S = center-to-centre girder spacing, m
 - W_e = the width of the design lane, m
 - W_c = the bridge deck width, m
 - C_f = a correction factor from tables
 - F = the width dimension that characterizes the load distribution for the bridge

Expressions for F and C_f for longitudinal moments in multi-spine bridges obtained from Table (2.1) depending on a factor, β

$$\beta = \pi \left[\frac{A}{L} \right] \left[\frac{D_x}{D_{xy}} \right]^{0.5} \quad (2.7)$$

Where :

- A = width of the bridge for ULS and FLS; but not greater than three times the spine spacing S for FLS
- D_x = total bending stiffness, EI , of the bridge cross-section divided by the width of the bridge
- D_{xy} = total torsional stiffness, GJ , of the bridge cross-section divided by the width of the bridge

For bridges having more than four design lanes, the values of F shall be calculated from the following:

$$F = F_4 \frac{nR_L}{2.80} \quad (2.8)$$

Where F_4 is the value of F for four design lanes obtained from table (2.1)

For the longitudinal bending moment per girder, M_g , for Fatigue Limit State:

$$M_g = F_m M_{g \text{ avg}} \quad (2.9)$$

Where:

$M_{g \text{ avg}}$ = the average moment per box girder determined by sharing equally the total moment on the bridge cross-section among all box girders in the cross section

F_m = an amplification factor for the transverse variation in maximum longitudinal moment intensity

$$M_{g \text{ avg}} = \frac{M_T}{N} \quad (2.10)$$

$$F_m = \frac{SN}{F(1 + \frac{\mu C_f}{100})} \geq 1.05 \quad (2.11)$$

$$\mu = \frac{w_e - 3.3}{0.6} \leq 1.0 \quad (2.12)$$

Where :

M_T = the maximum moment per design lane,

n = the number of design lanes

R_L = a modification factor for multilane loading

N = the number of longitudinal box girders

S = center-to-centre girder spacing in meter

W_e = the width of the design lane in meter

C_f = a correction factor obtained from tables

F = the width dimension that characterizes the load distribution for the bridge.

Expressions for F and C_f for multi-spine bridges are shown in Table 2.1.

For the longitudinal vertical shear per girder, V_g , for ultimate, serviceability and fatigue limit states:

$$V_g = F_v V_{g \text{ avg}} \quad (2.13)$$

Where:

$V_{g \text{ avg}}$ = the average shear per girder

F_v = an amplification factor for the transverse variation in maximum longitudinal vertical shear intensity

$$V_{g \text{ avg}} = \frac{nV_T R_L}{N} \quad (2.14)$$

$$F_v = \frac{SN}{F} \quad (2.15)$$

Where:

V_T = the maximum vertical shear per design lane

n = the number of design lanes

R_L = a modification factor for multilane loading

N = the number of longitudinal box girders

S = is center – to- center girder spacing in meter

W_e = the width of the design lane in meter

F = the width dimension that characterizes the load distribution for the bridge and can be obtained from provided tables.

For bridges having more than four design lanes, the values of F shall be calculated from the following:

$$F = F_4 \frac{nR_L}{2.80} \quad (2.16)$$

Where F_4 is the value of F for four design lanes obtained from Table (2.2)

CHAPTER 3

FINITE-ELEMENT ANALYSIS

3.1 General

The Finite Element Method (FEM) is one of the most important methods used currently in the engineering analysis and design. The approach was developed by utilizing the method of numerical analysis and minimization of variation calculus to obtain approximate solutions to vibration systems. The method is employed comprehensively in the analysis of solids and structures and of heat transfer and fluids and in several engineering applications. The rapid progress in using the method began by the advance in the digital computer since the method would require significant computations.

As the name indicates, the method takes a complex problem and breaks it down into a finite number of simple problems. A continuous structure theoretically has an infinite number of simple problems, but the finite-element method approximates the behavior of a continuous structure by dividing it into a finite number of elements. Then, each element is considered to be a simple problem. Each element has a certain number of nodes that define the element geometric boundaries. The entire continuous structure geometry is defined by the final geometry of all elements. Each node has a certain number of degrees of freedoms. Nodes also defined where boundary conditions and load applications need to be applied. In general, the finer the mesh, the closer the geometry of the structure can be approximated as well as the load application and the stress and strain gradients. However, there is a tradeoff: the finer the mesh, the more computational power is needed to solve complex problems. Mesh optimization approach is adopted to create the larger mesh size that would not reduce the accuracy of the results.

There are many commercially-available finite-element software programs packages utilized for structural engineering applications. “SAP2000 software” Wilson and Habibullah, 2010 is considered one of the most used finite-element program package for structural engineering

analysis and design. The package has the capability to preprocessor, analyze, and post processor the structure. The program is used for general purpose applications including bridges, buildings offshore structures and many others. The program was adopted throughout the parametric study conducted in this study.

3.2 Finite-Element Procedure

The analysis of an engineering application needs the idealization of the physical problem into a form of mathematical model that can be solved. The finite-element method offers a way to solve a complex problem in engineering and mathematical physics by means of subdividing it into a series of simpler interrelated problems. The key step in engineering analysis is to select the appropriate mathematical model. Since most refined mathematical model can not reproduce exactly the physical problem, the finite-element analysis can only predict the approximate response of the problem. However, a refined mathematical model will increase our insight into the response of the engineering problem. The finite-element model gives approximate values of the unknowns at discrete number of points in a continuum. Essentially, it gives a consistent technique for modeling the whole structure as an assemblage of discrete parts or finite-elements. This numerical method of analysis starts by discretizing a physical model. Discretization is the process where a body is divided into an equivalent system of smaller units (elements) interconnected at points (nodes) common to two or more elements and/or boundary lines and/or surfaces. All elements are combined in formulated equations to obtain the solution for the entire structure. Using a displacement formulation, the stiffness matrix of each element is derived and the global stiffness matrix of the entire structure can be formulated by the direct stiffness method. This global stiffness matrix, along with the given displacement boundary conditions and applied loads is then solved, thus the displacements and stresses for the entire system are determined. The global stiffness matrix represents the nodal force- displacement relationships and is expressed in a matrix equation form as follows:

$$[P] = [K] [U] \quad (3.1)$$

Where: $[P]$ = nodal load vector;

$[K]$ = global stiffness matrix;

$[U]$ = nodal displacement vector

The basic of the displacement-based finite-element solution is the principle of virtual work. The principal states that the equilibrium of a body requires that any compatible small virtual displacements imposed on the body in its state of equilibrium, the total internal virtual work is equal to the total external virtual work.

3.3 SAP2000 Computer Program

The commercially-available finite-element software SAP2000 is a powerful engineering program to provide a wide range of useful engineering capabilities suitable for practical structural engineering applications. SAP2000 is based on the idea of transferring the physical structural members into objects using the graphical user interface. The software is capable of modeling any complicated structure by dividing it into small and manageable pieces. The finite-element program contains several types of objects. Point objects that are automatically created at the corners or ends of all other objects or to model isolators, damper or multi-linear spring. Line objects are to represent Frame, Cable and Tendon elements. Connecting two joints using link elements can be modeled using Line objects. Area objects are to model Shell elements with three- or four-node three-dimensional element, which combines separate membrane and plate-bending behavior. The membrane behavior includes translational in-plane stiffness components and rotational stiffness components in the direction normal to the plane of the element. The plate bending behavior includes two-way, out of plane, plate rotational stiffness components and translational stiffness component in the direction normal to the plane of the element. Shell elements are to represent slab, walls or any other thin-walled members.

The graphical interface of the program is used to draw the model and select the appropriate objects to represent the actual physical structure. As closer the representation of the physical member to the finite-element model as more accurate the results obtained by the finite-element analysis. The number of elements should be sufficient to accurately describe the geometry of the actual structure. The locations of the structural boundaries and the type

of the boundary conditions used should be carefully considered. Changes in thickness and material properties need to be considered and introduced in the finite-element model.

For moving load analysis case, lanes, vehicle and vehicle class shall be modeled and defined. The line or the area where the traffic load can act upon the bridge superstructure should be first identified. The lane width can be specified in the program as well as the distance between the vehicle and the lane edge. Multiple lanes can be defined per the actual traffic pattern on the bridge. Truck and/or lane loads can be represented in the program by number of concentrated and/or distributed forces. Each truck axes can be represented by single or double loads with s defined axle width. The minimum or the maximum distances between each axes can be specified in the program. Vehicle class can be used to combine several vehicles together to run on the bridge at the same time. It can also be used to define the dynamic amplification factor for the truck loading used in the analysis. In the moving load analysis case, the program creates first the influence surface for each straining actions. Once the influence surfaces calculated, the envelope for each bridge response can be evaluated. The vehicles are automatically located at each possible location along the lanes and within the width of the lanes to produce the maximum and minimum response quantities throughout the structure.

As mentioned before, the linear static analysis of a structure involves the solution of the system of linear equations represented by equation 3.1. For each Load Case, the program automatically creates a corresponding stiffness matrix of the full structure and accordingly solving the system of linear equations. The software considers each loading position on the bridge to obtain the influence surface as a linear static analysis case. Load combinations option available in the software can be used to combine the results of Analysis Cases to obtain the determined values used for the design of the structural members. Moving Load Analysis available in SAP 2000 is used to determine the response of a bridge structure subjected to vehicular live loads. The maximum and minimum displacements, forces and stresses due to multiple-lane loads on bridges can be obtained using the “SAP2000 software” Wilson and Habibullah, 2010. Multiple lane reduction factors are defined in the Moving Load Analysis case.

3.4 Finite-Element Modeling of Composite Multiple Box Girder Bridges

The finite element technique was adopted to model two-equal-span continuous concrete deck-on multiple steel box-girder bridges. Three-dimensional finite-element models were constructed in a way to represent the actual physical structural geometry, boundary conditions, load locations, and material properties of the bridge components, namely: reinforced concrete for the deck slab and steel for the webs, bottom flange, diaphragms and cross bracings. The following subsections explain the element type selected for each component, the material modeling, and the boundary conditions used on the developed FEA models were described below.

3.4.1 Material Modeling

The material properties are very important to define in order to get accurate results. The bridge slab is made of reinforced concrete while the rest of the box girder is made of steel. Elastic material properties are defined and used throughout this study. Each material is defined with a unique name and properties. The required properties for SAP2000 are the modulus of elasticity, Poisson's ration, and the weight density. The compressive strength of concrete (f'_c) is considered 30 MPa and the weight density (γ_c) 24.5 kN/m³. The modulus of elasticity of concrete (E_c) considered in the analysis is 26000 MPa based on the following equation:

$$E_c = (3000 \sqrt{f'_c} + 6900) (\gamma_c / 2300)^{1.5} \quad (3.5)$$

The Poisson's ratio for elastic strain of concrete is taken as 0.20. The modulus of elasticity of steel (E_s) is taken as 200,000 MPa and the Poisson's ratio for elastic strain of steel is taken as 0.30.

3.4.2 Geometric Modeling

A three-dimensional finite-element model was developed to simulate each bridge considered in this study. Three-dimensional shell elements were selected to model the reinforced concrete deck slab, steel webs, steel bottom flanges, and three-dimensional beam elements were chosen in the finite-element model to represent the cross bracings. The arrangements of

elements in the transverse and longitudinal directions were selected to accurately simulate the actual structure geometric configurations.

3.4.2.1 Modeling of Deck Slab, Webs, Bottom Flange and End- Diaphragms

SAP2000 has a three- or four-node formulation for shell elements. The formulation combines the membrane and plate-bending behavior. The shell elements used in this study is a homogeneous one that combines the above-mentioned formulation. The element behavior includes two-way, out-of-plane, plate rotational stiffness components and a translational stiffness component in the direction normal to the plane of the element. The element has six degrees of freedom at each node, namely: three displacements (U_1 , U_2 , U_3) and three rotations (φ_1 , φ_2 , φ_3). Four-point numerical full integration formulation is used for the shell stiffness. Internal forces, moments, and stresses are evaluated at the 2 x 2 Gauss integration points and then extrapolated to the nodes representing the element. The four-node elements are more accurate than the three-node elements. Therefore, the four-node elements were used to model the plate components of the bridges studied herein. Figure 3.1 shows schematic diagrams of the four-node shell element used in this study

3.4.2.2 Modeling of Connections

The connection between the steel girder and concrete slab was assumed to be fully-connected, no slip between the steel girder and the concrete slab was considered in the analysis. The steel girder and the concrete slab share the same nodes at the interface. The six degrees of freedoms at each node, three displacements (U_1 , U_2 , and U_3) and three rotational (φ_1 , φ_2 , φ_3), at the interface of the steel girder and the concrete slab are equivalent. Schematic view of the bridge model is showing the intermittent connections between steel box-girder and concrete slab in Figure 3.2.

3.4.3 Boundary Conditions

There were two different boundary constraints considered in modeling of the continuous concrete deck on multiple steel box-girder bridges, namely: the roller support and the hinged support. The roller support was modeled by releasing the horizontal movement of the node in

the required directions. However, the hinged support was constrained from any horizontal movement but released for all rotations. In modeling the bridge supports in this study, all supports were constrained in the vertical direction, but allowed to rotate around the support line. All other supports except the far most south ones are released in all horizontal directions. The far most south supports for the bridge ends are released in the longitudinal direction (X-direction) only. All internal supports at the pier location are released in the transverse direction (Y-direction) except the far most south support, which is restrained in all directions. The support arrangement was chosen to allow the bridge to move freely due to temperature variations as in practice. All support conditions were applied at the lower end nodes of each web, at the external and internal support lines, as shown in Figure 3.3.

3.4.4 Aspect Ratio of shell elements

In the finite-element modeling, the aspect ratio is defined as the ratio of the longest dimension to the shortest dimension of a quadrilateral element. In many cases, as the aspect ratio increases, the inaccuracy of the solution increases (Logan, 2002). Logan presented a graph showing that as aspect ratio rises above 4, the percentage of error from the exact solution increases greater than 15% consequently. Three-dimensional finite element models were used to analyze the box-girder bridges considered within this study. A sensitivity study was conducted to choose the finite-element mesh. The finite-element mesh is usually chosen based on pilot runs and is a compromise between economy and accuracy. In this study, 40 elements in the longitudinal direction were used in the FEA model for bridges with span lengths of 20 m, 80 elements for bridges with span lengths of 40 m and so on. The number of elements was chosen to keep the maximum aspect ratio about 2.5 which is within the acceptable range and does not compromise the accuracy of the results.

3.5 Finite Element Analysis of Bridge Models

Pilot runs were also performed (Samaan 2004) to investigate the effect of vertical stiffeners and concrete steel reinforcement on the structural response of the finite-element models. It was found that the vertical stiffeners had an insignificant effect on the structural response of the finite-element model, so they were omitted in the modeling. Figure 3.4 illustrates the

final finite-element mesh used in the static and dynamic analyses of two-box girder bridges. The number of elements between webs varied depending on the number of girder and the number of elements in the longitudinal direction varied depends on the span length and aspect ratio. The aspect ratios of the elements used for the concrete deck slab and the bottom flanges ranged from 0.88 to 2.4 for all bridge prototypes. The aspect ratios of the shell element for the webs and end- diaphragms ranged between 0.93 and 2.5 for all bridge prototypes. The finite-element model was then adopted to conduct extensive parametric studies for static responses of continuous composite box girder bridges. Figure 3.5a and Figure 3.5b show views of the finite-element models for the straight bridge model with and without concrete deck slab, respectively.

Chapter 4

PARAMETRIC STUDY

4.1 General

A parametric study was performed on continuous two-equal-span bridges having a concrete deck on multiple steel box girder bridges. The main objectives of the parametric study were to (i) Investigate the influence of major parameters affecting the various distribution factors, for both ultimate and fatigue limit states;(ii) Establish a data base for the distribution factors, for maximum stresses, shear force and support reaction forces necessary for design to correlate them with available CHBDC and AASHTO-LRFR equations; and (iii) Develop more reliable empirical formulas for load distribution factors for such bridges.

The CL-625-ONT truck loading as well as the lane loading is considered in the design of bridges in Ontario. The lane loading consisted of superimposed load of 9 kN.m uniformly and centrally distributed within a strip of 3 m width along with 80% of the truck loading is shown in Figure 4.1 summarizes the configurations of the contains truck loading and lane loading. Whichever of the truck load types produces higher structural responses is applied. The modifications factors for multi presence of vehicles in lanes, shown in Table 4.1 are taken as 0.9, 0.8, 0.7, and 0.6 for two, three, four and five lane loading, respectively.

Sensitivity study on a prototype bridge 2L-80-2b was conducted to evaluate the load distribution factors due to the Truck load and Lane load. Table 4.2 shows that all load distribution factors for the Truck load were slightly higher than those obtained from the Lane load. Therefore, it was decided to carry out all parametric study for the load distribution factors using the Truck load only.

4.2 Composite box-girder Bridge Configurations

In this parametric study, Fifty five composite multiple box-girder bridges were analyzed to obtain the load distribution factors. The following main parameters were considered to influence the load distribution in that type of bridges:

- 1- Number of design lanes, n , as determined from Table 4.3;
- 2- Number of boxes, N ; and
- 3- Span length, L

Table 4.4 presents the cross-sectional configurations of bridges used in the parametric study. The symbols used in Table 4.4 represent designations of the bridge types considered in these parametric studies, namely: L stands for lane, b stands for box, and the number in the middle of the designation embodies the span length of the bridge in meters. For example, 3L-40-4b denotes a continuous two-equal-span bridge of three lanes, four boxes and each span being 40 m long. The cross-sectional symbols used in Table 4.4 are shown in Figure 4.2.

Five different lengths of 20, 40, 60, 80 and 100 m for each span were considered in the parametric study. The number of lanes was taken as 2, 3, 4 and 5 lanes. The total bridge widths were taken 9.00, 13.05, 17.00 and 20.50 m for two, three, four and five-lane bridges. The number of boxes ranged from two to three in the case of two-lane bridges, two to four in the case of three-lane bridges, three to five in the case four-lane bridges and three to five in the case five-lane bridges. Figure 4.3 presents the number of boxes along with the number of lanes considered in the parametric study. The practical span-to-depth ratio for box-girder bridges ranges from 20 to 30 (Hall, at el. 1999). For steel girders having a specified minimum yielding stress of 350 MPa or less, the preferred span-to-depth ratio of the steel girder is about 25. The thickness of steel plates forming the bottom flanges and the webs was taken 16mm. while the thickness of the concrete slab was taken 225 mm.

The above range of parameters in this study was based on a survey of constructed box girder bridges (Heins 1978). Steel plate diaphragms of 16 mm thickness were provided at the pier and abutment supports. The depth of the diaphragms was the same as that of the steel box. Cross bracings made from back-to-back angles, 150 x 150 x 10 mm in cross-section, were

provided inside and between the spread boxes at a spacing of 10 m for all bridge configurations.

4.3 Truck Loading Conditions of Composite Multiple Box-Girder Bridges

For live loading conditions, the Canadian Highway Bridge Design Code specifies a truck with a gross weight of 625 kN (CL-625). According to CHBDC, the truck were applied to the two-equal-span continuous straight girder bridges to determine which case would produce the maximum moment near the mid-span and at the pier location and the maximum shear force at the support for bridges with span lengths of 20, 40, 60, 80 and 100 m. The design of the bridge is characterized by three limit states, namely: the Serviceability Limit State (SLS), the Ultimate Limit State (ULS), and the Fatigue Limit State (FLS). As such, truck loading conditions considered herein include loading cases for each of the three limit states of design. Since, bridge configurations considered in this study include two-to five-lane bridges which reflect two to five design lanes, different loading cases were considered to calculate bending moment and shear distribution factors. Figures 4.4 to 4.11 Schematically indicate all possible live load cases considered for the bending moment and shear at both exterior and interior girders. The following loading cases were considered:

- (1) Exterior girder-partial load with CHBDC truck loading
- (2) Exterior girder-full load with CHBDC truck loading
- (3) Middle girders-partial load with CHBDC truck loading
- (4) Middle girders-full load with CHBDC truck loading
- (5) Exterior girder-fatigue load with CHBDC truck loading
- (6) Middle girders-fatigue load with CHBDC truck loading

In case of loading conditions for fatigue limit state design CHBDC specifies only one truck travelling at the center of the travelling lane.

In order to determine the maximum strain actions investigated in this study, truck loading cases as shown in figures 4.1 through 4.11 were applied to each bridge in the transverse direction using the finite-element analysis. In the partial loading case, the wheel loads close to the curbs were positioned at a distance of 0.6 m from the curb edge and the external lane was loaded to produce the maximum stress and shear effects. The modification factors

applied directly while instructing SAP2000 software to consider each load case these factors are 0.9, 0.8, 0.7, and 0.6 for two, three, four and five lanes, respectively.

4.4 Parametric Study for Load Distribution Factors

To calculate the load distribution factors for the studied bridges, an extensive parametric study was carried out. The parametric study was conducted on two-equal-span continuous straight concrete deck on multiple steel box-girder bridges to achieve all the objectives outlined in Section 4.1. Key parameters investigated in this parametric study were also mentioned in the previous section.

There are several assumptions considered in this parametric as follows:

- 1- The reinforced concrete slab deck had full composite interaction with the steel girder. No slip between the concrete and steel surfaces was introduced in the finite-element models.
- 2- The materials properties for steel and concrete used in the analyses were assumed to be elastic and homogenous. Thus, the effect of plastic deformation or buckling has not been investigated or captured in the finite-element analyses.
- 3- The bridges were simply-supported at the bridge ends, similar to semi-integral abutment bridge type. No integral abutment bridge types were simulated.
- 4- Solid end-diaphragms were used in the transverse direction and their material and thickness were taken to be the same as those of the webs.

4.4.1 Load Distribution Factors for Longitudinal Bending Moment

To calculate the longitudinal positive and negative stress load distribution factors, F_m^{+ve} and F_m^{-ve} , respectively, the maximum tensile and compressive stresses obtained for the exterior and interior girders from the finite-element analysis, $(\sigma)_{FEA}$, were divided by the maximum stresses obtain from simple two span beam or idealize girder, $(\sigma)_{beam}$.

The idealized girder was formulated by partitioning the two-span-continuous composite multiple box-girder cross-section of the bridge to a number of individual continuous girders as shown in Figure 4.12. Each girder represents one box and is loaded by the truck load. The span lengths for the idealized girder are exactly the corresponding span lengths of the

bridges. The longitudinal Positive and negative moment in idealized girders near the mid-span and at the pier location of the bottom of the girders $(\sigma^+)_{beam}$ and $(\sigma^-)_{beam}$, respectively were determined. Then, the maximum positive and negative stresses at the simple two span beam can be obtained from the following formulas:

$$(\sigma^+)_{beam} = \frac{M^+ Y_t}{I} \quad (4.1)$$

$$(\sigma^-)_{beam} = \frac{M^- Y_b}{I} \quad (4.2)$$

Where:

- M^+ = the maximum positive moment near the mid-span for a straight continuous box-girder due to CHBDC truck loading
- M^- = the maximum negative moment at the interior support for a straight continuous box girder due to CHBDC truck loading
- Y_t = the distance from the neutral axis to the top flange
- Y_b = the distance from the neutral axis to the bottom flange
- I = the moment of inertia of the box girder

The maximum positive stress, $(\sigma^+)_{FEA}$ was obtained from the three-dimensional finite-element models using the finite-element analysis. The maximum positive stresses obtained at the bottom flange of the girder near the mid-span for the partially loaded lanes, fully loaded lanes and fatigue loading conditions as shown in Figures 4.4. Reduction factors according to CHBDC were implemented in the finite-element models to account for the number of loaded lanes. Consequently, the distribution factor for positive stress for each bridge model, $(F_m)^{+ve}$ was calculated in accordance with CHBDC as follows:

$$F_m^{+ve} = \frac{R'_L \sigma_{FEA}^+}{R_L \left(\frac{\sigma_{beam}^+ n}{N} \right)} \quad (4.3)$$

In a same manner, the maximum negative stress, $(\sigma^-)_{FEA}$ at the bottom flange of the girder at the interior support was obtained by using the finite-element analysis. The distribution factor for negative stress, $(F_m)^{-ve}$ in the bridges was determined as:

$$F_m^{-ve} = \frac{R'_L \sigma_{FEA}^-}{R_L \left(\frac{\sigma_{beam}^- n}{N} \right)} \quad (4.4)$$

Where

N = number of boxes

n = number of design lanes, Table 4.3

R_L = modification factor for multi-design lanes based on the number of the design lanes, in accordance with CHBDC, Table 4.2

R'_L = modification factor for multilane loading based on the number of the loaded lanes, Table 4.2

4.4.2 Load Distribution Factor for Vertical Shear

In order to determine the shear distribution factor, F_v , for internal and external supports of two-equal-span bridges, the maximum shear force obtained from the finite-element analysis, $(V)_{FEA}$, was divided by the maximum shear force obtained from two span beam analysis (V)_{beam}.

It must be noted that the maximum shear forces of the bridges were obtained by considering the absolute maximum values, regardless of the loading case or the location of the shear force in the box girders. The distribution factor for vertical shear in bridges was calculated according to CHBDC as follows:

$$(F_v)_{inner} = \frac{R'_L (V_{FEA})_{pier}}{R_L \left(\frac{(V_{beam})_{pier} n}{N} \right)} \quad (4.5)$$

$$(F_v)_{outer} = \frac{R'_L (V_{FEA})_{end}}{R_L \left(\frac{(V_{beam})_{end} n}{N} \right)} \quad (4.6)$$

Where:

$(F_V)_{\text{internal}}$ = load distribution factor for vertical shear at internal support of two-equal-span bridge

$(F_V)_{\text{external}}$ = load distribution factor for vertical shear at external support of two-equal-span bridge

$(V_{\text{FEA}})_{\text{pier}}$ = vertical shear at internal support from finite-element analysis

$(V_{\text{FEA}})_{\text{end}}$ = vertical shear at external support from finite-element analysis

$(V_{\text{beam}})_{\text{pier}}$ = vertical shear at internal support from two span beam

$(V_{\text{beam}})_{\text{end}}$ = vertical shear at external support from two span beam n , N , R_L and R'_L are as defined before.

Similarly, the fatigue load distribution factors for stresses and shear forces are evaluated using the equations 4.3 to 4.5, by considering the truck location for the Fatigue Limit State loading case.

Chapter 5

RESULTS FROM THE PARAMETRIC STUDY

5.1 General

In this chapter the results from the parametric study are presented. Three dimensional finite–element models are used in the analyses, in which 55 two-span composite multiple box-girder bridges are investigated. Several loading conditions are considered to evaluate the results for the maximum structural responses of such bridges. The results from the parametric study are based on CHBDC truck loading conditions. Based on the data generated from the parametric study, the following load distribution factors are obtained: (i) the distribution factor for tensile stress at the positive moment region, (ii) the distribution factor for compressive stress at the negative moment region, (iii) the distribution factor for shear forces at supports. The effects of bridge span length, number of lanes and number of boxes on the structural responses of the bridges are discussed.

A sensitivity study was conducted to determine the different factors that may influence the load distribution factors. In terms of bracing effect, pervious work (Nour, 2000; Androus, 2003) showed that having internal bracings improved the ability of the cross-section to transfer loads from one girder to an adjacent one. However, the addition of external bracing didn't have a significant effect on the stress distribution. Also, pervious work by Sennah (1998) revealed that changing the type of cross-bracing system didn't have a significant effect on stress distribution. Such work showed that replacing the steel angle cross-section of bracing members by rectangular one, or changing the bracing cross-sectional area has no effect on moment distribution. In the case of straight reinforced and prestressed concrete multi-cell bridges, Nutt et al. (1988) and Sennah (1998) conducted sensitivity study that revealed that changing either the concrete slab thickness or the bottom flange thickness has an insignificant effect on the moment distribution. The sensitivity study also revealed that changing the span-to-depth ratio of steel boxes within the practical range of 20 to 30 found by Heins (1978) has also an insignificant effect on the stress distribution. It was also found (Samaan, 2004; Hassan, 2005; Nour, 2000) that the most crucial parameters that affect the

load distribution factors are the number of lanes, number of boxes and span length. Based on such findings, it was decided to consider the number of lanes, number of boxes and span lengths in this parametric study. Also, the parametric study was conducted using internal and external bracing in accordance with the minimum spacing required by CHBDC for all bridges, with X-type bracing having a 150x150 mm cross-section and using span-to-depth ratio of 25 for the steel boxes.

5.2 Positive Moment Distribution Factors at Ultimate Limit State (Fm+)

5.2.1 Effect of Span Length

Figure 5.1 shows the distribution factors for maximum positive moment in three-lane, two-box girder and three-lane, three-box girder bridges due to CHBDC truck loading at ULS. It can be observed that the moment distribution factor for straight bridges decrease from 1.60 to 1.30 with increasing span length from 20 m to 40 m (a decrease of 23%). However, it decreases from 1.30 to 1.10 when span length increases from 40 to 60 m (a decrease of 18%). For span length more than 60 m, the moment distribution factor decreases by less than 3%. It can be observed that the change in number of boxes from 2 to 3 has insignificant effect on the positive moment distribution factors.

5.2.2 Effect of Number of Lanes

In Figure 5.2, the effect of number of lanes on the positive moment distribution factors at ULS is presented. The distribution factors for maximum positive moment for bridges with three boxes and span lengths 40, 60, 80 and 100 m, subjected to CHBDC truck loading, is illustrated. It can be observed that the moment distribution factors for straight bridges is almost uniform with increasing number of lanes from 2 to 3 and it increases linearly with increase the number of lanes from 3 to 5 lanes. For example, for bridge with span length of 40 m, it can observed that the moment distribution factor increases slightly from 1.28 to 1.3 (an increase of 2%) when the number for lane changes from 2 to 3. However, when the number of lanes changed from 3 to 5, the moment distribution factor increases linearly from 1.3 to 1.59 (an increase of 22%).

5.2.3 Effect of Number of Boxes

Figure 5.3 shows the change in the maximum positive moment distribution factors for three-lane bridges with span lengths 40, 60, 80 and 100 m, with change in number of boxes. It can be observed that the positive moment distribution factors at ultimate limit state are almost uniform irrespective of the number of boxes for bridges. For example, the positive moment distribution factor for 40-m span bridge remains almost 1.30 with slight change with increase in number of boxes from 2 to 4.

5.3 Positive Moment Distribution Factors at Fatigue Limit State (F_{m+})

5.3.1 Effect of span length

The effect of span length on positive moment distribution factors at fatigue limit state is presented in Figure 5.4. The graph shows that the distribution factors for positive moment in three-lane, two-box, girder and three-lane, three-box, girder bridges as affected by the change in span length from 20 to 100 m. It can be observed that the fatigue positive moment distribution factor significantly decreases with increasing the span length from 20 m to 40. This rate decreases with increase in bridge span. For example, in case of 3L-2b bridge, the moment distribution factor changes from 3.55 in case of 20 m span length to 2.18 in case 40 m span length (a decrease of 38%). However, it changes from 2.18 to 1.67 with increase of span length from 40 to 60 m (a decrease of 23%). When span length changes from 60 to 100 m, the moment distribution factor decreases from 1.67 to 1.45 (a decrease of 13%).

5.3.2 Effect of Number of Lanes

To examine the effect of number of lanes, positive moment distribution factors for fatigue limit state for selected bridges are obtained from the parametric study and plotted in Figure 5.5. For three-box girder bridges and span lengths of 40, 60, 80, and 100 m, the distribution factors for positive moment are plotted against the change in number of lanes from 2 to 5. For a bridge with span length of 40 m, it can be observed that the positive moment distribution factor increases almost linearly from 1.8 to 3.35 with increase in number of lanes from 2 to 5 (a increase of 86%). Similar observations were made for bridges with span lengths of 60, 80

and 100 m. It is also interesting to note that the rate of increase in the positive moment distribution factors decreases with increasing the span length.

5.3.3 Effect of Number of Boxes

Figure 5.6 depicts the change in the position moment distribution factor for FLS design for span length of 40, 60, 80 and 100 m, as affected by the change in number of boxes. It is clear that the positive moment distribution factor slightly changes with increase in number of boxes from 2 to 4. For example, it can be observed that the positive moment distribution factor changes from 1.65 to 1.95 (an increase of 18%) when increase in number of boxes from 2 to 4 for bridges with span length of 60 m. It can be seen that the number of boxes slight effect on the moment distribution factors for fatigue state for bridges considered in this study.

5.4 Negative Moment Distribution Factors at Ultimate Limit State (Fm-)

5.4.1 Effect of Span Length

The changes in the load distribution factors for maximum negative moment are obtained from the detailed three-dimensional finite-element models. The results for the three-lane, two-box, girder and three-lane, three-box, girder bridges are compared in Figure 5.7. It can be observed that the negative moment distribution factors significantly decrease linearly with increase in span length from 20 to 60 m and remain almost unchanged with increase in span length from 60 to 100 m. For example, in 3L-2b bridges, the negative moment distribution factor decreases lineally from 3.25 to 2.16 with increase in span length from 20 to 60 m, while it remains around 2.16 with increase in span length from 60 to 100 m.

5.4.2 Effect of Number of Lanes

In Figure 5.8, the distribution factors for maximum negative moment at ULS in three-box girder bridges with span lengths of 40, 60, 80 and 100 m are presented. It can be observed that the moment distribution factor for 100-m span bridges decreases from 2.50 to 2.30 with increase in number of lanes from 2 to 3 (a decrease of 8%). On the contrary, it increases linearly from 2.30 to 3.25 with increase in number of lanes from 3 to 5 (an increase of 70%). Similar trend was observed for bridges of spans 40, 60 and 80 m. As such, the effect of

number of lanes on negative moment distribution factors is shown to be more significant when the number of lanes changing between 3 and 5.

5.4.3 Effect of Number of Boxes

Figure 5.9 shows the distribution factors for the maximum negative moment for three lanes and span lengths of 40, 60, 80 and 100 m due to CHBDC live load. In the figure, it can be observed that the moment distribution factor for straight bridges is almost uniform with increasing the number of boxes from 2 to 4. This means that the number of boxes girder has slightly effect on the negative moment distribution factor. For example, for two-equal span bridge with a span length of 60 m, the negative moment distribution factors change from 2.16 to 2.25 (less than 5%) by increasing the number of boxes from 2 to 4.

5.5 Negative Moment Distribution Factors at Fatigue Limit State

5.5.1 Effect of Span Length

The results for the change in the negative moment distribution factors at FLS for three-lane, two-box, girder bridges and three-lane, three-box, girder bridges are presented in Figure 5.10. It is clear that the distribution factors for fatigue limit state design significantly decrease with increase in span length from 20 to 60 m. However, insignificant increase is observed with increase in span length from 60 to 100 m. For example, for 3L-2b bridges, the negative moment distribution factor changes from 6.55 in case of 20-m span length to 2.9 in case 60-m span length (a decrease of 55%). While it remains almost 2.9 for bridges with span lengths ranging from 60 to 100 m.

5.5.2 Effect of Number of Lanes

Figure 5.11 depicts the change of the negative moment distribution factors for fatigue limit state design with change in number of lanes for three-box girder bridges of 40, 60, 80 and 100 m span lengths. It can be observed that the distribution factors increase when changing the number of lanes from 2 to 5. It is clear that the load distribution factors decrease by increasing the bridge span length. For example, the negative moment distribution factors for three lanes bridges decrease from 4.2 to 3.5 (about 17%) when the span lengths change from

40 to 100 m. The change rate of the load distribution factors generally increase by increasing the number of lanes for all span lengths considered in herein.

5.5.3 Effect of Number of Boxes

The distribution factors for negative moment for FLS design for three-lane bridges of span lengths of 40, 60, 80 and 100 m are depicted in Figure 5.12 for number of boxes ranging from 2 to 4. It can be observed that the moment distribution factor increases with increase in number of boxes. For examples, the 80-m span bridge has a negative moment distribution factor increasing from 1.55 to 1.7 (about 9%) with increase in number of boxes from 2 to 4. It is also interesting to note that the increase is almost the same for all span lengths.

5.6 Shear Distribution Factors for Ultimate Limit State

5.6.1 Effect of Span Length

The parametric study was conducted to determine the maximum vertical shear force in each web at the support lines under different truck loading conditions at ULS, from which the shear distribution factor is obtained. Figure 5.13 presents the shear distribution factors obtained for three-lane, two-box, girder and three-lane, three-box, girder bridges. The figure shows that the distribution factors for shear are slightly increasing with increase in span length from 20 to 100 m. This means that the bridge span length has insignificant effect on the shear distribution factors at ULS design. For example, the shear distribution factor for a 3L-3b bridge increases from 1.33 to 1.35 (an increase of 2%) with increase in span length from 20 to 40 m.

5.6.2 Effect of Number of Lanes

Figure 5.14 presents the load distribution factors for maximum vertical shear force evaluated for bridges having three-box girders and span lengths of 40, 60, 80 and 100 m, with the change in number of design lanes. It can be observed that the highest distribution factor for shear force occurs for two-lane bridges. These factors decrease with increasing the number of lanes from to 3. However, the distribution factors significantly increase with increase in number of lanes from 3 to 5. For example, the shear distribution factor for a 40-m span

bridge at ULS decreases from 1.68 to 1.35 (a decrease of 20%) with increase the number of lanes from 2 to 3. With increase the number of lanes from 3 to 5, the value changes from 1.35 to 1.60 (an increase of 19%). As it is considered later in this chapter, given the uneven trend in effect of number of lanes in shear distribution factor, it would be beneficial from the accuracy and best-fit point of view to deduce empirical expressions for shear distribution factors for each number of design lanes rather than considering number of lanes as a variable in the developed equations.

5.6.3 Effect Number of Boxes

In the parametric study, number of boxes reflects to the number of webs present in the bridge cross-section. Webs are the main members in resisting the shear forces in the bridge superstructure. Therefore, increasing the number of boxes affects the distribution factors for shear force. Figure 5.15 shows the distribution factors for shear with the change in number of boxes for bridges with different span lengths. It can be observed that the distribution factors increase with increase in number of boxes. For example, the shear distribution factor at ULS for a 100-m span bridge increases slightly from 1.3 to 1.38 (an increase of 6%) when the number of box increases from 2 to 3 and it continues increasing but with greater rate from 1.38 to 1.73 (an increase of 25%) with increase in number of boxes from 3 to 4. It is also interesting to note that the trend for all bridge spans is similar.

5.7 Vertical Shear Distribution Factors for Fatigue Limit State

5.7.1 Effect of Span Length

Figure 5.16 depicts the distribution factors for fatigue limit state design for vertical shear for three-lane bridges with different number of boxes and span lengths. It can be observed that the distribution factors are almost the same with increase in span length. On the other hand, the load distribution factors increase with increase in number of boxes from 2 to 3.

5.7.2 Effect of Number of Lanes

Figure 5.17 shows the change in the vertical shear distribution factors for bridges having different span lengths and number of design lanes. The graphs show slight changes in vertical

shear distribution factors with increase in number of lanes. For example, the factors increase from 2.3 to 2.55 with increase in the number of lanes from 2 to 3 (an increase 10%) and it increases linearly from 2.55 to 2.8 with increase in number of lanes from 3 to 5 (an increase of 9%). However, it is interesting to observe that the distribution factors for fatigue limit vertical shear are almost constant with increase in span lengths from 40 to 100 m as mentioned before in section 5.7.1.

5.7.3 Effect of Number of Boxes

The distribution factors for fatigue limit state design for vertical shear as a function of number of boxes are presented in Fig. 5.18. It can be observed that the shear distribution factor increases linearly with the increase in number of boxes as observed earlier. For example, the shear distribution factor changes from 1.8 in case of two-box cross-section to 3.2 in case of four-box cross-section (an increase of 77%). Similar behavior is observed in similar cases shown in the Appendix.

5.8 Correlation between the Load Distribution Factors Obtained from the FEA and CHBDC Equation

The following subsection presents correlation between the load distributions factors obtained from the finite-element modeling as those available in CHBDC to examine the level of underestimation of conservatism implied in the design of such bridges when using CHBDC load distribution factor expressions.

5.8.1 Comparison at the Ultimate Limit State Design

Since the CHBDC simplified method of analysis provides one expression for both shear and bending moment distribution factors at ULS and FLS as shown in Chapter 2, it is interesting to investigate the correlation between both factors calculated from the FEA and CHBDC Equations. Figures 5.19 and 5.20 present the comparison between the distribution factors for positive moment and negative moment, respectively, for two-equal-span bridges as obtained from the FEA and CHBDC. It should be noted that the results of positive moment distribution factor (F_m^+) obtained from CHBDC simplified method of analysis underestimates the structural response in most bridges considered in this study, with a difference up to 53%.

In addition, the negative moment distribution factor (F_m^-) obtained from CHBDC is always less than that obtained from FEA analysis as depicted in Fig. 5.20.

Figures 5.21 and 5.22 depict similar graphs for the shear force distribution factors at internal and external supports for two-equal-span straight bridges, respectively, obtained from the FEA and CHBDC. In contrast to moment distribution factors, CHBDC values for shear distribution at ULS correspond very well.

5.8.2 Fatigue Limit State Design

Figures 5.23 and 5.24 illustrate the comparison between the positive moment and negative moment distribution factors for two-equal-span bridges, respectively, as obtained from the FEA and CHBDC. It can be observed that for CHBDC positive may underestimate the moment distribution factor for FLS for most of the bridges considered in this study. In addition, the negative moment distribution factor obtained from CHBDC is always less than that obtained from FEA analysis as depicted in Fig. 5.24. For example, the positive and negative distribution factors for 3L-40-2b bridge, are 1.75 and 2.08, respectively, as obtained from CHBDC expressions given in Chapter 2, while the corresponding values as obtained from finite element analysis are 2.19 and 3.96, respectively (an underestimation of 25.14% and 90.38%, respectively).

Figures 5.25 and 5.26 present comparison between CHBDC and FEA results for the shear force distribution factors at the internal and external supports for two-equal-span bridges, respectively. The results calculated using CHBDC simplified method of analysis are conservative when compared to actual distribution factors calculated based on the finite-element analysis.

5.9 Correlation between the load Distribution Factors from the FEA and AASHTO-LRFD Equation

5.9.1 Ultimate Limit State Design

Figures 5.27 and 5.28 present the correlation between CHBDC and FEA results for the distribution factors for positive moment and negative moment for two-equal-span,

respectively. It can be observed that the AASHTO-LRFD values for positive moment distribution factors are significantly higher than those obtained from FEA analysis. On the other hand, AASHTO-LRFD values for the negative moment distribution factors are generally greater than those obtained from FEA analysis. This indicates that AASHTO-LRFD equation overestimates the structural response for the positive moment distribution factors and underestimate the response for the negative moment distribution factors. For example, the positive and negative moment distribution factors for 3L-40-3b bridge are 1.79, 2.08, respectively, as obtained from AASHTO-LRFD expression given in Chapter 2. The corresponding values as obtained from the finite-element analysis are 1.30 and 2.54, respectively (an overestimation of 38% and underestimation 22%, respectively).

The distribution factors for shear forces at ULS obtained from the FEA analysis and AASHTO-LRFD equation at the internal and external are shown in Figures 5.29 and 5.30, respectively. In both cases the AASHTO-LRFD values seem slightly conservative for some bridge geometries and highly conservative in others. For example, the internal and external shear distribution factors for 3L-40-3b bridge, are 2.08 and 1.75 as obtained from AASHTO expressions presented in Chapter 2. The corresponding values as obtained from finite-element analysis are 1.35 and 1.26, respectively (an overestimation of 35% and 39%, respectively).

5.9.2 Fatigue Limit State Design

Distribution factors for positive and negative moments are presented in Figures 5.31 and 5.32, respectively. The figures correlate values obtained based on the AASHTO-LRFD simplified method and those calculated from the finite-element analysis at FLS. It is clear the AASHTO-LRFD distribution factors for positive moment have no trend since AASHTO-LRFD equation underestimates the responses for some bridges and overestimates them in others. In case of negative moment distribution factors, AASHTO unconservatively predicts the responses of most bridge considered in this study. On the other hand, the distribution factors for shear forces at FLS obtained from the FEA analysis and AASHTO-LRFD equation at the internal and external supports are shown in Figures 5.33 and 5.34, respectively. In both cases, the AASHTO-LRFD values seem unconservative in most cases

of bridge when compared with those obtained from the FEA. For instance, the internal and external shear distribution factors in case of 3L-40-4b Bridge are 1.66 as obtained from AASHTO-LRFD expressions, while the corresponding values as evaluated based on the finite-element analysis are 3.18 and 2.82, respectively (a underestimation of 91.56% and 69.87% respectively).

5.10. Empirical Equations for the Load Distribution Factors

Based on the results obtained from the parametric study on 55 bridge configurations, empirical expressions were developed for the distribution factors for positive moment (F_{m+}), negative moment (F_{m-}), shear forces at the internal and external supports for two-equal-span continuous composite box-girder bridges for ultimate and fatigue limit states designs. The developed empirical formulas for vehicular load include the following parameters:

- 1- span length of the bridge (L)
- 2- number of box (N)
- 3- number of lanes (n)

Using a statistical computer package for best fit based on the method of least squares, the empirical formulas for distribution factors are developed with minimum error. It should be noted that the highest values for a specific girder from all the loading cases are considered in this the creation of the empirical equations.

The following expressions were derived in the same format, as those originally exist in CHBDC for multiple box girders.

- 1- For positive and negative moment distribution factors in the bottom flange along bridge span due to CHBDC live loading for Ultimate and Fatigue Limit States design:

$$F_m = \frac{SN}{F(1 + \frac{\mu C_f}{100})} \quad (5.1)$$

Where,

F_m = the moment distribution factor

S = the girder spacing

N = the number of box girders

F = a width dimension factor that characterizes load distribution for a bridge

C_f = a correction factor

$$\mu = \frac{w_e - 3.3}{0.6} \leq 1.0 \quad (5.2)$$

Where,

W_e = the width of a design lane, calculate with CHBDC clause 3.8.2.

It should be noted that the values of F and C_f in CHBDC equations are a linear function of β in case of ultimate and fatigue limit state designs for longitudinal moments. However, the value of F in CHBDC expressions to obtain the longitudinal shear at ultimate and fatigue limit state design is a constant irrespective of the value of β , number of boxes and bridge span. Based on the data generated from the parametric study, it was observed that the number of boxes, number of design lanes and span length have an effect on the response and they should be includes in the developed expressions. As such, it was decided to use F and C_f as follows to develop more reliable expressions for structural design.

$$F = (a + b\beta) N^c$$

$$C_f = C + d\beta$$

Where: a , b , c , d and e = are new constants in the proposed empirical equation.

Typical samples of the results from the finite-element analysis, parameters of empirical equations and variance between FEA and empirical equations are given more details in (Appendix A.1 to Appendix A.8).

In this study, new empirical expressions were developed for the positive and negative moment distribution factors for ULS and FLS. Data generated from the parametric study was used to develop the new parameters F , C_f and there constants a , b , c and e . Tables 5.1 and 5.2 present the developed parameters of the empirical equations of positive and negative moment distribution factors at ULS, respectively. While Tables 5.3 and 5.4 present the developed parameters of the empirical equations for positive and negative moment distribution factors at FLS, respectively. These parameters were developed to be in a similar format to that used in CHDDBC simplified method of analysis. These equations were developed with a condition that the resulting values underestimates the response by a maximum 5% to provide

confidence on the developed equations for the practice engineers (see Appendices A.1 to A.8 for more details).

The correlation between the developed formulas for positive moment and negative moment distribution factors and the values obtained from the finite-element analysis for the ultimate limit state design are shown in Figs. 5.35 through 5.42. While Figs. 5.43 through 5.50 depict the correlation for the same distribution factors at the Fatigue Limit State. It is obvious that all graphs show very good correlation between the estimated results from the developed formulas and calculated results from the finite-element analyses.

2- For the developed shear distribution factor equation, the following equation was proposed

$$F_v = \frac{SN}{F} \quad (5.3)$$

Few sets of equations to obtain F parameter were considered in this study after careful repetition of the regression analysis of the data generated from the parametric study. The first set of the equation for F is a multiplier of a linear function of span length (L) and exponential function of the number of boxes in a bridge cross-section as follows:

$$F = (a + b L) N^c \quad (5.4)$$

Figures 5.51 through 5.58 show the correlation between the shear distribution factors (F_v) at internal and external supports obtained from the proposed empirical equation and the finite-element analysis at the Ultimate Limit State design. Tables 5.5 and 5.6 present the developed parameters of the empirical equation for shear distribution factors at ULS at inner and outer support, respectively. It can be observed that in the new parameter empirical equation the value of a is different with different number of lanes, but the value of b is a constant value with different number of lane. Figures 5.59 through 5.66 show the same distribution factors but for the Fatigue Limit State design. Tables 5.7 and 5.8 present the developed parameters of the empirical equation of the shear distribution factors at the FLS at inner and outer supports, respectively. It is noted that in Tables 5.7 and 5.8 that the equation of F doesn't depend on the bridge span length in the case of the Fatigue Limit State.

The second set of equation when F is as a function of (β) in linear equation is presented as follows:

$$F = (a + b \beta) N^c \quad (5.5)$$

Figures 5.67 through 5.74 show the correlation between the shear distribution factors (F_v) at the internal and external supports obtained from the new empirical equation, which is a function in β , and the values obtained from the FEA at the Ultimate Limit State. The Summary of developed parameters is presented in Tables 5.9 and 5.10. Figures 5.75 through 5.82 present correlation between the values obtained from the developed equation and those obtained from the FEA analysis. Good agreement is observed. It should be noted that the developed parameters used in the imperial equation are listed in Tables 5.11 and 5.12.

The third set of equations when F is as a function of (β) in polynomial equation is considered as follows:

$$F = (a + b \beta + c \beta^2) N^c \quad (5.6)$$

Figures 5.83 through 5.90 show the correlation between the shear force distribution factors (F_v) at the internal and external supports obtained from the new empirical equation, which is function of β in polynomial equation, and the finite-element analysis at the Ultimate Limit State. The Summary of developed parameters is presented in Tables 5.13 and 5.14. Figures 5.91 through 5.98 show good correlation between the values obtained from the developed expressions and the FEA results. It is obvious that the results obtained based on the empirical equations developed for distribution factors for shear forces are very close to those obtained from the finite-element analyses.

Chapter 6

SUMMARY AND CONCLUSIONS

6.1 Summary

An extensive theoretical investigation was conducted to determine the effect of several variables on the moment and shear force distributions among box girders in two-equal-span continuous straight composite concrete deck-on multiple steel box-girder bridges due to the passage of CHBDC truck loading for both Ultimate and Fatigue Limit State designs. A detailed literature review was carried out to set up the basis for this research work. The results of the literature review indicated lack of expressions to describe the load distribution factors for such bridges. Different truck loading conditions were considered in this study to determine the maximum response from which empirical expressions for load distribution factors can be deduced. The influences of the key parameters, namely: span length (L), number of lane (n), and number of box (N), were investigated. Results obtained from the FEA analysis of 55 bridge prototypes were used to deduce empirical expressions for moment and shear distribution factors for such bridges.

6.2 Conclusions

Calculation of accurate distribution factors for design live loads is very important to bridge design. The design values need to be close to actual values to allow engineers to design bridges to be safe and as economical as possible.

Based on the theoretical investigations carried out on continuous straight concrete deck-on multiple steel box-girder bridges, the following conclusions can be drawn:

- 1- The bridge span length, number of boxes and number of design lanes play a significant effect on the value of the load distribution factors of such bridges.
- 2- The moment distribution factors of these bridges decrease with increasing span length and increases linearly with increasing number of lanes. On the other hand, the moment distribution factors remain almost uniform with increasing the number of boxes.

- 3- Shear distribution factor is almost uniform with increasing span length and decrease with increase in number of lanes from 2 to 3. However, this trend changes by increasing the number of lanes from 3 to 5. On the other hand, the shear distribution factor increased with increased number of boxes.
- 4- In case of ultimate limit state design, the CHBDC simplified method of analysis seems to be conservative for shear distribution factors when compared to data generated from the finite-element analysis. On the other hand, the CHBDC simplified method underestimates the moment distribution factors by up to 150% when compared to those obtained from the finite-element analysis.
- 5- The CHBDC values are the most conservative (i.e. highest overestimation) for all distribution factors in case of fatigue limit state with a range up to 80% difference compared with the values calculated based on the finite-element analysis.
- 6- Generally, the AASHTO-LRFD load distribution factors for ULS and FLS overestimate the structural response of bridges up to 80%. Few cases were observed to underestimate the structural response with a difference up to 80% when compared to the FEA results.
- 7- Based on the data generated from the parametric study on two-span-length straight bridges, empirical expressions for the moment and shear distribution factors were developed. Correlations with FEA results show that the proposed expressions are more accurate and reliable than the available simplified method specified in the CHBDC simplified method of analysis.

6.3 Recommendations for Future Research

It is recommended that further research efforts be directed to address the following:

- 1- Study the effect of material and geometric nonlinearity on the load distribution factors of such bridges.
- 2- Investigate the effect of skewness of bridge superstructure on the load distribution of such bridges.
- 3- Extension of the developed load distribution factors to integral abutment bridges.

Table 2.1 Expression for F and C_f for longitudinal moments in multi-box bridges as determined by CHBDC 2006

Limit state	Number of design lanes	F, m	$C_f, \%$
ULS or SLS	2	$8.5 - 0.3 \beta$	$16 - 2\beta$
	3	$11.5 - 0.5 \beta$	$16 - 2\beta$
	4	$14.5 - 0.7 \beta$	$16 - 2\beta$
FLS	2 or more	$8.5 - 0.9 \beta$	$16 - 2\beta$

Table 2.2 Expression for F for longitudinal vertical shear in multi-box bridges as determined by CHBDC 2006

Limit state	Number of design lanes	F, m
ULS or SLS	2	7.20
	3	9.60
	4	11.20
FLS	2 or more	4.25

Table 4.1 Modification factors for multilane loading as determined by CHBDC 2006

Number of loaded design lanes	Modification factor (R_L)
1	1.00
2	0.90
3	0.80
4	0.70
5	0.60
6 or more	0.55

Table 4.2 Comparison between truck load and lane load in the calculation of the load distribution factors

Bridge type	Track cases	LDF	CL-625-ONT Truck Load	CL-625-ONT Lane Load
2L-80-2b	Partial Load	F_m^{+ve}	0.79	0.74
		F_m^{-ve}	1.27	1.05
		$(F_v)_{inner}$	0.98	0.90
		$(F_v)_{outer}$	0.92	0.83
	Full Load	F_m^{+ve}	1.18	1.15
		F_m^{-ve}	1.80	1.56
		$(F_v)_{inner}$	1.26	1.18
		$(F_v)_{outer}$	1.20	1.14

Table 4.3 Number of design lanes as determined by CHBDC 2006

W_c	n
6.0 m or less	1
Over 6.0 m to 10.0 m incl.	2
Over 10.0 m to 13.5 m incl.	2 or 3
Over 13.5 m to 17.0 m incl.	4
Over 17.0 m to 20.5 m incl.	5
Over 20.5 m to 24.0 m incl.	6
Over 24.0 m to 27.5 m incl.	7
Over 27.5 m	8

Table 4.4 Geometries of bridges used in parametric study for load distribution factor

Bridge type	Number of lanes (n)	Span Length (L)	Number of Boxes (N)	Cross Section Dimensions (m)				
				Bridge Width (B)	Deck width (W_c)	Width of Design Lane (W_e)	width (B_1)	Depth of Box (D)
2L-20-2b	2 Lane	20	2	10.00	9.00	4.50	2.50	0.80
2L-20-3b		20	3	10.00	9.00	4.50	1.67	0.80
2L-40-2b		40	2	10.00	9.00	4.50	2.50	1.60
2L-40-3b		40	3	10.00	9.00	4.50	1.67	1.60
2L-60-2b		60	2	10.00	9.00	4.50	2.50	2.40
2L-60-3b		60	3	10.00	9.00	4.50	1.67	2.40
2L-80-2b		80	2	10.00	9.00	4.50	2.50	3.20
2L-80-3b		80	3	10.00	9.00	4.50	1.67	3.20
2L-100-2b		100	2	10.00	9.00	4.50	2.50	4.00
2L-100-3b		100	3	10.00	9.00	4.50	1.67	4.00
3L-20-2b	3 Lane	20	2	13.50	12.50	4.17	3.38	0.80
3L-20-3b		20	3	13.50	12.50	4.17	2.25	0.80
3L-20-4b		20	4	13.50	12.50	4.17	1.69	0.80
3L-40-2b		40	2	13.50	12.50	4.17	3.38	1.60
3L-40-3b		40	3	13.50	12.50	4.17	2.25	1.60
3L-40-4b		40	4	13.50	12.50	4.17	1.69	1.60
3L-60-2b		60	2	13.50	12.50	4.17	3.38	2.40
3L-60-3b		60	3	13.50	12.50	4.17	2.25	2.40
3L-60-4b		60	4	13.50	12.50	4.17	1.69	2.40
3L-80-2b		80	2	13.50	12.50	4.17	3.38	3.20
3L-80-3b		80	3	13.50	12.50	4.17	2.25	3.20
3L-80-4b		80	4	13.50	12.50	4.17	1.69	3.20
3L-100-2b		100	2	13.50	12.50	4.17	3.38	4.00
3L-100-3b		100	3	13.50	12.50	4.17	2.25	4.00
3L-100-4b	100	4	13.50	12.50	4.17	1.69	4.00	
4L-20-3b	4 Lane	20	3	17.00	16.00	4.00	2.83	0.80
4L-20-4b		20	4	17.00	16.00	4.00	2.13	0.80
4L-20-5b		20	5	17.00	16.00	4.00	1.70	0.80
4L-40-3b		40	3	17.00	16.00	4.00	2.83	1.60
4L-40-4b		40	4	17.00	16.00	4.00	2.13	1.60
4L-40-5b		40	5	17.00	16.00	4.00	1.70	1.60
4L-60-3b		60	3	17.00	16.00	4.00	2.83	2.40
4L-60-4b		60	4	17.00	16.00	4.00	2.13	2.40
4L-60-5b		60	5	17.00	16.00	4.00	1.70	2.40
4L-80-3b		80	3	17.00	16.00	4.00	2.83	3.20
4L-80-4b		80	4	17.00	16.00	4.00	2.13	3.20
4L-80-5b		80	5	17.00	16.00	4.00	1.70	3.20
4L-100-3b		100	3	17.00	16.00	4.00	2.83	4.00
4L-100-4b		100	4	17.00	16.00	4.00	2.13	4.00
4L-100-5b	100	5	17.00	16.00	4.00	1.70	4.00	
5L-20-3b	5 Lane	20	3	20.50	19.50	3.90	3.42	0.80
5L-20-4b		20	4	20.50	19.50	3.90	2.56	0.80
5L-20-5b		20	5	20.50	19.50	3.90	2.05	0.80
5L-40-3b		40	3	20.50	19.50	3.90	3.42	1.60
5L-40-4b		40	4	20.50	19.50	3.90	2.56	1.60
5L-40-5b		40	5	20.50	19.50	3.90	2.05	1.60
5L-60-3b		60	3	20.50	19.50	3.90	3.42	2.40
5L-60-4b		60	4	20.50	19.50	3.90	2.56	2.40
5L-60-5b		60	5	20.50	19.50	3.90	2.05	2.40
5L-80-3b		80	3	20.50	19.50	3.90	3.42	3.20
5L-80-4b		80	4	20.50	19.50	3.90	2.56	3.20
5L-80-5b		80	5	20.50	19.50	3.90	2.05	3.20
5L-100-3b		100	3	20.50	19.50	3.90	3.42	4.00
5L-100-4b		100	4	20.50	19.50	3.90	2.56	4.00
5L-100-5b	100	5	20.50	19.50	3.90	2.05	4.00	

Table 5.1 Summary of parameters of empirical equation for positive moment distribution factors at ULS

Number of design lanes	Value of F	Value of C_f	Parameter (e)
2	$(7 + \beta) N^{-e}$	$15 - 27 \beta$	0.75
3	$(9.5 - 0.9\beta) N^{-e}$	$17 - 7 \beta$	0.75
4	$(13 - 0.9\beta) N^{-e}$	$1.4 - 7 \beta$	0.75
5	$(10 - 0.9\beta) N^{-e}$	$51 - 7 \beta$	0.75

Table 5.2 Summary of parameters of empirical equation for negative moment distribution factors at ULS

Number of design lanes	Value of F	Value of C_f	Parameter (e)
2	$(4.6 - 0.34 \beta) N^{-e}$	$17 - 7 \beta$	0.95
3	$(5.6 - 0.25\beta) N^{-e}$	$18 - 5 \beta$	0.95
4	$(4.4 - 0.07\beta) N^{-e}$	$14 - 2 \beta$	0.8
5	$(3.6 - 0.06 \beta) N^{-e}$	$12 - 2 \beta$	0.62

Table 5.3 Summary of parameters of empirical equation for positive moment distribution factors at FLS

Number of design lanes	Value of F	Value of C_f	Parameter (e)
2	$(7.3 - 1.92\beta) N^{-e}$	$5 - 2\beta$	0.75
3	$(9.34 - 1.18\beta) N^{-e}$	$4 - 13.15 \beta$	0.86
4	$(8.16 - 0.85\beta) N^{-e}$	$-7.5 - 10 \beta$	0.7
5	$(8.38 - 0.85\beta) N^{-e}$	$7 - 10.85 \beta$	0.77

Table 5.4 Summary of parameters of empirical equation for negative moment distribution factors at FLS

Number of design lanes	Value of F	Value of C_f	Parameter (e)
2	$(4.5 - 0.37 \beta) N^{-e}$	$6.4 - 7.77 \beta$	1.09
3	$(5.25 - 0.33\beta) N^{-e}$	$9.25 - 6.9 \beta$	1.18
4	$(4 - 0.15\beta) N^{-e}$	$6 - 3.86 \beta$	1.07
5	$(3.7 - 0.14 \beta) N^{-e}$	$5 - 3.74 \beta$	1

The First set of equation when F is a function of (L) Span length

Table 5.5 Summary of parameters of empirical equation for shear distribution factors at ULS state at inner support

Number of design lanes	Value of F	parameter (e)
2	$(14.5 - 0.01 L) N^{-e}$	1.80
3	$(15.8 - 0.01 L) N^{-e}$	1.45
4	$(18.5 - 0.01 L) N^{-e}$	1.40
5	$(13.6 - 0.01 L) N^{-e}$	1.11

Table 5.6 Summary of parameters of empirical equation for shear distribution factors at ULS state at outer support

Number of design lanes	Value of F	Parameter (e)
2	$(14.5 - 0.01 L) N^{-e}$	1.72
3	$(15.8 - 0.01 L) N^{-e}$	1.40
4	$(18.5 - 0.01 L) N^{-e}$	1.33
5	$(15 - 0.01 L) N^{-e}$	1.10

Table 5.7 Summary of parameters of empirical equation for shear distribution factors at FLS state at inner support

Number of design lanes	Value of F	Parameter (e)
2	$(9) N^{-e}$	1.67
3	$(12.6) N^{-e}$	1.8
4	$(14.7) N^{-e}$	1.78
5	$(17.23) N^{-e}$	1.8

Table 5.8 Summary of parameters of empirical equation for shear distribution factors at FLS state at outer support

Number of design lanes	Value of F	Parameter (e)
2	$(9.3) N^{-e}$	1.6
3	$(13) N^{-e}$	1.74
4	$(15.45) N^{-e}$	1.74
5	$(18) N^{-e}$	1.77

The Second set of equation when F is a function of (β)

Table 5.9 Summary of parameters of empirical equation for shear distribution factors at ULS state at inner support

Number of design lanes	Value of F	Parameter (e)
2	$(13.6 - 0.30 \beta) N^{-e}$	1.80
3	$(15 - 0.2\beta) N^{-e}$	1.45
4	$(17.4 - 0.24 \beta) N^{-e}$	1.40
5	$(17.4 - 0.24 \beta) N^{-e}$	1.12

Table 5.10 Summary of parameters of empirical equation for shear distribution factors at ULS state at outer support

Number of design lanes	Value of F	Parameter (e)
2	$(14 - 0.30 \beta) N^{-e}$	1.80
3	$(15 - 0.20 \beta) N^{-e}$	1.42
4	$(18.5 - 0.24 \beta) N^{-e}$	1.40
5	$(14 - 0.14 \beta) N^{-e}$	1.12

Table 5.11 Summary of parameters of empirical equation for shear distribution factors at FLS state at inner support

Number of design lanes	Value of F	Parameter (e)
2	$(9) N^{-e}$	1.66
3	$(12.8 - 0.27\beta) N^{-e}$	1.78
4	$(14.9 - 0.15\beta) N^{-e}$	1.77
5	$(17.45 - 0.06\beta) N^{-e}$	1.80

Table 5.12 Summary of parameters of empirical equation for shear distribution factors at FLS state at outer support

Number of design lanes	Value of F	Parameter (e)
2	$(9) N^{-e}$	1.60
3	$(13.25 - 0.14\beta) N^{-e}$	1.73
4	$(15.6 - 0.08 \beta) N^{-e}$	1.73
5	$(18.2 - 0.07\beta) N^{-e}$	1.76

The third set of equation when F is a function of (β^2)

Table 5.13 Summary of parameters of empirical equation for shear distribution factors at ULS state at inner support

Number of design lanes	Value of F	Parameter (e)
2	$(12.6 + 2\beta - 0.46\beta^2) N^e$	1.8
3	$(13.4 + 1.9\beta - 0.36\beta^2) N^e$	1.46
4	$(15 + 2.33\beta - 0.36\beta^2) N^e$	1.4
5	$(12.3 + 0.7\beta - 0.1\beta^2) N^e$	1.12

Table 5.14 Summary of parameters of empirical equation for shear distribution factors at ULS state at outer support

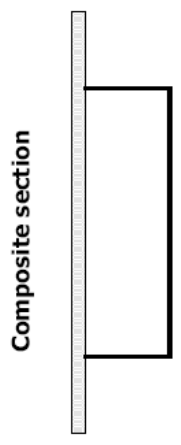
Number of design lanes	Value of F	Parameter (e)
2	$(12 + 0.86\beta - 0.01\beta^2) N^e$	1.75
3	$(13.4 + 1.18\beta - 0.13\beta^2) N^e$	1.4
4	$(15 + 1.85\beta - 0.17\beta^2) N^e$	1.4
5	$(12.8 + 0.7\beta - 0.05\beta^2) N^e$	1.12

Table 5.15 Summary of parameters of empirical equation for shear distribution factors at FLS state at inner support

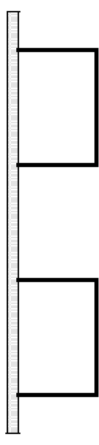
Number of design lanes	Value of F	Parameter (e)
2	$(8 + 1.18\beta - 0.36\beta^2) N^e$	1.65
3	$(11.77 + 0.84\beta - 0.22\beta^2) N^e$	1.79
4	$(13.94 + 0.7\beta - 0.15\beta^2) N^e$	1.78
5	$(16 + 0.94\beta - 0.15\beta^2) N^e$	1.8

Table 5.16 Summary of parameters of empirical equation for shear distribution factors at FLS state at outer support

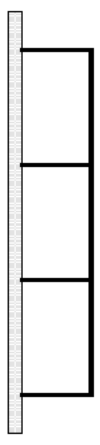
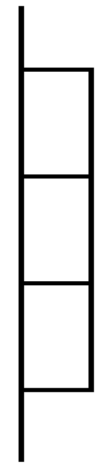
Number of design lanes	Value of F	Parameter (e)
2	$(8.3 + 0.9\beta - 0.17\beta^2) N^e$	1.63
3	$(11.9 + 0.74\beta - 0.11\beta^2) N^e$	1.74
4	$(14 + 0.8\beta - 0.09\beta^2) N^e$	1.74
5	$(16.8 + 0.66\beta - 0.07\beta^2) N^e$	1.77



a) Types of single-box girders



b) Types of multiple box girders



c) Types of cellular girders

Figure 1.1 Various box girder cross-sections

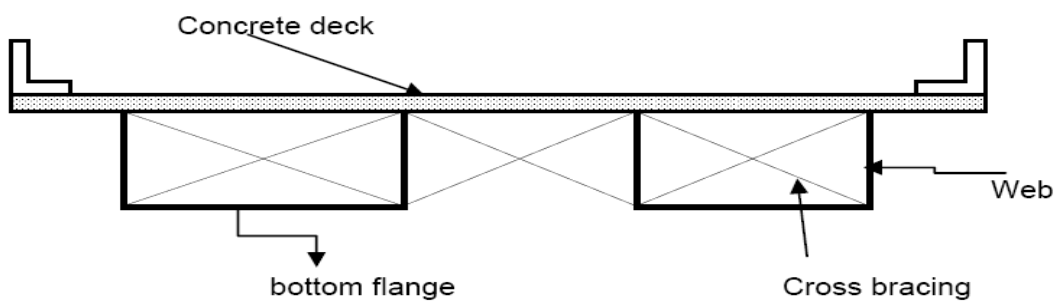


Figure 1.2 Typical twin-box girder bridge cross section



Figure 1.3 View of a Twin- box girder bridge

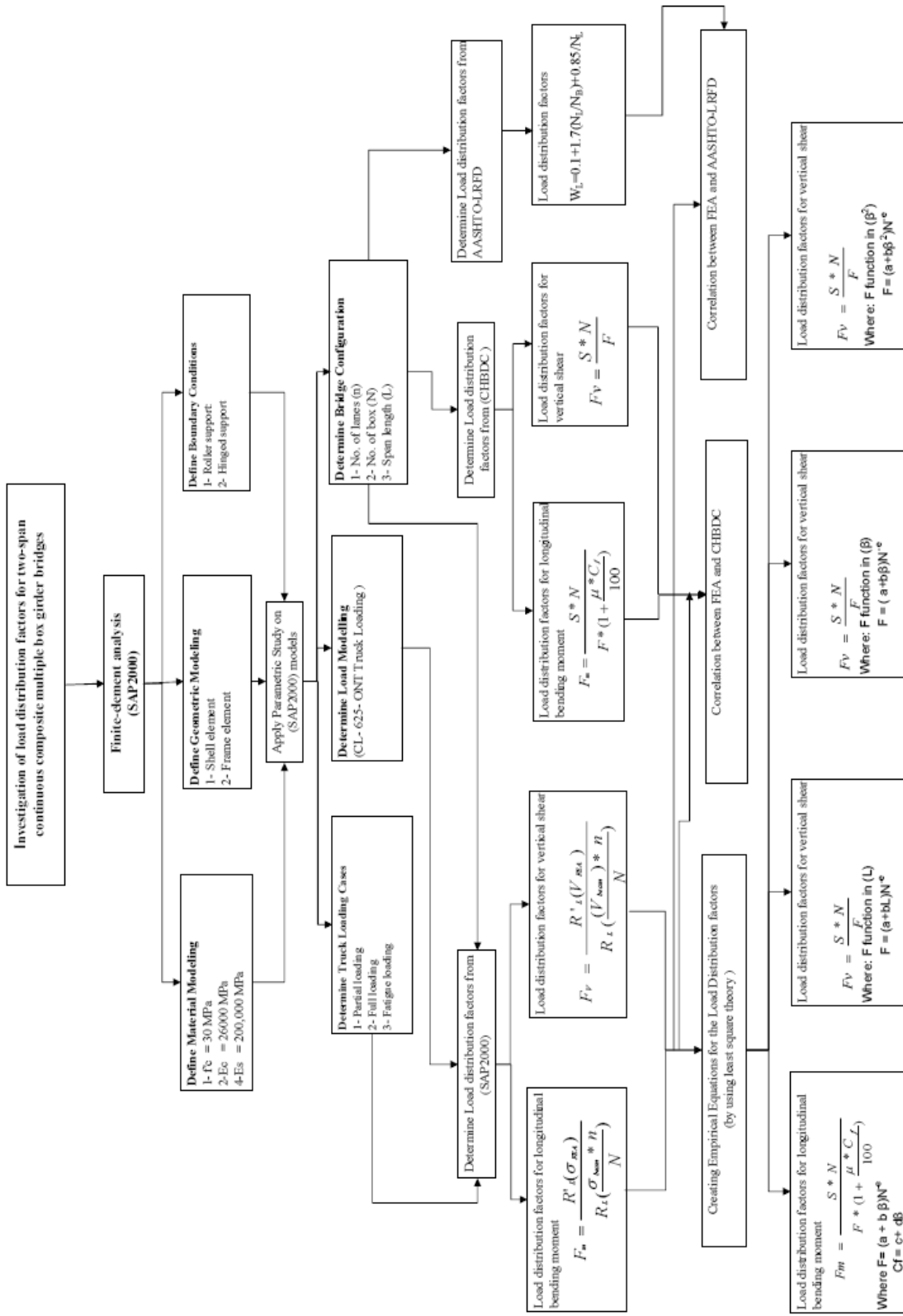
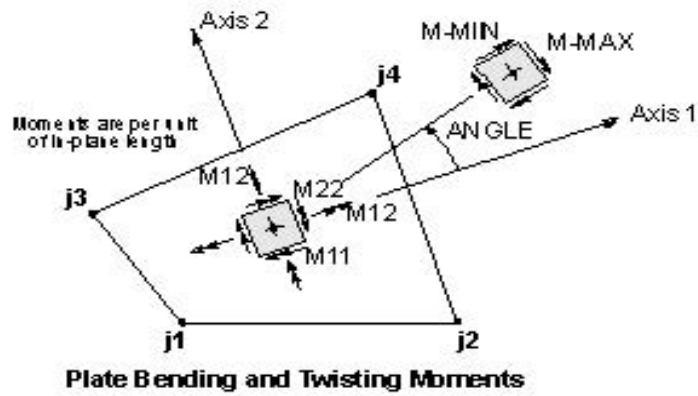
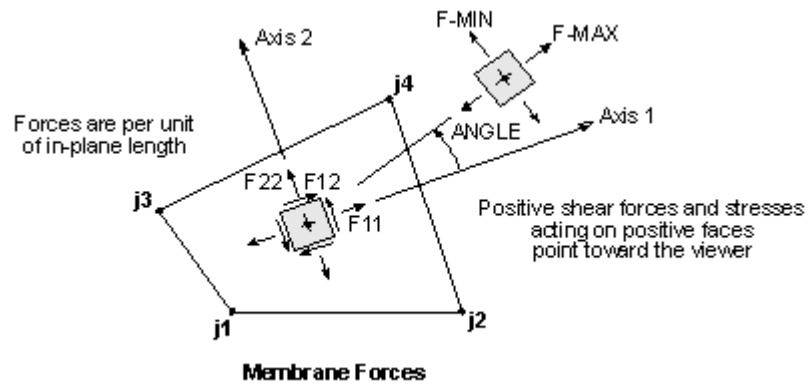


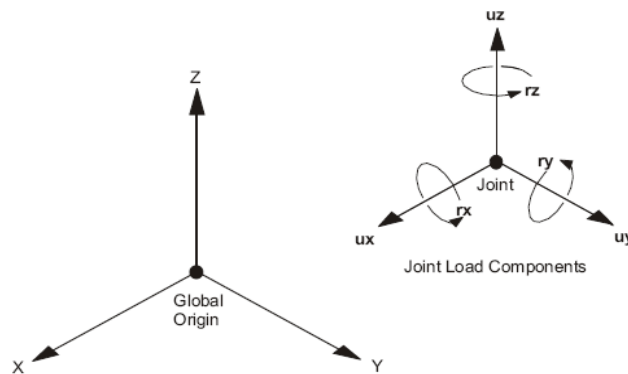
Figure 1.4 Organization chart of the research study



A) Plate bending moments



b) Stress and membrane forces



C) Global and local coordinates

Figure 3.1 Sketches of the four-node shell element used in the analysis, “SAP2000 software” Wilson and Habibullah, 2010

Connection between concrete slab
and steel box-girder

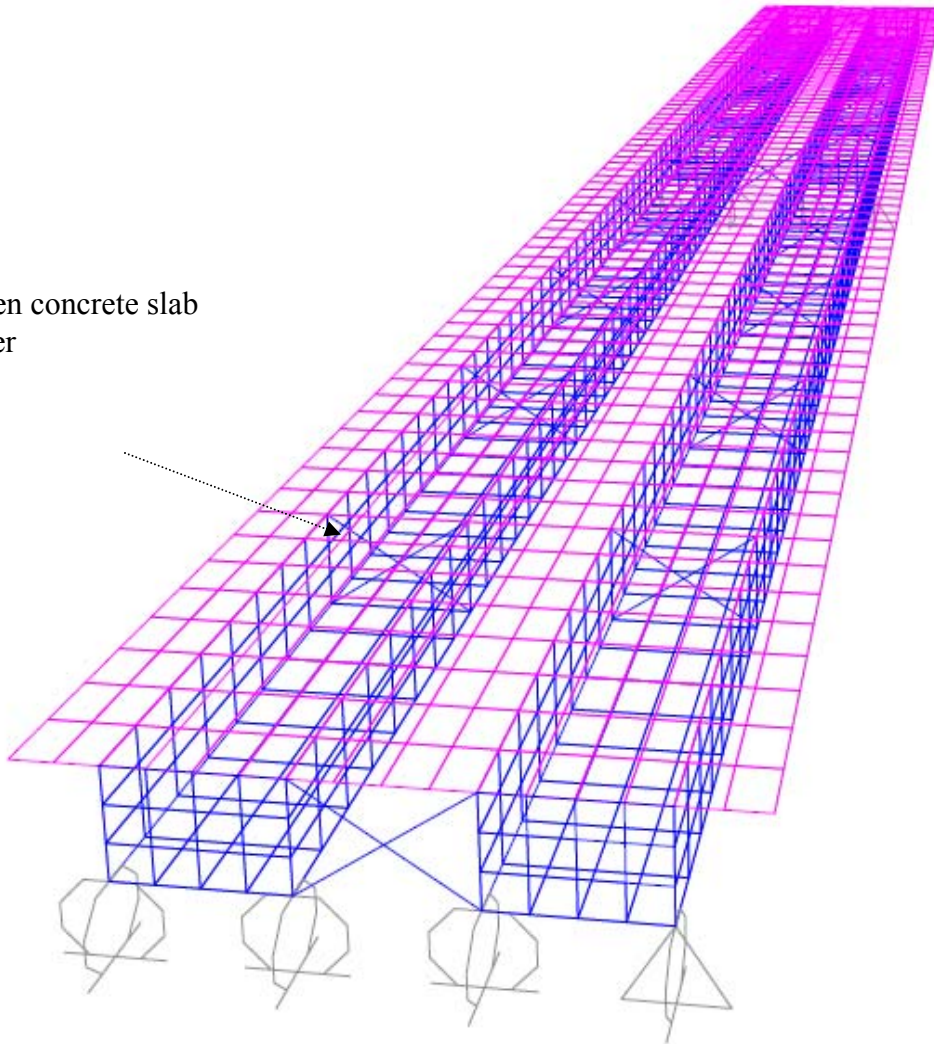
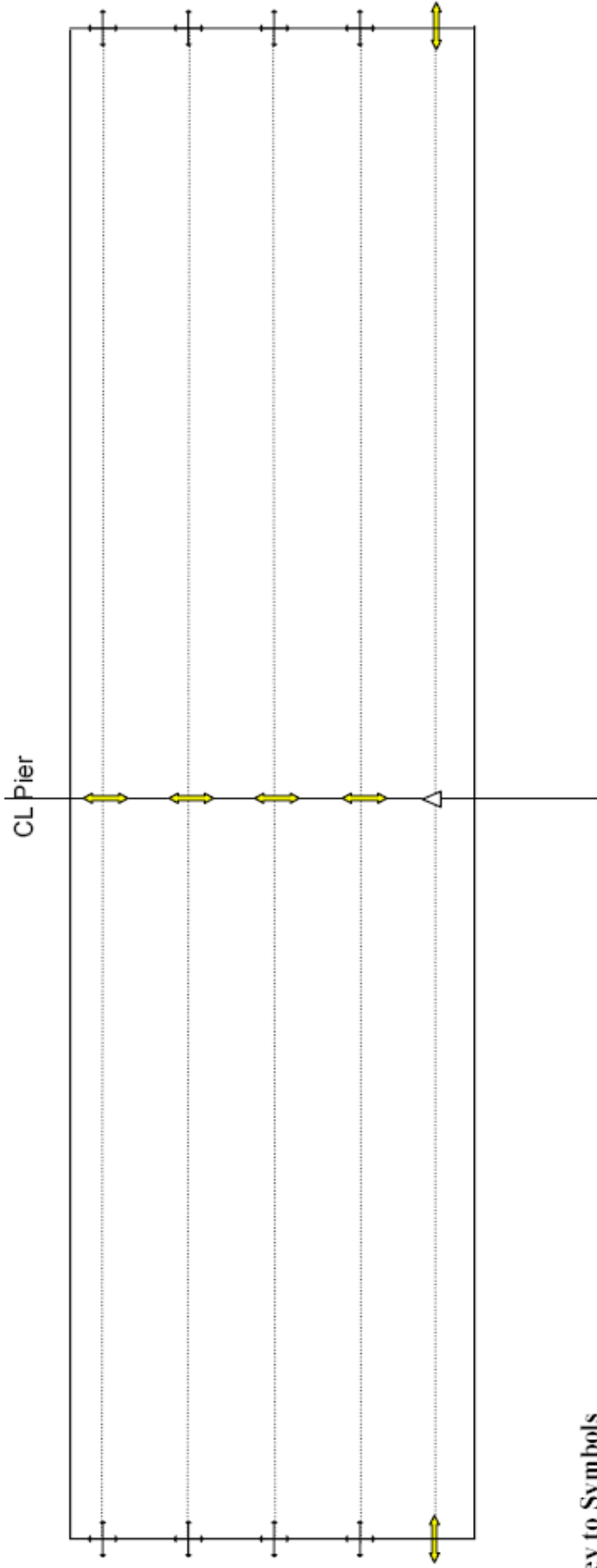


Figure 3.2 Schematic view of the bridge model showing the intermittent connections between steel box-girder and concrete slab



Key to Symbols

\triangle Fixed in the three dimensions

 Free in one direction

 Free in two direction

Figure 3.3 Boundary conditions of the bridges used in the parametric study

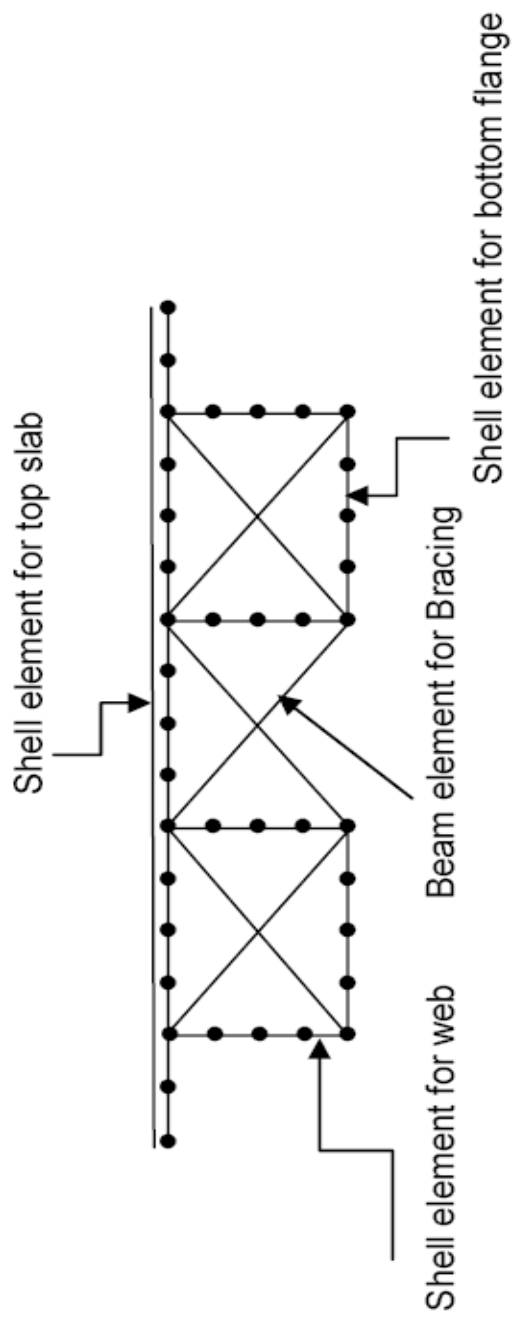
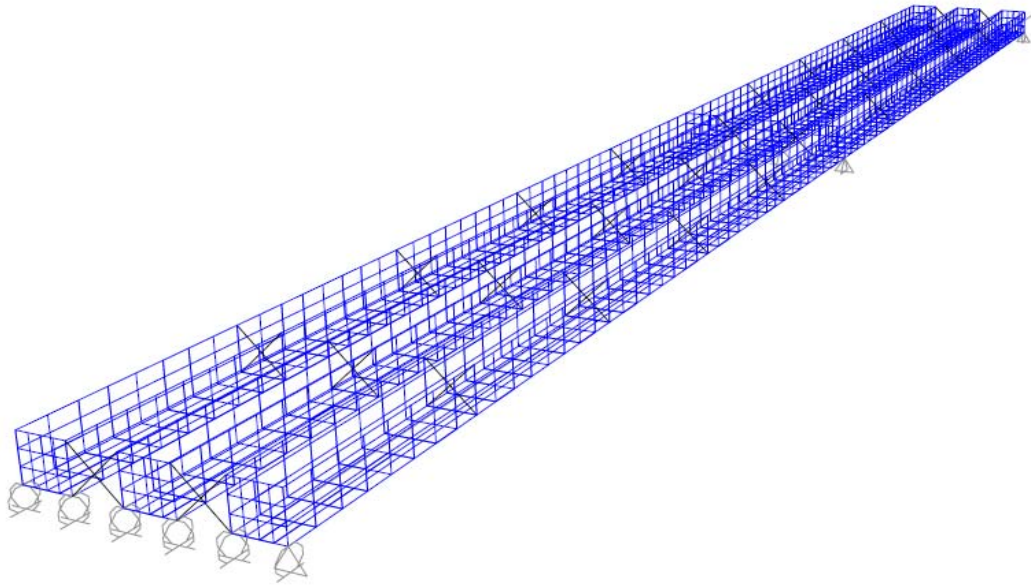
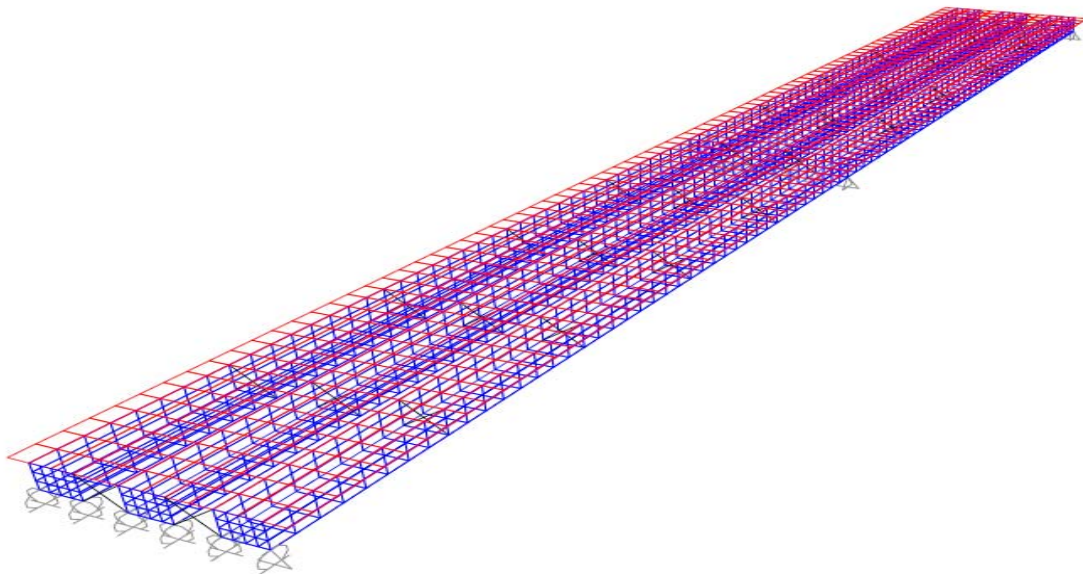


Figure 3.4 Finite element discretization of two-box girder cross-section

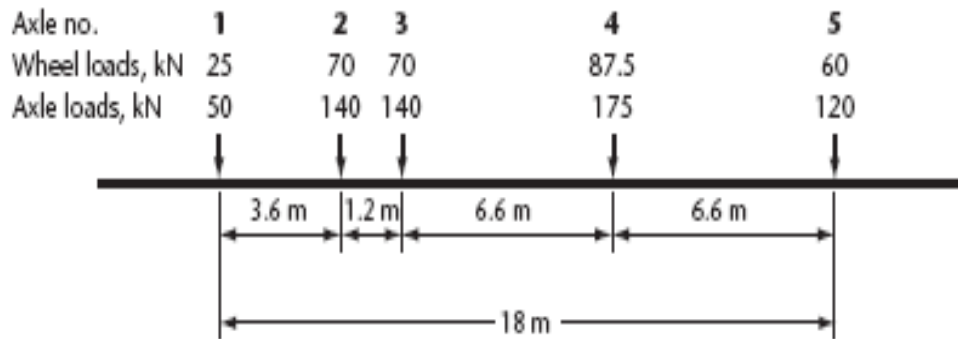


(a) The non-composite bridge model

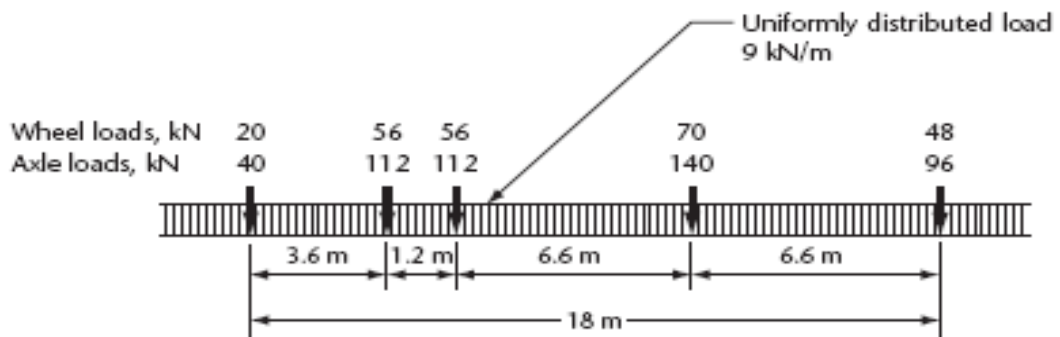


(b) The composite bridge model

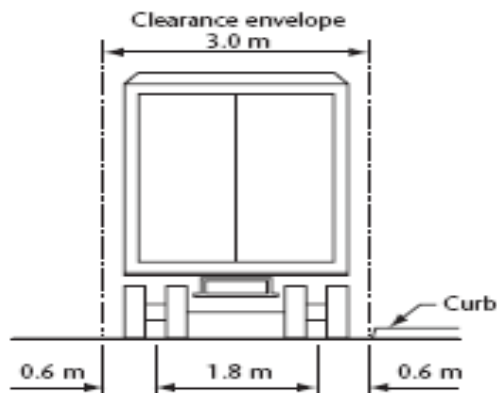
Figure 3.5 Typical finite-element meshes obtained from “SAP2000 Software” Wilson and Habibullah, 2010



CL-625-ONT Truck Loading



CL-625-ONT Lane Load



CL-W Truck

Figure 4.1 CL- 625-ONT Truck Loading and Lane Load

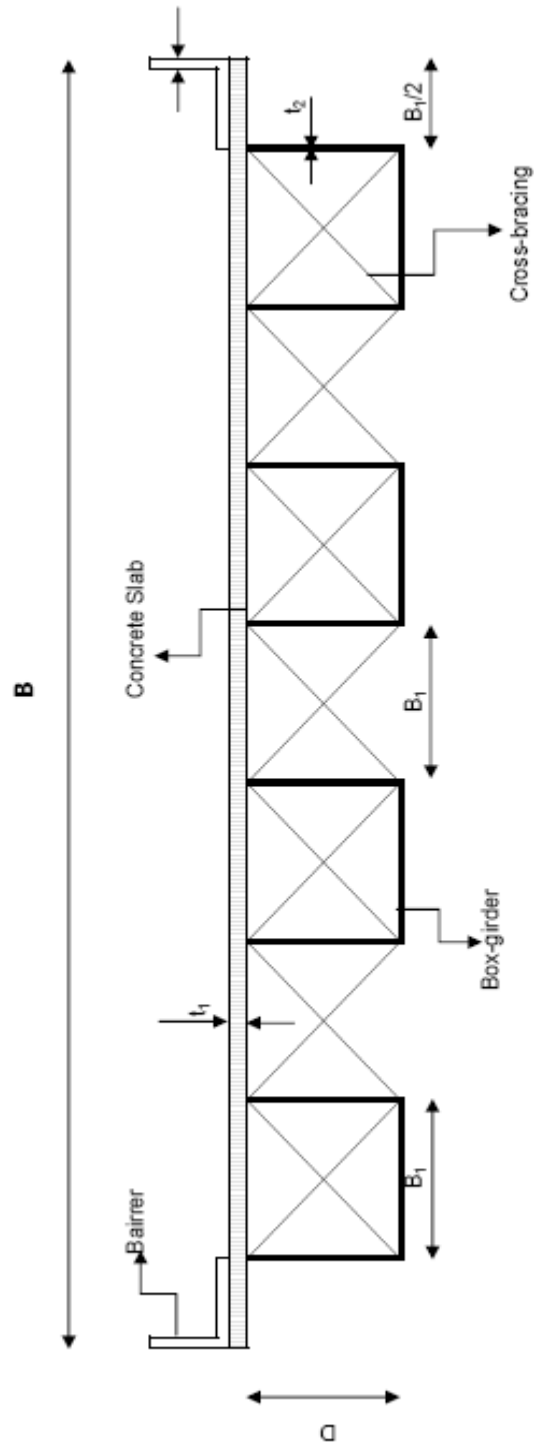


Figure 4.2 Symbols used for cross-section of a four-box girder bridge

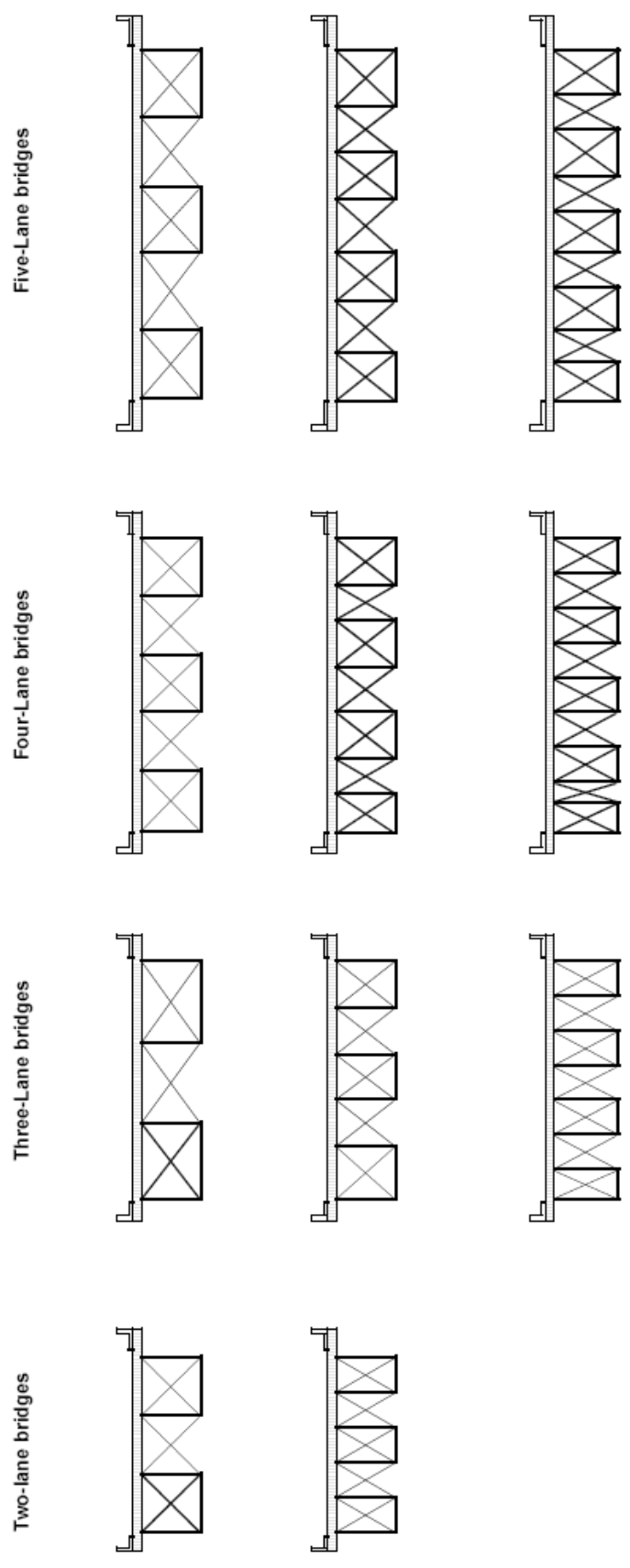
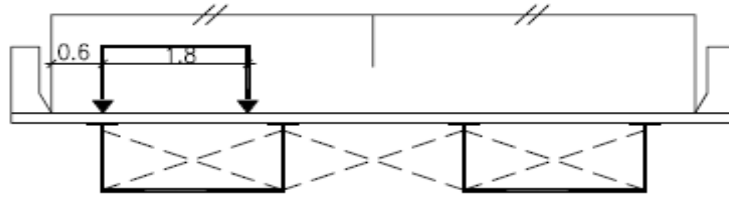
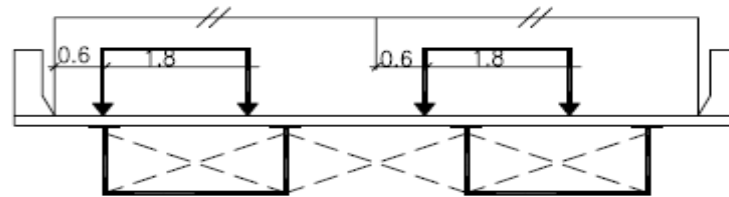


Figure 4.3 Cross-section configurations used in the parametric study

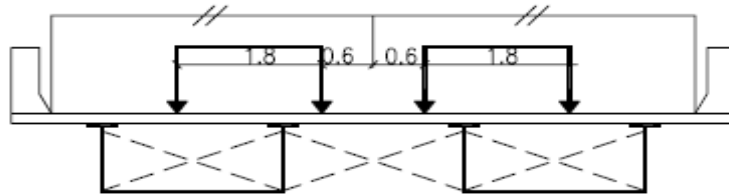
Exterior girder –
Partial load



Exterior girder –
Full load



Middle girder –
Full load



Fatigue loading

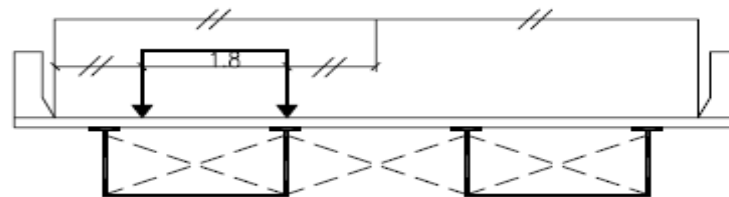


Figure 4.4 Loading cases for two–design lane, two-girder bridges

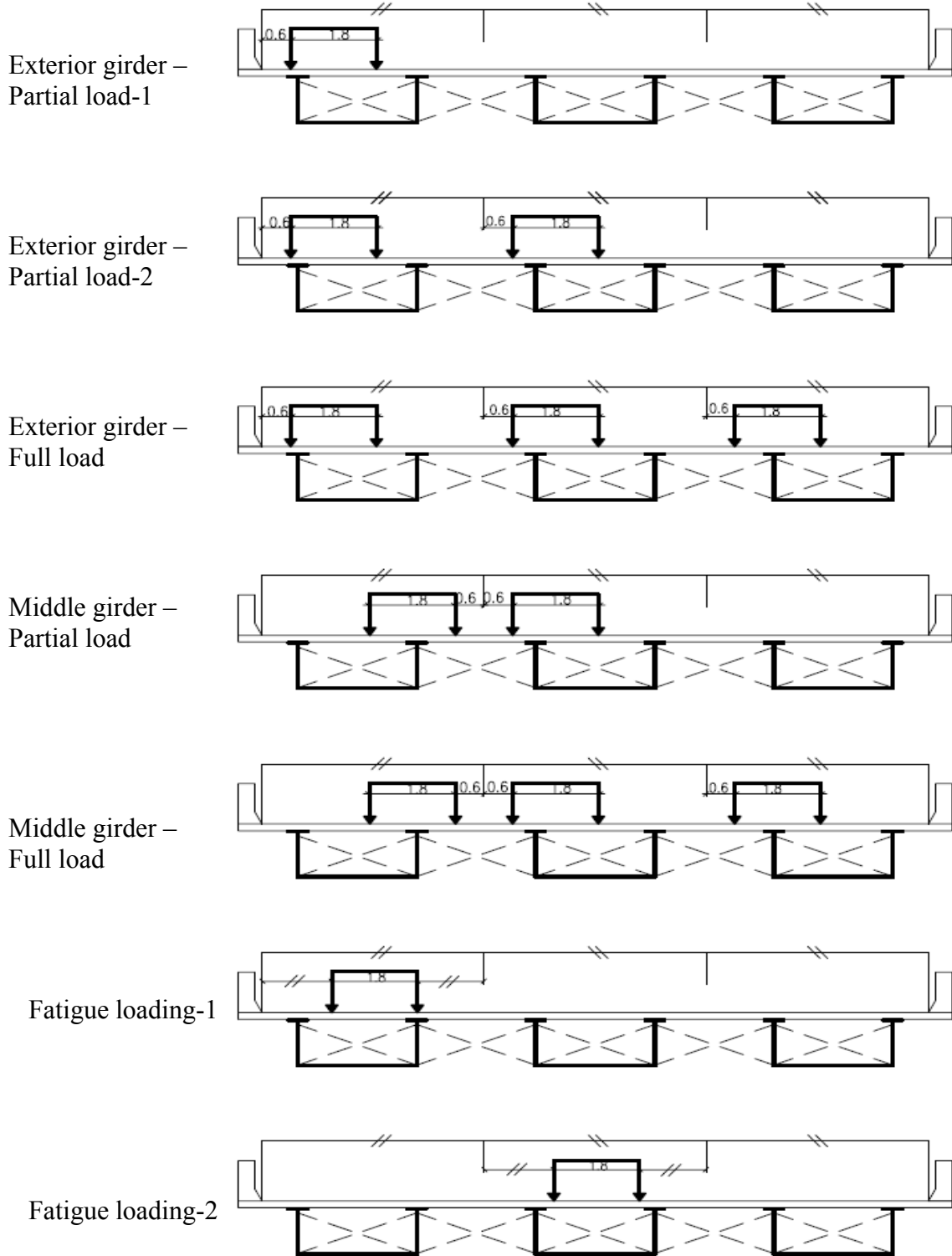


Figure 4.5 Loading cases for three–design lane, three-girder bridges

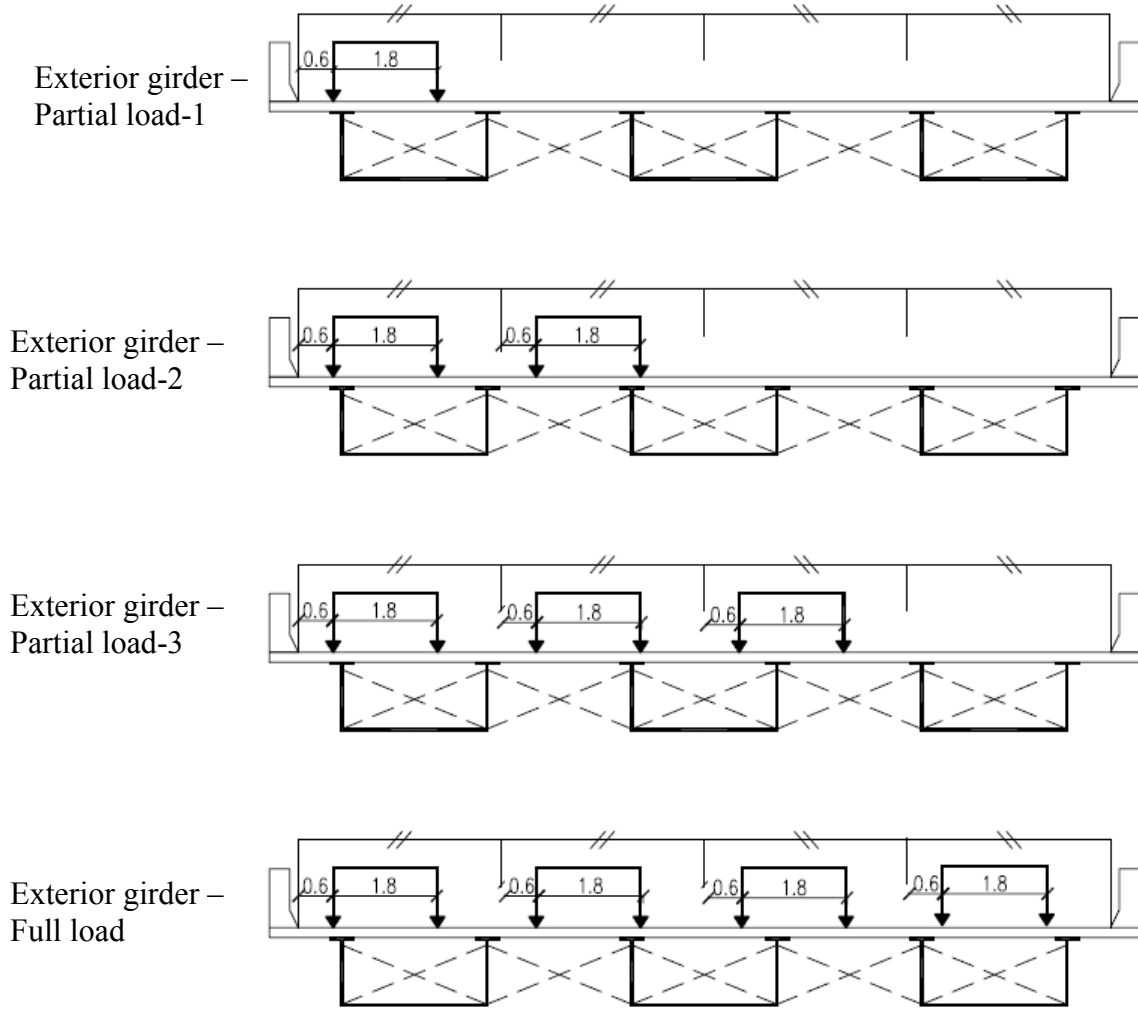


Figure 4.6 Loading cases for exterior girder for four–design lane, three-girder bridges

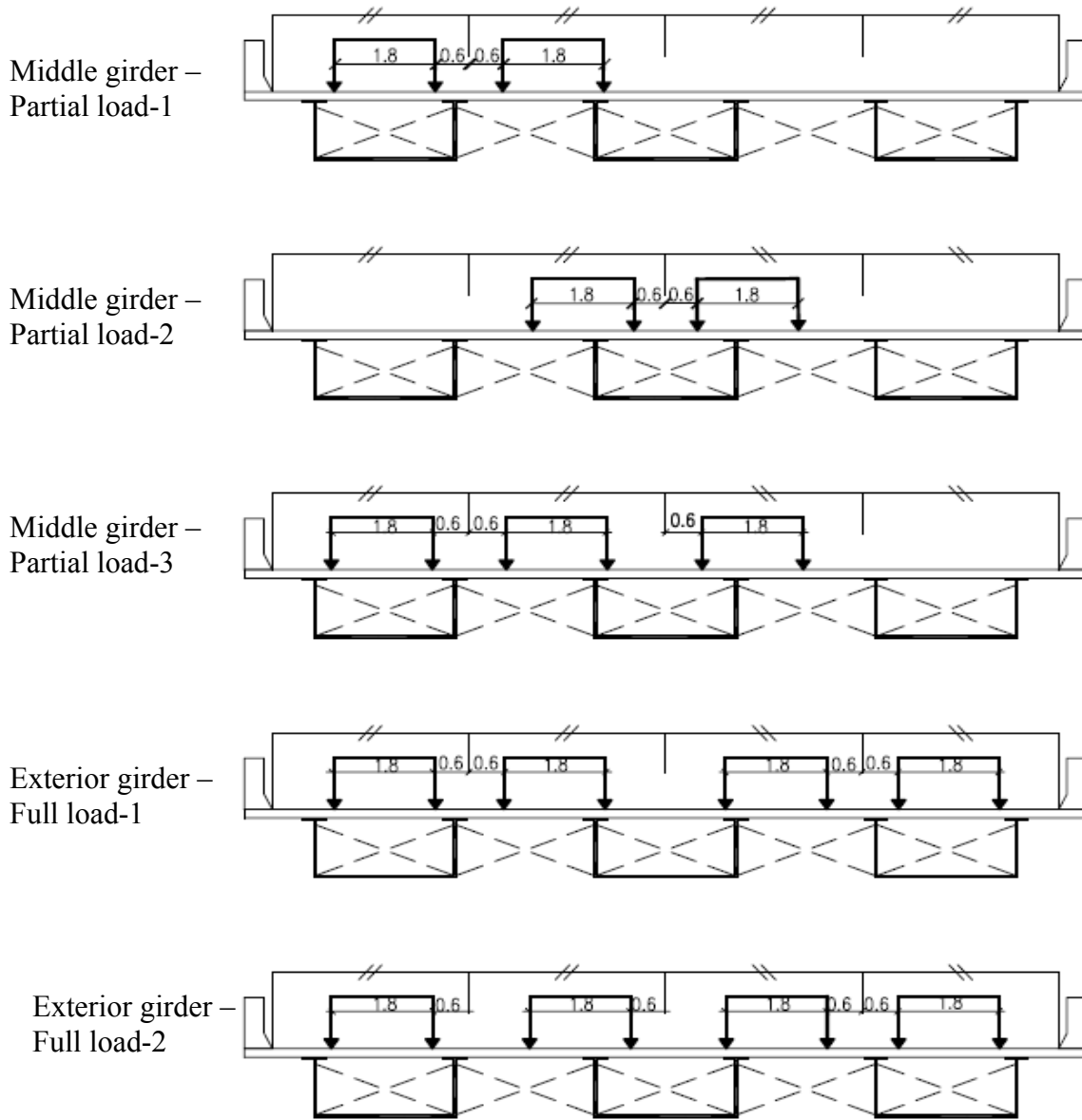


Figure 4.7 Loading cases for middle girder for four–design lane, three-girder bridges

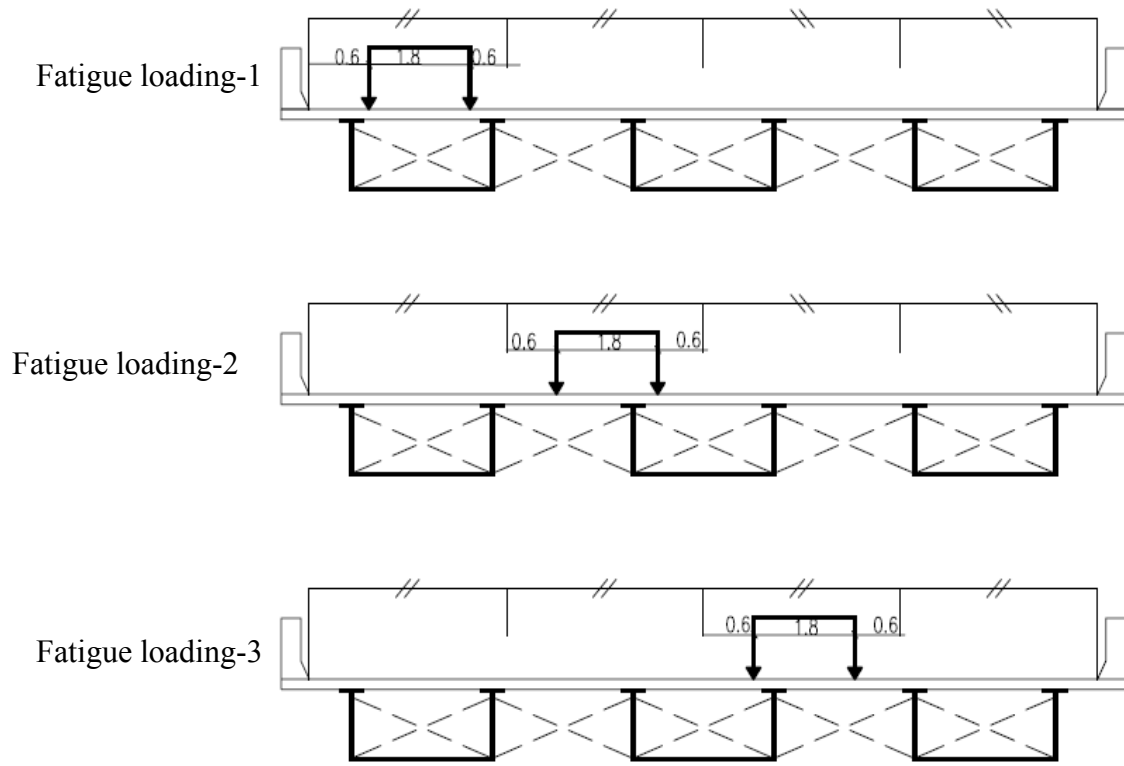


Figure 4.8 Loading cases for fatigue load for four–design lane, three-girder bridges

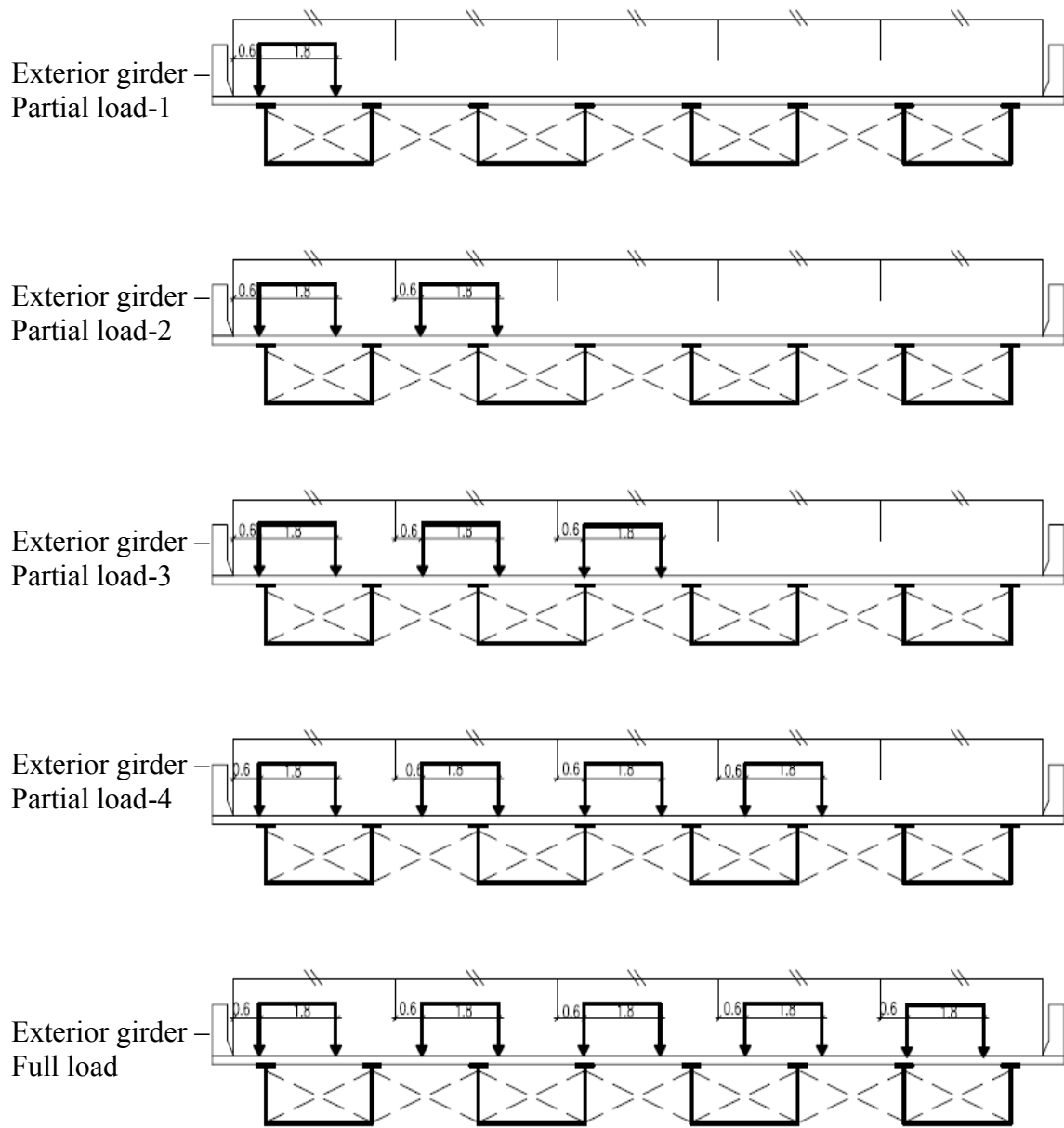


Figure 4.9 Loading cases for exterior girder for five–design lane, four-girder bridges

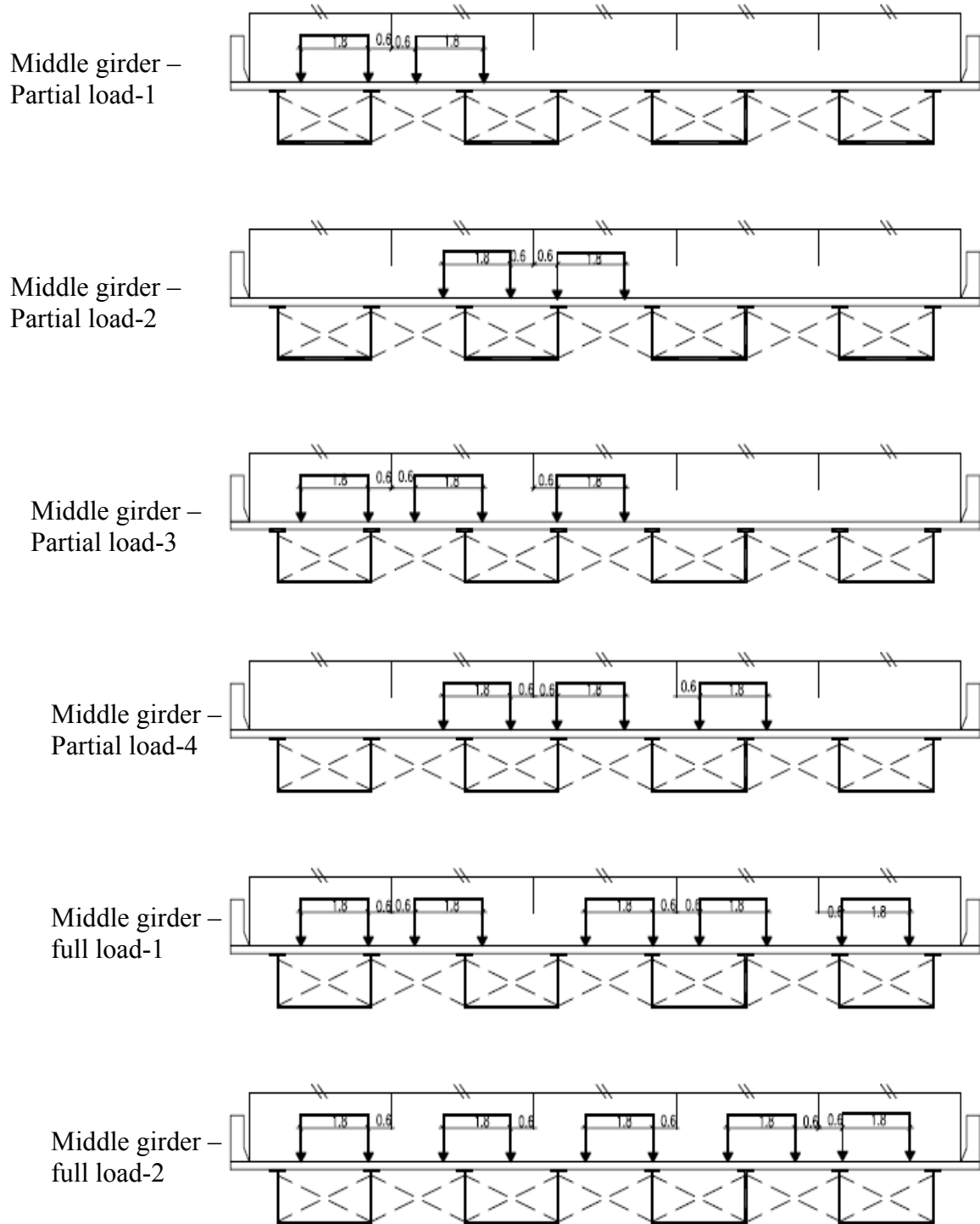


Figure 4.10 Loading cases for middle girder for five–design lane, four-girder bridges

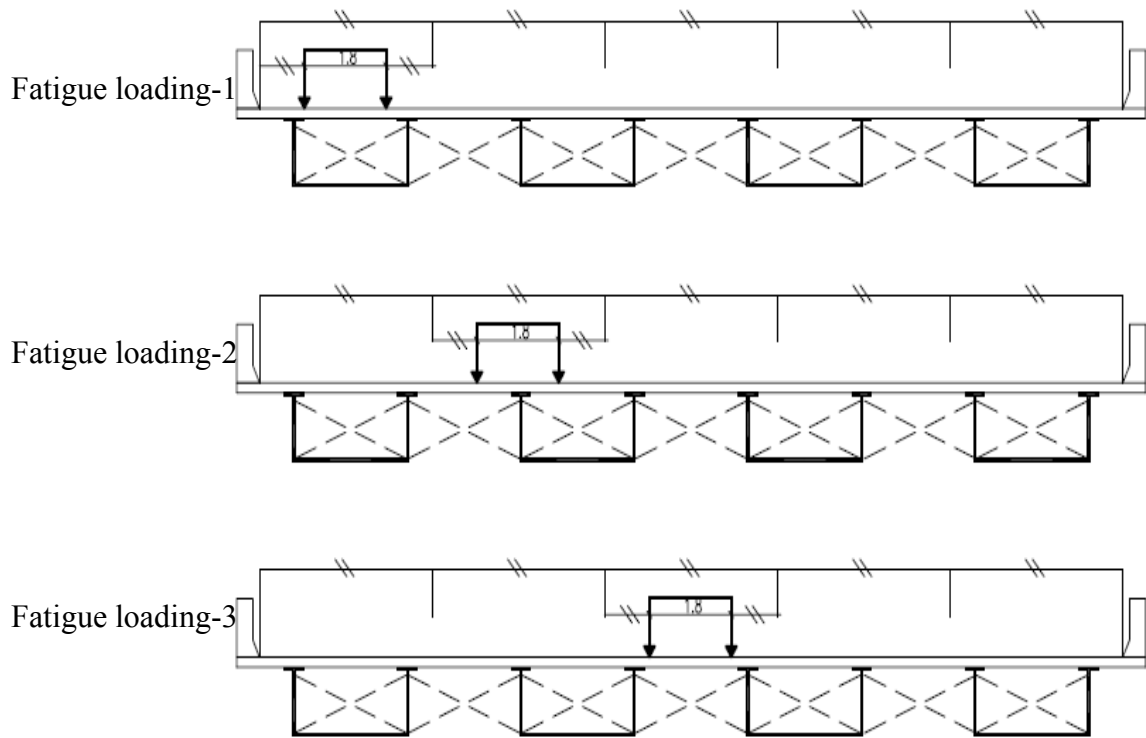


Figure 4.11 loading cases for fatigue load for five–design lane, four-girder bridges

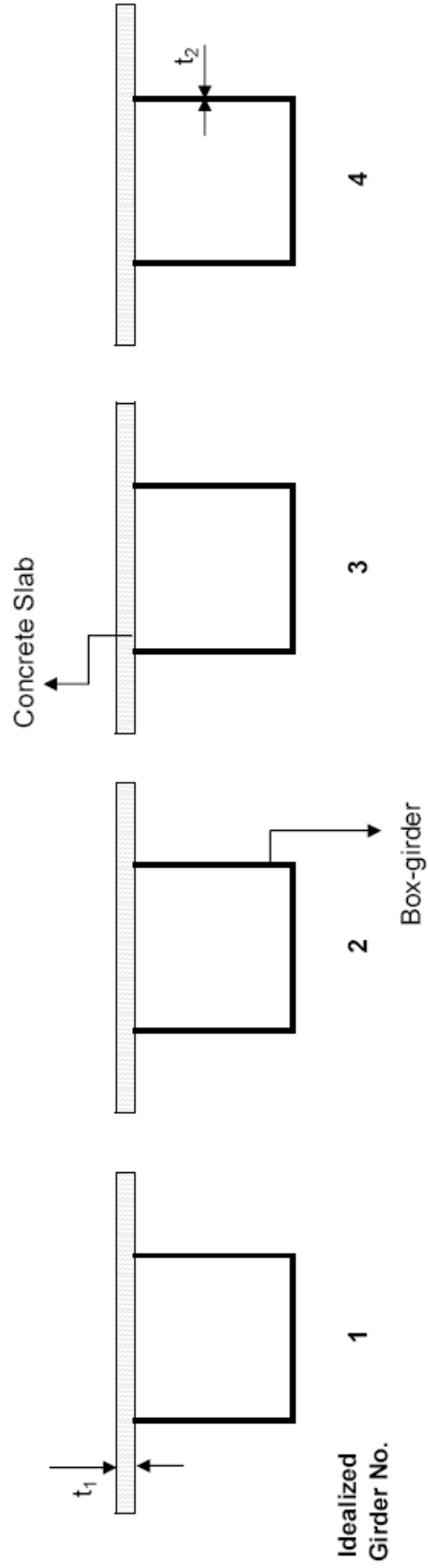


Figure 4.12 Idealized four-box bridge cross-section

Figure 5.1 Effect of span length on positive moment distribution factors at ULS due to CHBDC truck load

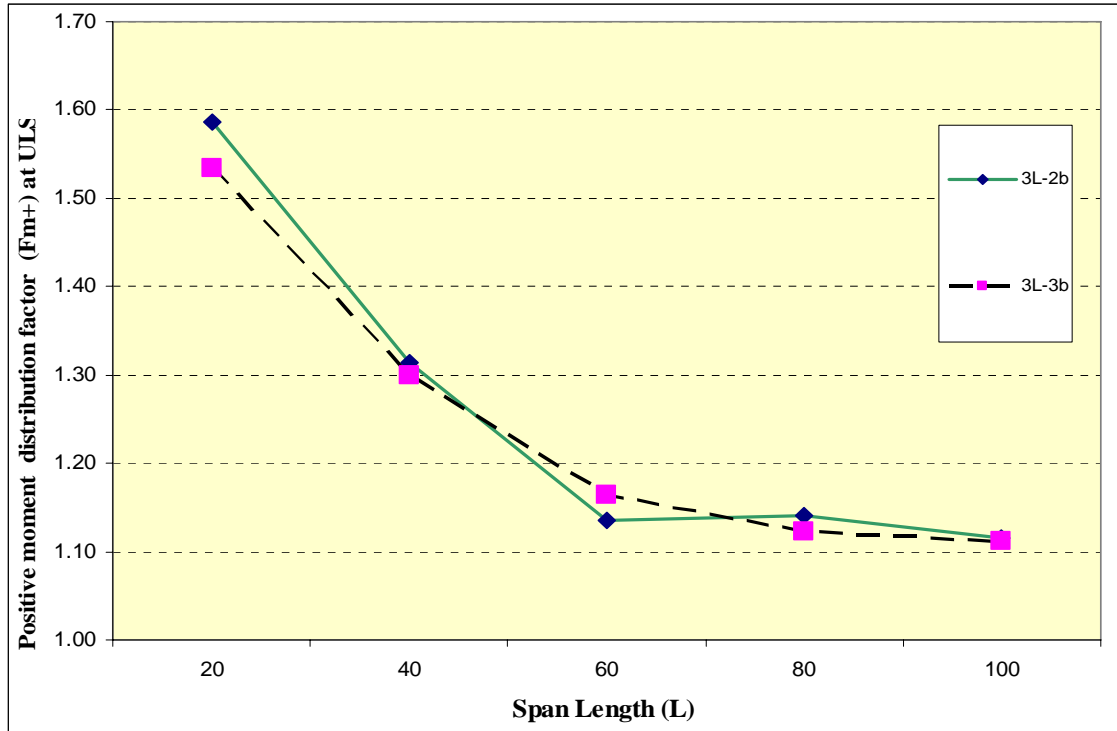


Figure 5.2 Effect of no. of lanes on positive moment distribution factors at ULS due to CHBDC truck load

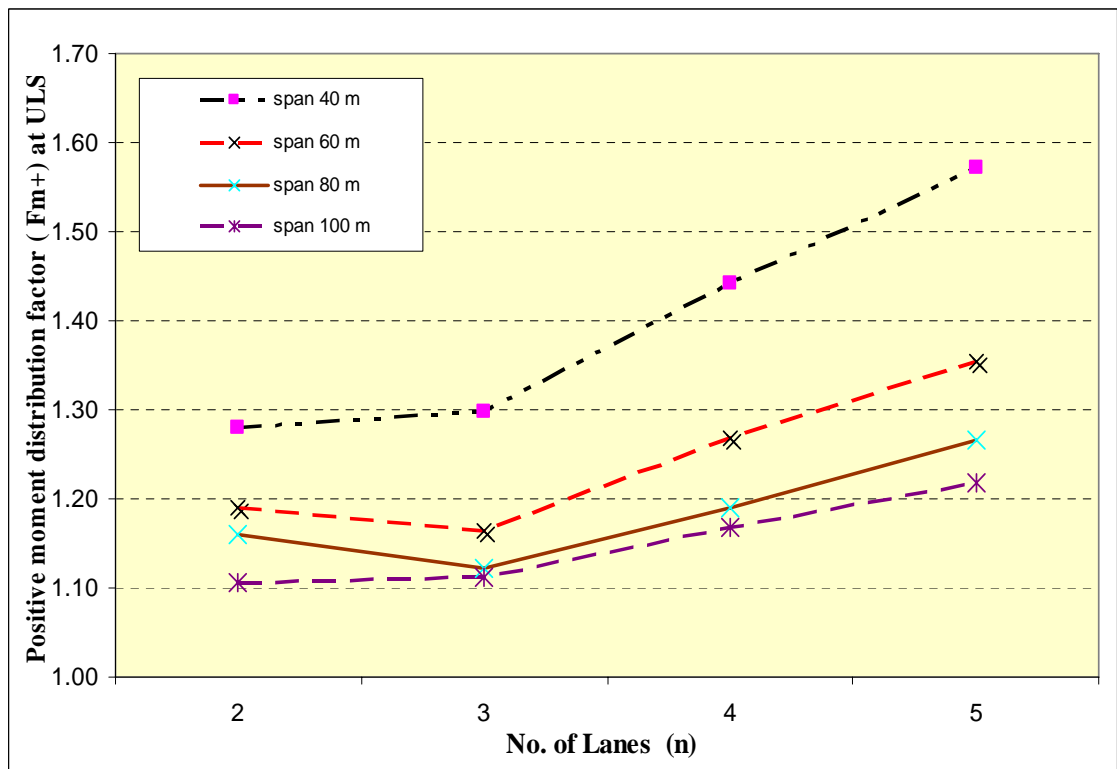


Figure 5.3 Effect of no. of boxes on positive moment distribution factors at ULS due to CHBDC truck load

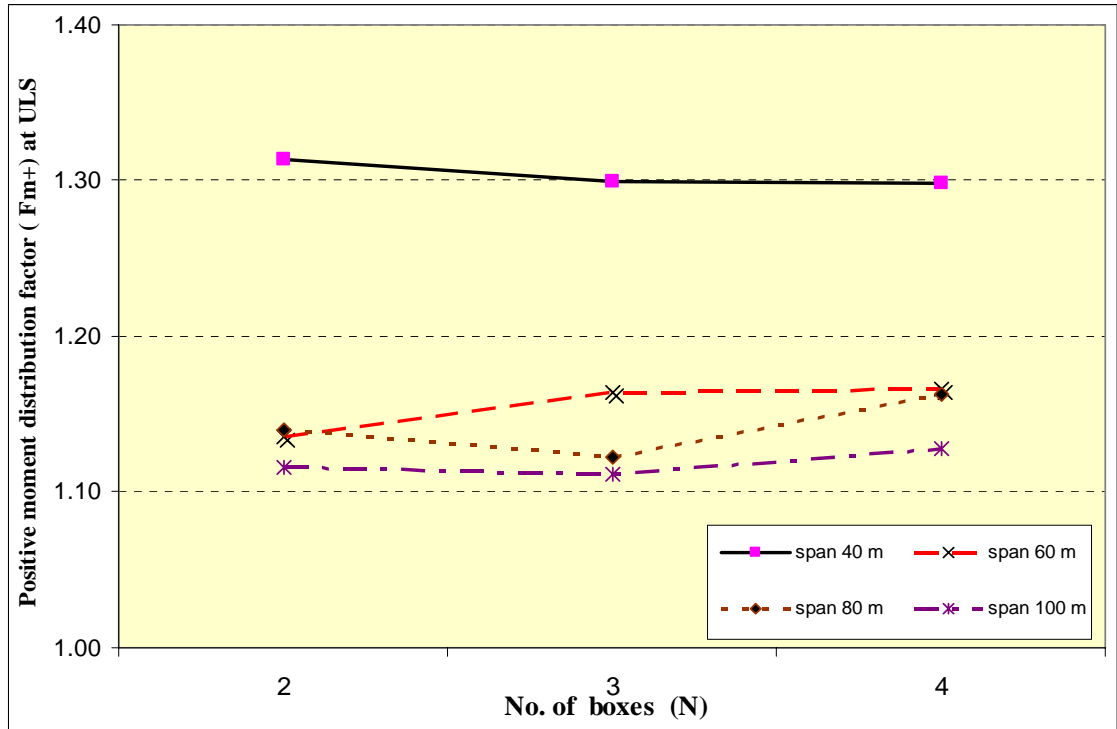


Figure 5.4 Effect of span length on positive moment distribution factors at FLS due to CHBDC truck load

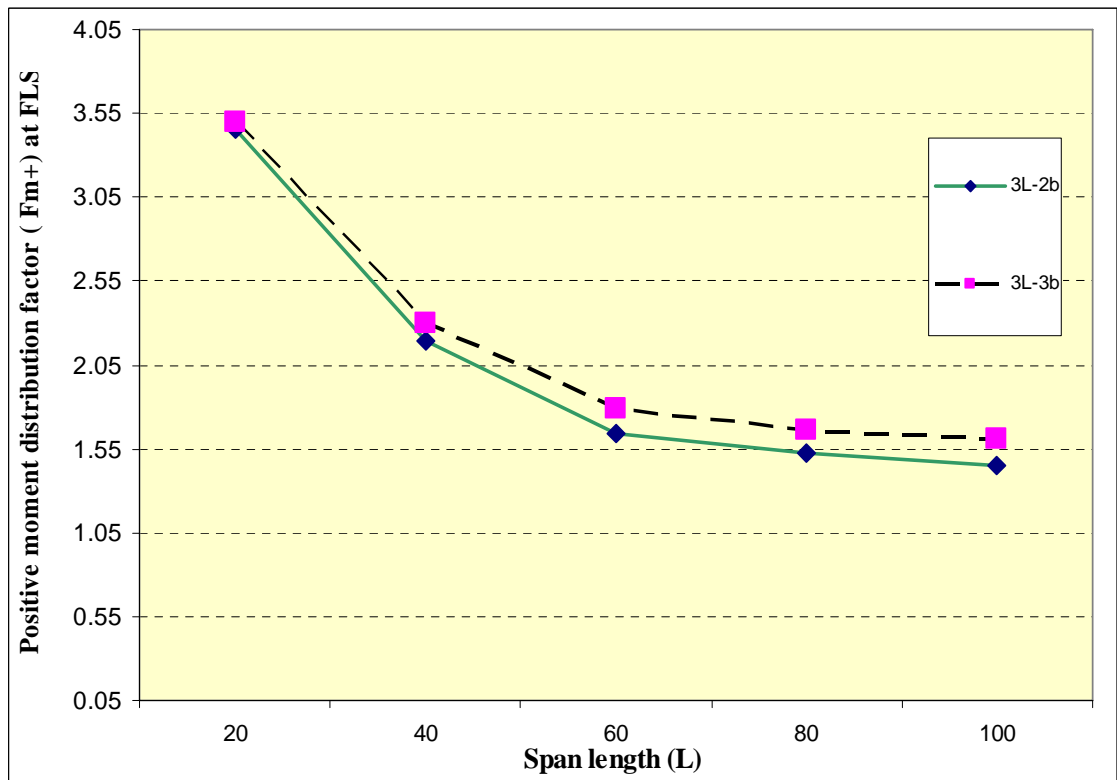


Figure 5.5 Effect of no. of lanes on positive moment distribution factor at FLS due to CHBDC truck load

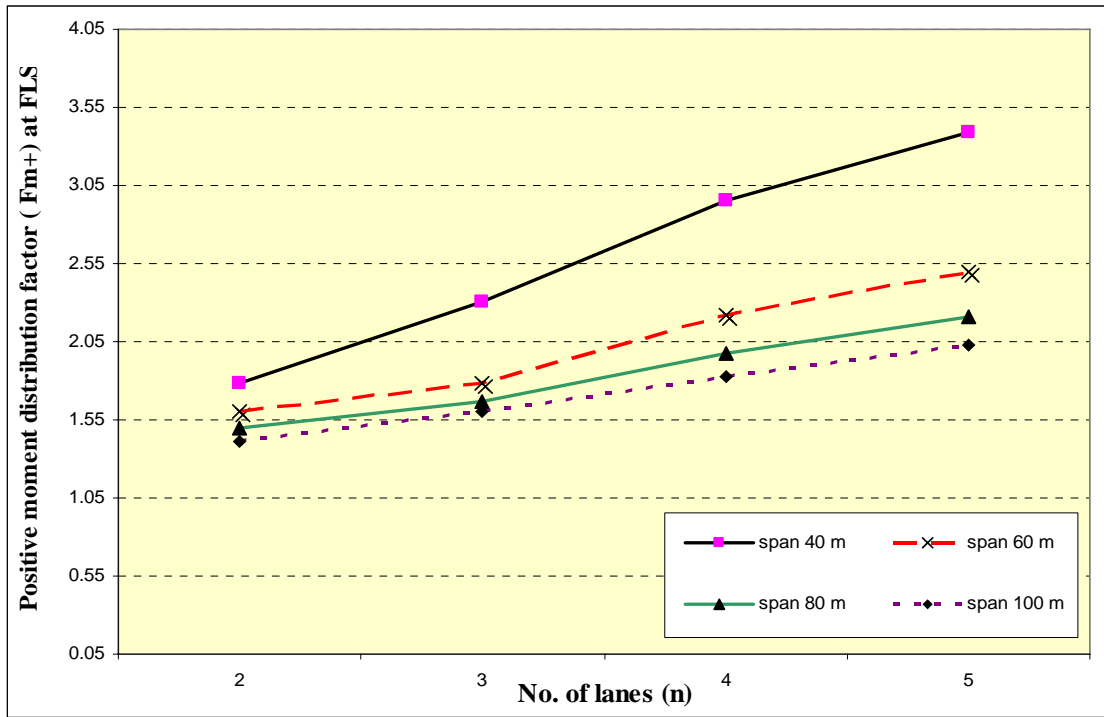


Figure 5.6 Effect of no. of boxes on positive moment distribution factor at FLS due to CHBDC truck load

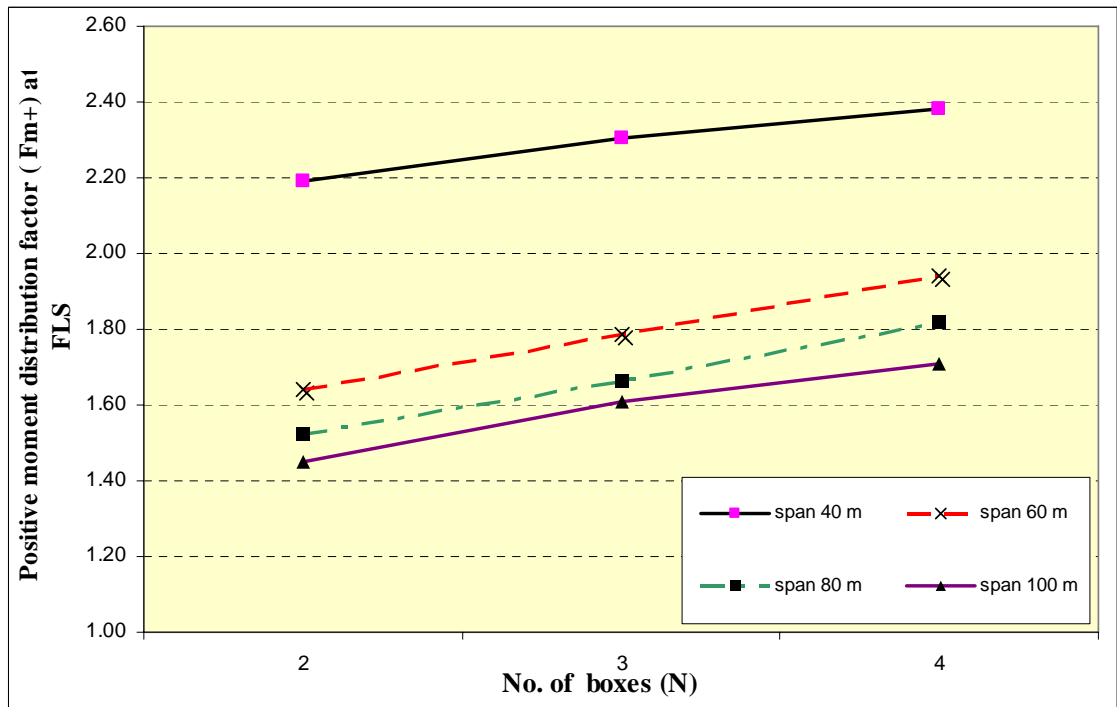


Figure 5.7 Effect of span length on negative moment distribution factors at ULS due to CHBDC truck load

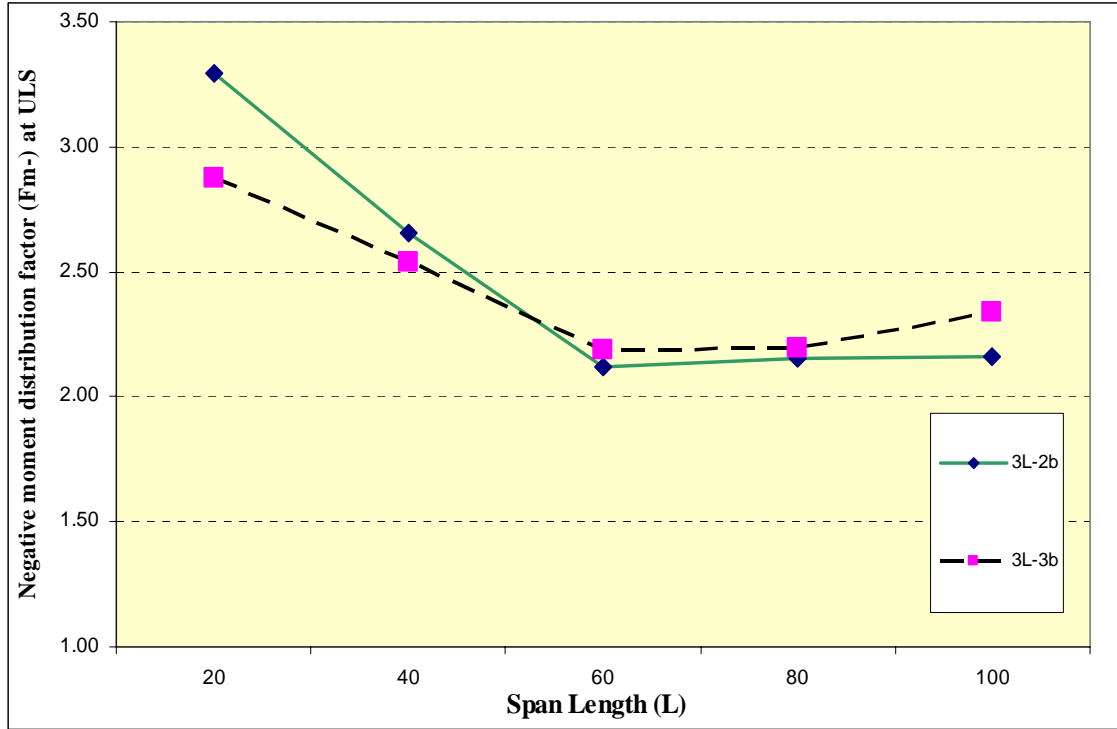


Figure 5.8 Effect of no. of lanes on negative moment distribution factors at ULS due to CHBDC truck load

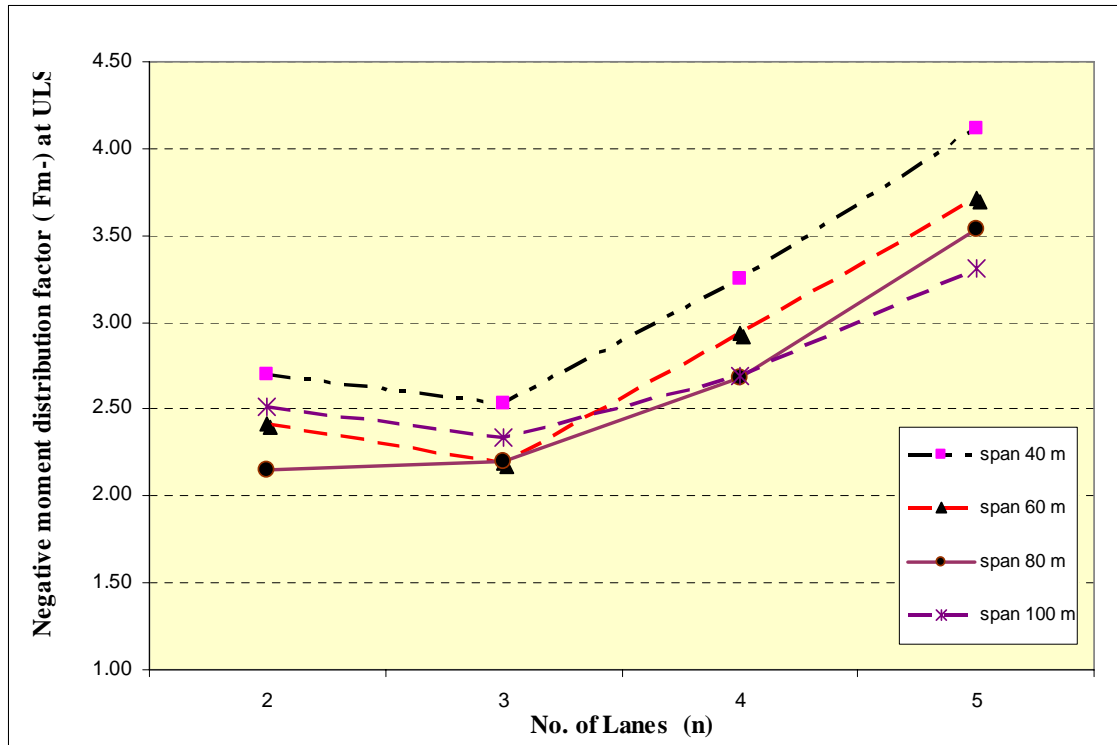


Figure 5.9 Effect of no. of boxes on negative moment distribution factor at ULS due to CHBDC truck load

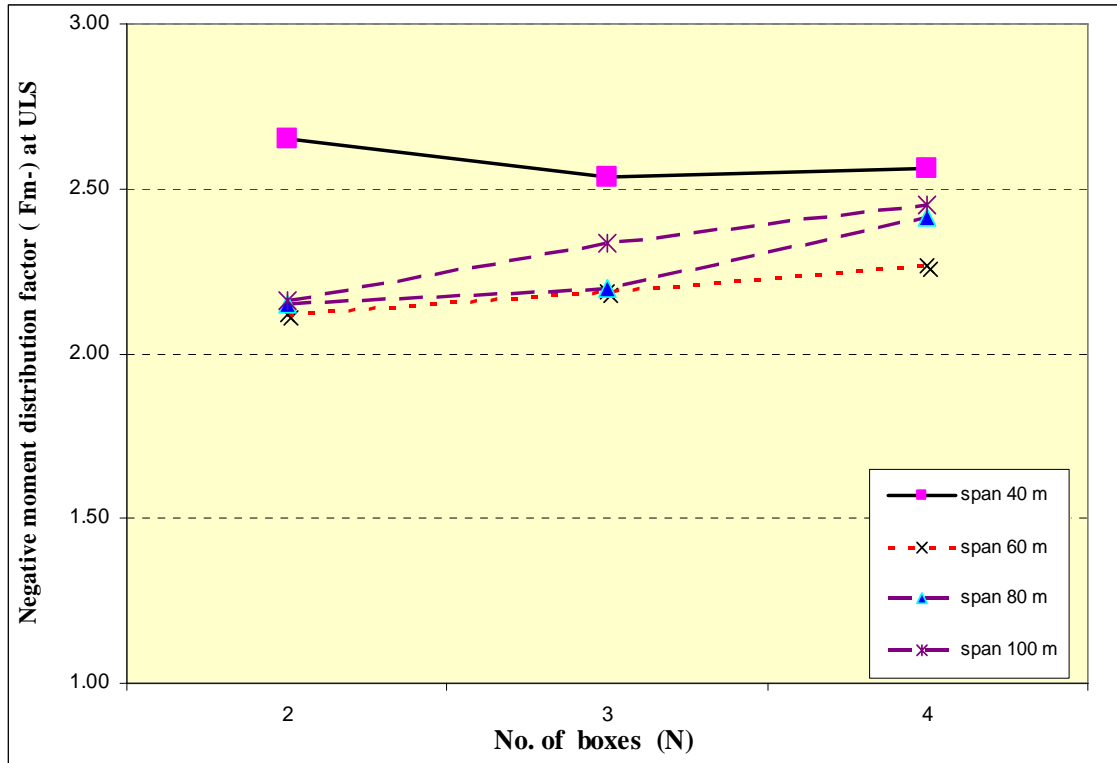


Figure 5.10 Effect of span length on negative moment distribution factor at FLS due to CHBDC truck load

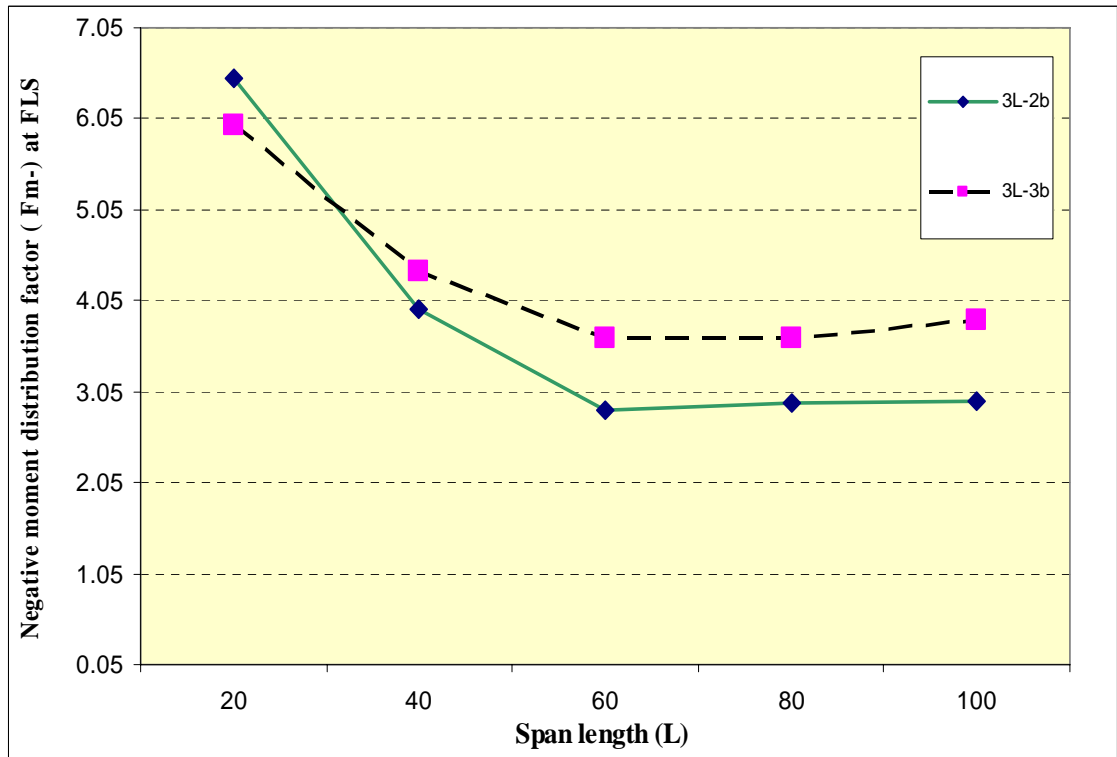


Figure 5.11 Effect of no. of lanes on negative moment distribution factors at FLS due to CHBDC truck load

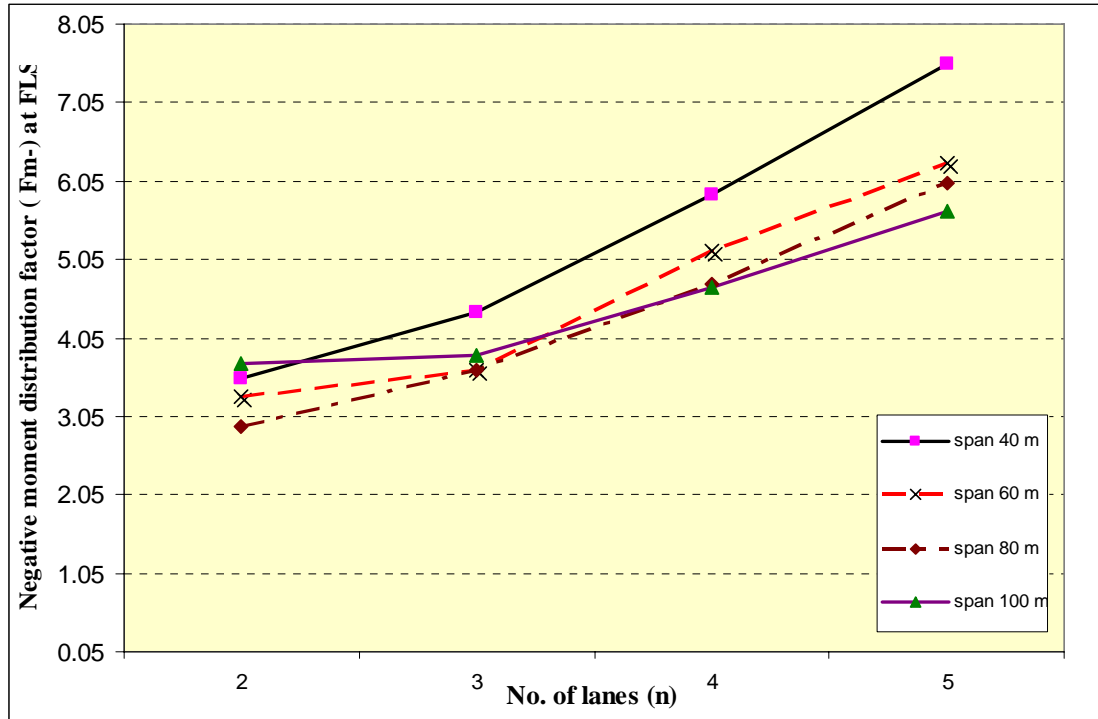


Figure 5.12 Effect of no. of boxes negative moment distribution factors at FLS due to CHBDC Truck load

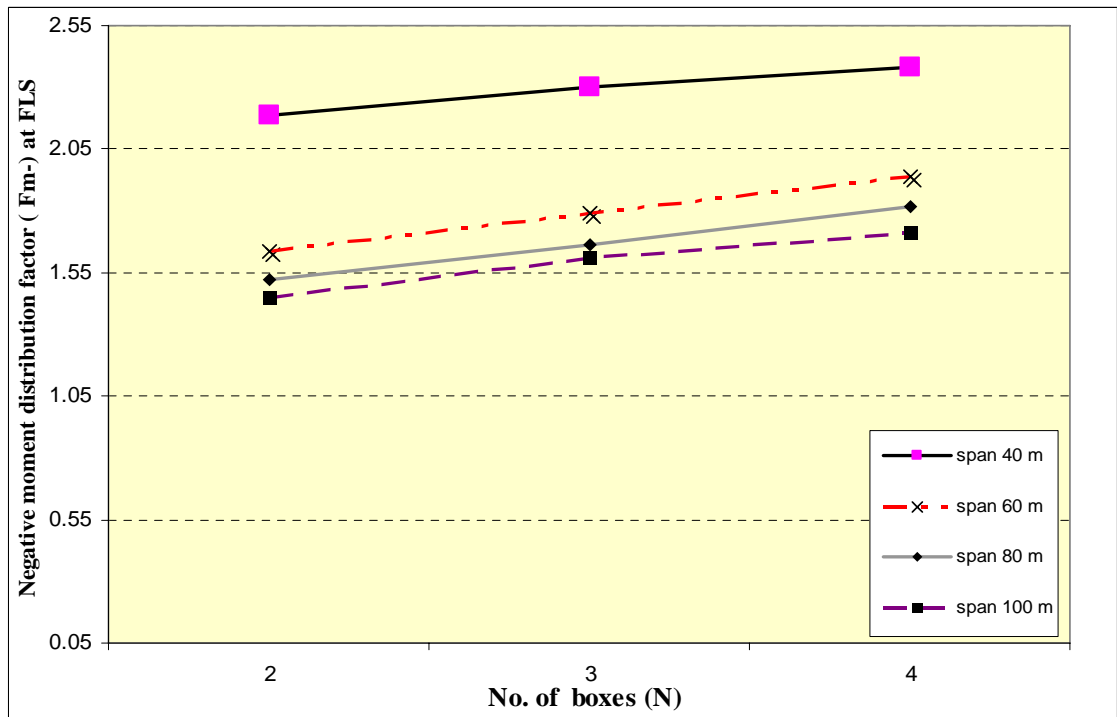


Figure 5.13 Effect of span length on shear distribution factors at ULS due to CHBDC truck load

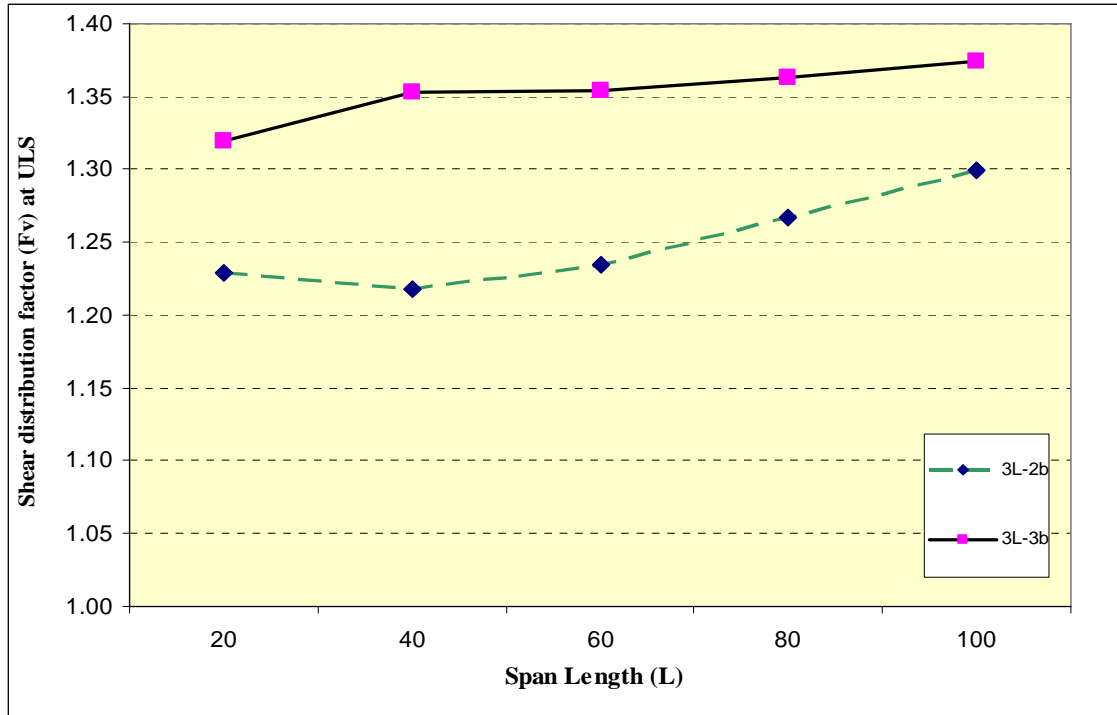


Figure 5.14 Effect of no. of lanes on shear distribution factors at ULS due to CHBDC truck load

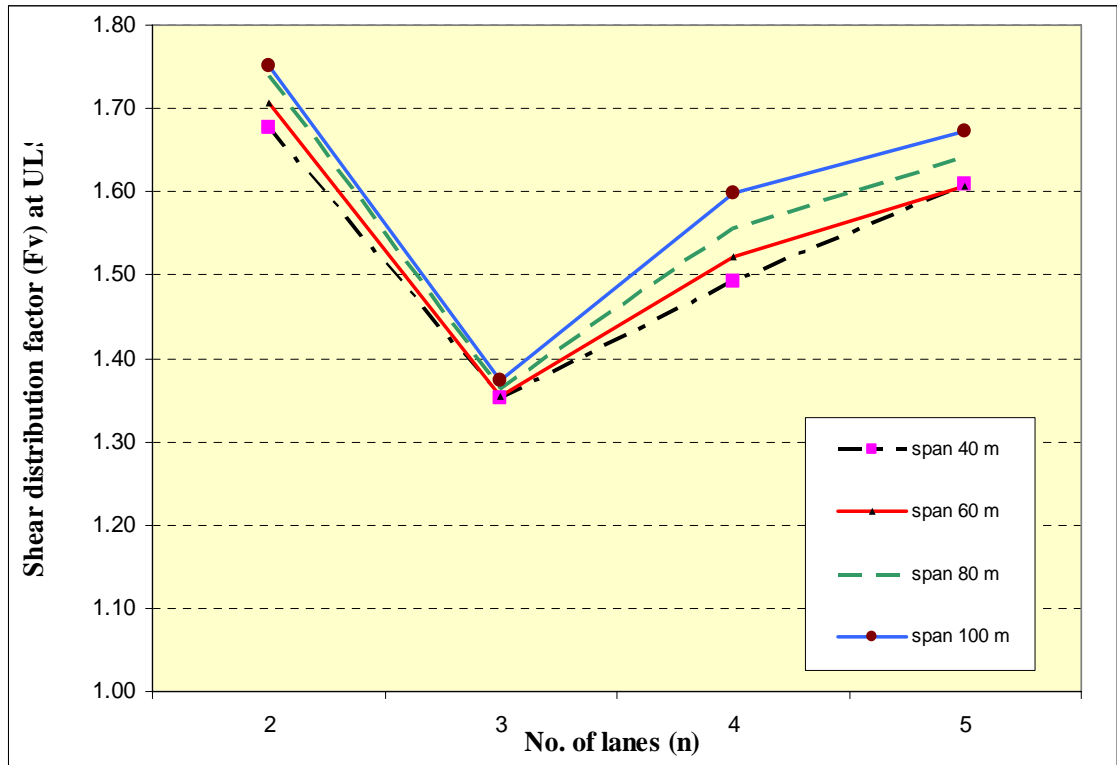


Figure 5.15 Effect of no. of boxes on shear distribution factors at ULS due to CHBDC truck load

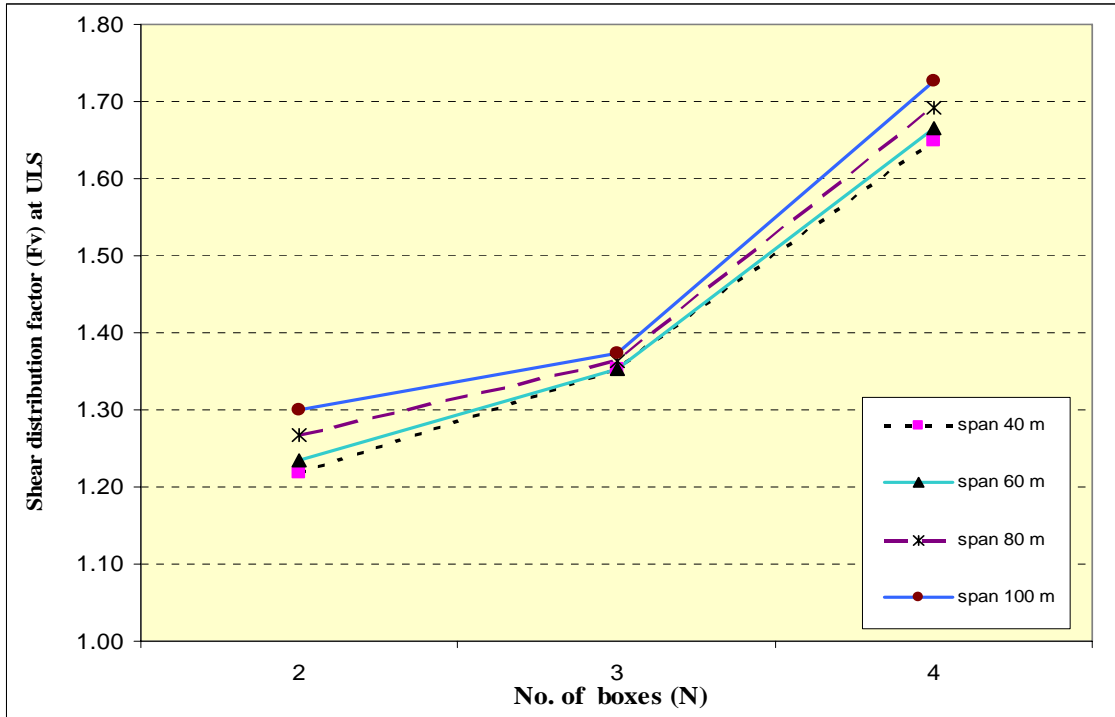


Figure 5.16 Effect of span length on shear distribution factors at FLS due to CHBDC truck load

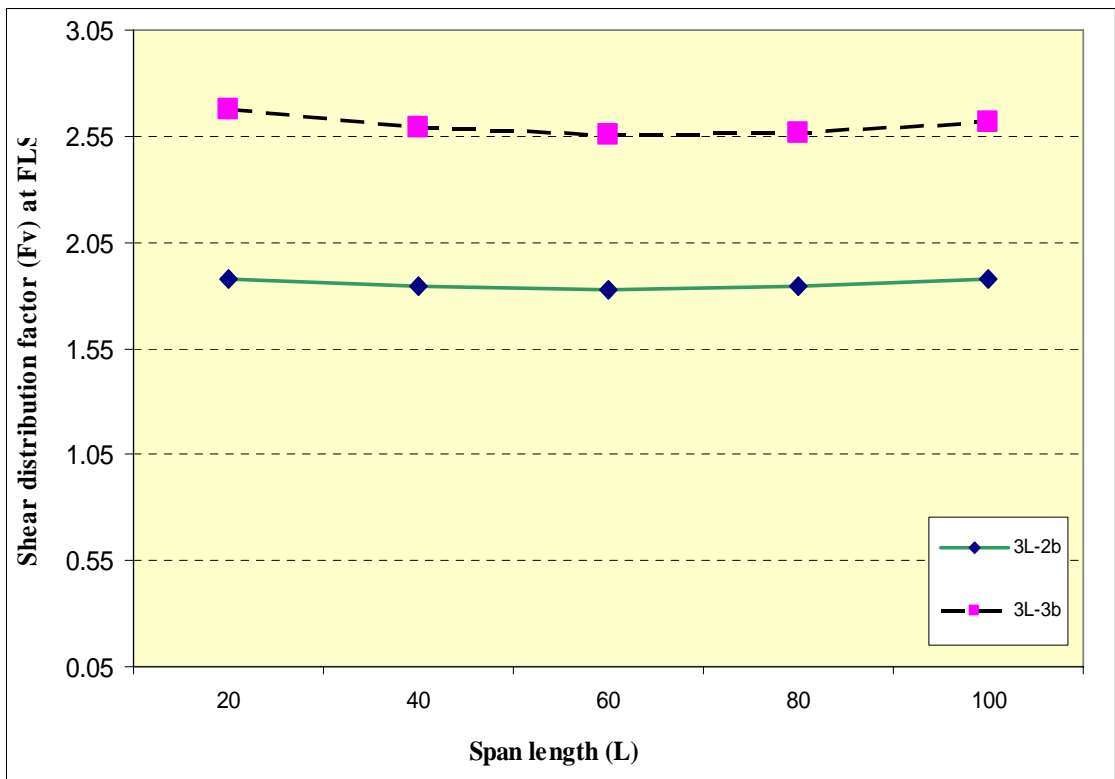


Figure 5.17 Effect of no. of lanes on shear distribution factors at FLS due to CHBDC truck load

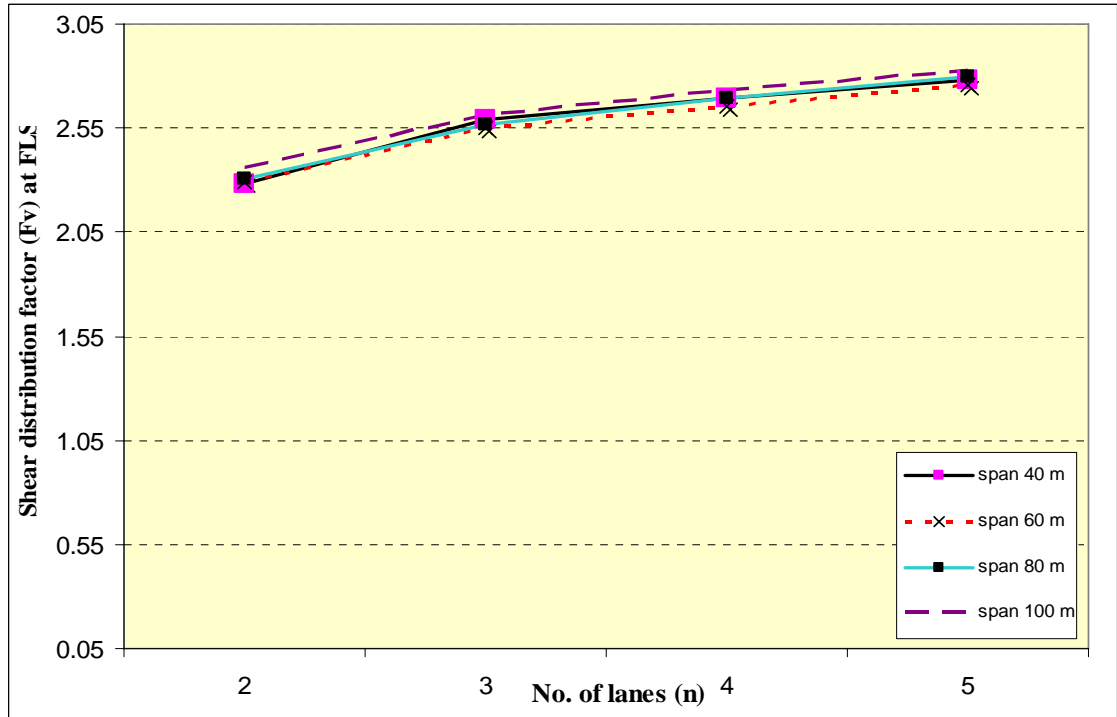


Figure 5.18 Effect of no. of boxes on shear distribution factor at FLS due to CHBDC truck load

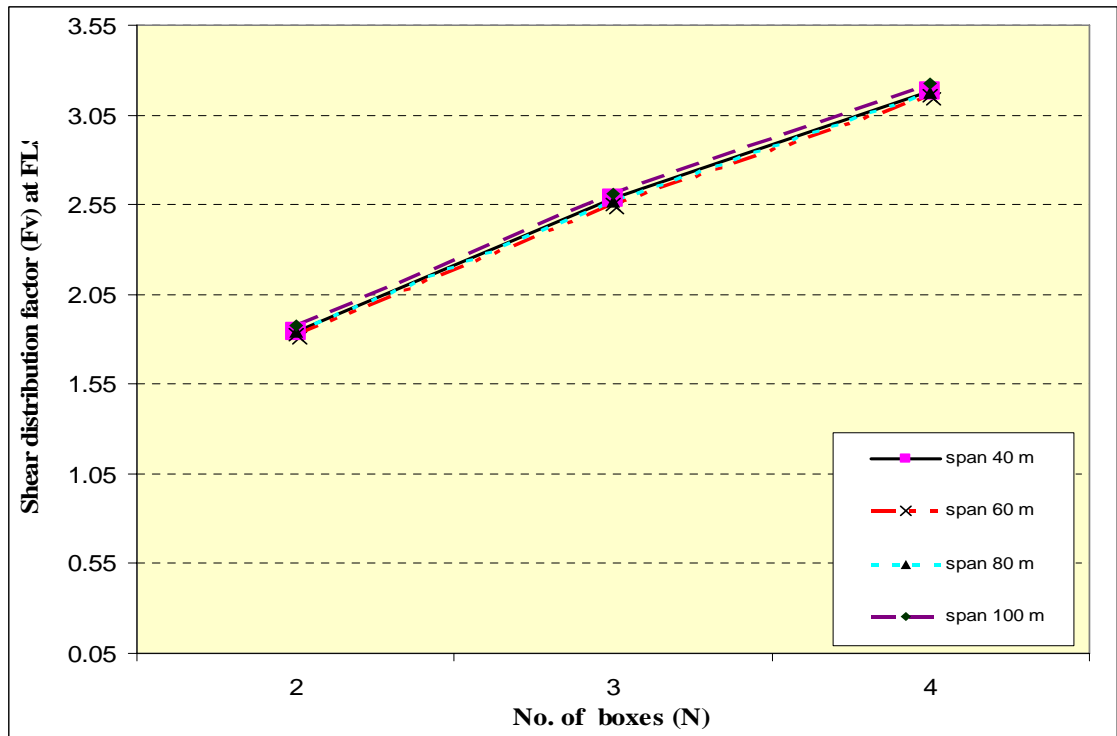


Figure 5.19 Correlation between positive moment distribution factor (F_{m+}) from FEA and CHBDC results at ULS

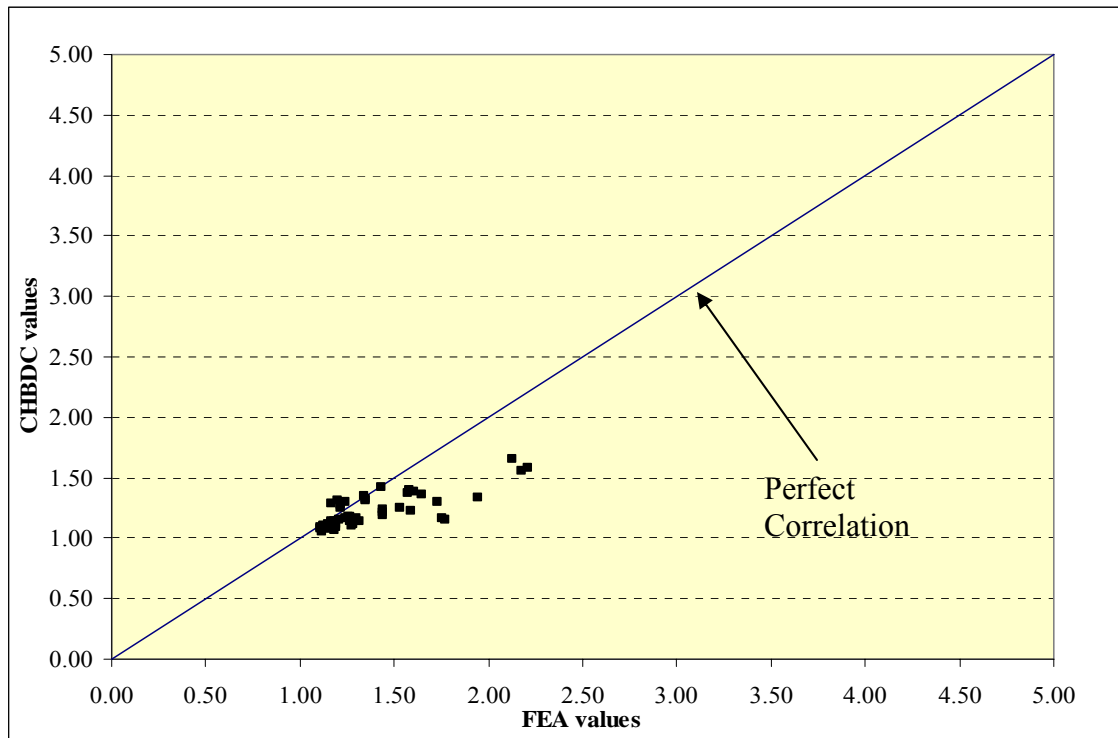


Figure 5.20 Correlation between negative moment distribution factor (F_{m-}) from FEA and CHBDC results at ULS.

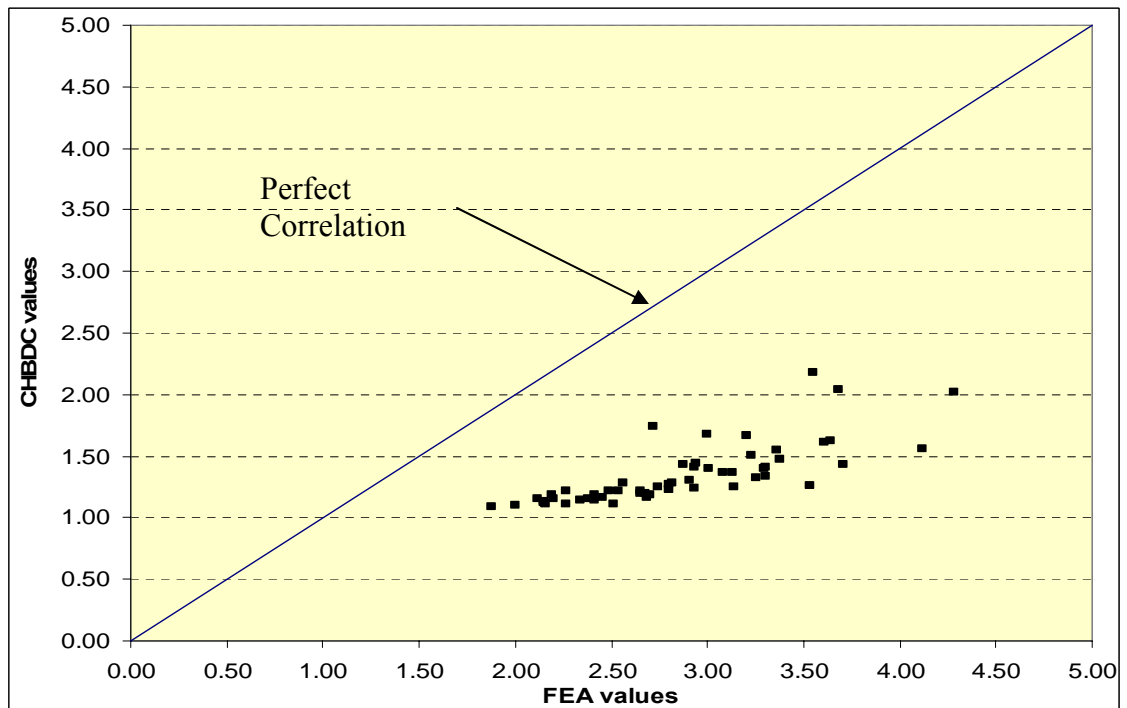


Figure 5.21 Correlation between Shear Distribution factors (F_v) at internal support from FEA and CHBDC results at ULS.

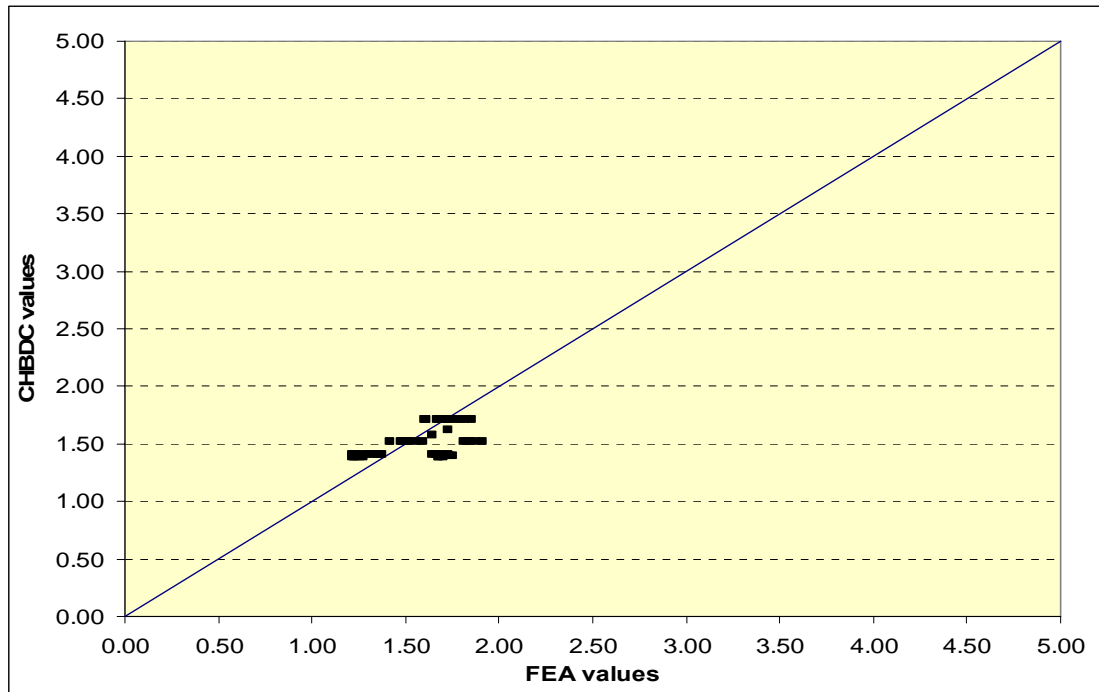


Figure 5.22 Correlation between shear distribution factors (F_v) at external support from FEA and CHBDC results at ULS.

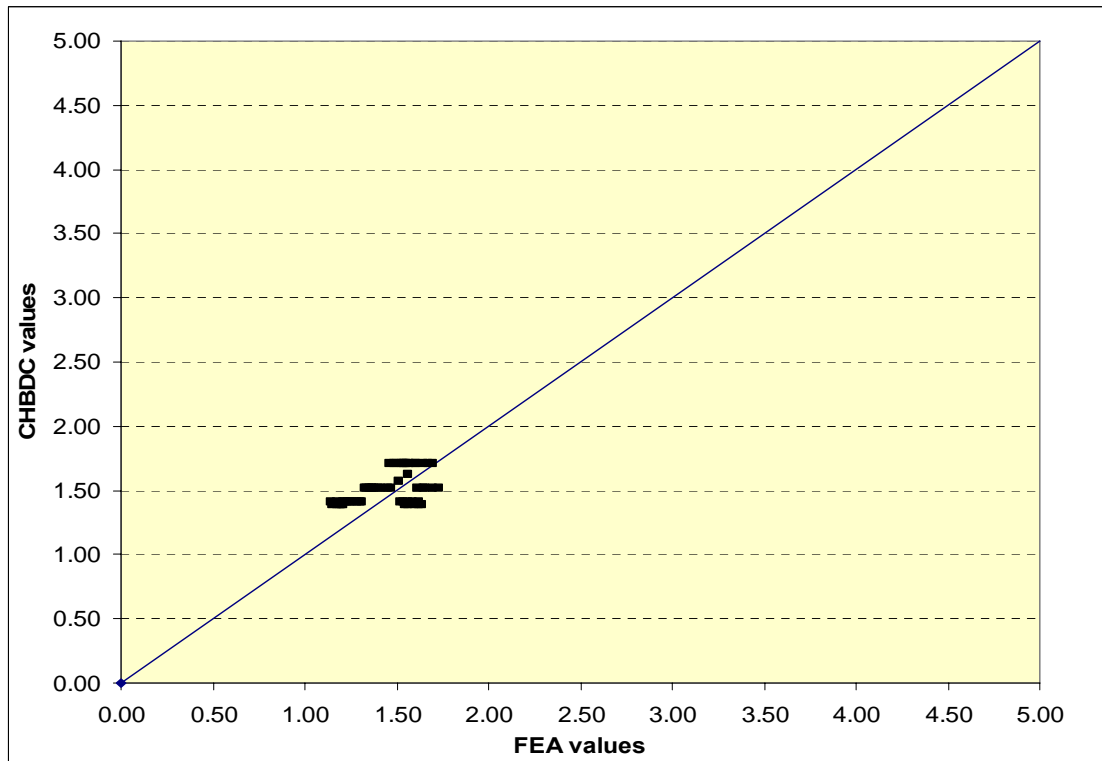


Figure 5.23 Correlation between positive moment distribution factors (F_{m+}) from FEA and CHBDC results at FLS

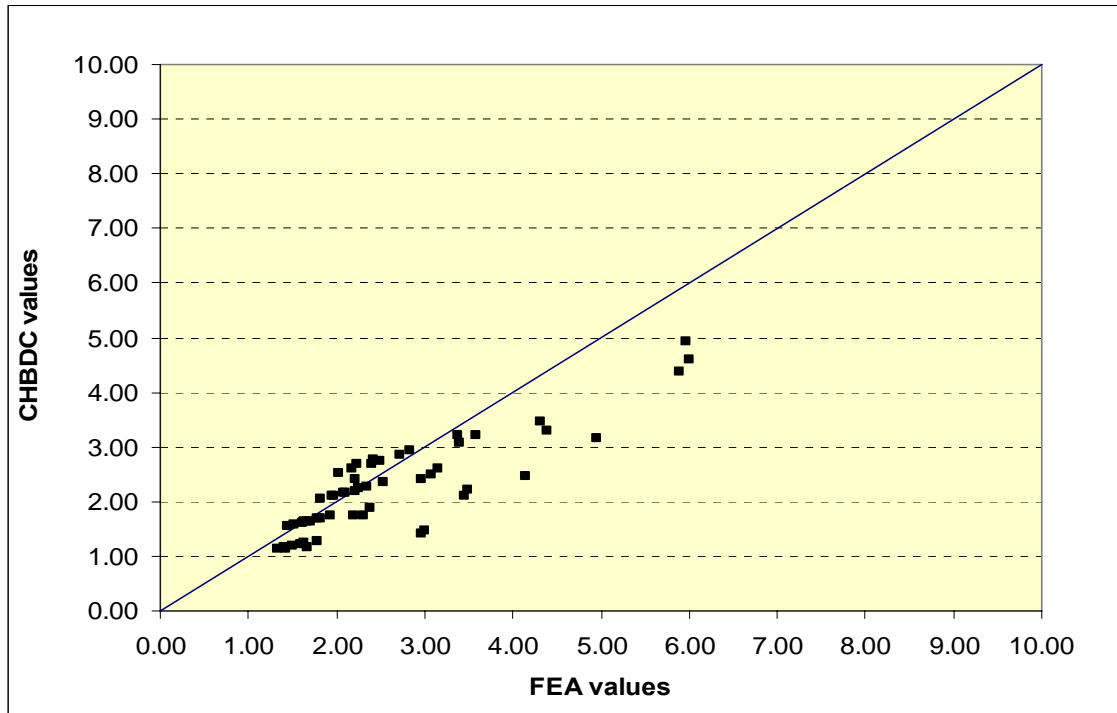


Figure 5.24 Correlation between negative moment distribution factor (F_{m-}) from FEA and CHBDC results at FLS

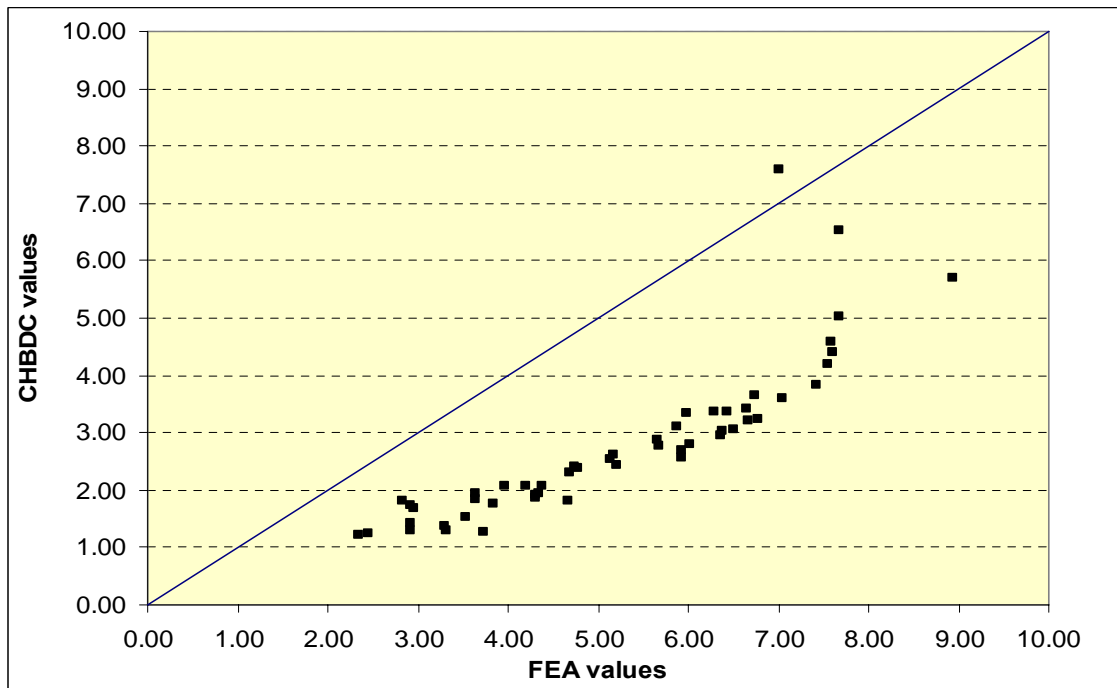


Figure 5.25 Correlation between shear distribution factors (F_v) at internal support from FEA and CHBDC results at FLS

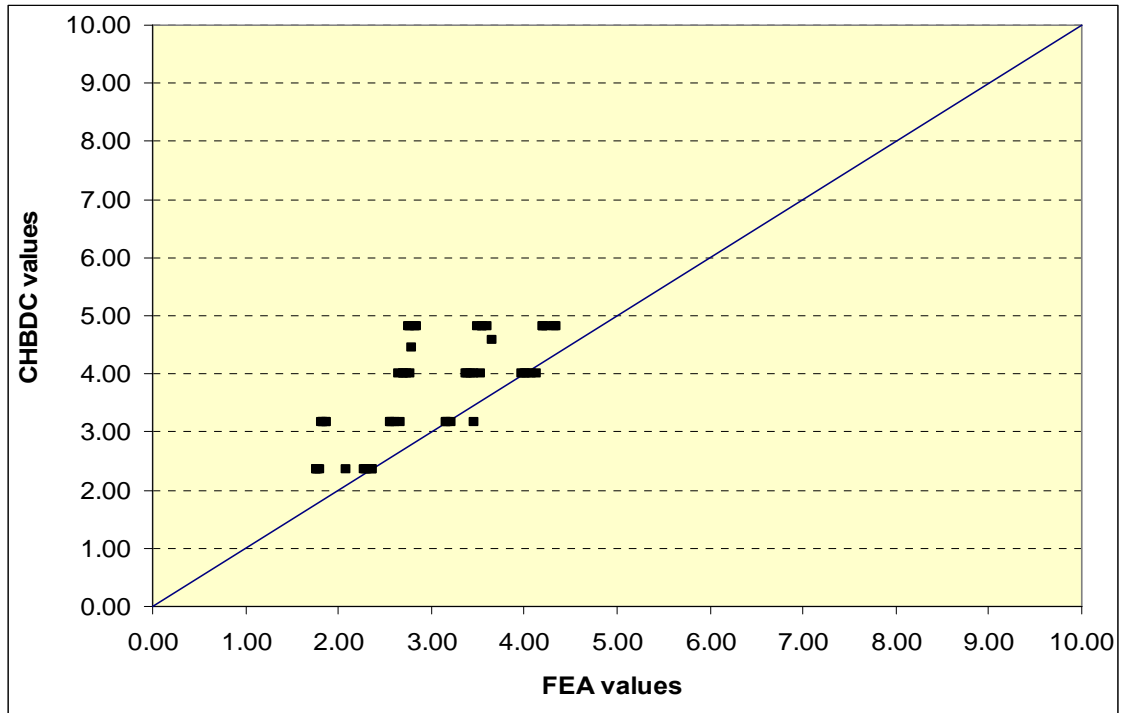


Figure 5.26 Correlation between shear distribution factor (F_v) at external support from FEA and CHBDC results at FLS

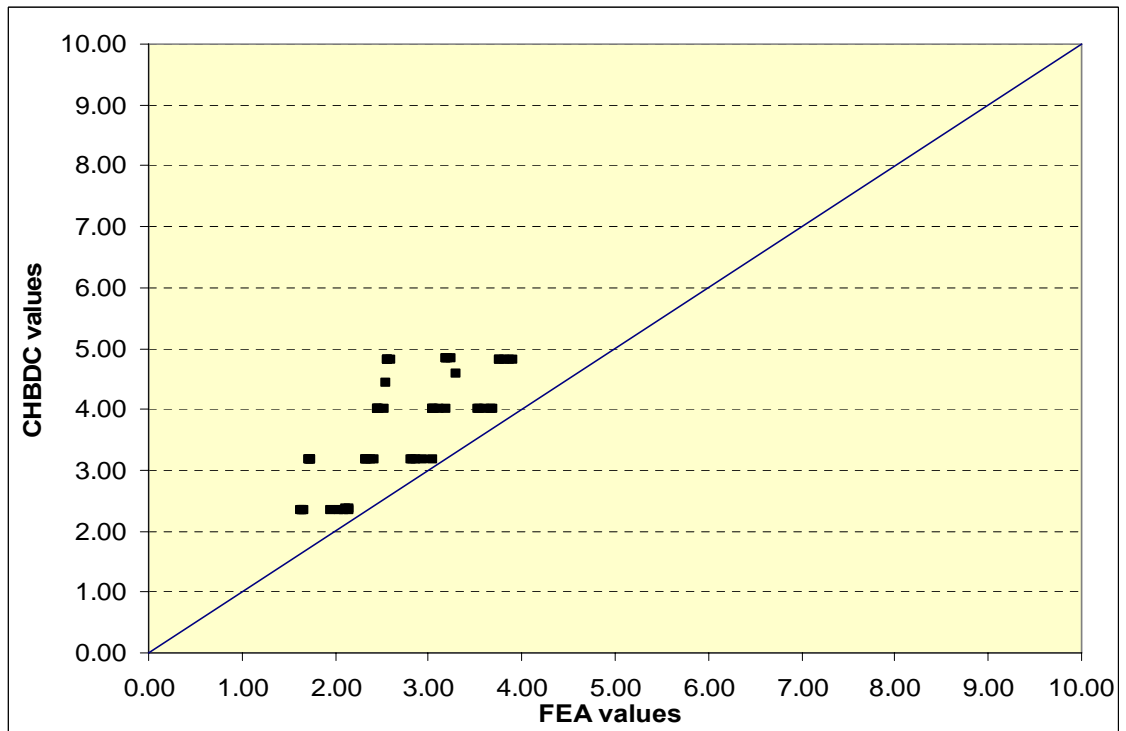


Figure 5.27 Correlation between positive moment distribution factors (F_{m+}) from FEA and AASHTO results at ULS

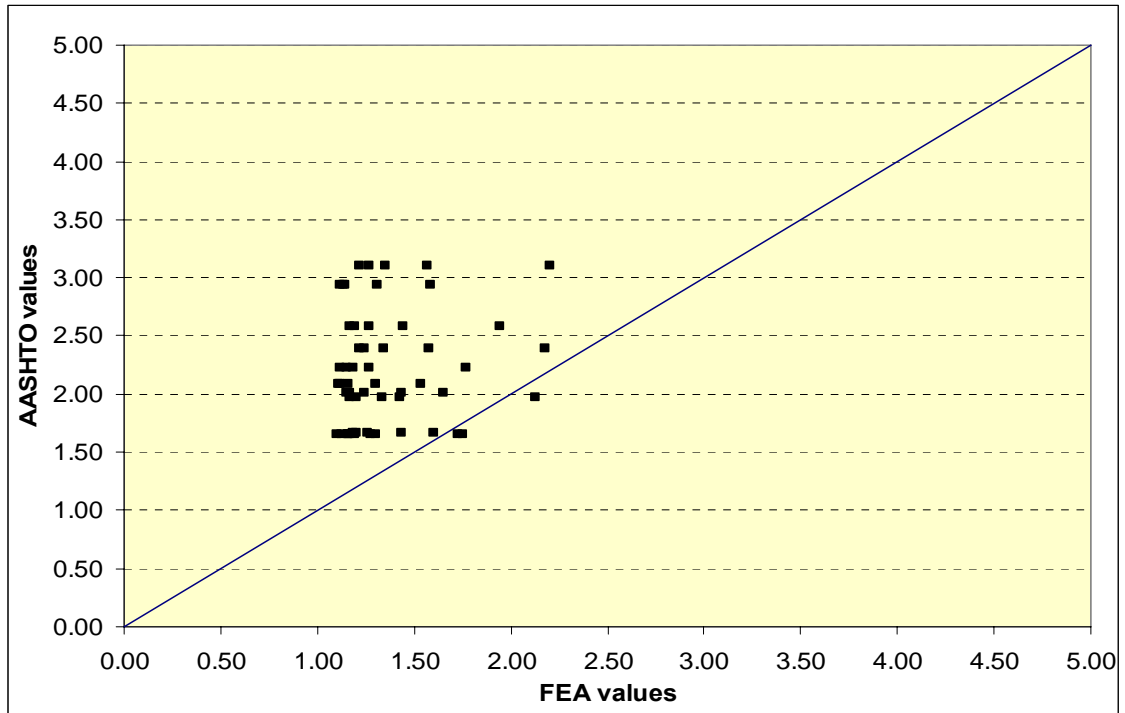


Figure 5.28 Correlation between negative moment distribution factor (F_{m-}) from FEA and AASHTO results at ULS

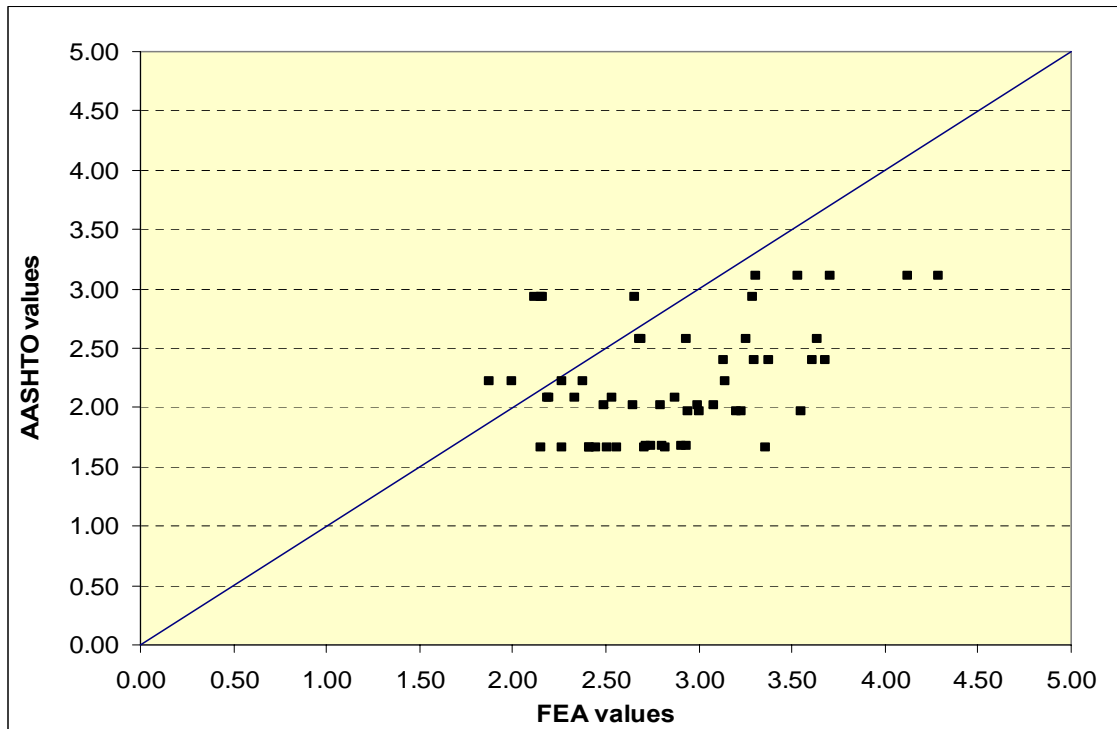


Figure 5.31 Correlation between positive moment distribution factors (F_{m+}) from FEA and AASHTO results at FLS

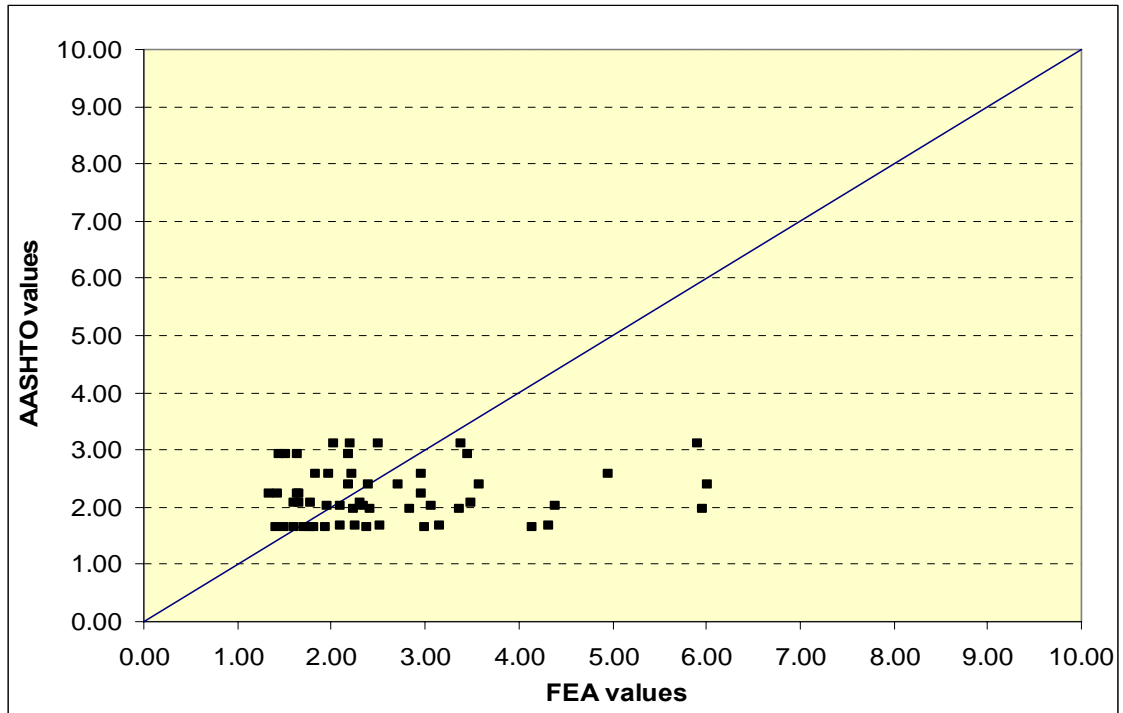


Figure 5.32 Correlation between negative moment distribution factor (F_{m-}) from FEA and AASHTO results at FLS

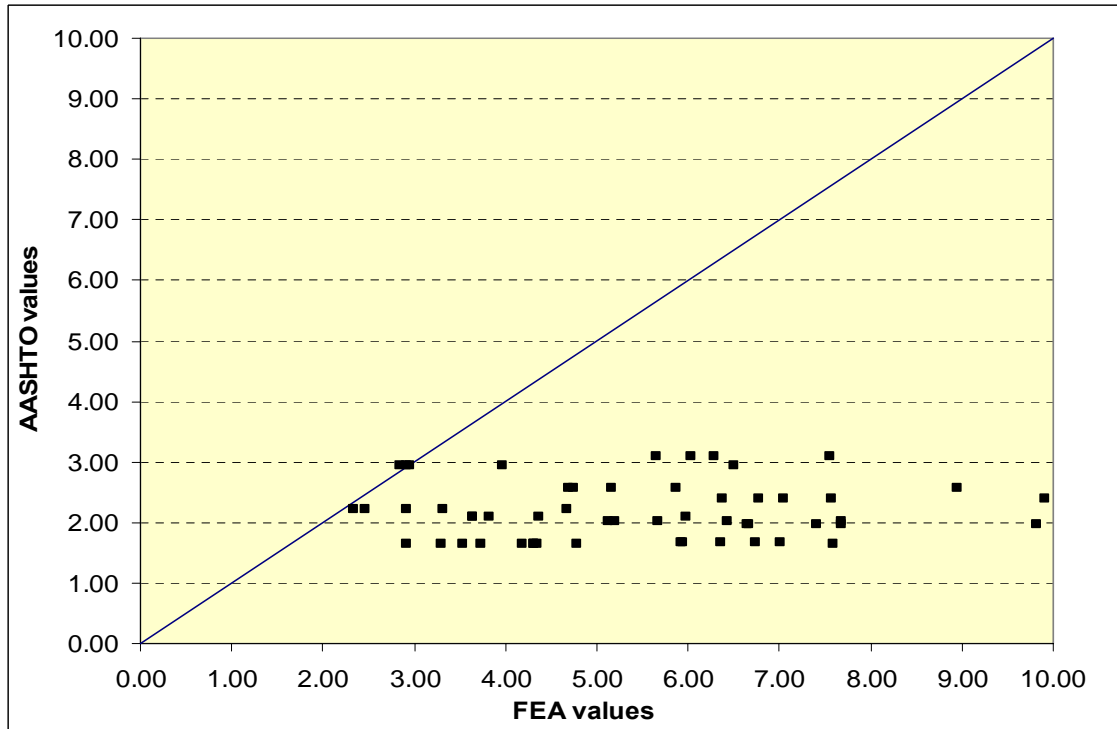


Figure 5.33 Correlation between shear distribution factor (F_v) at internal support from FEA and AASHTO results at FLS

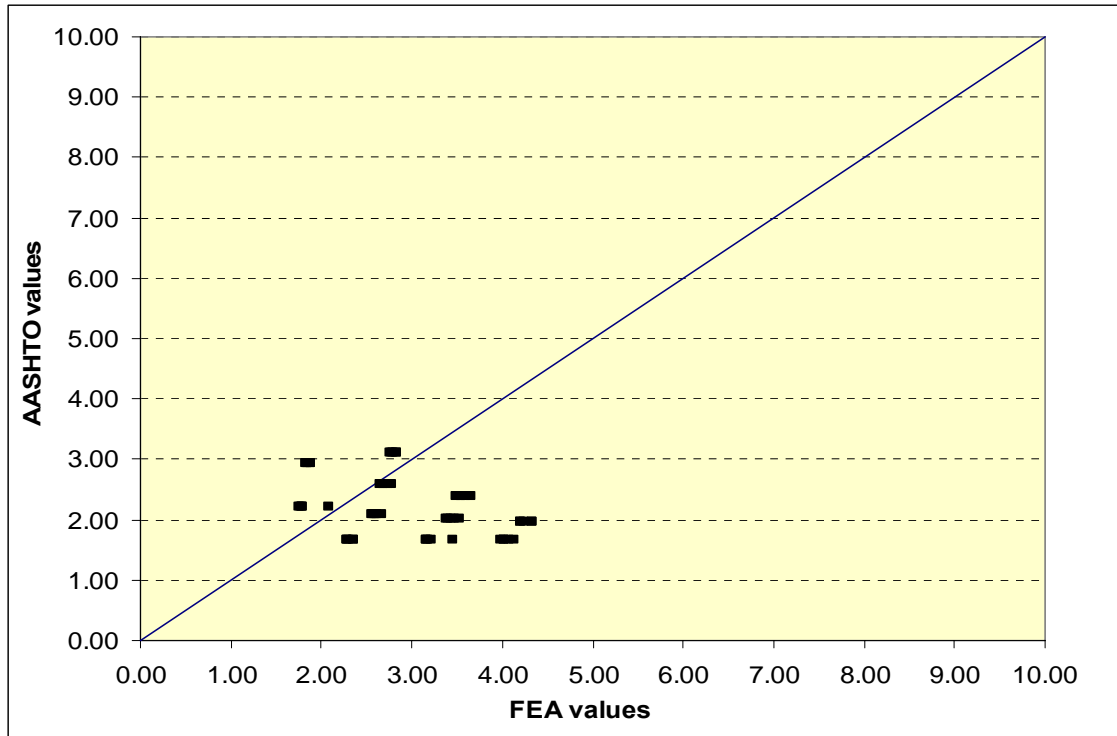


Figure 5.34 Correlation between shear distribution factors (F_v) at external support from FEA and AASHTO results at FLS

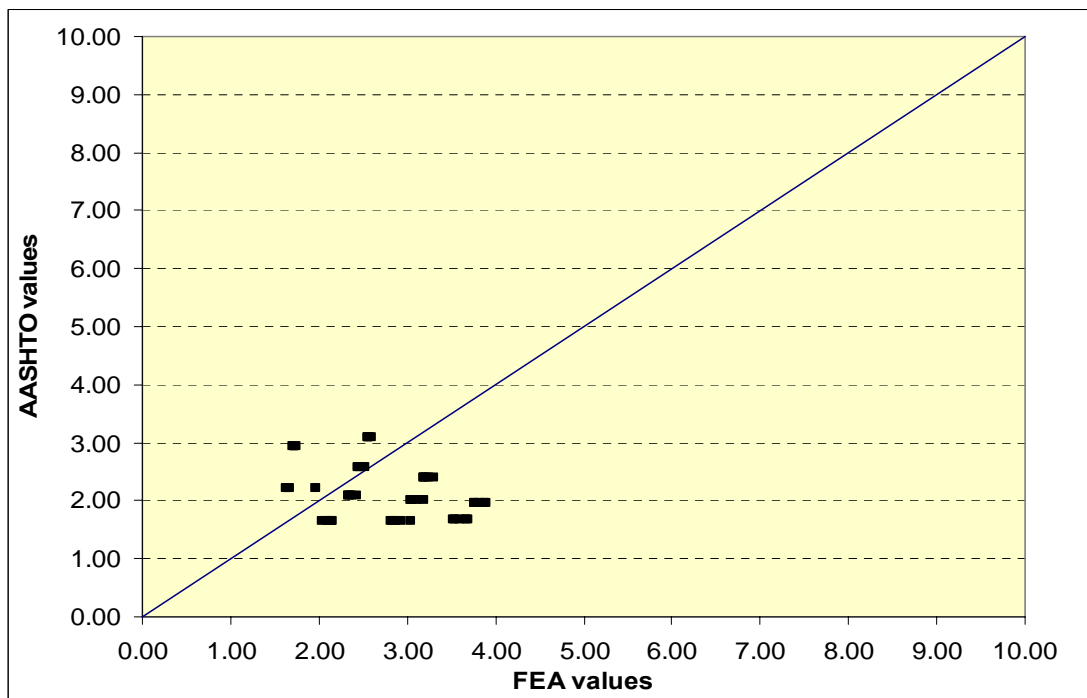


Figure 5.35 Comparison between positive moment distribution factors from the empirical equation and FEA for two lanes bridges at ULS

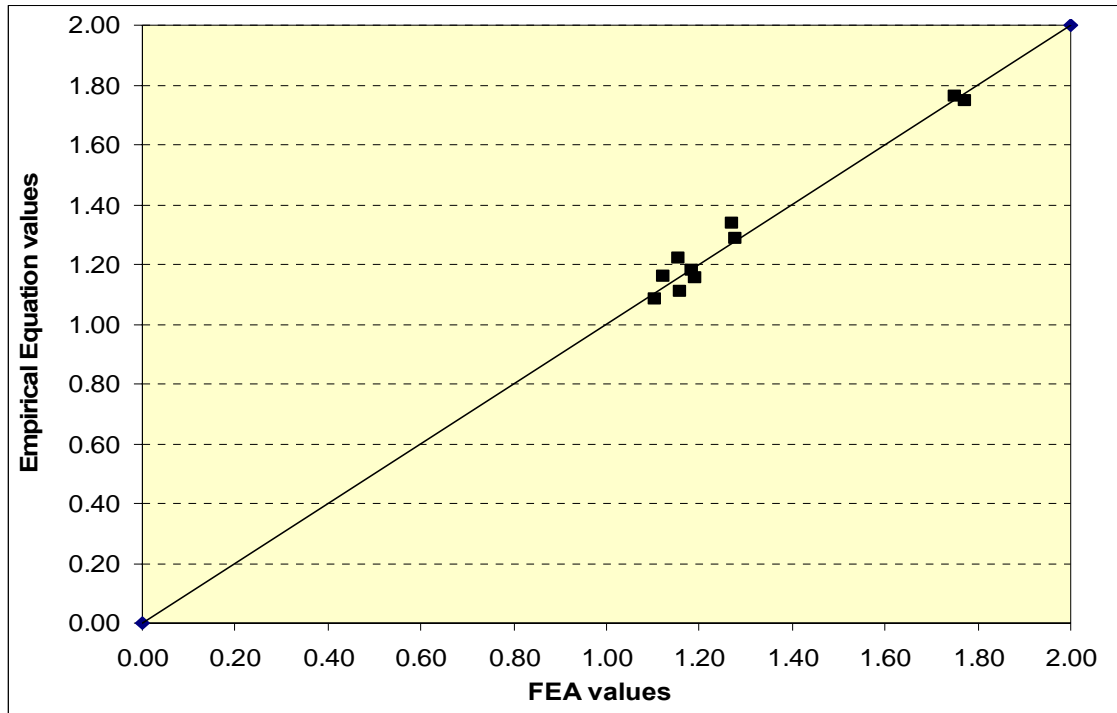


Figure 5.36 Comparison between negative moment distribution factors from the empirical equation and FEA for two lanes bridges at ULS

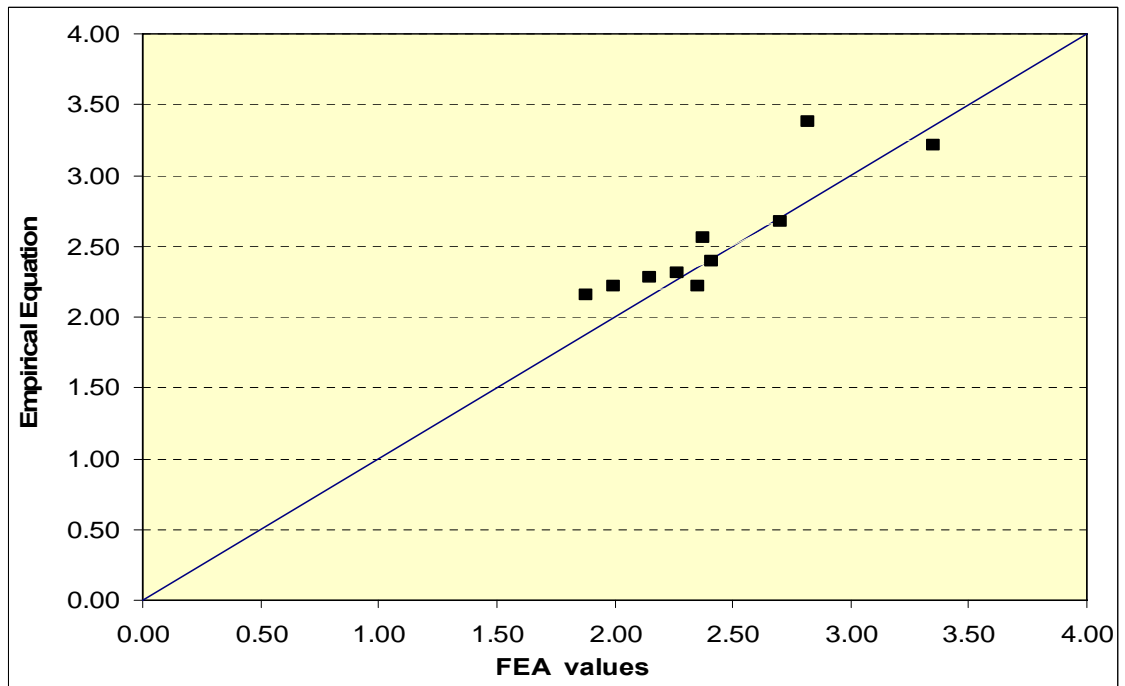


Figure 5.37 Comparison between positive moment distribution factors from the empirical equation and FEA for three lanes bridges at ULS

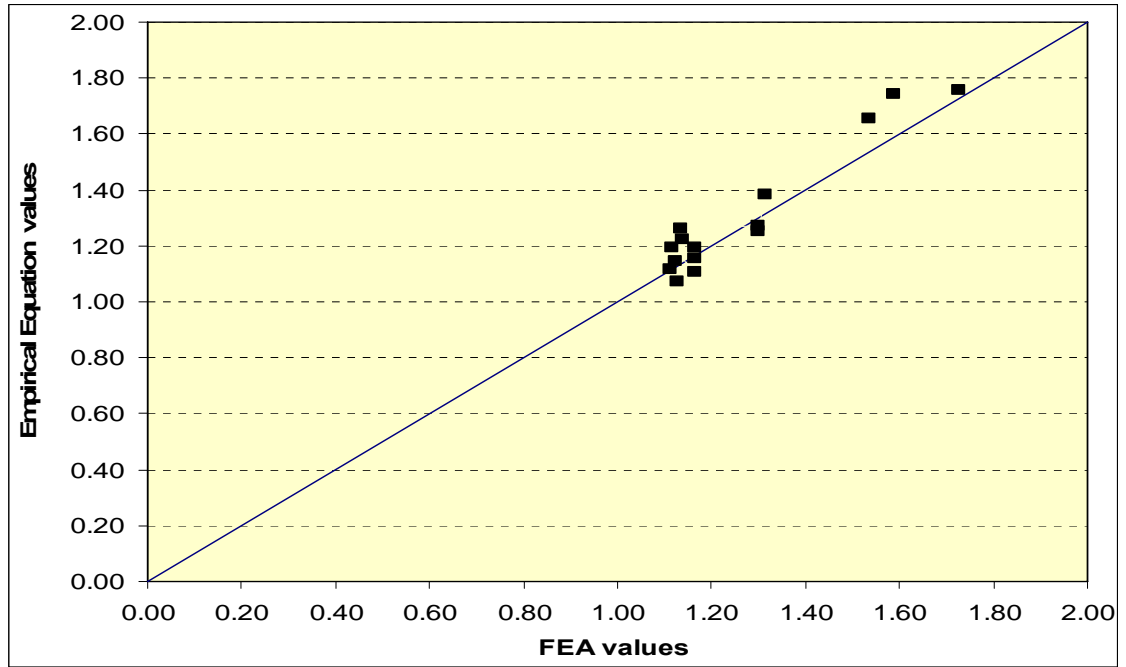


Figure 5.38 Comparison between negative moment distribution factors from the empirical equation and FEA for three lanes bridges at ULS

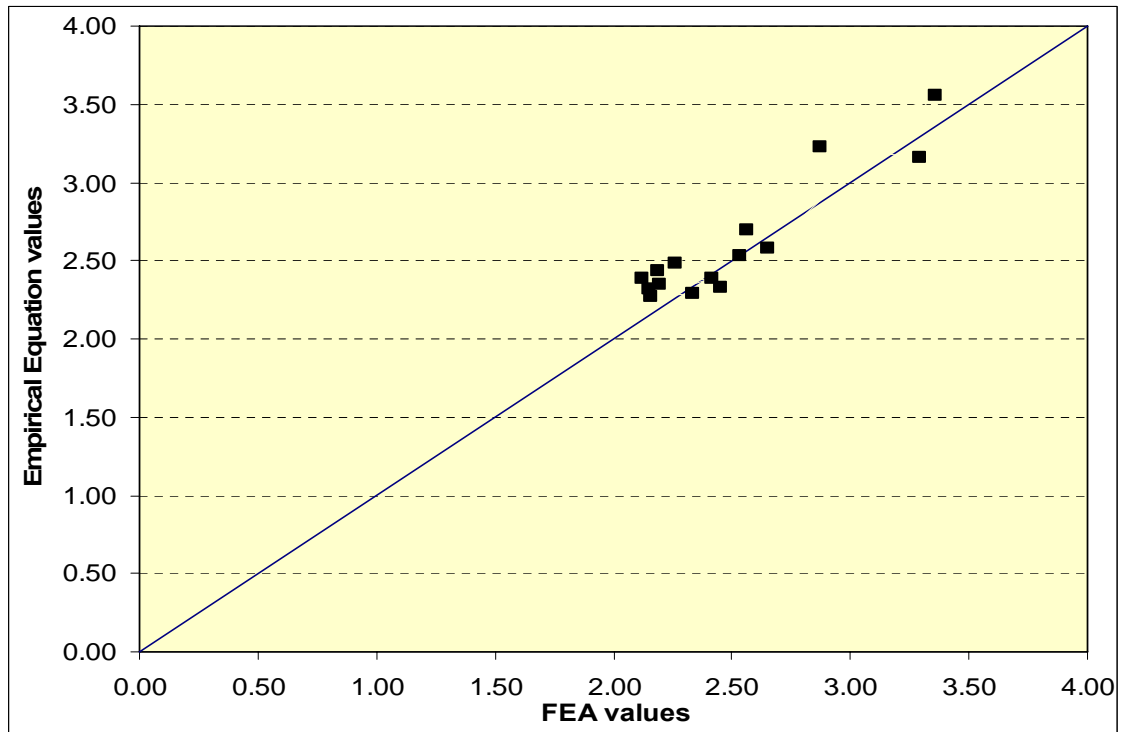


Figure 5.39 Comparison between positive moment distribution factors from the empirical equation and FEA for four lanes bridges at ULS

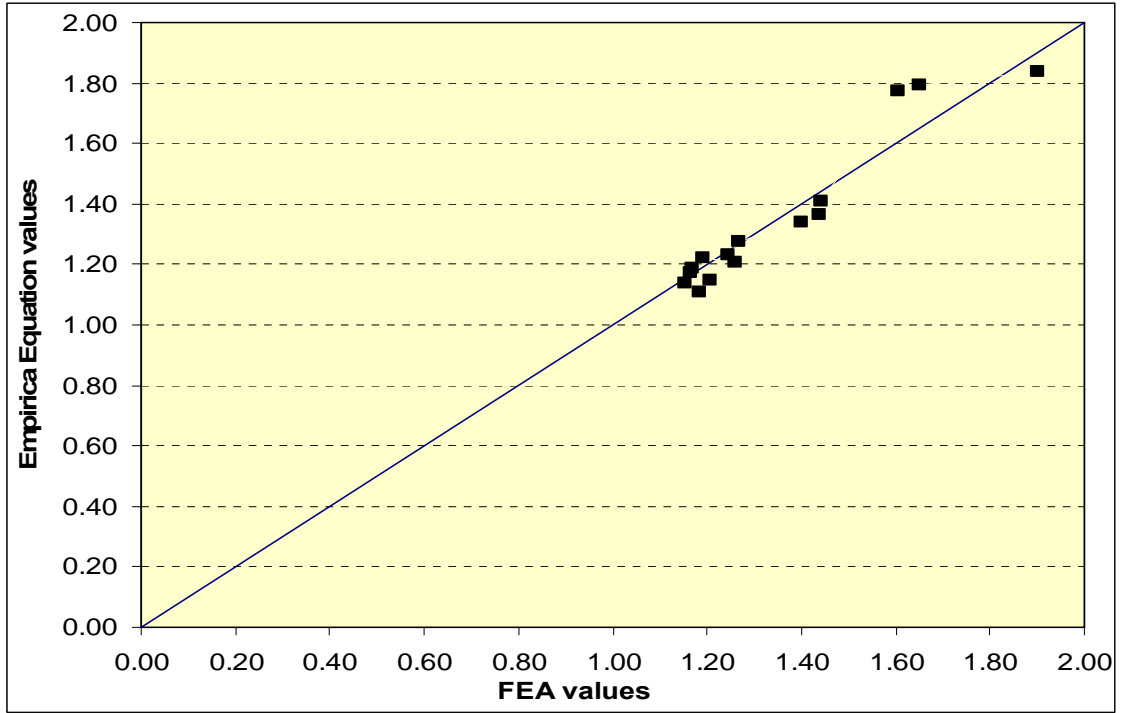


Figure 5.40 Comparison between positive moment distribution factors from the empirical equation and FEA for four lanes bridges at ULS

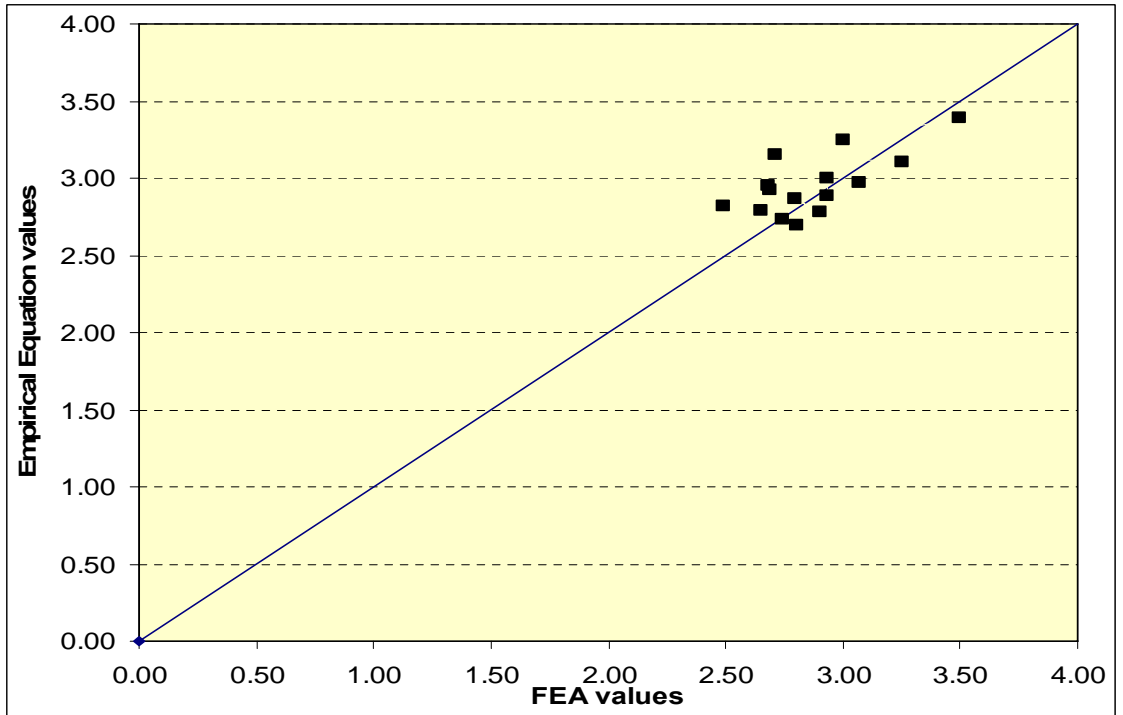


Figure 5.41 Comparison between positive moment distribution factors from the empirical equation and FEA for five lanes bridges at ULS

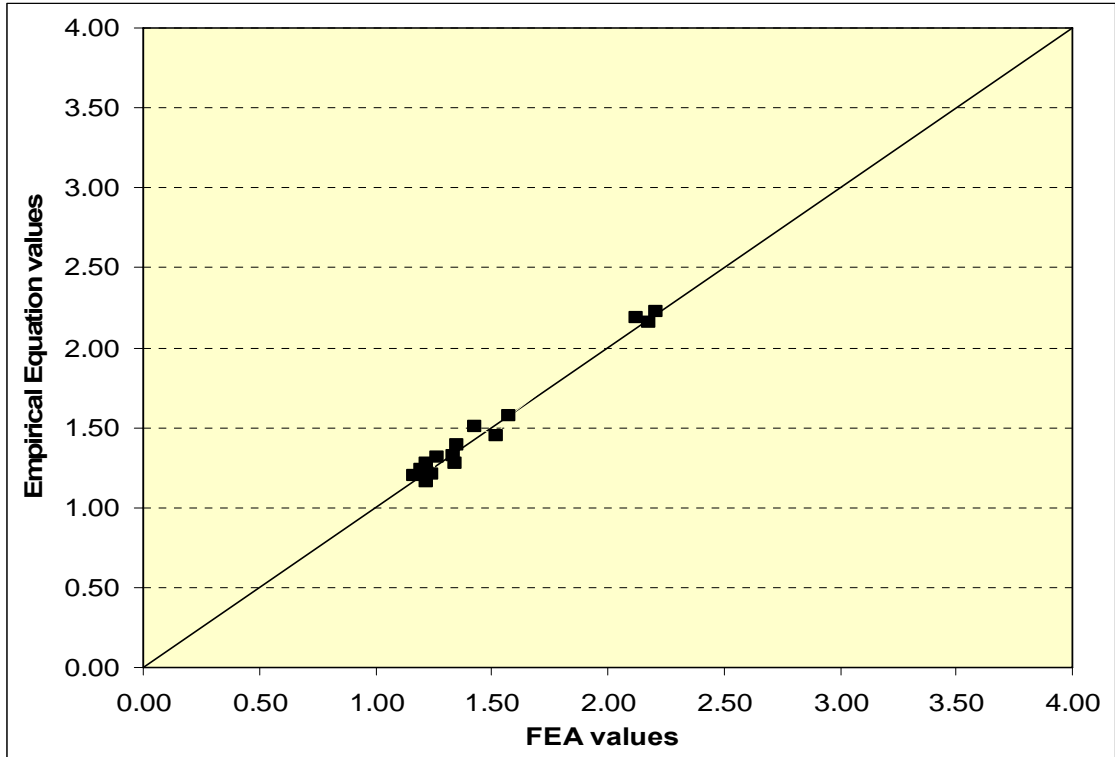


Figure 5.42 Comparison between negative moment distribution factors from the empirical equation and FEA for five lanes bridges at ULS

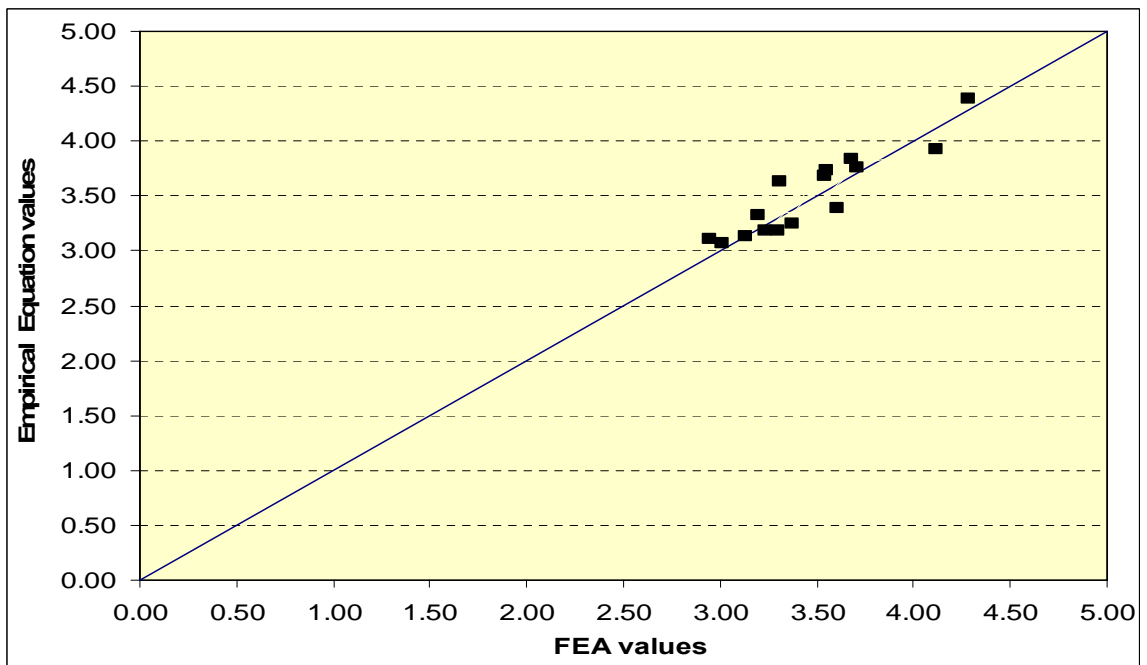


Figure 5.43 Comparison between positive moment distribution factors from the empirical equation and FEA for two lanes bridges at FLS

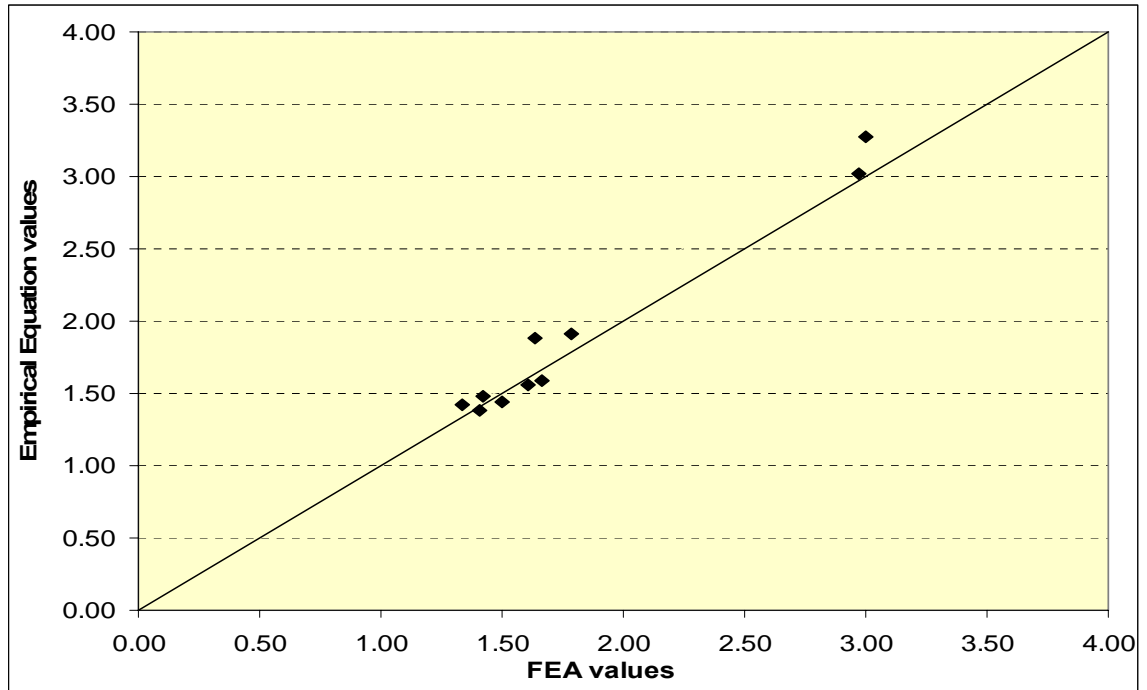


Figure 5.44 Comparison between negative moment distribution factors from the empirical equation and FEA for two lanes bridges at FLS

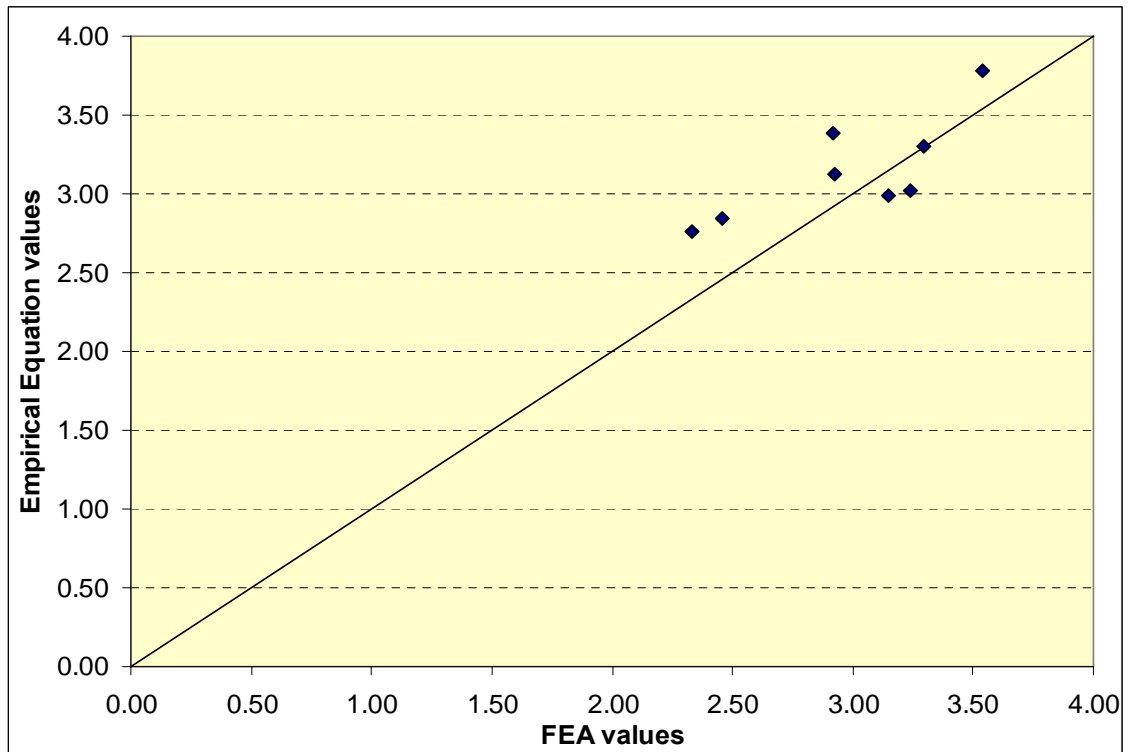


Figure 5.45 Comparison between positive moment distribution factors from the empirical equation and FEA for three lanes bridges at FLS

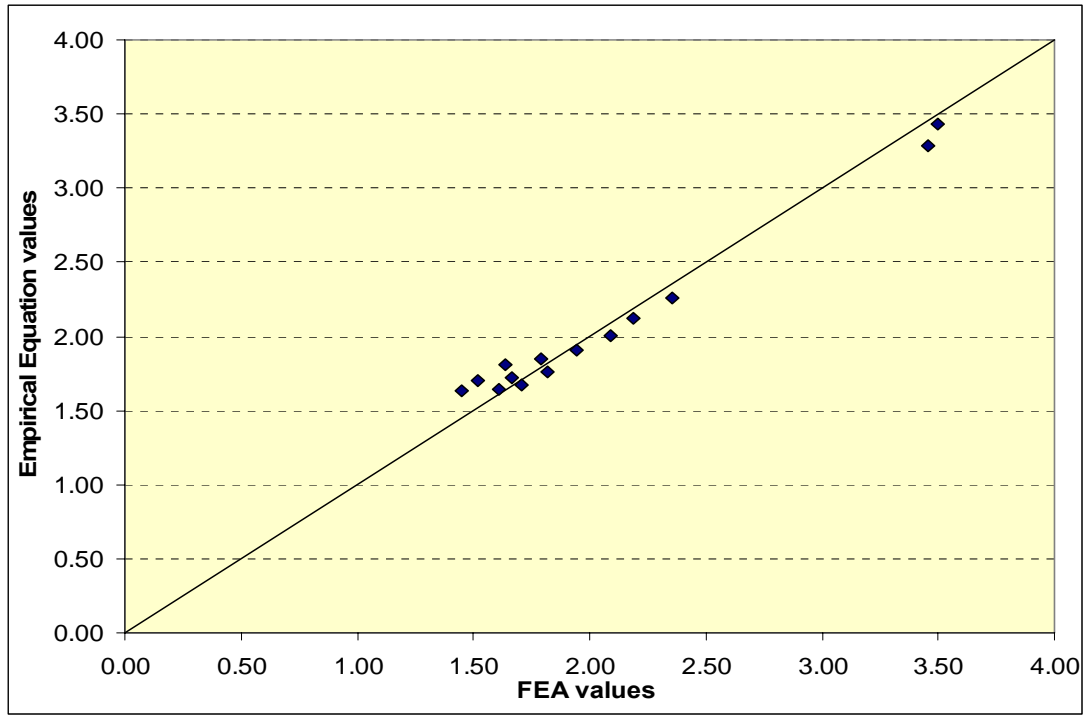


Figure 5.46 Comparison between negative moment distribution factors from the empirical equation and FEA for three lanes bridges at FLS

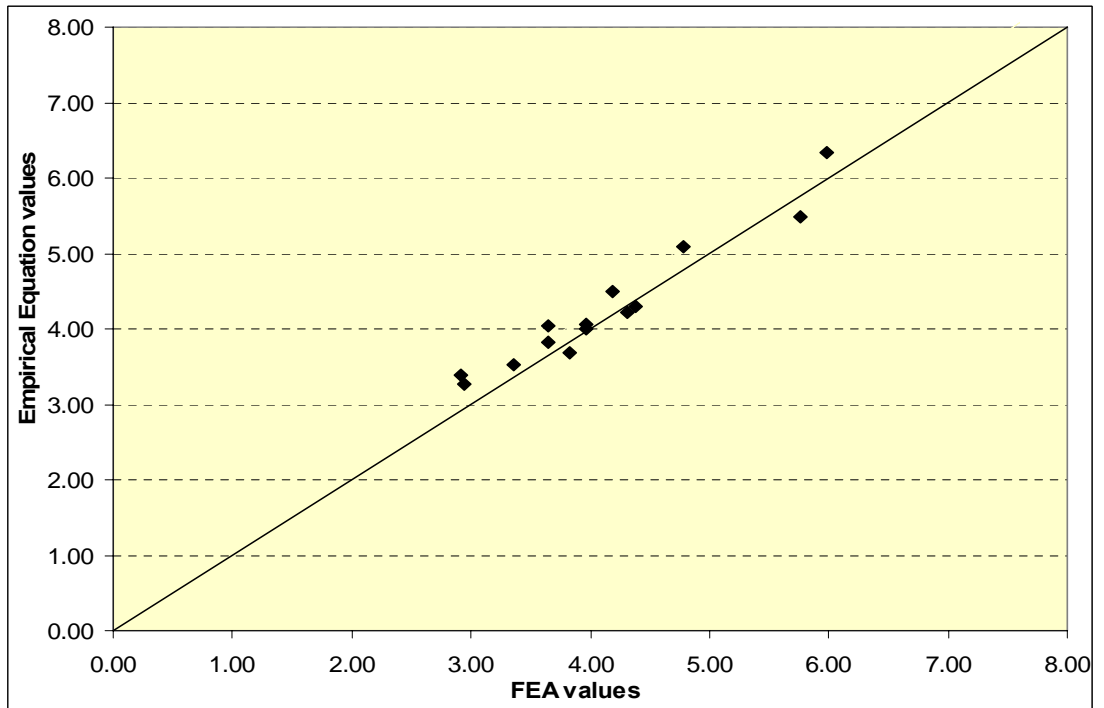


Figure 5.47 Comparison between positive moment distribution factors from the empirical equation and those from FEA for four lanes bridges at FLS

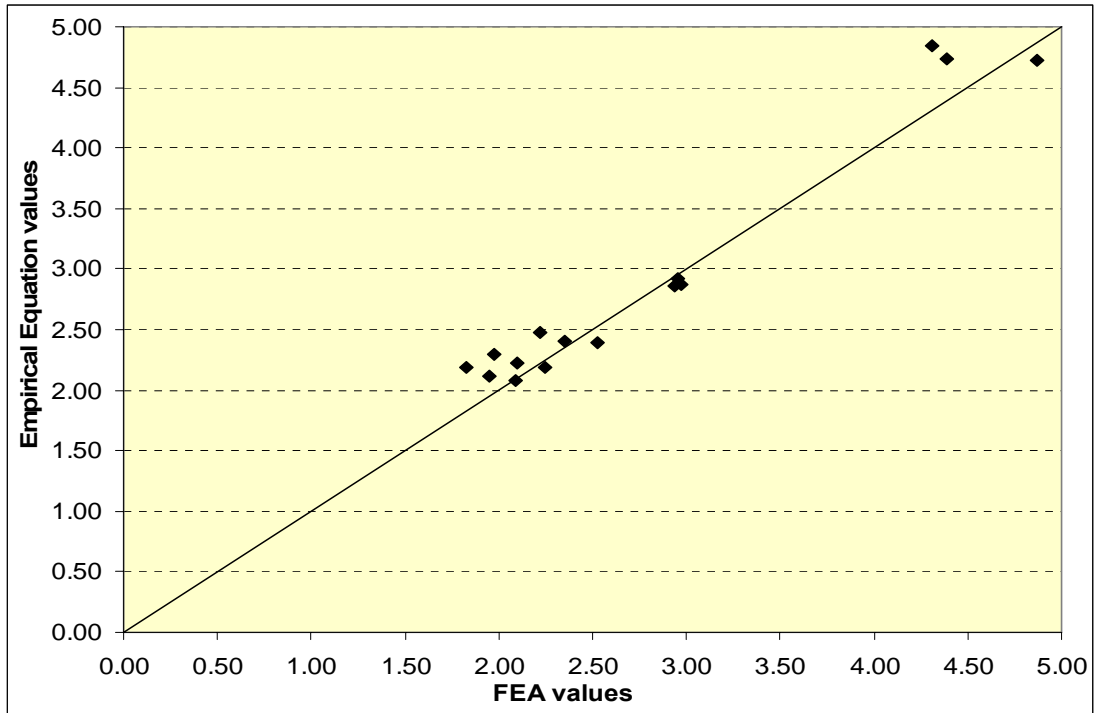


Figure 5.48 Comparison between negative moment distribution factors from the empirical equation and those from FEA for four lanes bridges at FLS

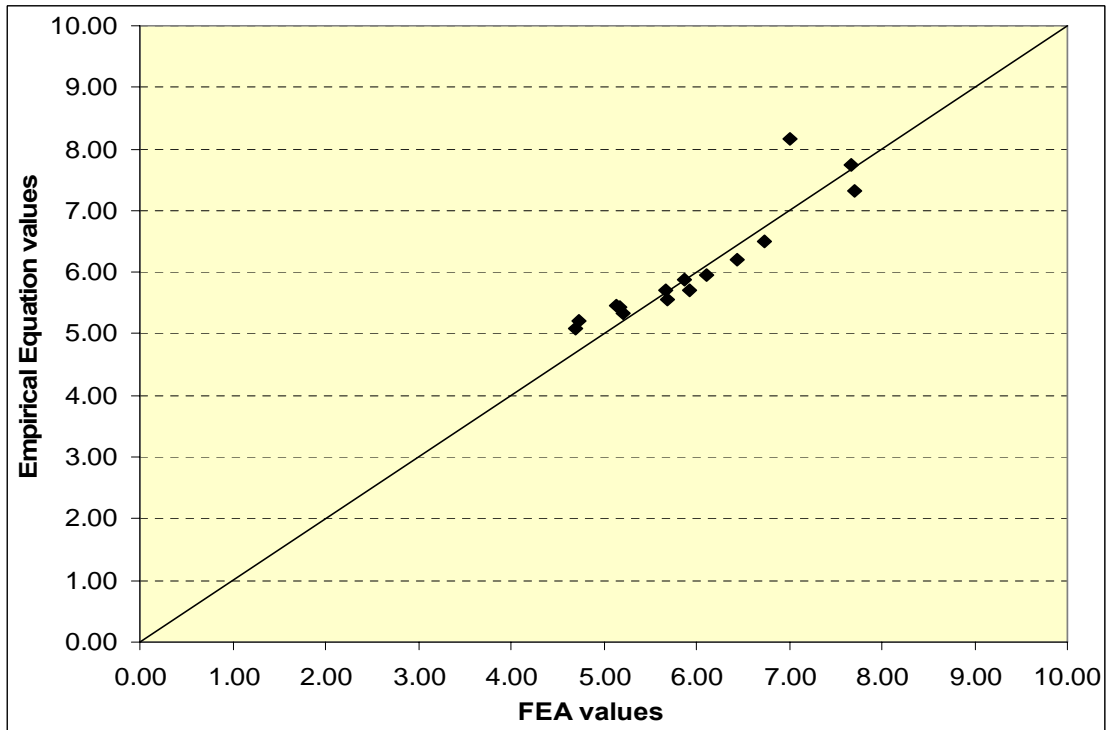


Figure 5.49 Comparison between positive moment distribution factors from the empirical equation and FEA for five lanes bridges at FLS

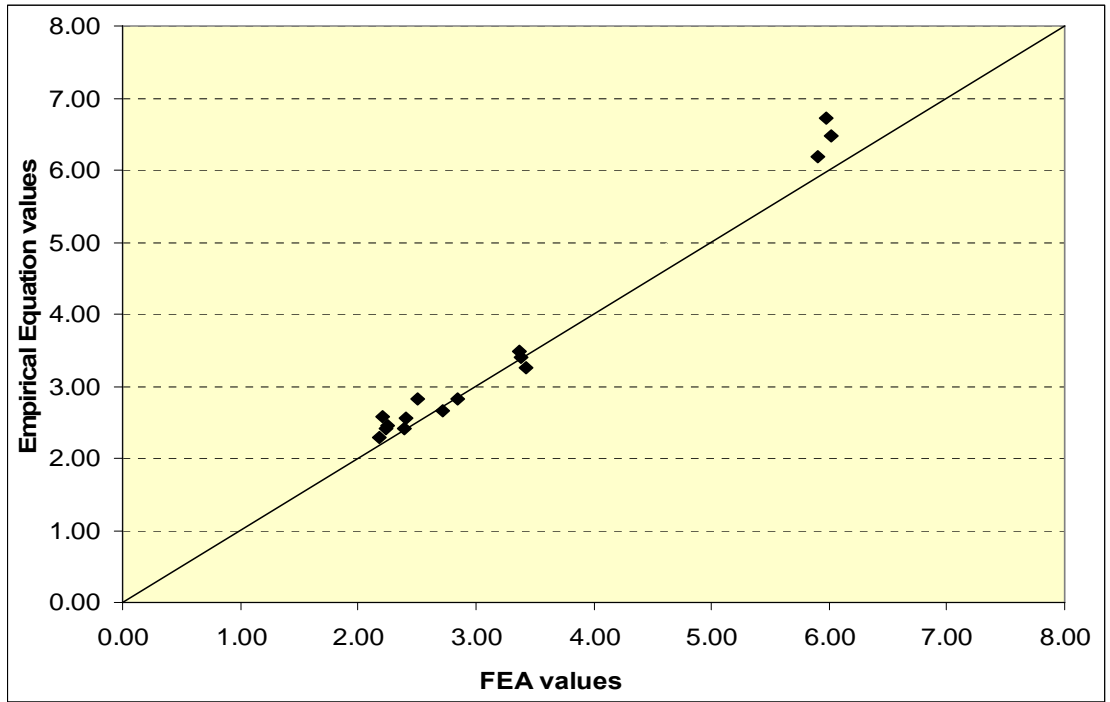


Figure 5.50 Comparison between negative moment distribution factors from the empirical equation and FEA for five lanes bridges at FLS

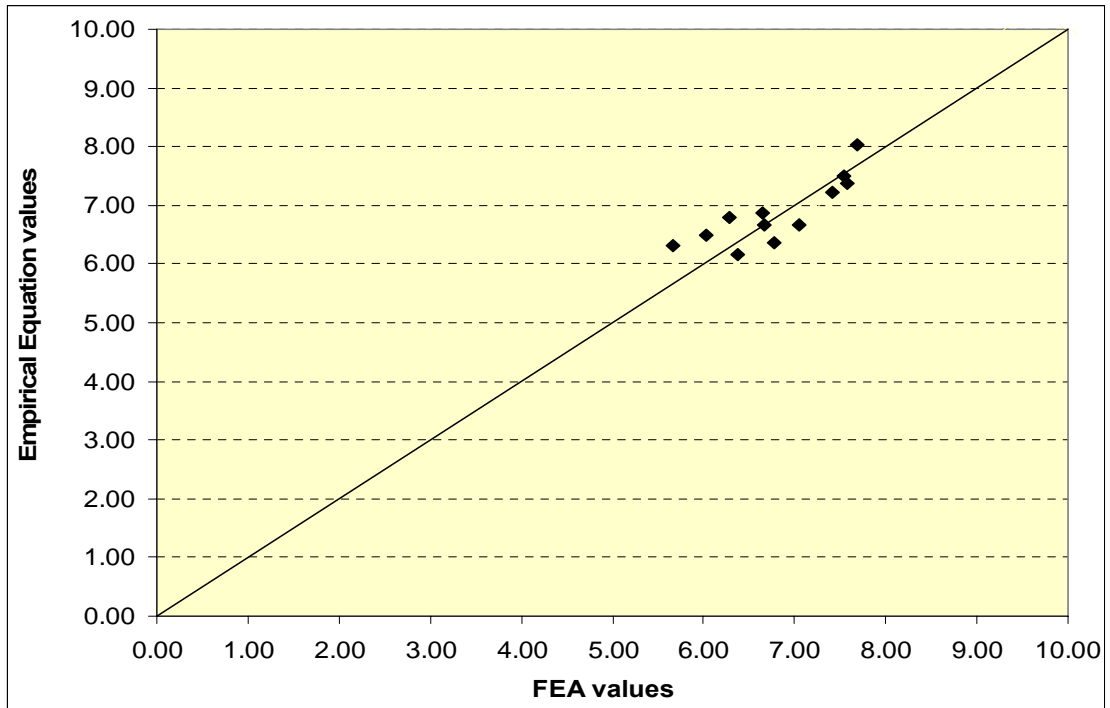


Figure 5.51 Comparison between vertical shear at internal support from the empirical equation and FEA for two lanes bridges at ULS as function of (L)

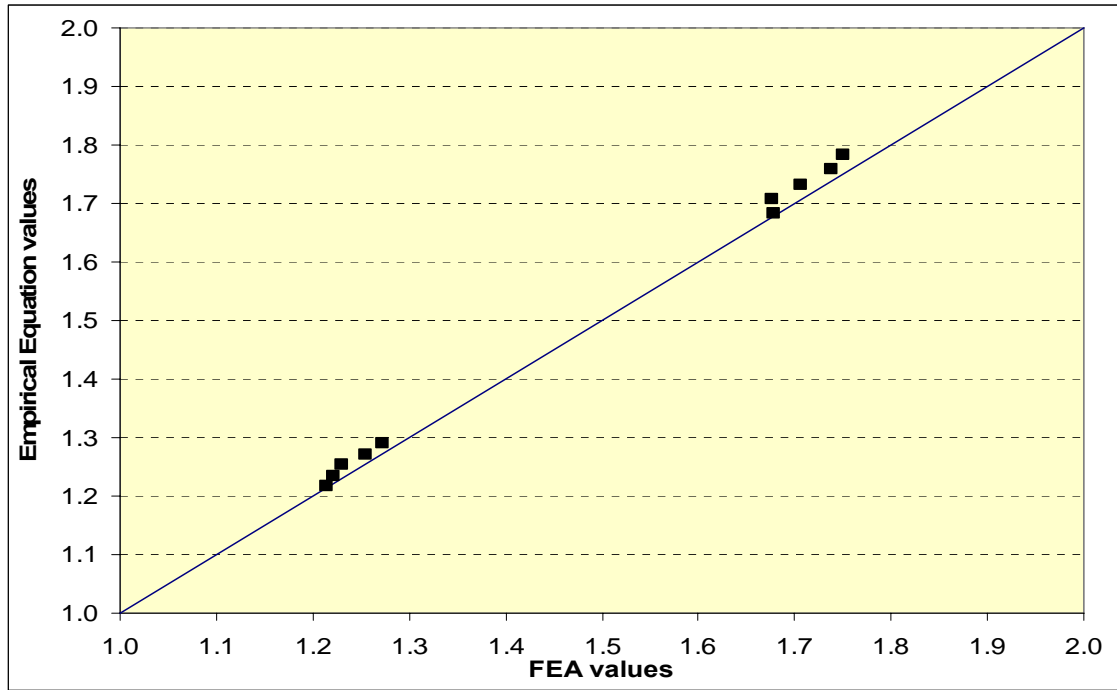


Figure 5.52 Comparison between vertical shear at external support from the empirical equation and FEA for two lanes bridges at ULS as function of (L)

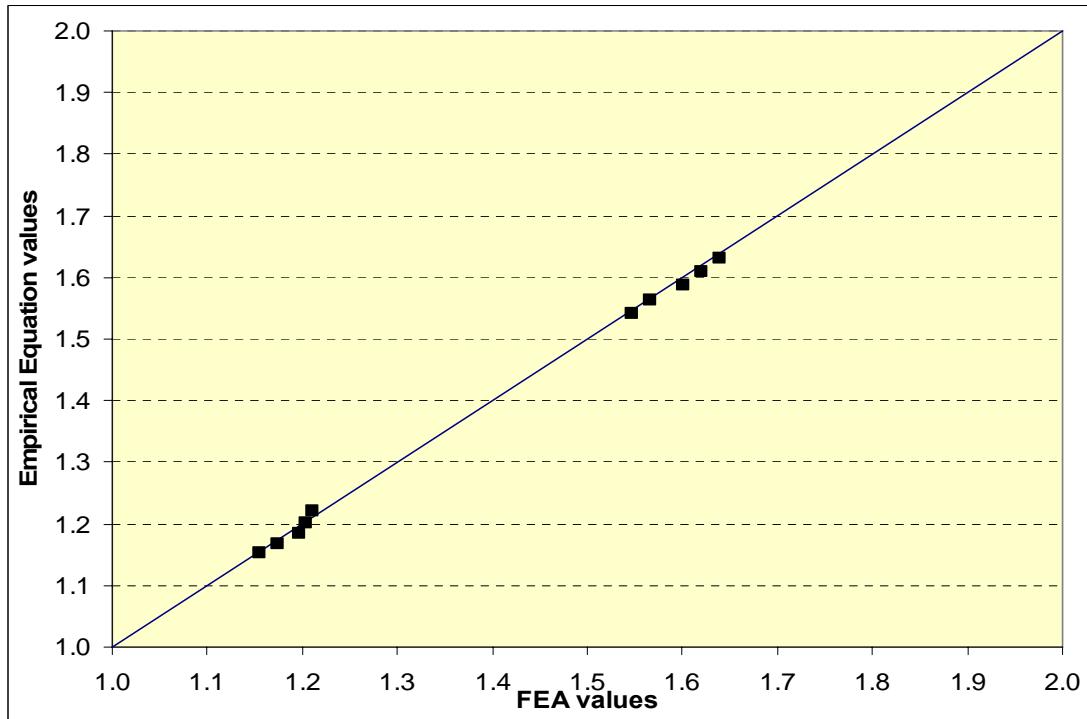


Figure 5.53 Comparison between vertical shear at internal support from the empirical equation and FEA for three lanes bridges at ULS as function of (L)

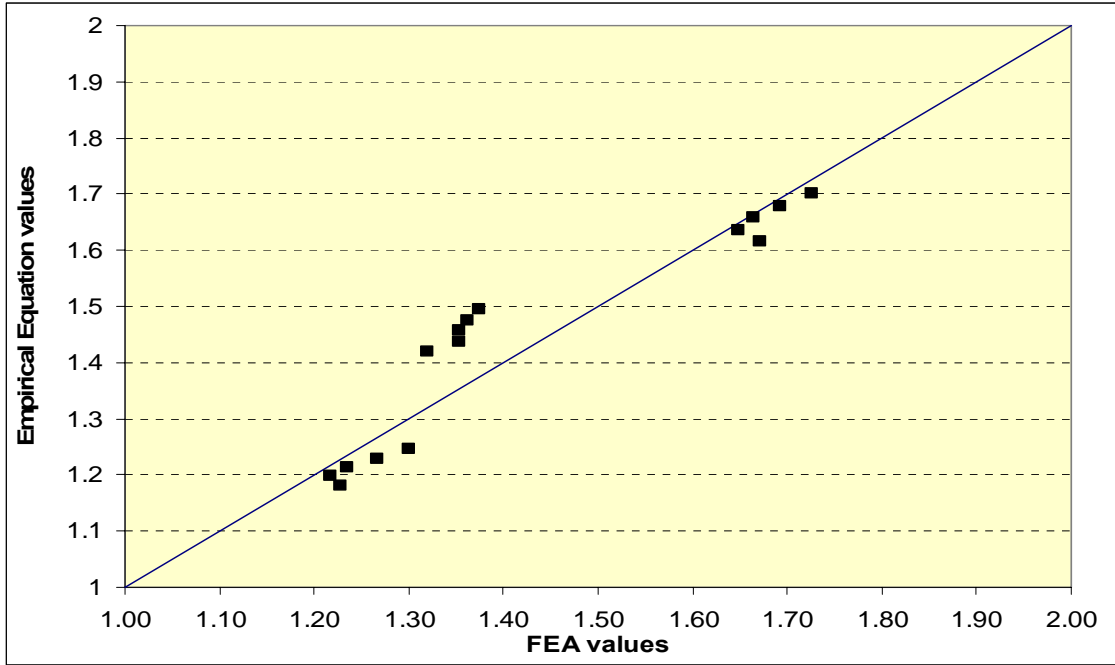


Figure 5.54 Comparison between vertical shear at external support from the empirical equation and FEA for three lanes bridges at ULS as function of (L)

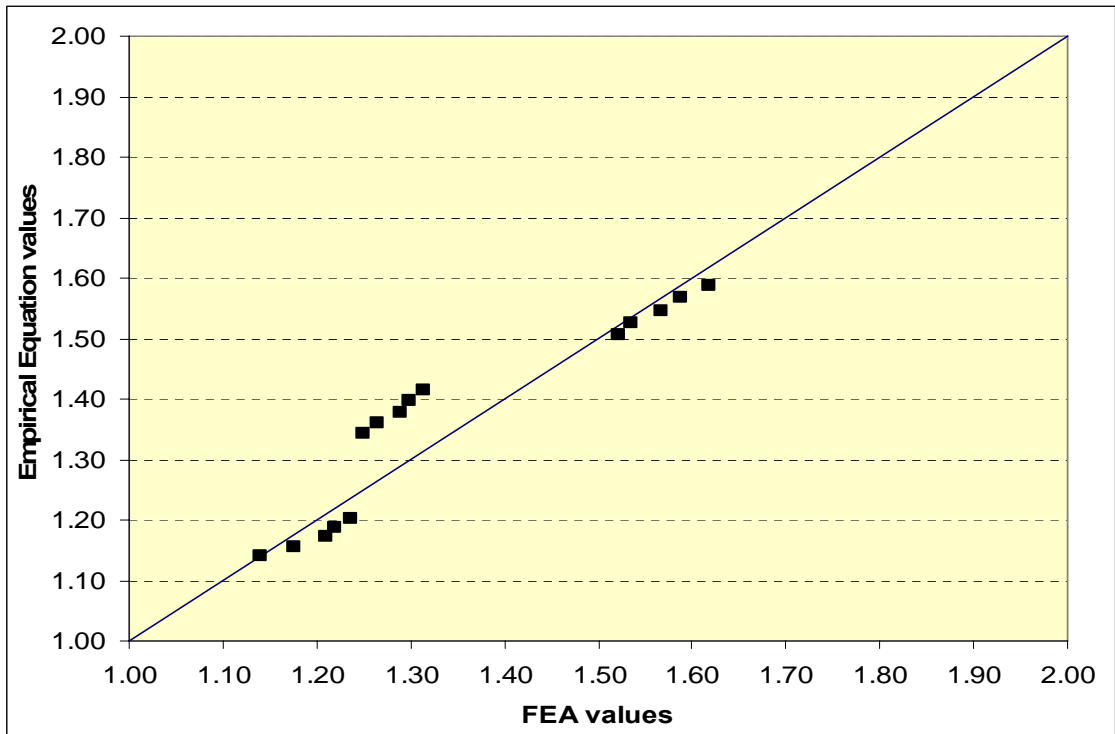


Figure 5.55 Comparison between vertical shear at internal support from the empirical equation and FEA for four lanes bridges at ULS as function of (L)

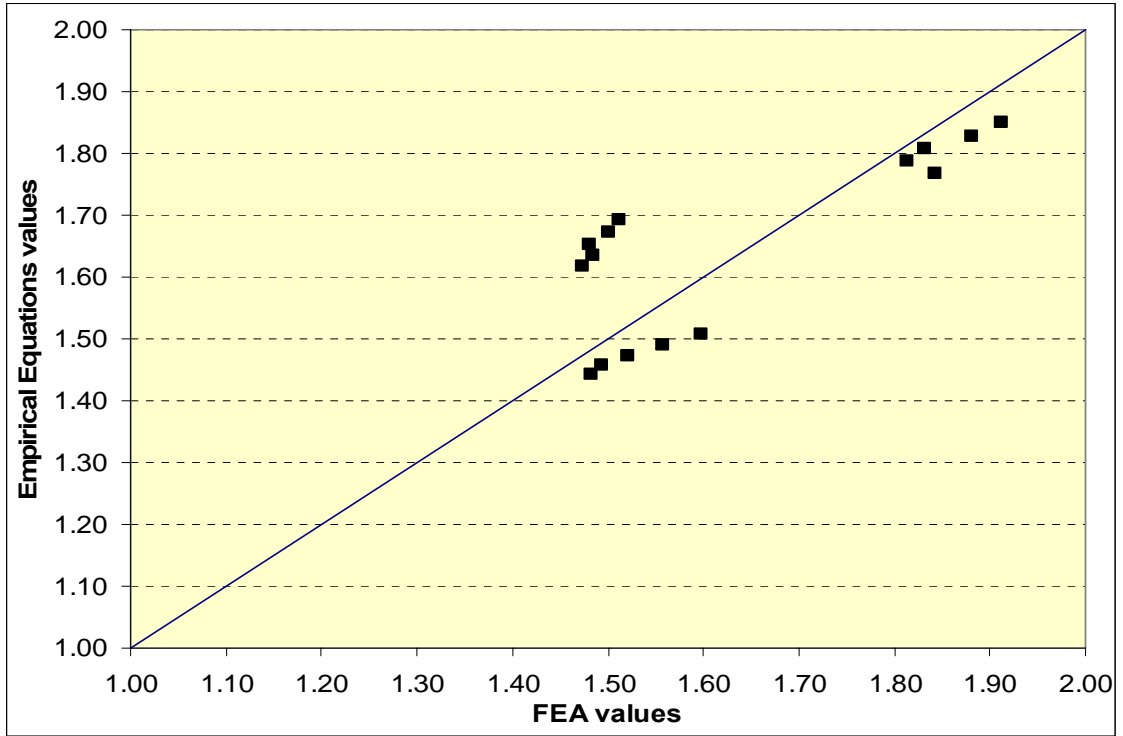


Figure 5.56 Comparison between vertical shear at external support from the empirical equation and FEA for four lanes bridges at ULS as function of (L)

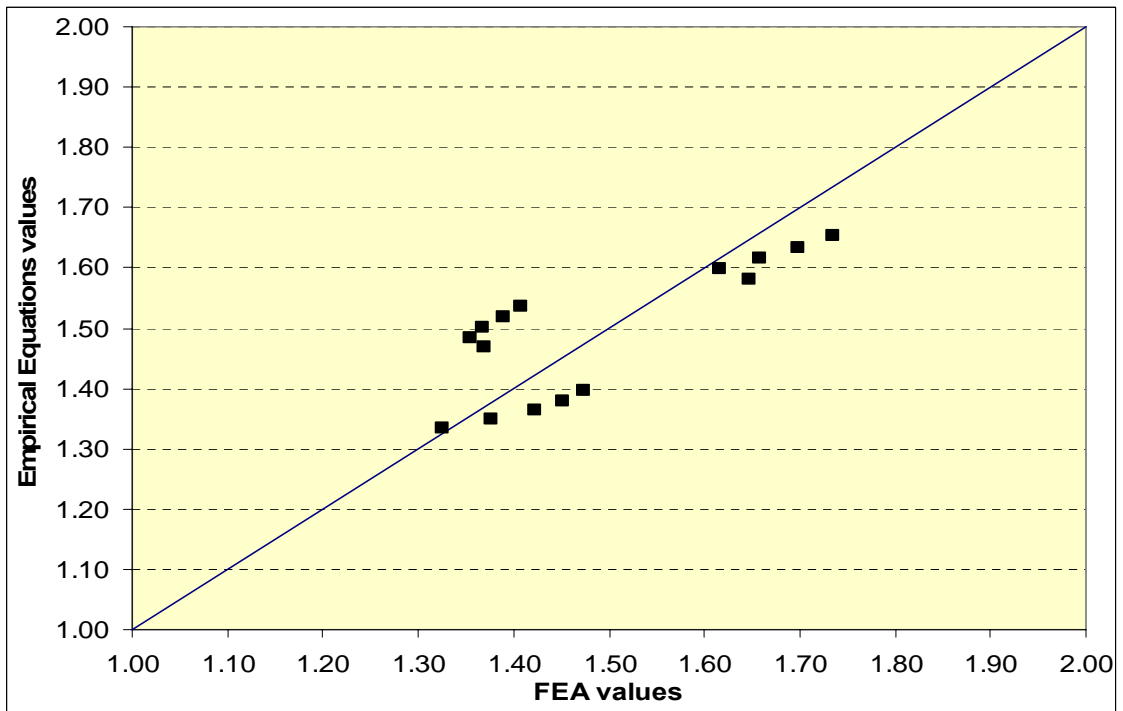


Figure 5.57 Comparison between vertical shear at internal support from the empirical equation and FEA for five lanes bridges at ULS as function of (L)

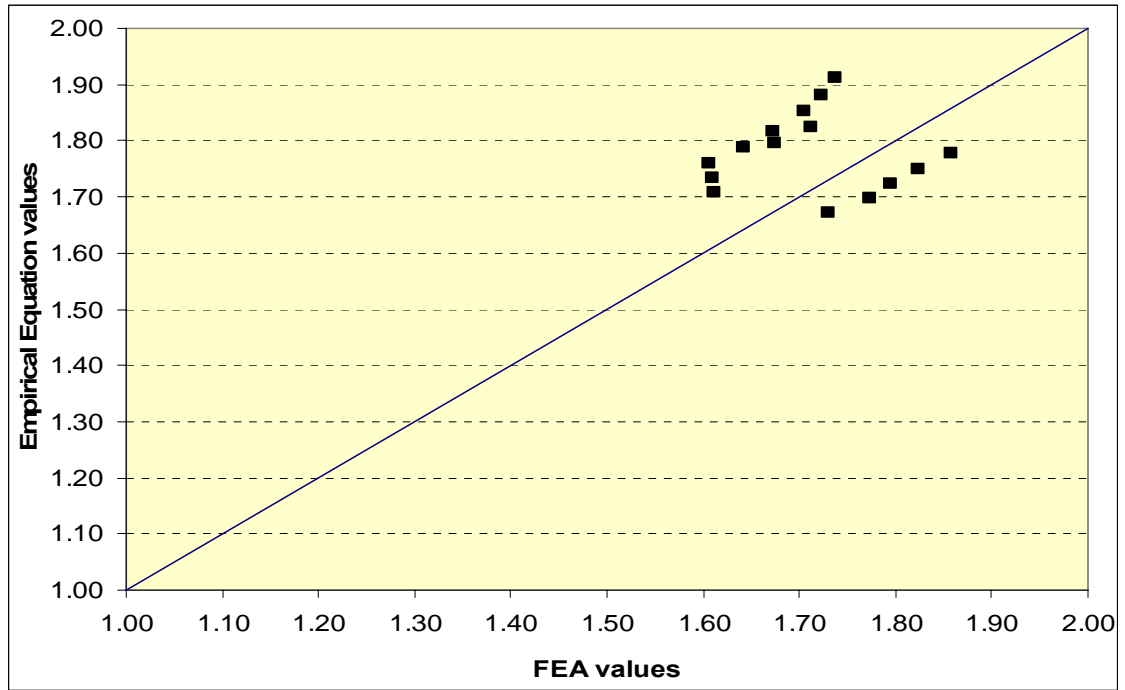


Figure 5.58 Comparison between vertical shear at external support from the empirical equation and FEA for five lanes bridges at ULS as function of (L)

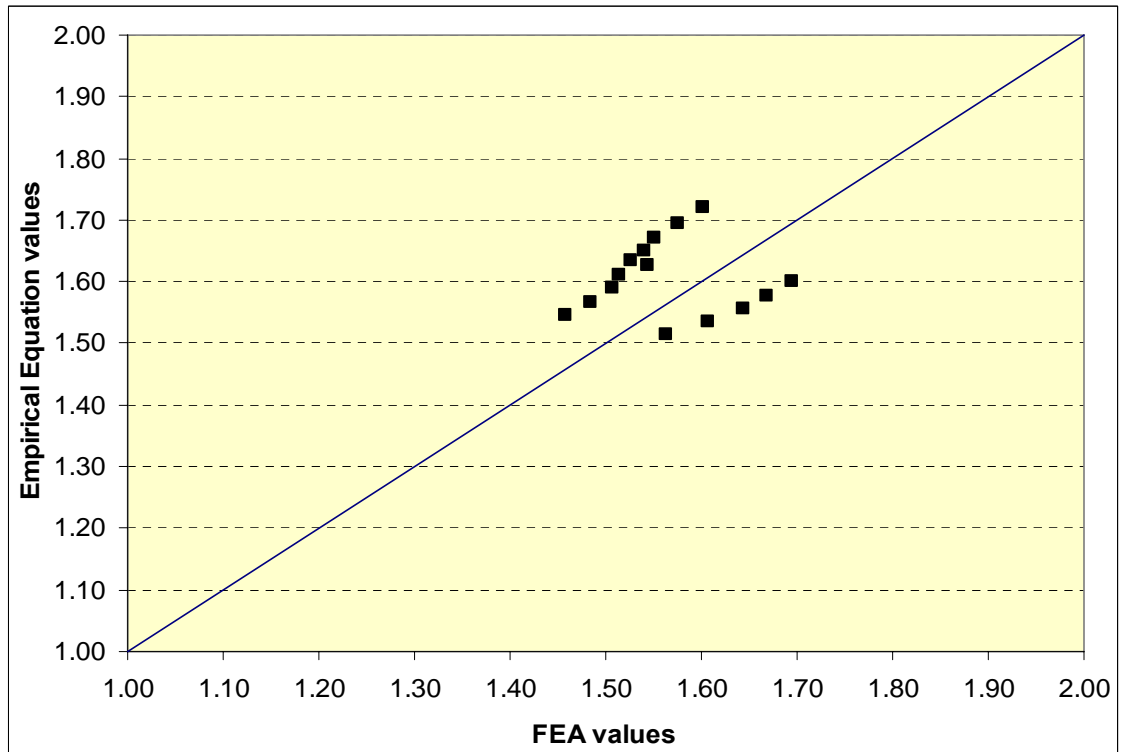


Figure 5.59 Comparison between vertical shear at internal support from the empirical equation and FEA for two lanes bridges at FLS as function of (L)

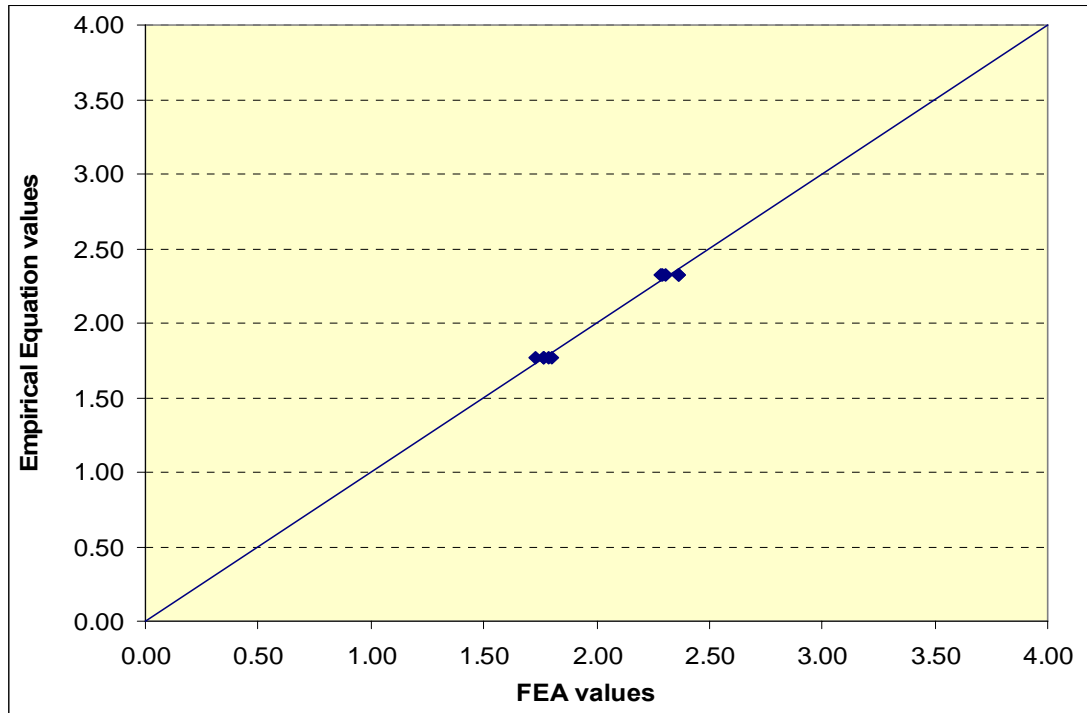


Figure 5.60 Comparison between vertical shear at external support from the empirical equation and FEA for two lanes bridges at FLS as function of (L)

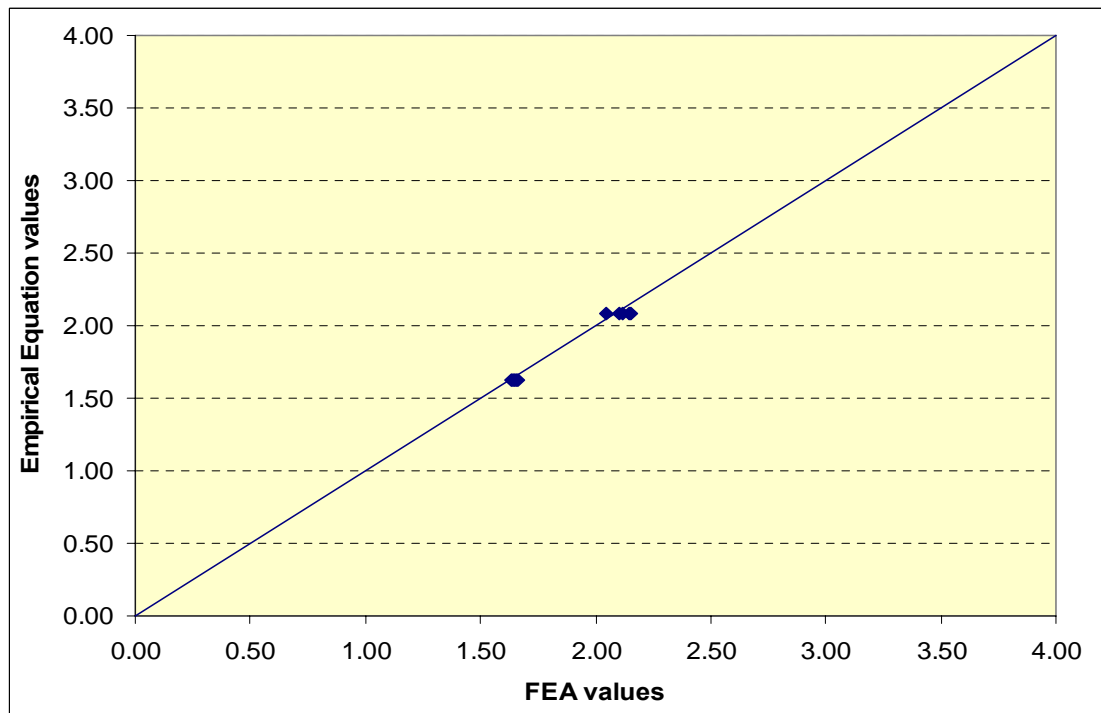


Figure 5.61 Comparison between vertical shear at internal support from the empirical equation and FEA for three lanes bridges at FLS as function of (L)

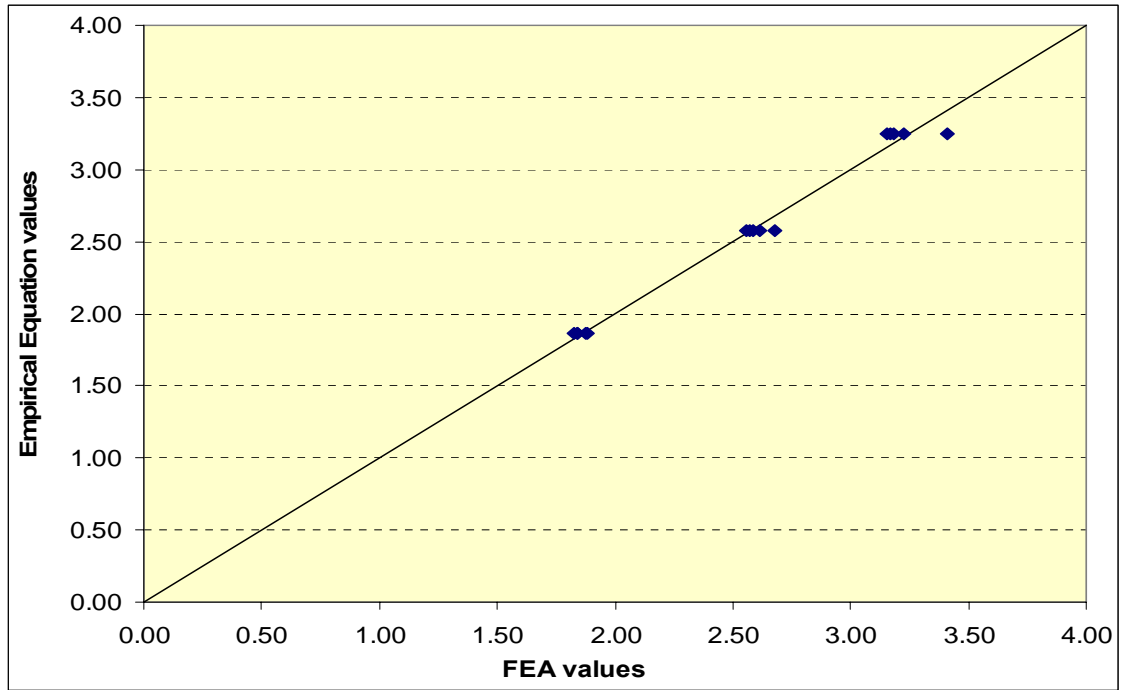


Figure 5.62 Comparison between vertical shear at external support from the empirical equation and FEA for three lanes bridges at FLS as function of (L)

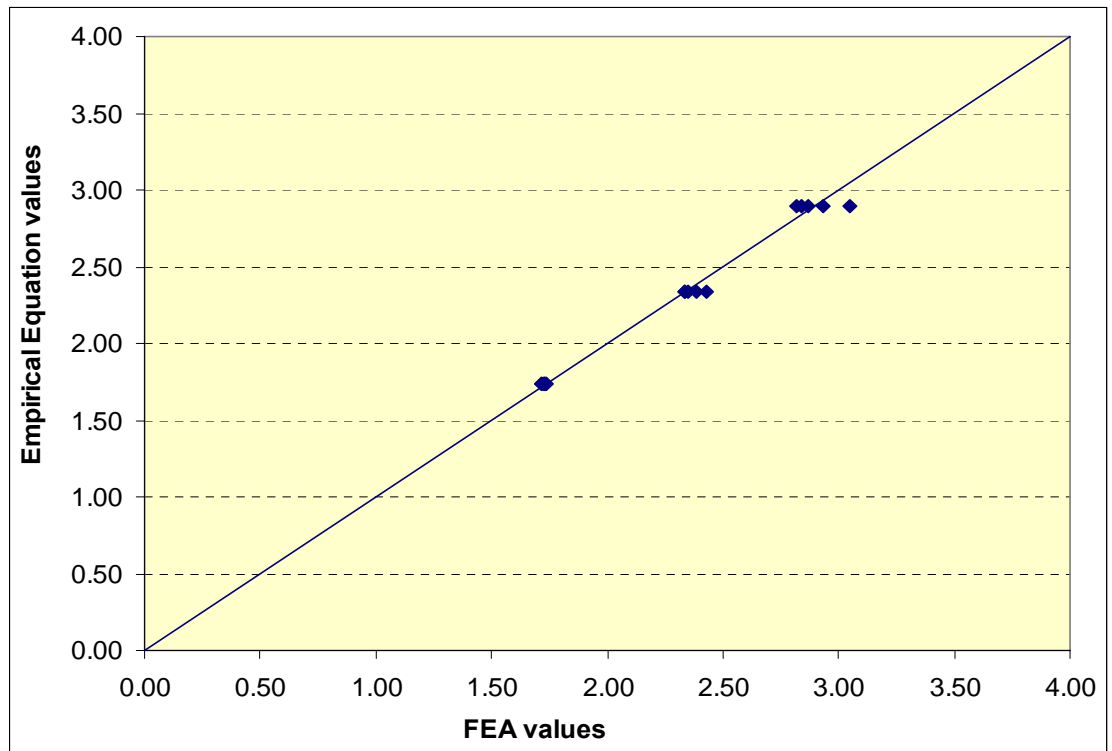


Figure 5.63 Comparison between vertical shear at internal support from the empirical equation and FEA for four lanes bridges at FLS as function of (L)

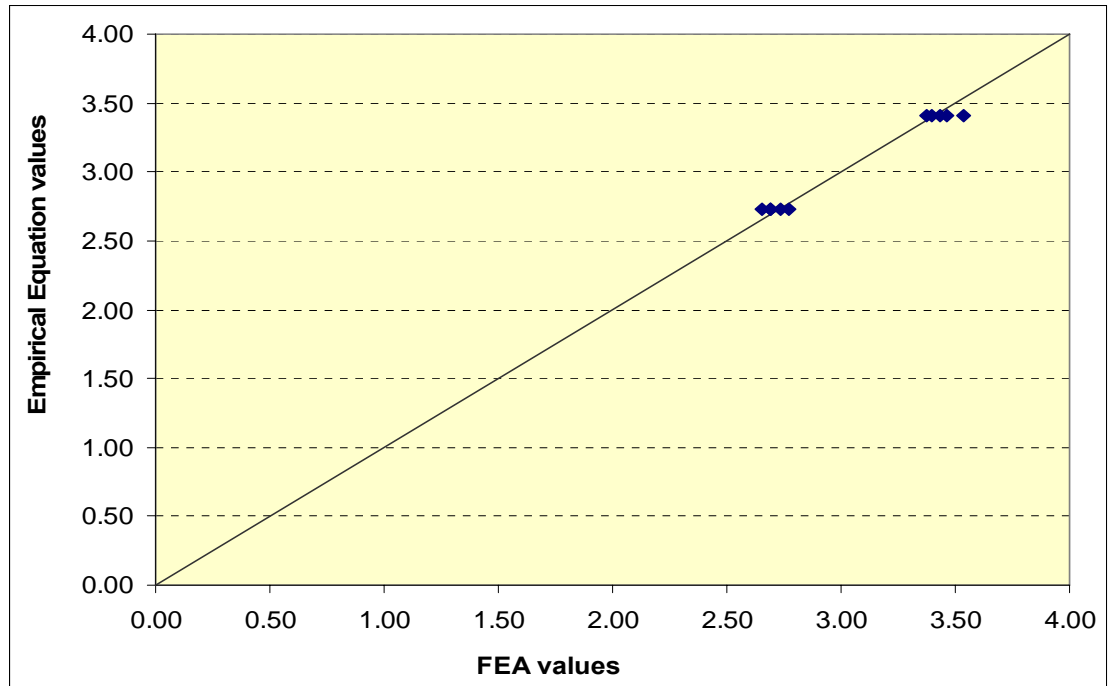


Figure 5.64 Comparison between vertical shear at external support from the empirical equation and FEA for four lanes bridges at FLS as function of (L)

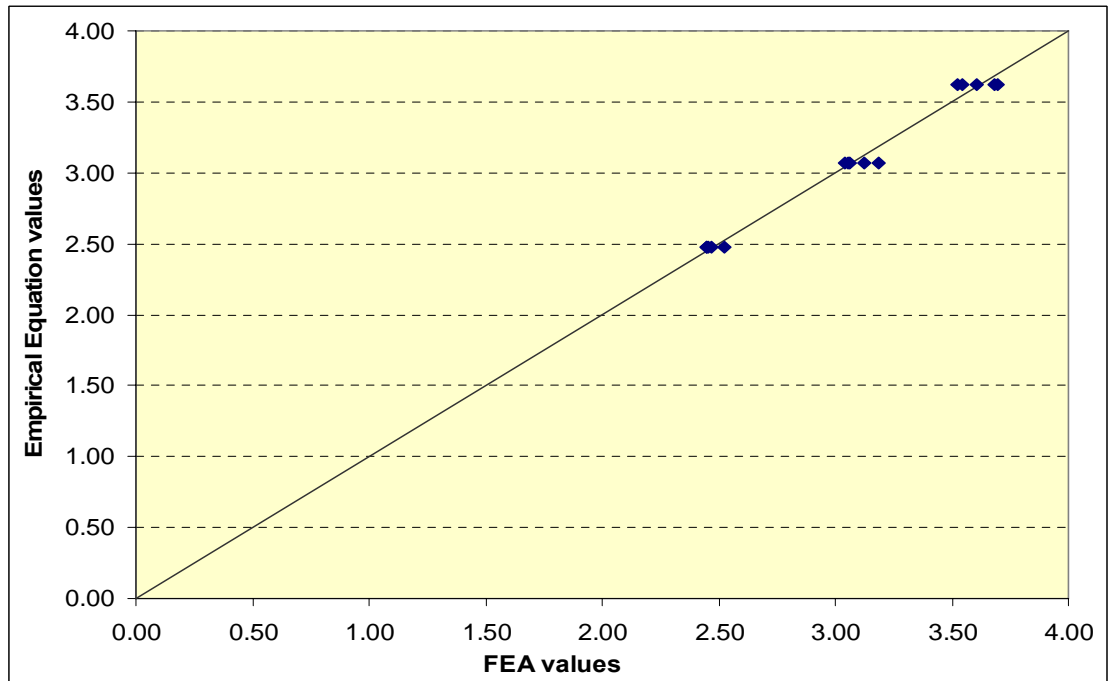


Figure 5.65 Comparison between vertical shear at internal support from the empirical equation and FEA for five lanes bridges at FLS as function of (L)

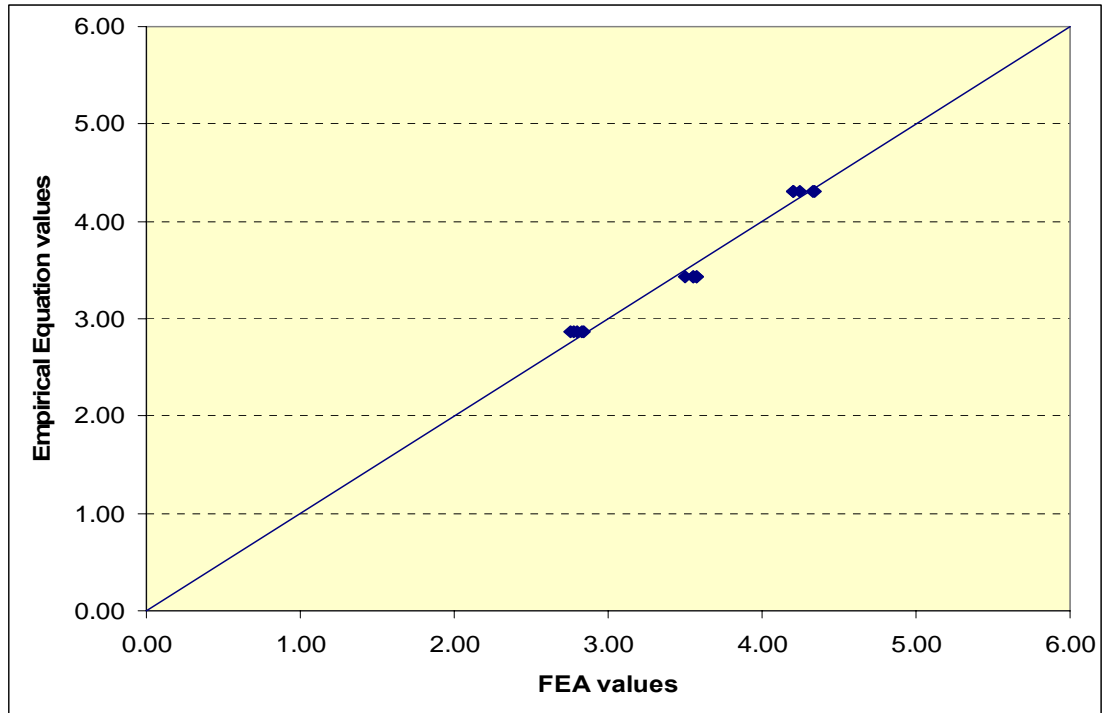


Figure 5.66 Comparison between vertical shear at external support from the empirical equation and FEA for five lanes bridges at FLS as function of (L)

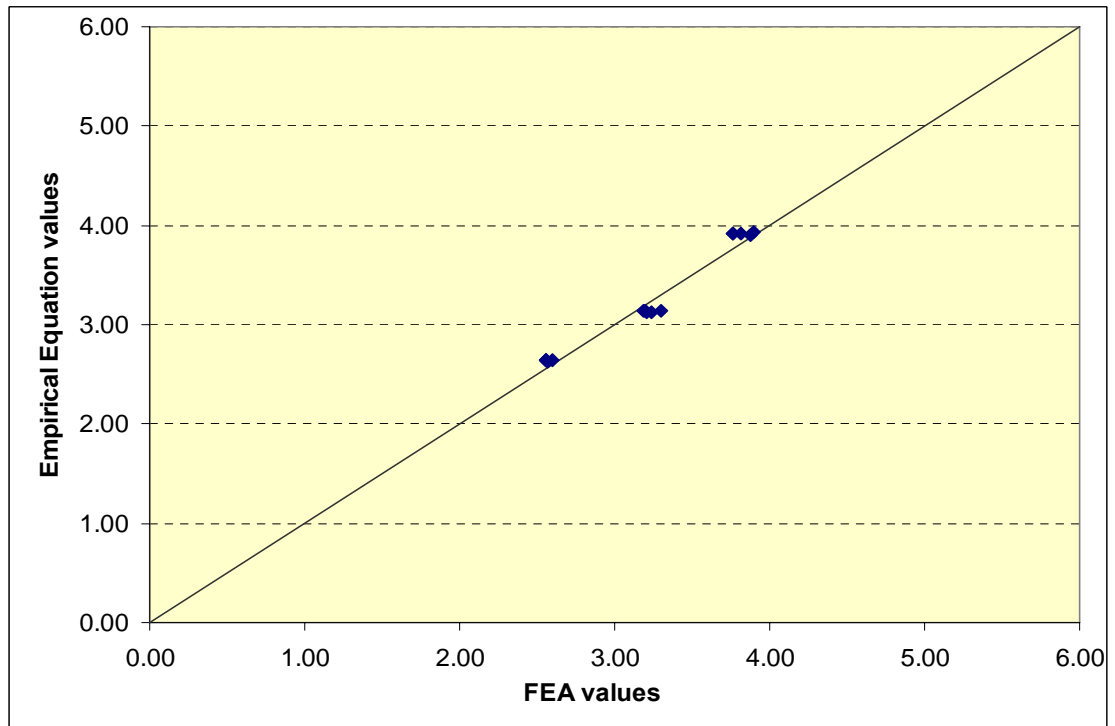


Figure 5.67 Comparison between vertical shear at internal support from the empirical equation and FEA for two lanes bridges at ULS as function of (β)

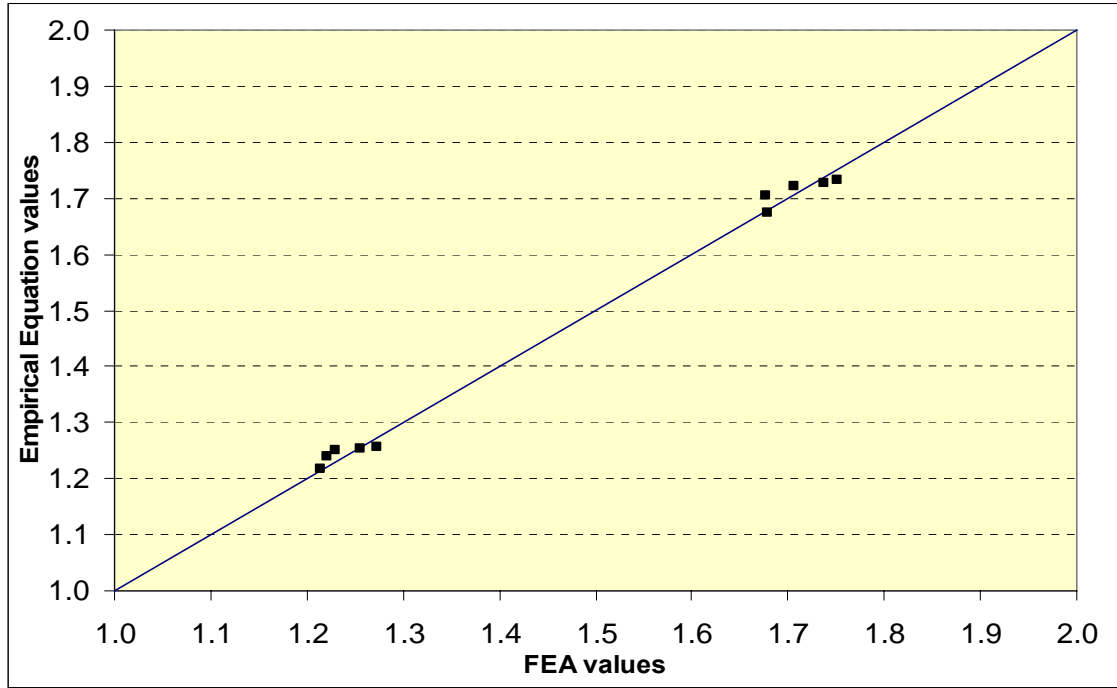


Figure 5.68 Comparison between vertical shear at external support from the empirical equation and FEA for two lanes bridges at ULS as function of (β)

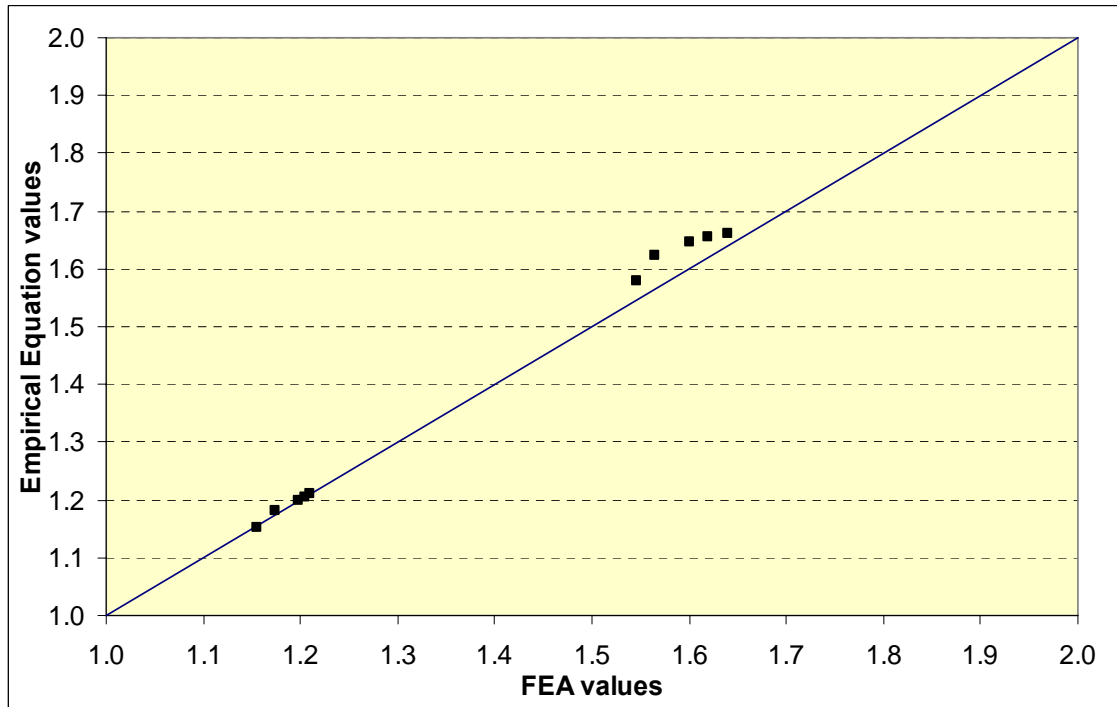


Figure 5.69 Comparison between vertical shear at internal support from the empirical equation and FEA for three lanes bridges at ULS as function of (β)

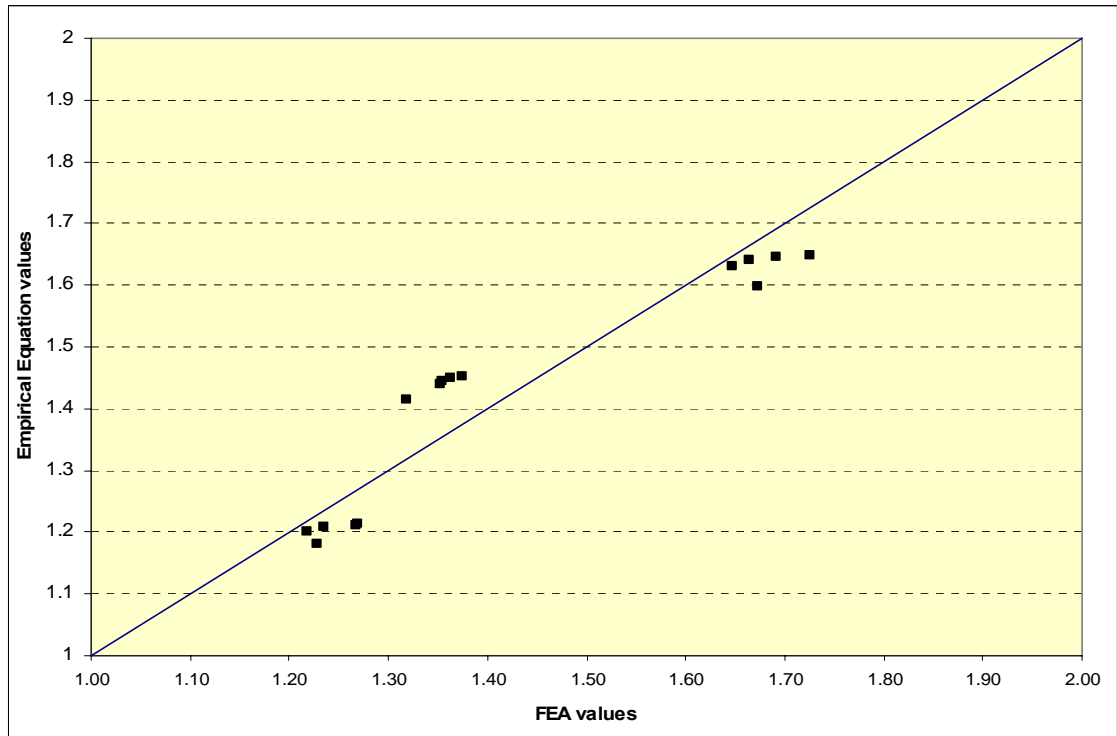


Figure 5.70 Comparison between vertical shear at external support from the empirical equation and FEA for three lanes bridges at ULS as function of (β)

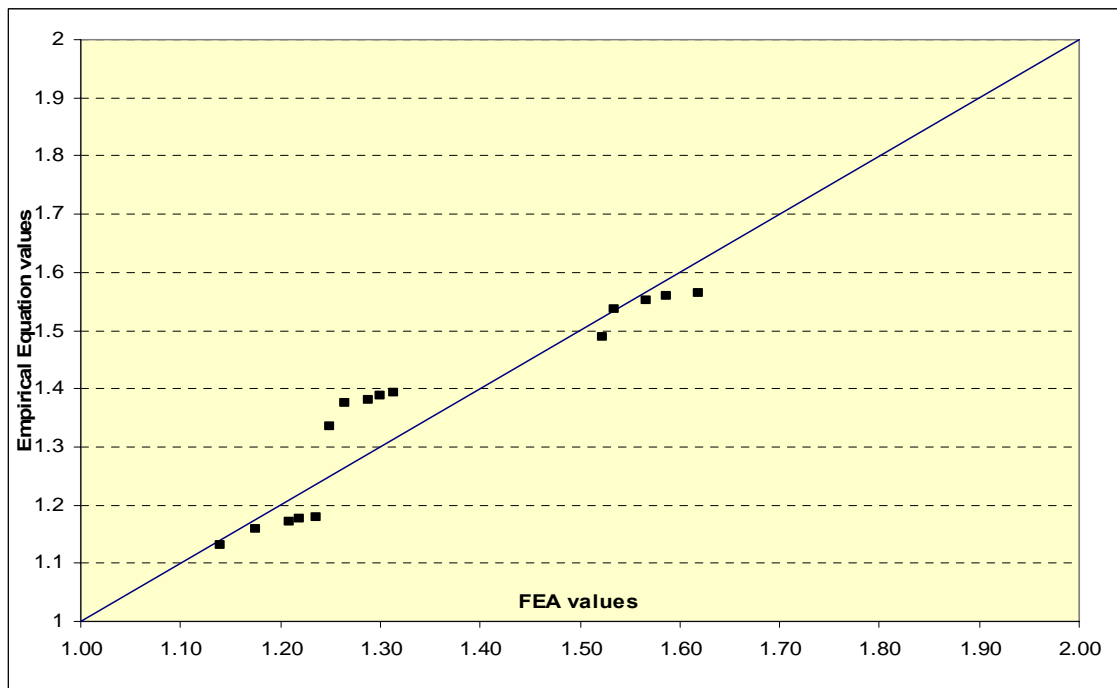


Figure 5.71 Comparison between vertical shear at internal support from the empirical equation and FEA for four lanes bridges at ULS as function of (β)

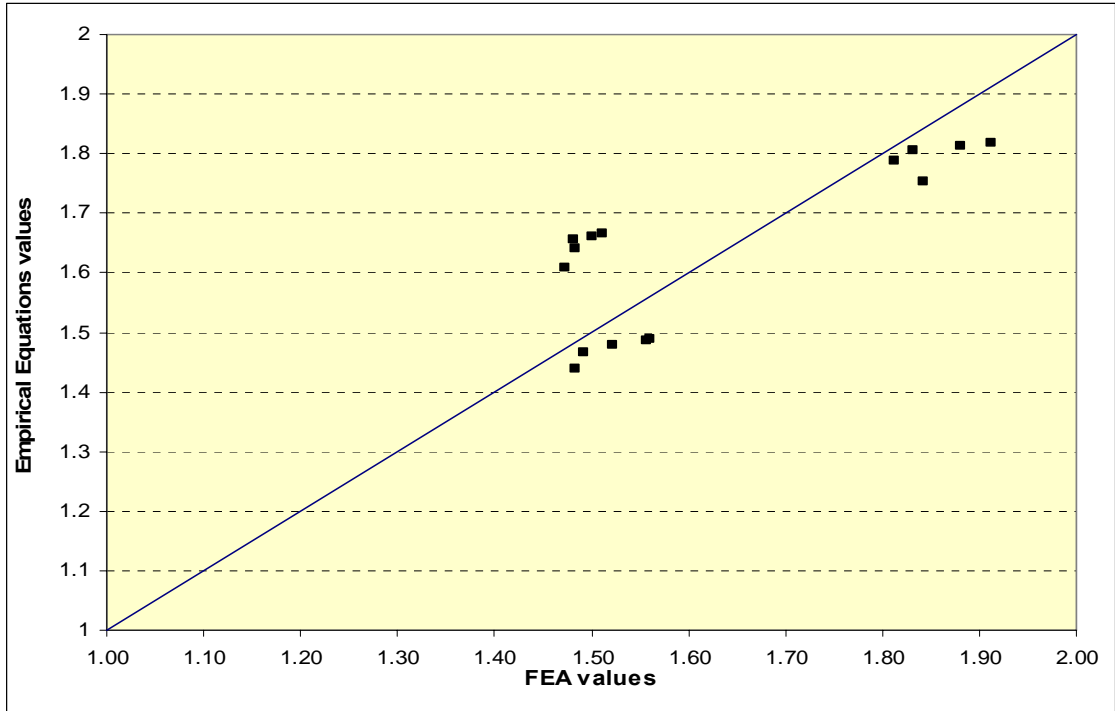


Figure 5.72 Comparison between vertical shear at external support from the empirical equation and FEA for four lanes bridges at ULS as function of (β)

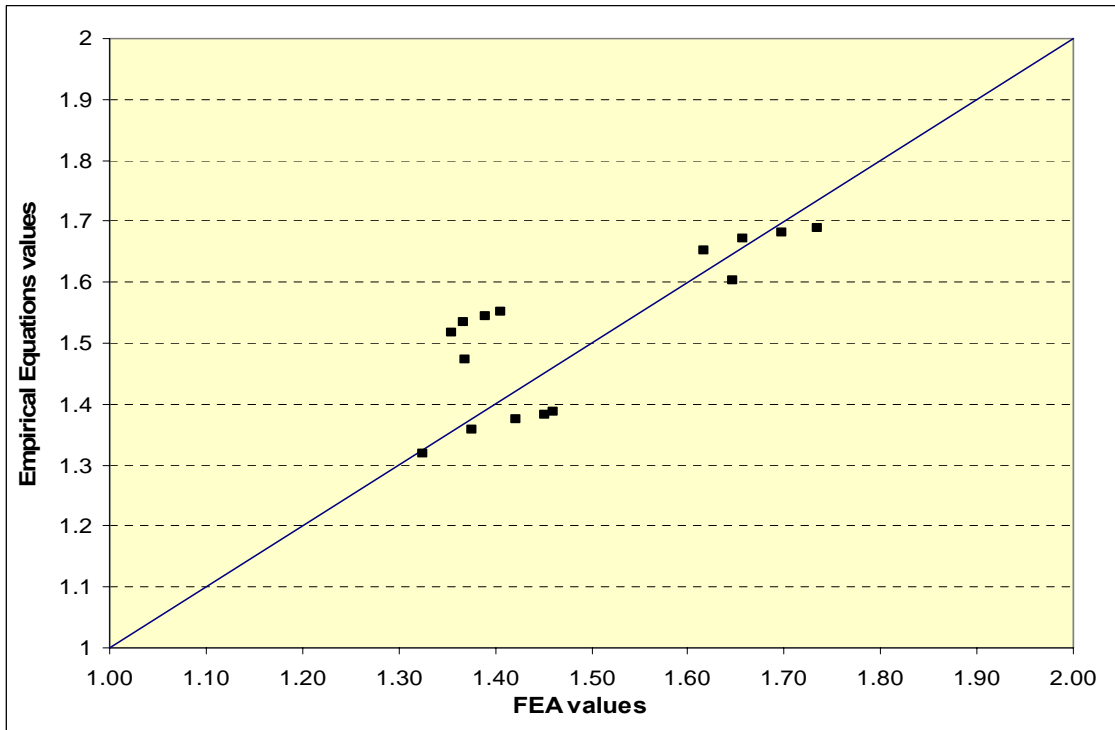


Figure 5.73 Comparison between vertical shear at internal support from the empirical equation and FEA for five lanes bridges at ULS as function of (β)

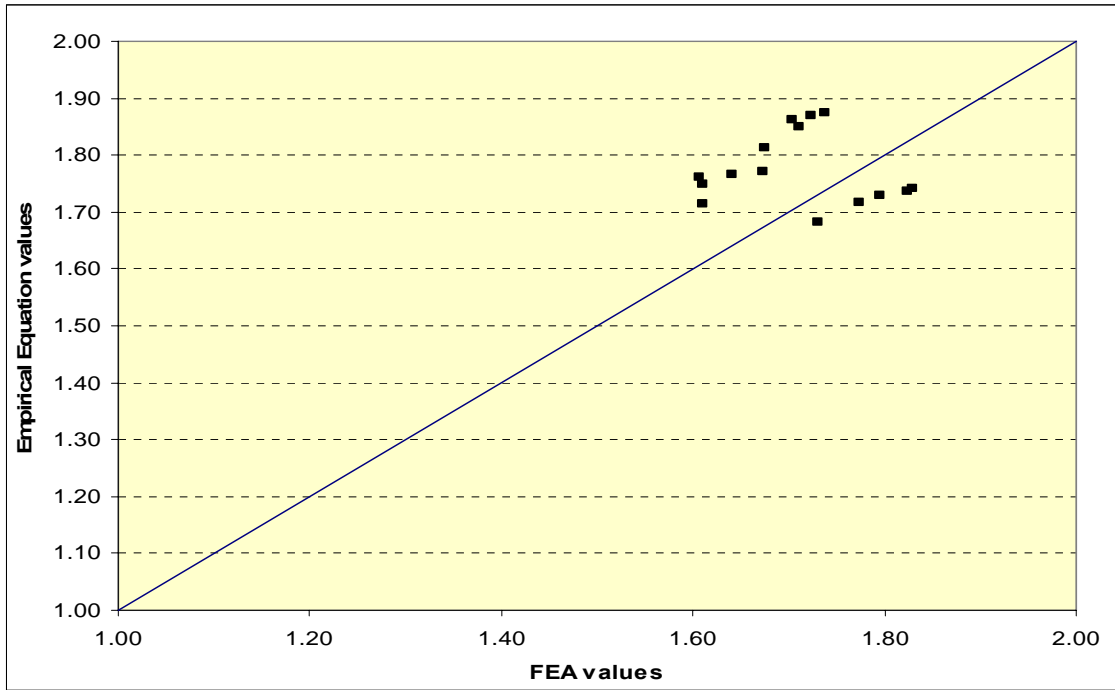


Figure 5.74 Comparison between vertical shear at external support from the empirical equation and FEA for five lanes bridges at ULS as function of (β)

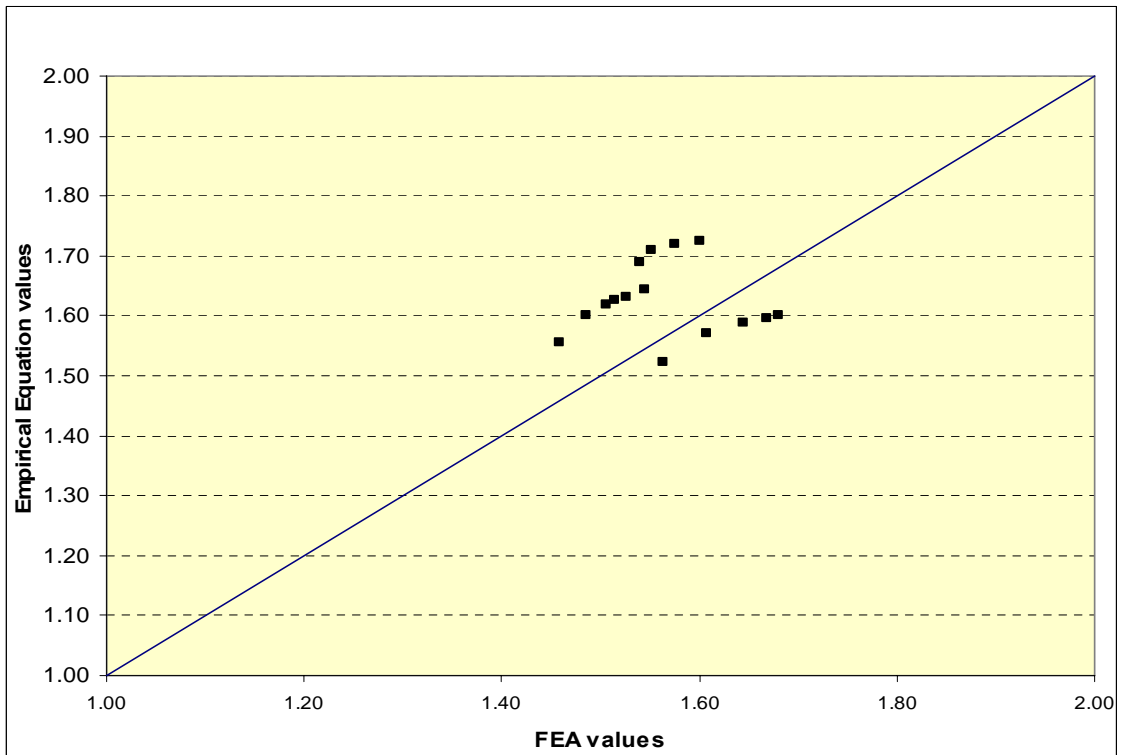


Figure 5.75 Comparison between vertical shear at internal support from the empirical equation and FEA for two lanes bridges at FLS as function of (β)

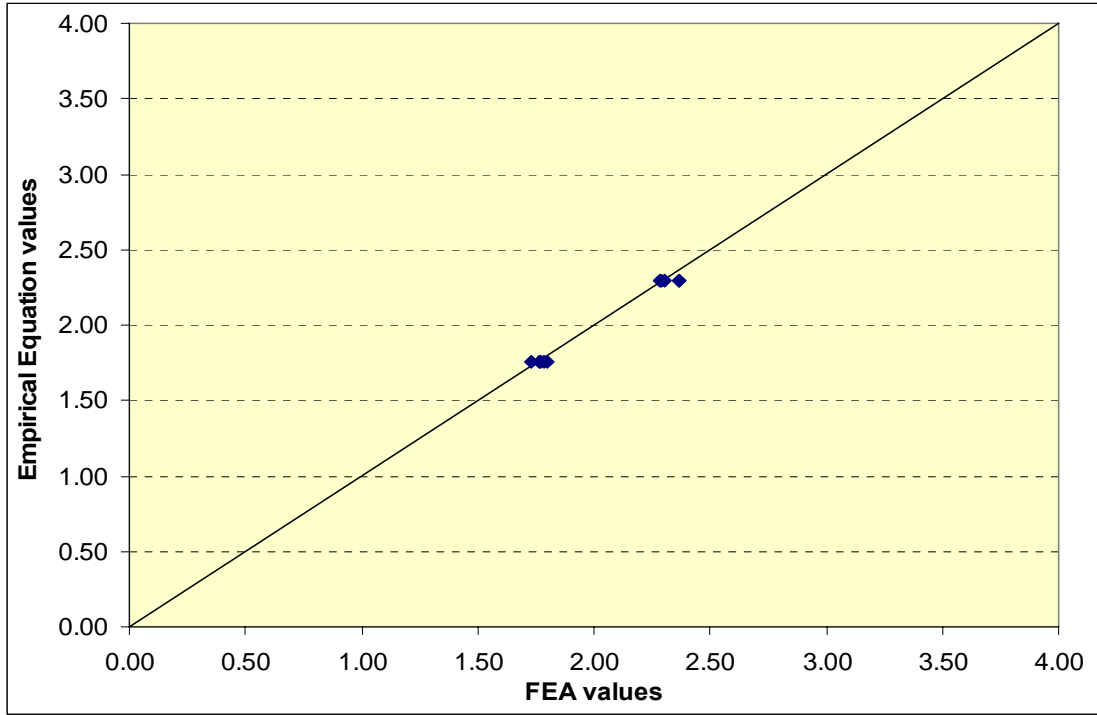


Figure 5.76 Comparison between vertical shear at external support from the empirical equation and FEA for two lanes bridges at FLS as function of (β)

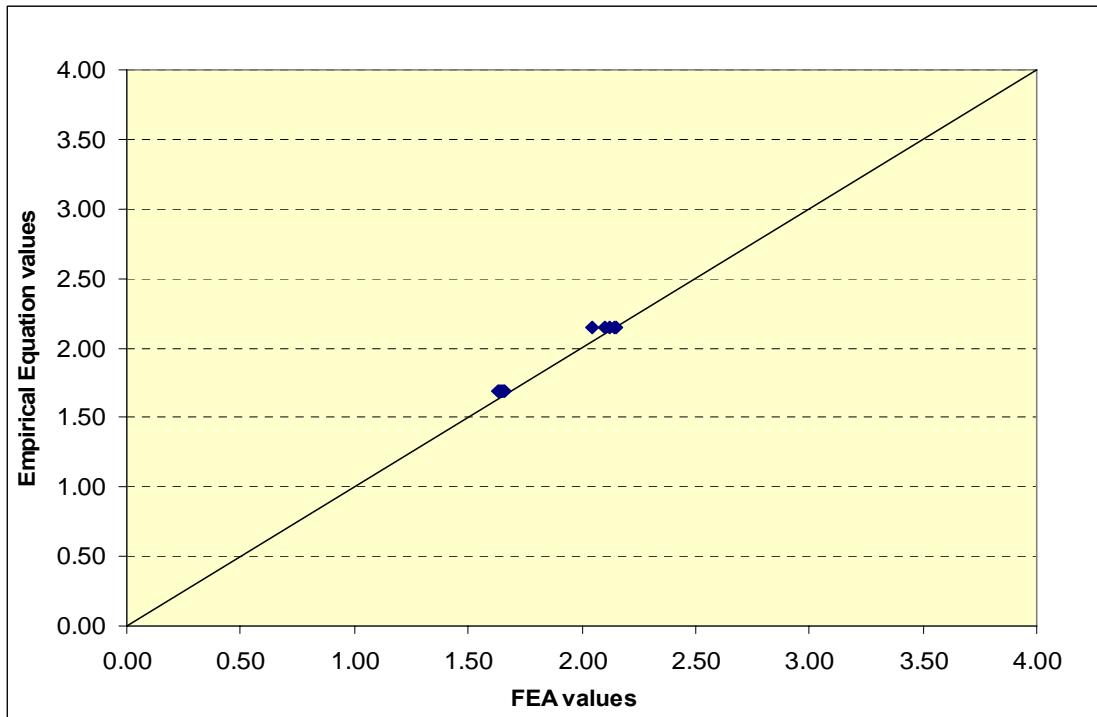


Figure 5.77 Comparison between vertical shear at internal support from the empirical equation and FEA for three lanes bridges at FLS as function of (β)

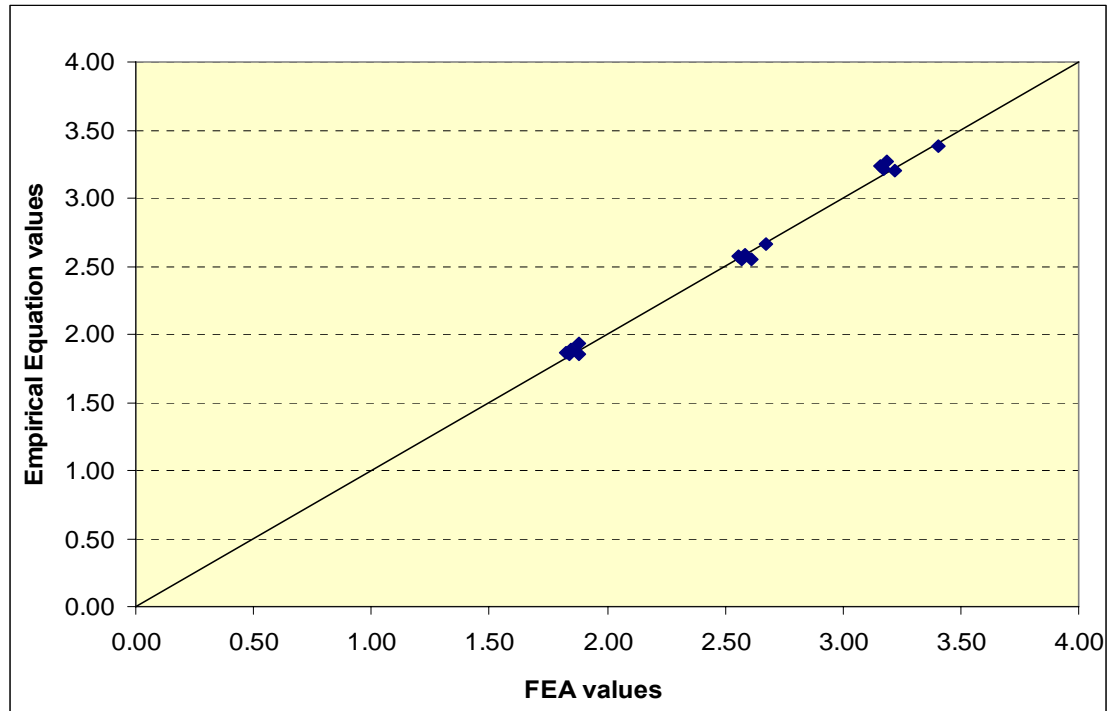


Figure 5.78 Comparison between vertical shear at external support from the empirical equation and FEA for three lanes bridges at FLS as function of (β)

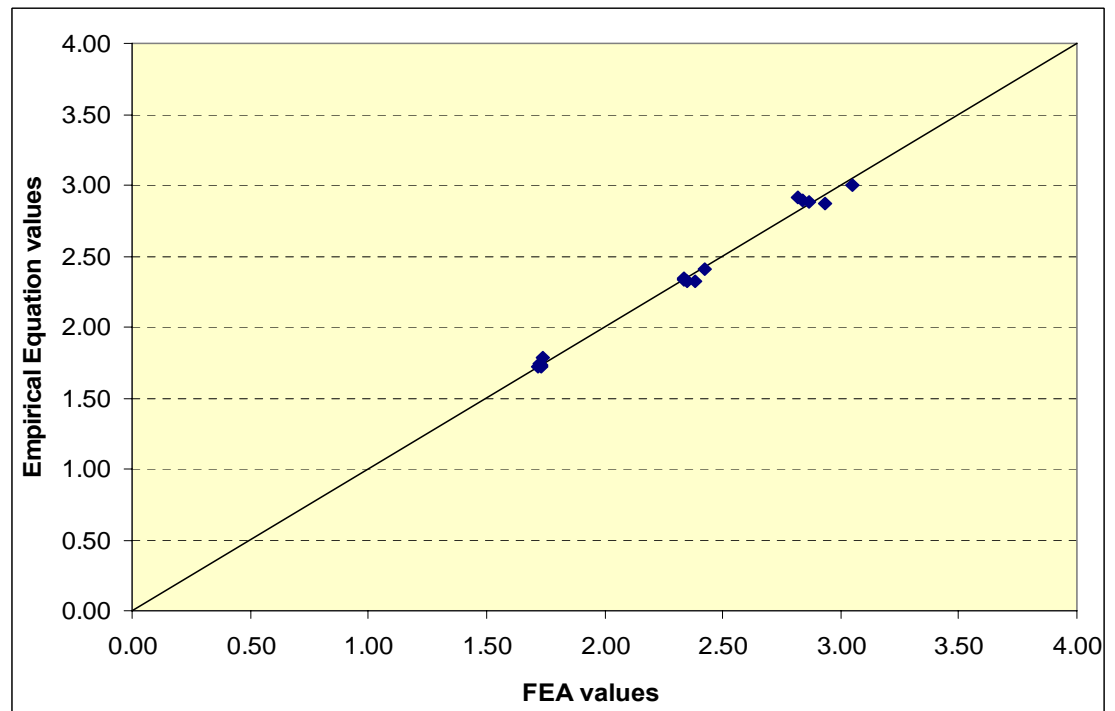


Figure 5.79 Comparison between vertical shear at internal support from the empirical equation and FEA for four lanes bridges at FLS as function of (β)

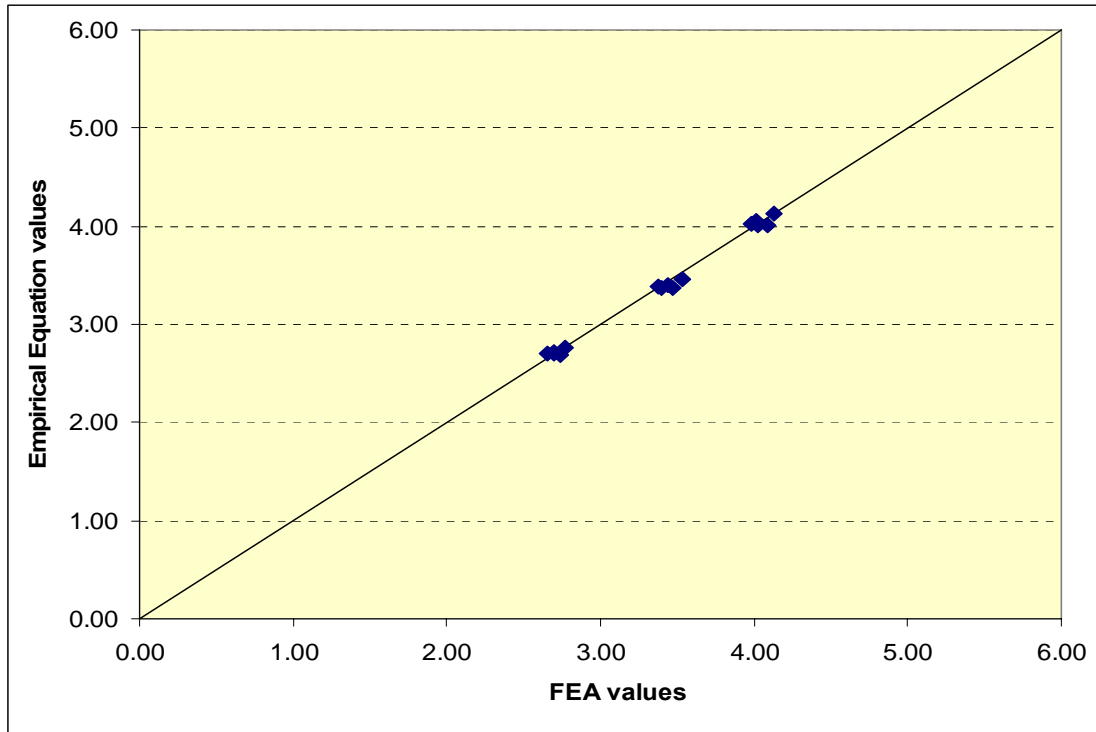


Figure 5.80 Comparison between vertical shear at external support from the empirical equation and FEA for four lanes bridges at FLS as function of (β)

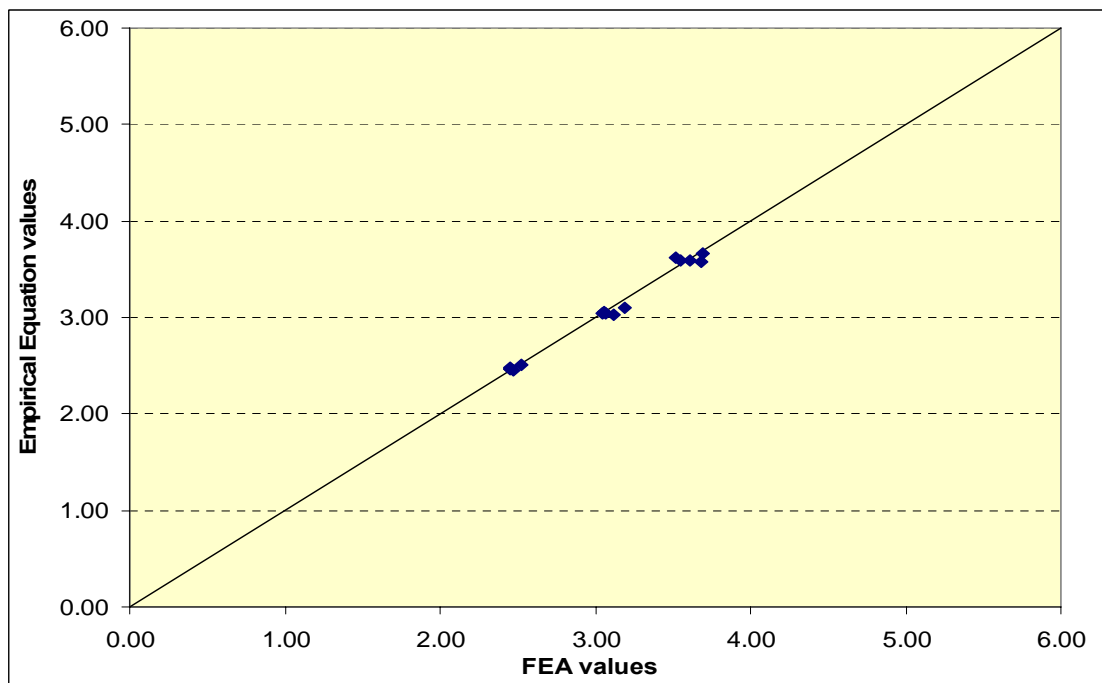


Figure 5.81 Comparison between vertical shear at internal support from the empirical equation and FEA for five lanes bridges at FLS as function of (β)

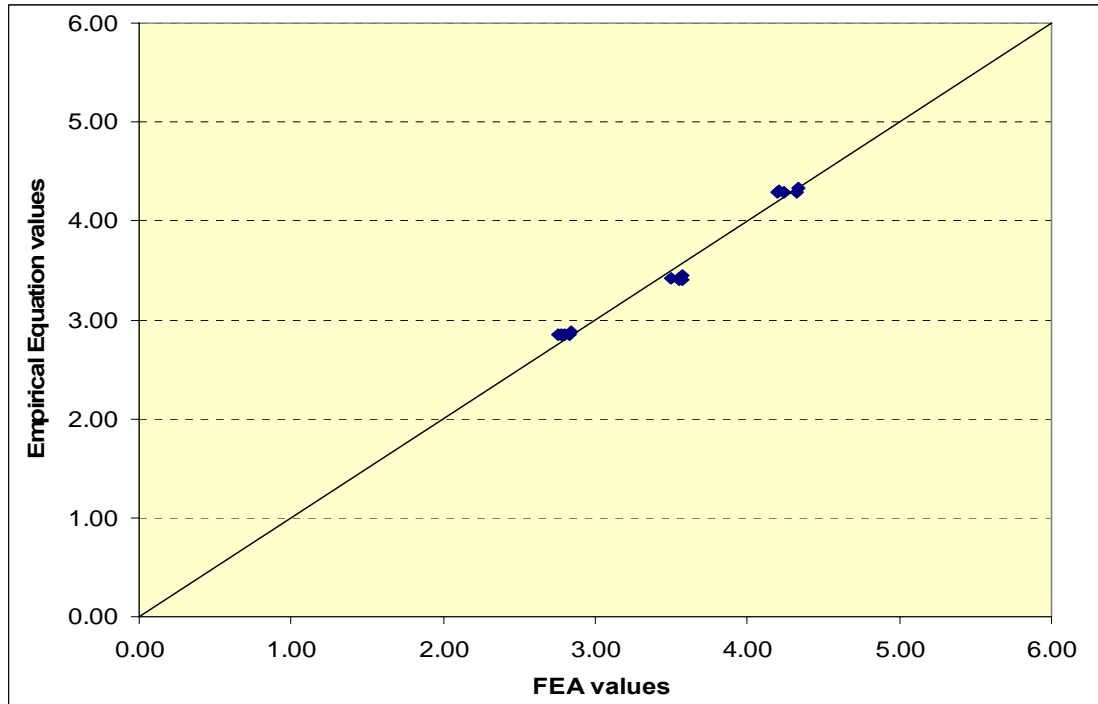


Figure 5.82 Comparison between vertical shear at external support from the empirical equation and FEA for five lanes bridges at FLS as function of (β)

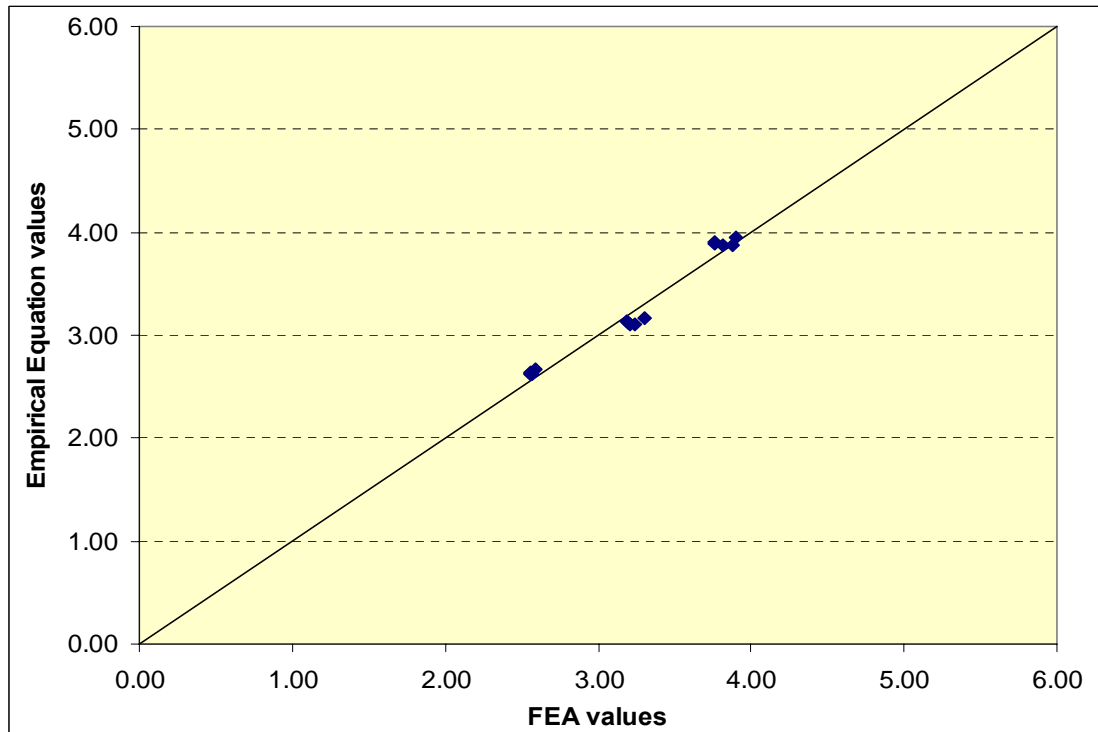


Figure 5.83 Comparison between vertical shear at internal support from the empirical equation and FEA for two lanes bridges at ULS as function of (β^2)

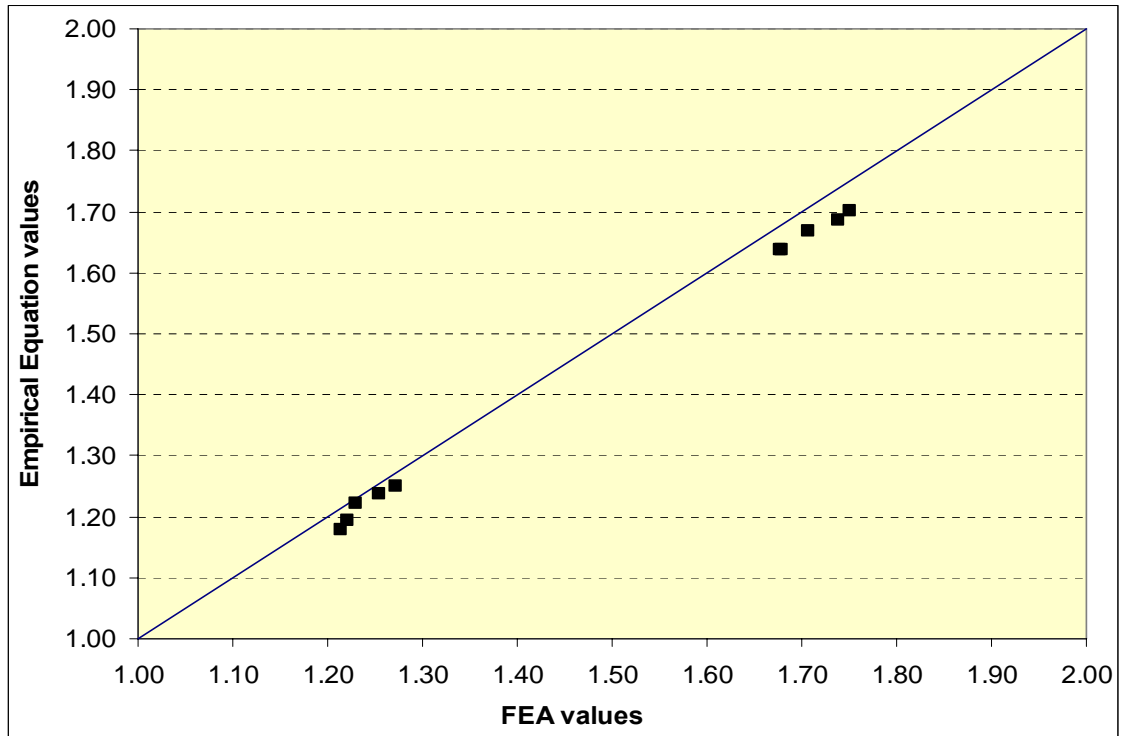


Figure 5.84 Comparison between vertical shear at external support from the empirical equation and FEA for two lanes bridges at ULS as function of (β^2)

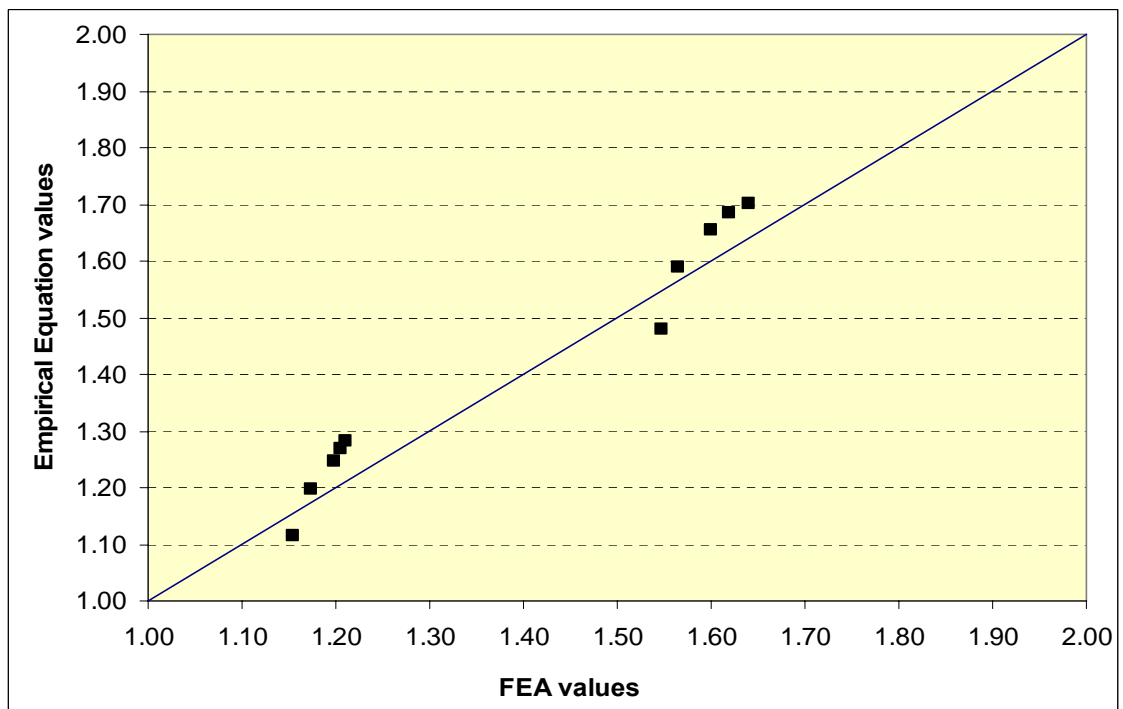


Figure 5.85 Comparison between vertical shear at internal support from the empirical equation and FEA for three lanes bridges at ULS as function of (β^2)

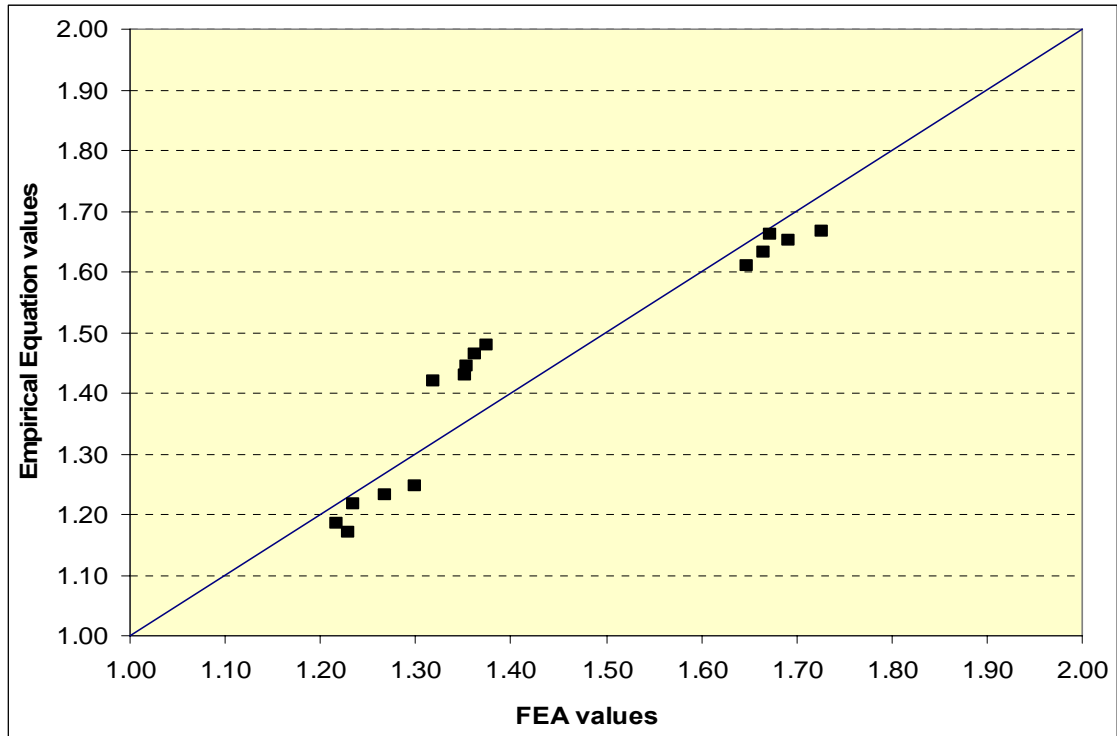


Figure 5.86 Comparison between vertical shear at external support from the empirical equation and FEA for three lanes bridges at ULS as function of (β^2)

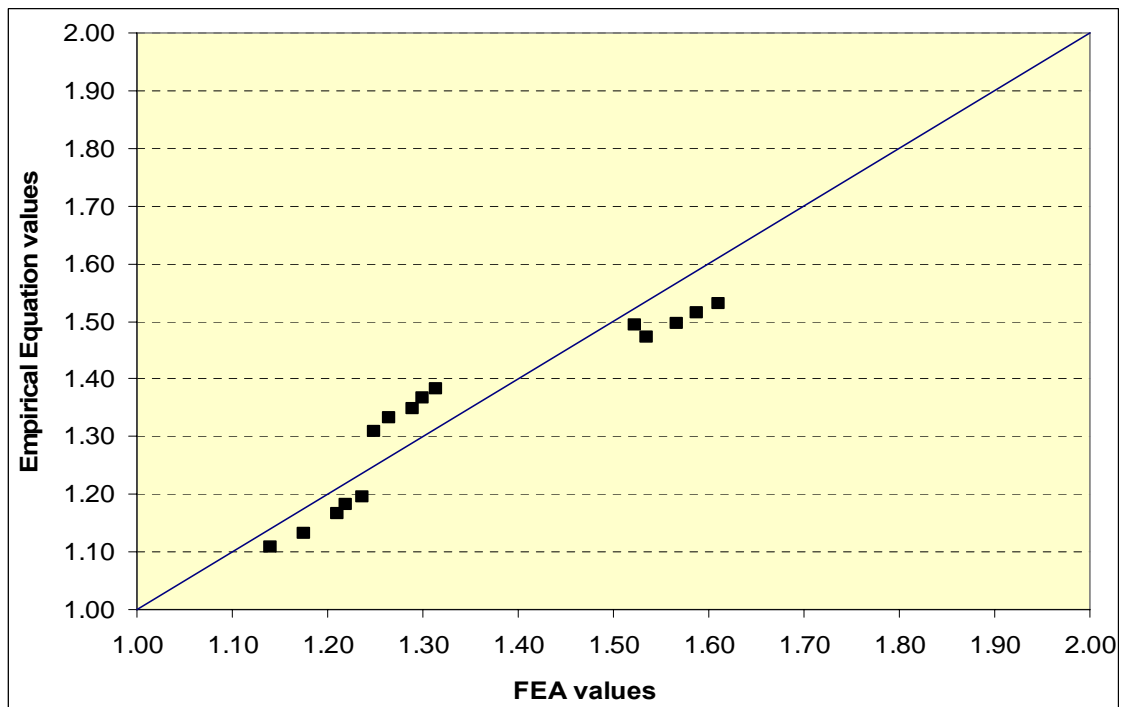


Figure 5.87 Comparison between vertical shear at internal support from the empirical equation and FEA for four lanes bridges at ULS as function of (β^2)

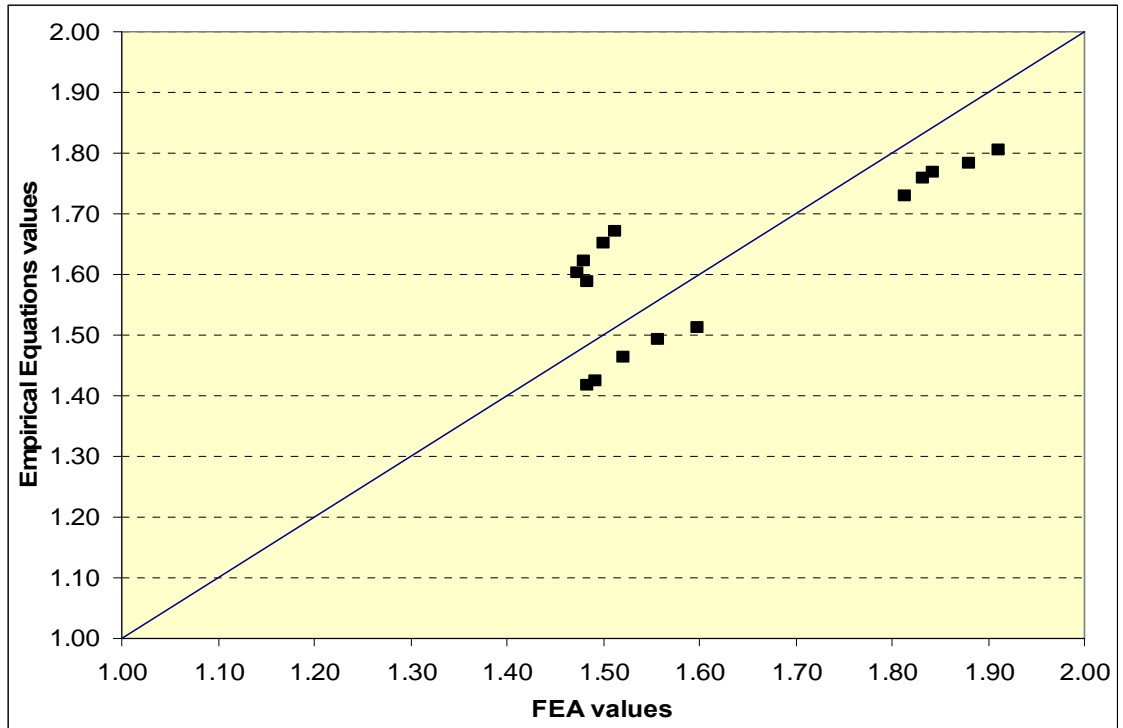


Figure 5.88 Comparison between vertical shear at external support from the empirical equation and FEA for four lanes bridges at ULS as function of (β^2)

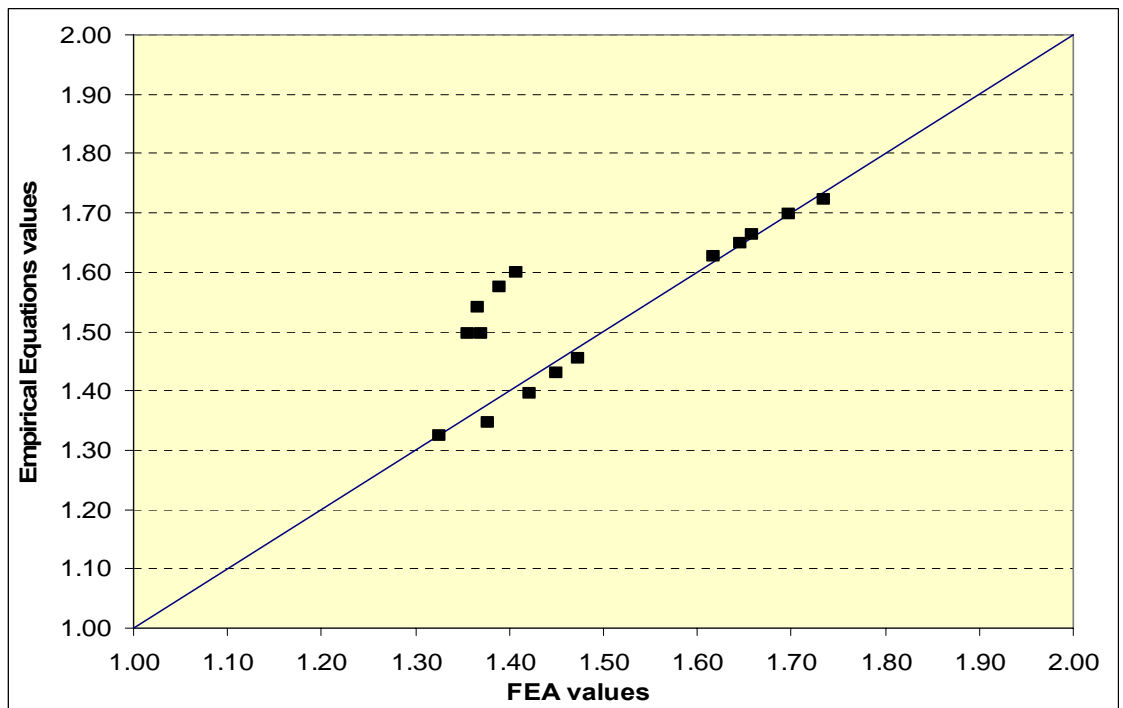


Figure 5.89 Comparison between vertical shear at internal support from the empirical equation and FEA for five lanes bridges at ULS as function of (β^2)

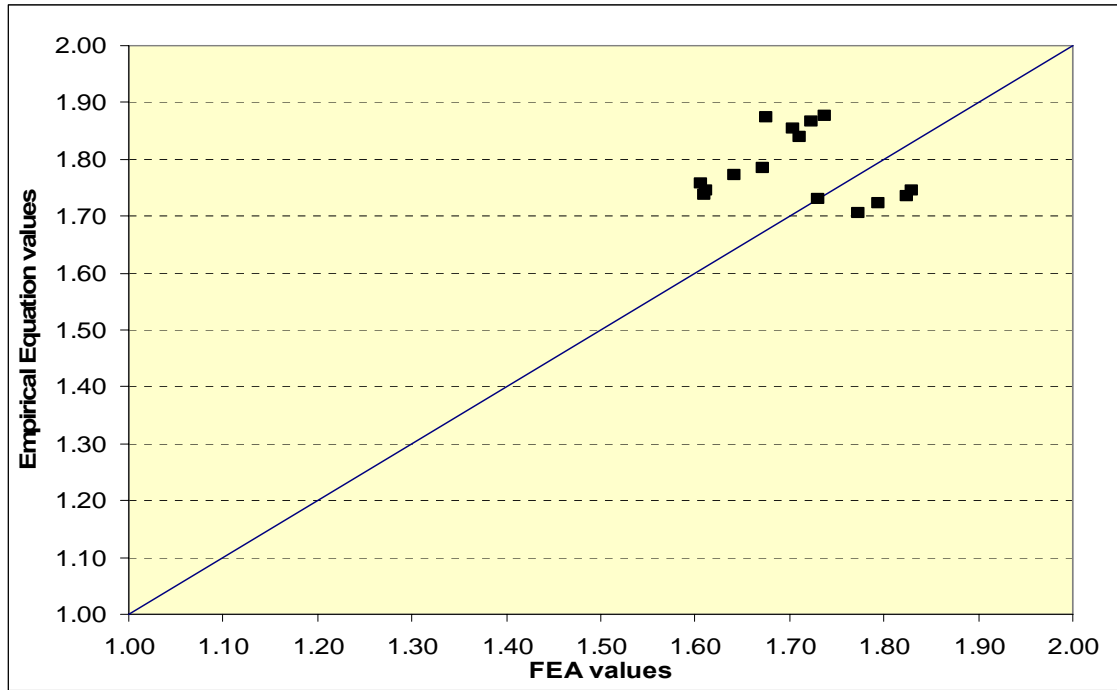


Figure 5.90 Comparison between vertical shear at external support from the empirical equation and FEA for five lanes bridges at ULS as function of (β^2)

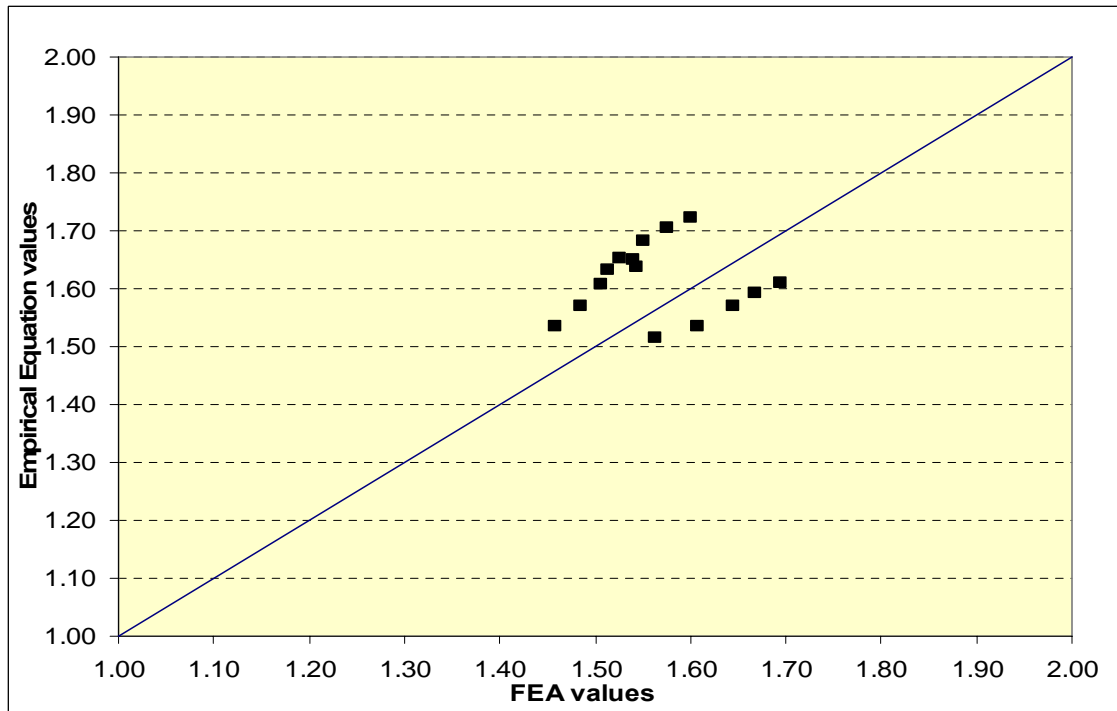


Figure 5.91 Comparison between vertical shear at internal support from the empirical equation and FEA for two lanes bridges at FLS as function of (β^2)

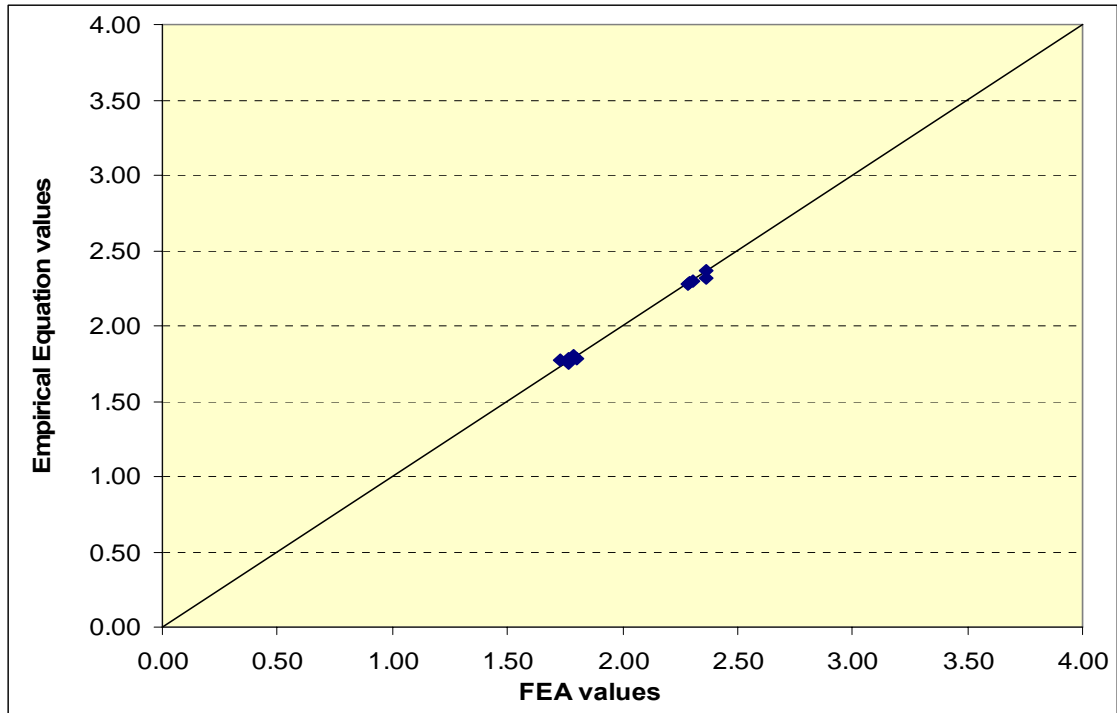


Figure 5.92 Comparison between vertical shear at external support from the empirical equation and FEA for two lanes bridges at FLS as function of (β^2)

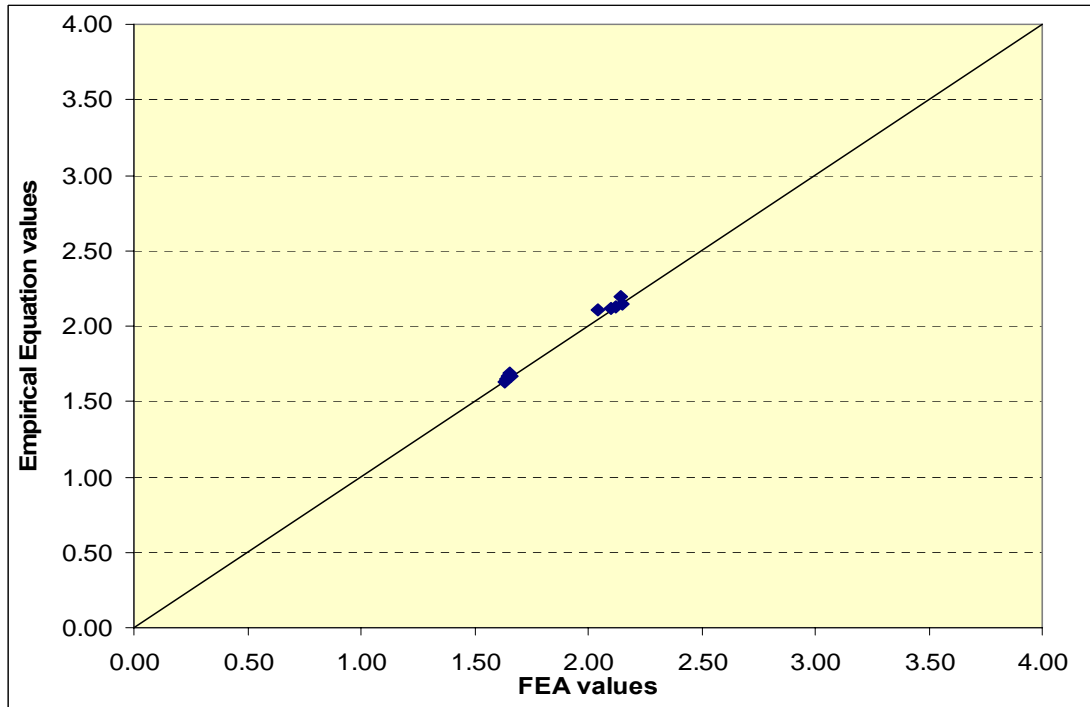


Figure 5.93 Comparison between vertical shear at internal support from the empirical equation and FEA for three lanes bridges at FLS as function of (β^2).

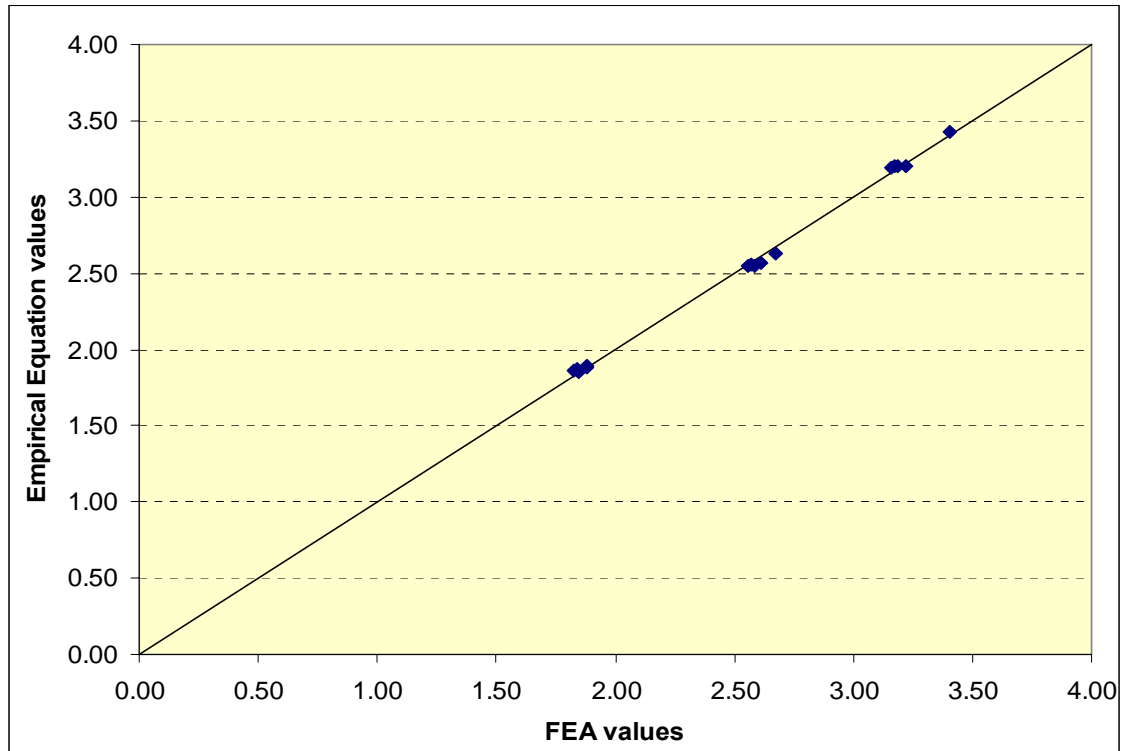


Figure 5.94 Comparison between vertical shear at external support from the empirical equation and FEA for three lanes bridges at FLS as function of (β^2).

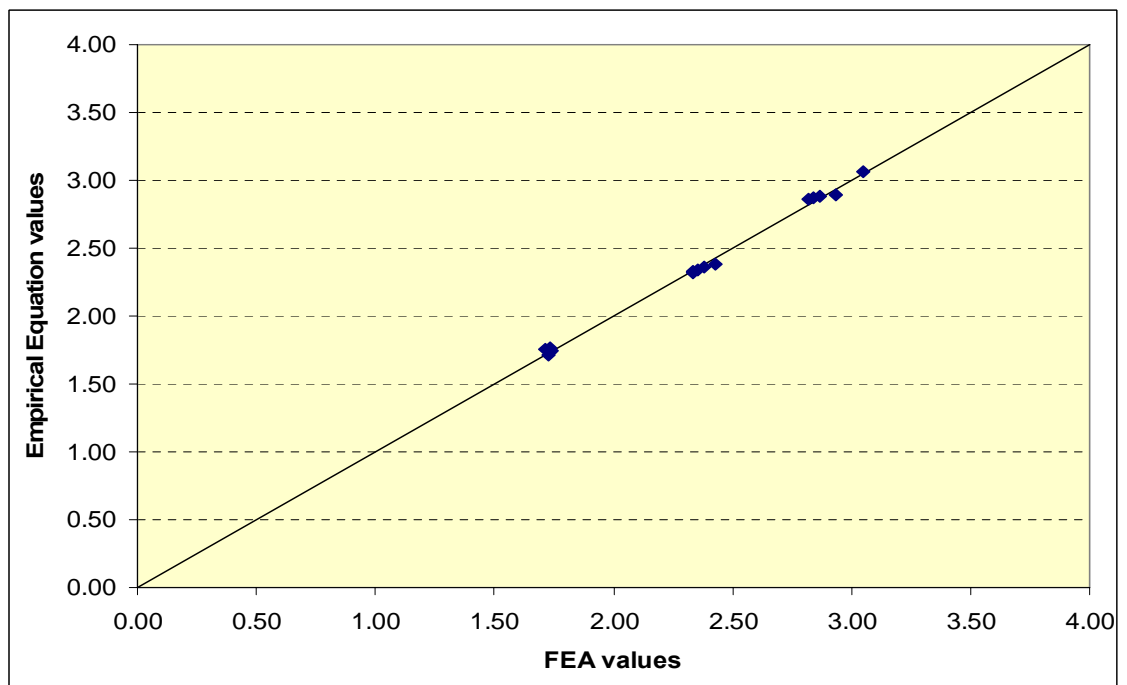


Figure 5.95 Comparison between vertical shear at internal support from the empirical equation and FEA for four lanes bridges at FLS as function of (β^2) .

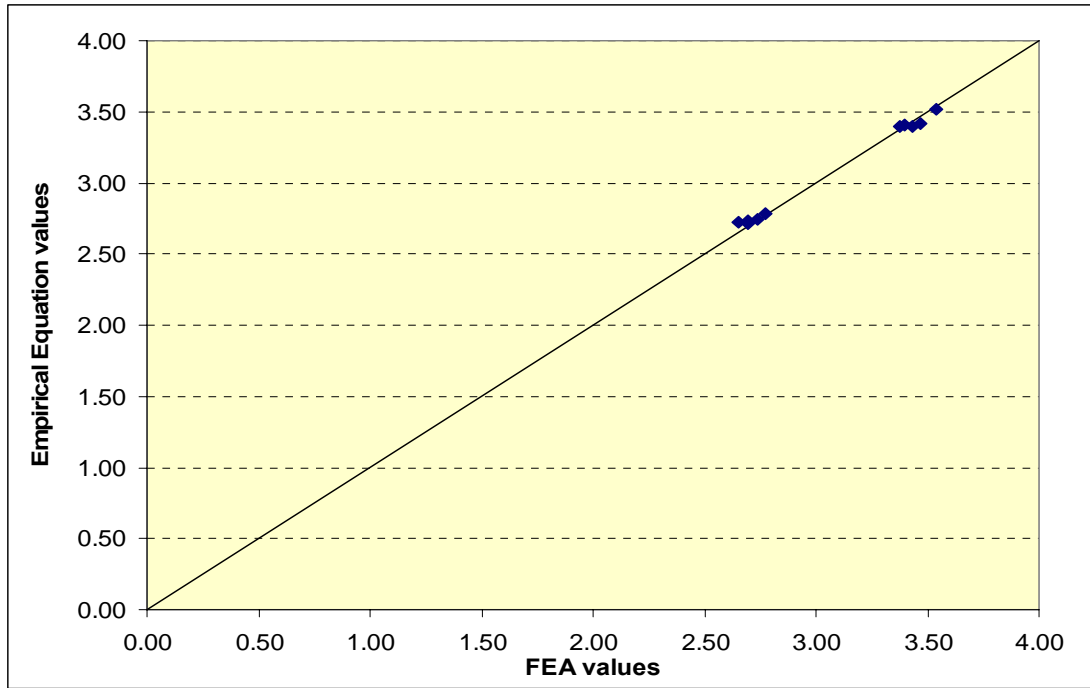


Figure 5.96 Comparison between vertical shear at external support from the empirical equation and FEA for four lanes bridges at FLS as function of (β^2) .

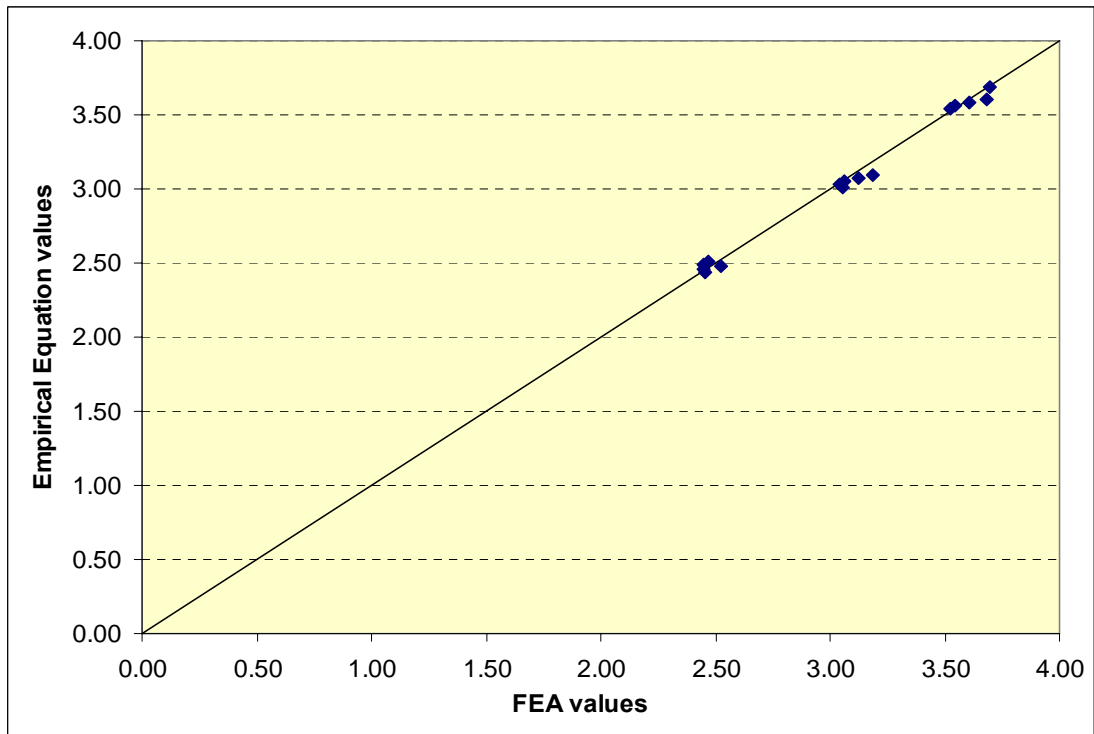


Figure 5.97 Comparison between vertical shear at internal support from the empirical equation and FEA for five lanes bridges at FLS as function of (β^2).

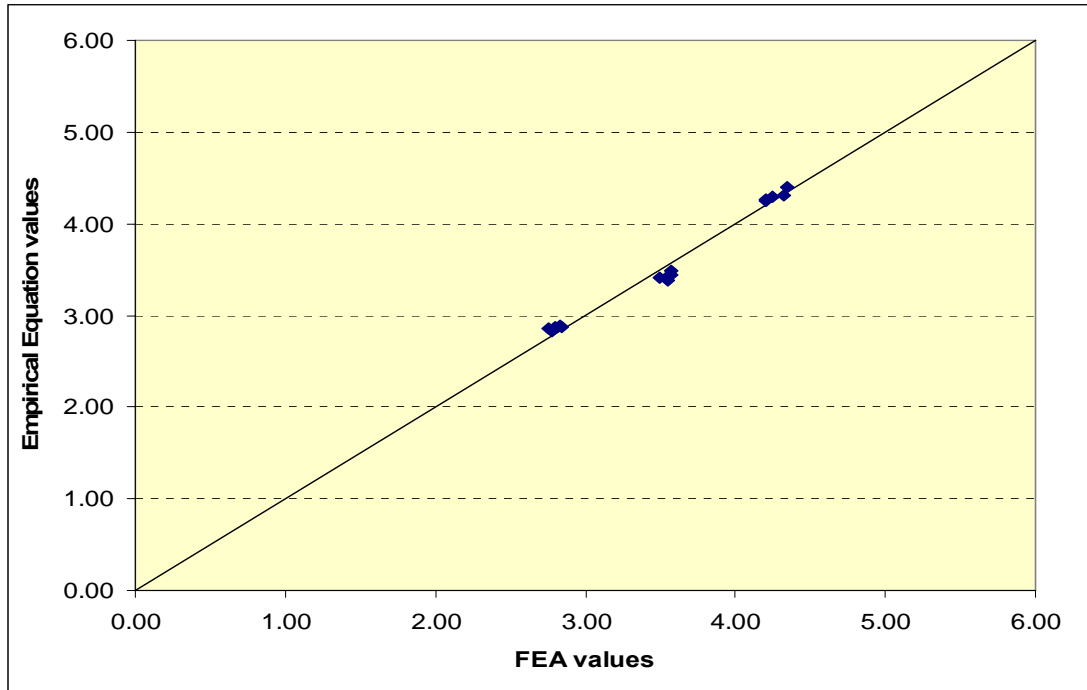
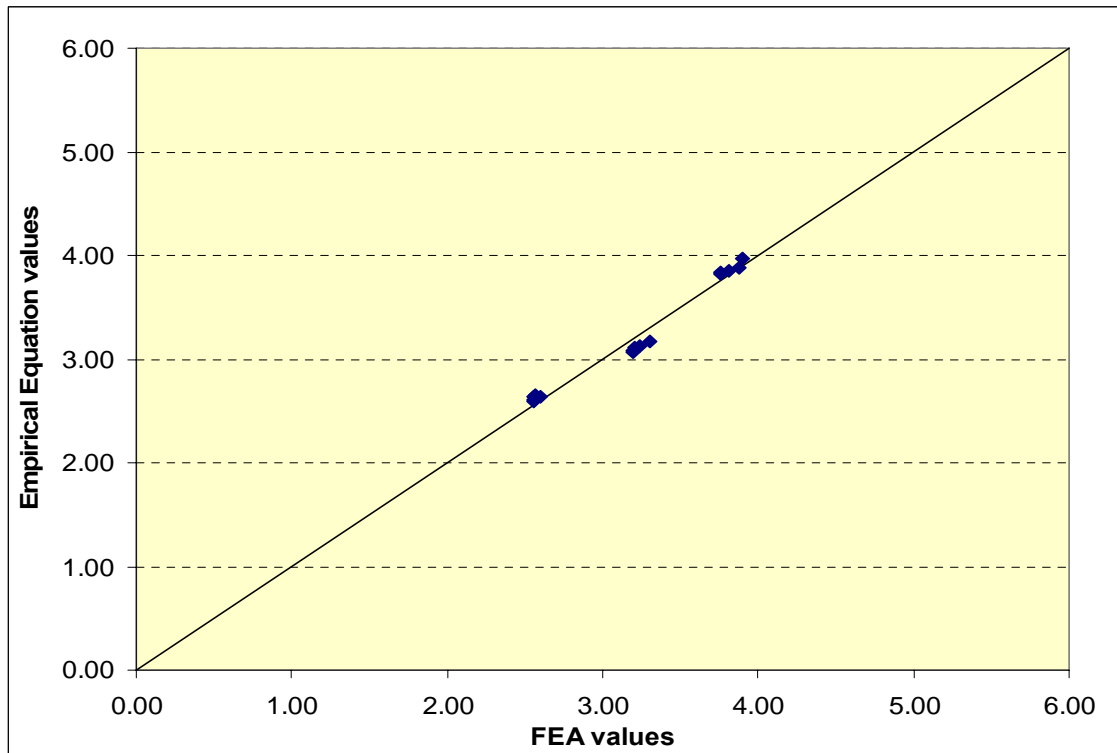


Figure 5.98 Comparison between vertical shear at external support from the empirical equation and FEA for five lanes bridges at FLS as function of (β^2).



Appendix A.1 Parameters of empirical equation of moment distribution factors at ULS

Bridge type	# of Trucks	# of lanes (u)	R _i	Number of Box (N)	Center to center girder spacing (S)	μ	Result from FEA		Parameters of empirical equation					Empirical equation	Variance		
							(β) of Fm+	Fm+	Fm-	a	b	c	d			e	
2 Lanes																	
2L-20-2b	2	Full Load	2	0.9	2	5.00	1	2.35	1.77		7	1	15	-27	0.75	1.75	-1.45
2L-20-3b	2	Full Load	2	0.9	3	3.33	1	2.59	1.75		7	1	15	-27	0.75	1.76	0.52
2L-40-2b	2	Full Load	2	0.9	2	5.00	1	1.52	1.27		7	1	15	-27	0.75	1.34	5.10
2L-40-3b	2	Full Load	2	0.9	3	3.33	1	1.77	1.28		7	1	15	-27	0.75	1.29	0.60
2L-60-2b	2	Full Load	2	0.9	2	5.00	1	1.11	1.15		7	1	15	-27	0.75	1.22	5.68
2L-60-3b	2	Full Load	2	0.9	3	3.33	1	1.33	1.19		7	1	15	-27	0.75	1.15	-3.14
2L-80-2b	2	Full Load	2	0.9	2	5.00	1	0.93	1.18		7	1	15	-27	0.75	1.18	-0.20
2L-80-3b	2	Full Load	2	0.9	3	3.33	1	1.14	1.16		7	1	15	-27	0.75	1.11	-4.48
2L-100-2b	2	Full Load	2	0.9	2	5.00	1	0.82	1.12		7	1	15	-27	0.75	1.16	3.34
2L-100-3b	2	Full Load	2	0.9	3	3.33	1	1.02	1.11		7	1	15	-27	0.75	1.08	-2.01

2 Lanes																	
(β) of Fm-																	
Bridge type	# of Trucks	# of lanes (u)	R _i	Number of Box (N)	Center to center girder spacing (S)	μ	(β) of Fm+	Fm+	Fm-	a	b	c	d	e	Empirical equation	Variance	
2L-20-2b	2	Full Load	2	0.9	2	5.00	1	3.77		3.35	4.6	-0.34	17	-7	0.95	3.21	-4.14
2L-20-3b	2	Full Load	2	0.9	3	3.33	1	4.15		2.82	4.6	-0.34	17	-7	0.95	3.37	19.61
2L-40-2b	2	Full Load	2	0.9	2	5.00	1	2.44		2.38	4.6	-0.34	17	-7	0.95	2.56	7.78
2L-40-3b	2	Full Load	2	0.9	3	3.33	1	2.82		2.71	4.6	-0.34	17	-7	0.95	2.67	-1.15
2L-60-2b	2	Full Load	2	0.9	2	5.00	1	1.78		2.26	4.6	-0.34	17	-7	0.95	2.31	2.17
2L-60-3b	2	Full Load	2	0.9	3	3.33	1	2.12		2.41	4.6	-0.34	17	-7	0.95	2.39	-0.96
2L-80-2b	2	Full Load	2	0.9	2	5.00	1	1.49		2.00	4.6	-0.34	17	-7	0.95	2.22	10.87
2L-80-3b	2	Full Load	2	0.9	3	3.33	1	1.82		2.15	4.6	-0.34	17	-7	0.95	2.28	6.12
2L-100-2b	2	Full Load	2	0.9	2	5.00	1	1.32		1.88	4.6	-0.34	17	-7	0.95	2.16	14.93
2L-100-3b	2	Full Load	2	0.9	3	3.33	1	1.63		2.35	4.6	-0.34	17	-7	0.95	2.21	-5.76

3 Lanes																	
(β) of Fm+																	
Bridge type	# of Trucks	# of lanes (u)	R _i	Number of Box (N)	Center to center girder spacing (S)	μ	(β) of Fm+	Fm+	Fm-	a	b	c	d	e	Empirical equation	Variance	
3L-20-2b	3	Full Load	3	0.8	2	6.75	1	3.01	1.59		9.5	-0.9	17	-7	0.75	1.74	9.81
3L-20-3b	3	Full Load	3	0.8	3	4.50	1	3.25	1.53		9.5	-0.9	17	-7	0.75	1.66	7.91
3L-20-4b	3	Full Load	3	0.8	4	3.38	1	3.85	1.73		9.5	-0.9	17	-7	0.75	1.76	1.67
3L-40-2b	3	Full Load	3	0.8	2	6.75	1	1.81	1.31		9.5	-0.9	17	-7	0.75	1.38	5.26
3L-40-3b	3	Full Load	3	0.8	3	4.50	1	1.82	1.30		9.5	-0.9	17	-7	0.75	1.25	-3.71
3L-40-4b	3	Full Load	3	0.8	4	3.38	1	2.28	1.30		9.5	-0.9	17	-7	0.75	1.27	-2.20
3L-60-2b	3	Full Load	3	0.8	2	6.75	1	1.30	1.14		9.5	-0.9	17	-7	0.75	1.26	11.13
3L-60-3b	3	Full Load	3	0.8	3	4.50	1	1.57	1.16		9.5	-0.9	17	-7	0.75	1.20	2.71
3L-60-4b	3	Full Load	3	0.8	4	3.38	1	1.78	1.17		9.5	-0.9	17	-7	0.75	1.16	-0.84
3L-80-2b	3	Full Load	3	0.8	2	6.75	1	1.11	1.14		9.5	-0.9	17	-7	0.75	1.22	7.19
3L-80-3b	3	Full Load	3	0.8	3	4.50	1	1.32	1.12		9.5	-0.9	17	-7	0.75	1.15	2.12
3L-80-4b	3	Full Load	3	0.8	4	3.38	1	1.53	1.16		9.5	-0.9	17	-7	0.75	1.11	-5.00
3L-100-2b	3	Full Load	3	0.8	2	6.75	1	0.97	1.12		9.5	-0.9	17	-7	0.75	1.19	6.97
3L-100-3b	3	Full Load	3	0.8	3	4.50	1	1.17	1.11		9.5	-0.9	17	-7	0.75	1.12	0.49
3L-100-4b	3	Full Load	3	0.8	4	3.38	1	1.37	1.13		9.5	-0.9	17	-7	0.75	1.08	-4.67

Cont.

Bridge type	# of Trucks	# of lanes (n)	R _L	Number of Box (N)	Center to center girder spacing (S)	μ	Result from FEA		Parameters of empirical equation					Empirical equation	Variance		
							(β) of Fm+	Fm+	Fm-	a	b	c	d			e	
3 Lanes (β) of Fm-																	
3L-20-2b	3	Full Load	3	0.8	2	6.75	1	4.81		3.29	5.6	-0.25	18	-5	0.95	3.16	-4.12
3L-20-3b	3	Full Load	3	0.8	3	4.50	1	5.20		2.87	5.6	-0.25	18	-5	0.95	3.23	12.41
3L-20-4b	3	Full Load	3	0.8	4	3.38	1	6.16		3.36	5.6	-0.25	18	-5	0.95	3.56	5.90
3L-40-2b	3	Full Load	3	0.8	2	6.75	1	2.90		2.65	5.6	-0.25	18	-5	0.95	2.58	-2.59
3L-40-3b	3	Full Load	3	0.8	3	4.50	1	2.91		2.54	5.6	-0.25	18	-5	0.95	2.53	-0.13
3L-40-4b	3	Full Load	3	0.8	4	3.38	1	3.65		2.56	5.6	-0.25	18	-5	0.95	2.70	5.16
3L-60-2b	3	Full Load	3	0.8	2	6.75	1	2.08		2.12	5.6	-0.25	18	-5	0.95	2.38	12.48
3L-60-3b	3	Full Load	3	0.8	3	4.50	1	2.51		2.19	5.6	-0.25	18	-5	0.95	2.44	11.26
3L-60-4b	3	Full Load	3	0.8	4	3.38	1	2.85		2.26	5.6	-0.25	18	-5	0.95	2.48	9.70
3L-80-2b	3	Full Load	3	0.8	2	6.75	1	1.77		2.15	5.6	-0.25	18	-5	0.95	2.32	7.72
3L-80-3b	3	Full Load	3	0.8	3	4.50	1	2.12		2.20	5.6	-0.25	18	-5	0.95	2.35	6.73
3L-80-4b	3	Full Load	3	0.8	4	3.38	1	2.44		2.41	5.6	-0.25	18	-5	0.95	2.39	-1.17
3L-100-2b	3	Full Load	3	0.8	2	6.75	1	1.55		2.16	5.6	-0.25	18	-5	0.95	2.27	4.97
3L-100-3b	3	Full Load	3	0.8	3	4.50	1	1.88		2.34	5.6	-0.25	18	-5	0.95	2.29	-1.85
3L-100-4b	3	Full Load	3	0.8	4	3.38	1	2.19		2.45	5.6	-0.25	18	-5	0.95	2.33	-4.97
4 Lanes (β) of Fm+																	
4L-20-3b	4	Full Load	4	0.7	3	5.67	1	3.90	1.90		13	-0.9	1.4	-7	0.75	1.84	-3.31
4L-20-4b	4	Full Load	4	0.7	4	4.25	1	4.14	1.65		13	-0.9	1.4	-7	0.75	1.79	8.54
4L-20-5b	4	Full Load	4	0.7	5	3.40	1	4.38	1.61		13	-0.9	1.4	-7	0.75	1.77	10.47
4L-40-3b	4	Full Load	4	0.7	3	5.67	1	2.40	1.44		13	-0.9	1.4	-7	0.75	1.41	-2.40
4L-40-4b	4	Full Load	4	0.7	4	4.25	1	2.64	1.44		13	-0.9	1.4	-7	0.75	1.36	-5.16
4L-40-5b	4	Full Load	4	0.7	5	3.40	1	2.87	1.40		13	-0.9	1.4	-7	0.75	1.34	-4.18
4L-60-3b	4	Full Load	4	0.7	3	5.67	1	1.80	1.27		13	-0.9	1.4	-7	0.75	1.28	0.77
4L-60-4b	4	Full Load	4	0.7	4	4.25	1	2.02	1.25		13	-0.9	1.4	-7	0.75	1.23	-1.05
4L-60-5b	4	Full Load	4	0.7	5	3.40	1	2.24	1.26		13	-0.9	1.4	-7	0.75	1.21	-4.30
4L-80-3b	4	Full Load	4	0.7	3	5.67	1	1.50	1.19		13	-0.9	1.4	-7	0.75	1.22	2.44
4L-80-4b	4	Full Load	4	0.7	4	4.25	1	1.71	1.17		13	-0.9	1.4	-7	0.75	1.17	0.54
4L-80-5b	4	Full Load	4	0.7	5	3.40	1	1.92	1.20		13	-0.9	1.4	-7	0.75	1.15	-4.92
4L-100-3b	4	Full Load	4	0.7	3	5.67	1	1.32	1.17		13	-0.9	1.4	-7	0.75	1.19	1.52
4L-100-4b	4	Full Load	4	0.7	4	4.25	1	1.52	1.15		13	-0.9	1.4	-7	0.75	1.14	-1.21
4L-100-5b	4	Full Load	4	0.7	5	3.40	1	1.72	1.18		13	-0.9	1.4	-7	0.75	1.11	-6.24
4 Lanes (β) of Fm-																	
4L-20-3b	4	Full Load	4	0.7	3	5.67	1	6.24		3.50	4.4	-0.07	14	-2	0.8	3.39	-3.10
4L-20-4b	4	Full Load	4	0.7	4	4.25	1	6.63		3.00	4.4	-0.07	14	-2	0.8	3.25	8.36
4L-20-5b	4	Full Load	4	0.7	5	3.40	1	7.00		2.72	4.4	-0.07	14	-2	0.8	3.15	16.05
4L-40-3b	4	Full Load	4	0.7	3	5.67	1	3.84		3.25	4.4	-0.07	14	-2	0.8	3.11	-4.52
4L-40-4b	4	Full Load	4	0.7	4	4.25	1	4.22		3.07	4.4	-0.07	14	-2	0.8	2.97	-3.15
4L-40-5b	4	Full Load	4	0.7	5	3.40	1	4.59		2.94	4.4	-0.07	14	-2	0.8	2.88	-1.84
4L-60-3b	4	Full Load	4	0.7	3	5.67	1	2.88		2.93	4.4	-0.07	14	-2	0.8	3.00	2.34
4L-60-4b	4	Full Load	4	0.7	4	4.25	1	3.23		2.80	4.4	-0.07	14	-2	0.8	2.87	2.65
4L-60-5b	4	Full Load	4	0.7	5	3.40	1	3.58		2.91	4.4	-0.07	14	-2	0.8	2.78	-4.37
4L-80-3b	4	Full Load	4	0.7	3	5.67	1	2.40		2.68	4.4	-0.07	14	-2	0.8	2.95	10.14
4L-80-4b	4	Full Load	4	0.7	4	4.25	1	2.74		2.49	4.4	-0.07	14	-2	0.8	2.82	13.23
4L-80-5b	4	Full Load	4	0.7	5	3.40	1	3.06		2.74	4.4	-0.07	14	-2	0.8	2.73	-0.55
4L-100-3b	4	Full Load	4	0.7	3	5.67	1	2.11		2.69	4.4	-0.07	14	-2	0.8	2.92	8.78
4L-100-4b	4	Full Load	4	0.7	4	4.25	1	2.44		2.65	4.4	-0.07	14	-2	0.8	2.79	5.35
4L-100-5b	4	Full Load	4	0.7	5	3.40	1	2.75		2.80	4.4	-0.07	14	-2	0.8	2.70	-3.62

Cont.

Bridge type	# of Trucks	# of lanes (n)	R _L	Number of Box (N)	Center to center girder spacing (S)	μ	Result from FEA		Parameters of empirical equation					Empirical equation	Variance
							(β) of Fm+	Fm+	Fm-	a	b	c	d		

5 Lanes							(β) of Fm+										
5L-20-3b	5	Full Load	5	0.6	3	6.83	1	4.58	2.21		10	-0.9	51	-7	0.75	2.23	0.87
5L-20-4b	5	Full Load	5	0.6	4	4.88	1	4.99	2.18		10	-0.9	51	-7	0.75	2.16	-1.15
5L-20-5b	5	Full Load	5	0.6	5	4.10	1	5.08	2.13		10	-0.9	51	-7	0.75	2.19	2.85
5L-40-3b	5	Full Load	5	0.6	3	6.83	1	2.74	1.57		10	-0.9	51	-7	0.75	1.57	-0.18
5L-40-4b	5	Full Load	5	0.6	4	4.88	1	2.98	1.52		10	-0.9	51	-7	0.75	1.45	-4.69
5L-40-5b	5	Full Load	5	0.6	5	4.10	1	3.22	1.43		10	-0.9	51	-7	0.75	1.50	4.98
5L-60-3b	5	Full Load	5	0.6	3	6.83	1	2.03	1.35		10	-0.9	51	-7	0.75	1.39	2.97
5L-60-4b	5	Full Load	5	0.6	4	4.88	1	2.26	1.35		10	-0.9	51	-7	0.75	1.28	-4.98
5L-60-5b	5	Full Load	5	0.6	5	4.10	1	2.48	1.34		10	-0.9	51	-7	0.75	1.32	-1.36
5L-80-3b	5	Full Load	5	0.6	3	6.83	1	1.68	1.27		10	-0.9	51	-7	0.75	1.32	3.97
5L-80-4b	5	Full Load	5	0.6	4	4.88	1	1.89	1.24		10	-0.9	51	-7	0.75	1.21	-2.83
5L-80-5b	5	Full Load	5	0.6	5	4.10	1	2.10	1.20		10	-0.9	51	-7	0.75	1.24	3.44
5L-100-3b	5	Full Load	5	0.6	3	6.83	1	1.46	1.22		10	-0.9	51	-7	0.75	1.27	4.57
5L-100-4b	5	Full Load	5	0.6	4	4.88	1	1.67	1.22		10	-0.9	51	-7	0.75	1.16	-4.43
5L-100-5b	5	Full Load	5	0.6	5	4.10	1	1.87	1.17		10	-0.9	51	-7	0.75	1.20	2.18

5 Lanes							(β) of Fm-										
5L-20-3b	5	Full Load	5	0.6	3	6.83	1	7.32		4.28	3.6	-0.06	12	-2	0.62	4.39	2.44
5L-20-4b	5	Full Load	5	0.6	4	4.88	1	7.98		3.68	3.6	-0.06	12	-2	0.62	3.84	4.39
5L-20-5b	5	Full Load	5	0.6	5	4.10	1	8.12		3.55	3.6	-0.06	12	-2	0.62	3.73	5.14
5L-40-3b	5	Full Load	5	0.6	3	6.83	1	4.39		4.12	3.6	-0.06	12	-2	0.62	3.92	-4.86
5L-40-4b	5	Full Load	5	0.6	4	4.88	1	4.77		3.61	3.6	-0.06	12	-2	0.62	3.39	-6.04
5L-40-5b	5	Full Load	5	0.6	5	4.10	1	5.15		3.20	3.6	-0.06	12	-2	0.62	3.32	3.81
5L-60-3b	5	Full Load	5	0.6	3	6.83	1	3.25		3.71	3.6	-0.06	12	-2	0.62	3.76	1.33
5L-60-4b	5	Full Load	5	0.6	4	4.88	1	3.61		3.38	3.6	-0.06	12	-2	0.62	3.25	-3.77
5L-60-5b	5	Full Load	5	0.6	5	4.10	1	3.96		3.23	3.6	-0.06	12	-2	0.62	3.18	-1.69
5L-80-3b	5	Full Load	5	0.6	3	6.83	1	2.68		3.54	3.6	-0.06	12	-2	0.62	3.68	4.12
5L-80-4b	5	Full Load	5	0.6	4	4.88	1	3.03		3.30	3.6	-0.06	12	-2	0.62	3.18	-3.67
5L-80-5b	5	Full Load	5	0.6	5	4.10	1	3.36		2.94	3.6	-0.06	12	-2	0.62	3.11	5.58
5L-100-3b	5	Full Load	5	0.6	3	6.83	1	2.34		3.31	3.6	-0.06	12	-2	0.62	3.64	10.00
5L-100-4b	5	Full Load	5	0.6	4	4.88	1	2.67		3.13	3.6	-0.06	12	-2	0.62	3.14	0.14
5L-100-5b	5	Full Load	5	0.6	5	4.10	1	2.99		3.01	3.6	-0.06	12	-2	0.62	3.07	2.00

Appendix A.2 Parameters of empirical equation of moment distribution factors at FLS

Bridge type	# of Trucks	# of lanes (n)	R_L	Number of Box (N)	Center to center girder spacing (S)	μ	(β) of F_{M+}	Result from FEA		Parameters of empirical equation					Empirical equation	Variance	
								F_{M+}	F_{M-}	a	b	c	d	e			
2 Lanes																	
2L-20-2b	1	Fatigue_1	2	0.9	2	5.00	1	2.35	2.97		7.30	-1.92	5.00	-2.00	0.75	3.02	1.63
2L-20-3b	1	Fatigue_1	2	0.9	3	3.33	1	2.59	3.00		7.30	-1.92	5.00	-2.00	0.75	3.28	9.38
2L-40-2b	1	Fatigue_1	2	0.9	2	5.00	1	1.52	1.64		7.30	-1.92	5.00	-2.00	0.75	1.89	15.12
2L-40-3b	1	Fatigue_1	2	0.9	3	3.33	1	1.77	1.79		7.30	-1.92	5.00	-2.00	0.75	1.91	7.12
2L-60-2b	1	Fatigue_1	2	0.9	2	5.00	1	1.11	1.67		7.30	-1.92	5.00	-2.00	0.75	1.58	-4.93
2L-60-3b	1	Fatigue_1	2	0.9	3	3.33	1	1.33	1.60		7.30	-1.92	5.00	-2.00	0.75	1.56	-2.63
2L-80-2b	1	Fatigue_1	2	0.9	2	5.00	1	0.93	1.42		7.30	-1.92	5.00	-2.00	0.75	1.48	4.24
2L-80-3b	1	Fatigue_1	2	0.9	3	3.33	1	1.14	1.50		7.30	-1.92	5.00	-2.00	0.75	1.45	-3.45
2L-100-2b	1	Fatigue_1	2	0.9	2	5.00	1	0.82	1.33		7.30	-1.92	5.00	-2.00	0.75	1.42	6.69
2L-100-3b	1	Fatigue_1	2	0.9	3	3.33	1	1.02	1.41		7.30	-1.92	5.00	-2.00	0.75	1.38	-1.93
2 Lanes (β) of F_{M-}																	
2L-20-2b	1	Fatigue_1	2	0.9	2	5.00	1	3.77		4.50	4.50	-0.37	6.40	-7.77	1.09	4.44	-1.26
2L-20-3b	1	Fatigue_1	2	0.9	3	3.33	1	4.15		4.34	4.50	-0.37	6.40	-7.77	1.09	5.02	15.69
2L-40-2b	1	Fatigue_1	2	0.9	2	5.00	1	2.44		2.92	4.50	-0.37	6.40	-7.77	1.09	3.38	16.04
2L-40-3b	1	Fatigue_1	2	0.9	3	3.33	1	2.82		3.54	4.50	-0.37	6.40	-7.77	1.09	3.78	6.89
2L-60-2b	1	Fatigue_1	2	0.9	2	5.00	1	1.78		3.15	4.50	-0.37	6.40	-7.77	1.09	2.99	-5.00
2L-60-3b	1	Fatigue_1	2	0.9	3	3.33	1	2.12		3.30	4.50	-0.37	6.40	-7.77	1.09	3.31	0.24
2L-80-2b	1	Fatigue_1	2	0.9	2	5.00	1	1.49		2.46	4.50	-0.37	6.40	-7.77	1.09	2.84	15.70
2L-80-3b	1	Fatigue_1	2	0.9	3	3.33	1	1.82		2.92	4.50	-0.37	6.40	-7.77	1.09	3.13	6.98
2L-100-2b	1	Fatigue_1	2	0.9	2	5.00	1	1.32		2.33	4.50	-0.37	6.40	-7.77	1.09	2.76	18.21
2L-100-3b	1	Fatigue_1	2	0.9	3	3.33	1	1.63		3.24	4.50	-0.37	6.40	-7.77	1.09	3.02	-6.67
3 Lanes (β) of F_{M+}																	
3L-20-2b	1	Fatigue_1	3	0.8	2	6.75	1	3.01	3.46		9.34	-1.18	4.00	-13.15	0.86	3.28	-4.98
3L-20-3b	1	Fatigue_1	3	0.8	3	4.50	1	3.25	3.50		9.34	-1.18	4.00	-13.15	0.86	3.43	-1.88
3L-20-4b	1	Fatigue_1	3	0.8	4	3.38	1	3.85	4.14		9.34	-1.18	4.00	-13.15	0.86	4.34	4.67
3L-40-2b	1	Fatigue_1	3	0.8	2	6.75	1	1.81	2.19		9.34	-1.18	4.00	-13.15	0.86	2.12	-3.13
3L-40-3b	1	Fatigue_1	3	0.8	3	4.50	1	1.82	2.09		9.34	-1.18	4.00	-13.15	0.86	2.01	-3.82
3L-40-4b	1	Fatigue_1	3	0.8	4	3.38	1	2.28	2.35		9.34	-1.18	4.00	-13.15	0.86	2.26	-3.81
3L-60-2b	1	Fatigue_1	3	0.8	2	6.75	1	1.30	1.64		9.34	-1.18	4.00	-13.15	0.86	1.80	10.09
3L-60-3b	1	Fatigue_1	3	0.8	3	4.50	1	1.57	1.79		9.34	-1.18	4.00	-13.15	0.86	1.85	3.65
3L-60-4b	1	Fatigue_1	3	0.8	4	3.38	1	1.78	1.94		9.34	-1.18	4.00	-13.15	0.86	1.91	-1.76
3L-80-2b	1	Fatigue_1	3	0.8	2	6.75	1	1.11	1.52		9.34	-1.18	4.00	-13.15	0.86	1.71	12.10
3L-80-3b	1	Fatigue_1	3	0.8	3	4.50	1	1.32	1.66		9.34	-1.18	4.00	-13.15	0.86	1.72	3.22
3L-80-4b	1	Fatigue_1	3	0.8	4	3.38	1	1.53	1.82		9.34	-1.18	4.00	-13.15	0.86	1.76	-3.45
3L-100-2b	1	Fatigue_1	3	0.8	2	6.75	1	0.97	1.45		9.34	-1.18	4.00	-13.15	0.86	1.64	13.09
3L-100-3b	1	Fatigue_1	3	0.8	3	4.50	1	1.17	1.61		9.34	-1.18	4.00	-13.15	0.86	1.64	2.14
3L-100-4b	1	Fatigue_1	3	0.8	4	3.38	1	1.37	1.71		9.34	-1.18	4.00	-13.15	0.86	1.67	-1.90

Cont.

Bridge type	# of Trucks	# of lanes (n)	R _L	Number of Box (N)	Center to center girder spacing (S)	μ	(β) of F _{M+}	Result from FEA		Parameters of empirical equation					Empirical equation	Variance	
								F _{M+}	F _{M-}	a	b	c	d	e			
3 Lanes								(β) of F_{M-}									
3L-20-2b	1	Fatigue_1	3	0.8	2	6.75	1	4.81		5.76	5.25	-0.33	9.25	-6.90	1.18	5.49	-4.64
3L-20-3b	1	Fatigue_1	3	0.8	3	4.50	1	5.20		5.98	5.25	-0.33	9.25	-6.90	1.18	6.35	6.04
3L-20-4b	1	Fatigue_1	3	0.8	4	3.38	1	6.16		7.60	5.25	-0.33	9.25	-6.90	1.18	8.06	6.11
3L-40-2b	1	Fatigue_1	3	0.8	2	6.75	1	2.90		3.96	5.25	-0.33	9.25	-6.90	1.18	3.99	0.76
3L-40-3b	1	Fatigue_1	3	0.8	3	4.50	1	2.91		4.37	5.25	-0.33	9.25	-6.90	1.18	4.30	-1.68
3L-40-4b	1	Fatigue_1	3	0.8	4	3.38	1	3.65		4.78	5.25	-0.33	9.25	-6.90	1.18	5.10	6.66
3L-60-2b	1	Fatigue_1	3	0.8	2	6.75	1	2.08		3.36	5.25	-0.33	9.25	-6.90	1.18	3.53	5.03
3L-60-3b	1	Fatigue_1	3	0.8	3	4.50	1	2.51		3.64	5.25	-0.33	9.25	-6.90	1.18	4.05	11.05
3L-60-4b	1	Fatigue_1	3	0.8	4	3.38	1	2.85		4.19	5.25	-0.33	9.25	-6.90	1.18	4.49	7.13
3L-80-2b	1	Fatigue_1	3	0.8	2	6.75	1	1.77		2.92	5.25	-0.33	9.25	-6.90	1.18	3.38	15.74
3L-80-3b	1	Fatigue_1	3	0.8	3	4.50	1	2.12		3.85	5.25	-0.33	9.25	-6.90	1.18	3.82	4.71
3L-80-4b	1	Fatigue_1	3	0.8	4	3.38	1	2.44		4.31	5.25	-0.33	9.25	-6.90	1.18	4.22	-2.20
3L-100-2b	1	Fatigue_1	3	0.8	2	6.75	1	1.55		2.95	5.25	-0.33	9.25	-6.90	1.18	3.27	11.02
3L-100-3b	1	Fatigue_1	3	0.8	3	4.50	1	1.88		3.83	5.25	-0.33	9.25	-6.90	1.18	3.69	-3.68
3L-100-4b	1	Fatigue_1	3	0.8	4	3.38	1	2.19		3.96	5.25	-0.33	9.25	-6.90	1.18	4.07	2.70
4 Lanes								(β) of F_{M+}									
4L-20-3b	1	Fatigue_1	4	0.7	3	5.67	1	3.90	4.87		8.16	-0.85	-7.50	-10.00	0.70	4.72	-3.14
4L-20-4b	1	Fatigue_1	4	0.7	4	4.25	1	4.14	4.39		8.16	-0.85	-7.50	-10.00	0.70	4.73	7.78
4L-20-5b	1	Fatigue_1	4	0.7	5	3.40	1	4.38	4.31		8.16	-0.85	-7.50	-10.00	0.70	4.85	12.41
4L-40-3b	1	Fatigue_1	4	0.7	3	5.67	1	2.40	2.96		8.16	-0.85	-7.50	-10.00	0.70	2.92	-1.44
4L-40-4b	1	Fatigue_1	4	0.7	4	4.25	1	2.64	2.94		8.16	-0.85	-7.50	-10.00	0.70	2.86	-2.56
4L-40-5b	1	Fatigue_1	4	0.7	5	3.40	1	2.87	2.97		8.16	-0.85	-7.50	-10.00	0.70	2.87	-3.26
4L-60-3b	1	Fatigue_1	4	0.7	3	5.67	1	1.80	2.22		8.16	-0.85	-7.50	-10.00	0.70	2.48	11.43
4L-60-4b	1	Fatigue_1	4	0.7	4	4.25	1	2.02	2.35		8.16	-0.85	-7.50	-10.00	0.70	2.41	2.56
4L-60-5b	1	Fatigue_1	4	0.7	5	3.40	1	2.24	2.52		8.16	-0.85	-7.50	-10.00	0.70	2.39	-5.35
4L-80-3b	1	Fatigue_1	4	0.7	3	5.67	1	1.50	1.97		8.16	-0.85	-7.50	-10.00	0.70	2.29	16.17
4L-80-4b	1	Fatigue_1	4	0.7	4	4.25	1	1.71	2.10		8.16	-0.85	-7.50	-10.00	0.70	2.22	5.74
4L-80-5b	1	Fatigue_1	4	0.7	5	3.40	1	1.92	2.25		8.16	-0.85	-7.50	-10.00	0.70	2.19	-2.66
4L-100-3b	1	Fatigue_1	4	0.7	3	5.67	1	1.32	1.83		8.16	-0.85	-7.50	-10.00	0.70	2.19	19.72
4L-100-4b	1	Fatigue_1	4	0.7	4	4.25	1	1.52	1.9522		8.16	-0.85	-7.50	-10.00	0.70	2.11	8.27
4L-100-5b	1	Fatigue_1	4	0.7	5	3.40	1	1.72	2.0918		8.16	-0.85	-7.50	-10.00	0.70	2.08	-0.62
4 Lanes								(β) of F_{M-}									
4L-20-3b	1	Fatigue_1	4	0.7	3	5.67	1	6.24		7.70	4.00	-0.15	6.00	-3.86	1.07	7.32	-4.99
4L-20-4b	1	Fatigue_1	4	0.7	4	4.25	1	6.63		7.67	4.00	-0.15	6.00	-3.86	1.07	7.75	1.01
4L-20-5b	1	Fatigue_1	4	0.7	5	3.40	1	7.00		7.00	4.00	-0.15	6.00	-3.86	1.07	8.17	16.65
4L-40-3b	1	Fatigue_1	4	0.7	3	5.67	1	3.84		5.87	4.00	-0.15	6.00	-3.86	1.07	5.88	0.23
4L-40-4b	1	Fatigue_1	4	0.7	4	4.25	1	4.22		6.44	4.00	-0.15	6.00	-3.86	1.07	6.20	-3.70
4L-40-5b	1	Fatigue_1	4	0.7	5	3.40	1	4.59		6.74	4.00	-0.15	6.00	-3.86	1.07	6.51	-3.42
4L-60-3b	1	Fatigue_1	4	0.7	3	5.67	1	2.88		5.17	4.00	-0.15	6.00	-3.86	1.07	5.42	4.97
4L-60-4b	1	Fatigue_1	4	0.7	4	4.25	1	3.23		5.68	4.00	-0.15	6.00	-3.86	1.07	5.70	0.37
4L-60-5b	1	Fatigue_1	4	0.7	5	3.40	1	3.58		6.10	4.00	-0.15	6.00	-3.86	1.07	5.96	-2.37
4L-80-3b	1	Fatigue_1	4	0.7	3	5.67	1	2.40		4.74	4.00	-0.15	6.00	-3.86	1.07	5.21	10.01
4L-80-4b	1	Fatigue_1	4	0.7	4	4.25	1	2.74		5.13	4.00	-0.15	6.00	-3.86	1.07	5.47	6.57
4L-80-5b	1	Fatigue_1	4	0.7	5	3.40	1	3.06		5.92	4.00	-0.15	6.00	-3.86	1.07	5.71	-3.67
4L-100-3b	1	Fatigue_1	4	0.7	3	5.67	1	2.11		4.69	4.00	-0.15	6.00	-3.86	1.07	5.09	8.62
4L-100-4b	1	Fatigue_1	4	0.7	4	4.25	1	2.44		5.20	4.00	-0.15	6.00	-3.86	1.07	5.34	2.51
4L-100-5b	1	Fatigue_1	4	0.7	5	3.40	1	2.75		5.68	4.00	-0.15	6.00	-3.86	1.07	5.56	-2.18

Cont.

Bridge type	# of Trucks	# of lanes (n)	R _L	Number of Box (N)	Center to center girder spacing (S)	μ	(β) of F _{m+}	Result from FEA		Parameters of empirical equation					Empirical equation	Variance	
								F _{M+}	F _{M-}	a	b	c	d	e			
5 Lanes																	
(β) of F_{m+}																	
5L-20-3b	1	Fatigue_1	5	0.6	3	6.83	1	4.58	5.90		8.38	-0.85	7.00	-10.85	0.77	6.19	4.87
5L-20-4b	1	Fatigue_1	5	0.6	4	4.88	1	4.99	6.01		8.38	-0.85	7.00	-10.85	0.77	6.48	7.75
5L-20-5b	1	Fatigue_1	5	0.6	5	4.10	1	5.08	5.97		8.38	-0.85	7.00	-10.85	0.77	6.71	12.43
5L-40-3b	1	Fatigue_1	5	0.6	3	6.83	1	2.74	3.39		8.38	-0.85	7.00	-10.85	0.77	3.41	0.50
5L-40-4b	1	Fatigue_1	5	0.6	4	4.88	1	2.98	3.42		8.38	-0.85	7.00	-10.85	0.77	3.25	-4.96
5L-40-5b	1	Fatigue_1	5	0.6	5	4.10	1	3.22	3.37		8.38	-0.85	7.00	-10.85	0.77	3.48	3.33
5L-60-3b	1	Fatigue_1	5	0.6	3	6.83	1	2.03	2.50		8.38	-0.85	7.00	-10.85	0.77	2.82	12.66
5L-60-4b	1	Fatigue_1	5	0.6	4	4.88	1	2.26	2.72		8.38	-0.85	7.00	-10.85	0.77	2.66	-2.09
5L-60-5b	1	Fatigue_1	5	0.6	5	4.10	1	2.48	2.84		8.38	-0.85	7.00	-10.85	0.77	2.82	-0.93
5L-80-3b	1	Fatigue_1	5	0.6	3	6.83	1	1.68	2.21		8.38	-0.85	7.00	-10.85	0.77	2.58	16.64
5L-80-4b	1	Fatigue_1	5	0.6	4	4.88	1	1.89	2.39		8.38	-0.85	7.00	-10.85	0.77	2.42	1.09
5L-80-5b	1	Fatigue_1	5	0.6	5	4.10	1	2.10	2.41		8.38	-0.85	7.00	-10.85	0.77	2.55	5.73
5L-100-3b	1	Fatigue_1	5	0.6	3	6.83	1	1.46	2.25		8.38	-0.85	7.00	-10.85	0.77	2.45	8.79
5L-100-4b	1	Fatigue_1	5	0.6	4	4.88	1	1.67	2.18		8.38	-0.85	7.00	-10.85	0.77	2.29	4.95
5L-100-5b	1	Fatigue_1	5	0.6	5	4.10	1	1.87	2.24		8.38	-0.85	7.00	-10.85	0.77	2.40	7.31

5 Lanes																	
(β) of F_{m-}																	
5L-20-3b	1	Fatigue_1	5	0.6	3	6.83	1	7.32		10.20	3.70	-0.14	5.00	-3.74	1.00	9.88	-3.18
5L-20-4b	1	Fatigue_1	5	0.6	4	4.88	1	7.98		9.91	3.70	-0.14	5.00	-3.74	1.00	10.05	1.38
5L-20-5b	1	Fatigue_1	5	0.6	5	4.10	1	8.12		9.82	3.70	-0.14	5.00	-3.74	1.00	10.72	9.15
5L-40-3b	1	Fatigue_1	5	0.6	3	6.83	1	4.39		7.55	3.70	-0.14	5.00	-3.74	1.00	7.50	-0.63
5L-40-4b	1	Fatigue_1	5	0.6	4	4.88	1	4.77		7.58	3.70	-0.14	5.00	-3.74	1.00	7.38	-2.61
5L-40-5b	1	Fatigue_1	5	0.6	5	4.10	1	5.15		7.68	3.70	-0.14	5.00	-3.74	1.00	8.03	4.51
5L-60-3b	1	Fatigue_1	5	0.6	3	6.83	1	3.25		6.28	3.70	-0.14	5.00	-3.74	1.00	6.80	8.29
5L-60-4b	1	Fatigue_1	5	0.6	4	4.88	1	3.61		7.05	3.70	-0.14	5.00	-3.74	1.00	6.67	-5.40
5L-60-5b	1	Fatigue_1	5	0.6	5	4.10	1	3.96		7.42	3.70	-0.14	5.00	-3.74	1.00	7.23	-2.57
5L-80-3b	1	Fatigue_1	5	0.6	3	6.83	1	2.68		6.02	3.70	-0.14	5.00	-3.74	1.00	6.49	7.78
5L-80-4b	1	Fatigue_1	5	0.6	4	4.88	1	3.03		6.77	3.70	-0.14	5.00	-3.74	1.00	6.35	-6.14
5L-80-5b	1	Fatigue_1	5	0.6	5	4.10	1	3.36		6.64	3.70	-0.14	5.00	-3.74	1.00	6.87	3.40
5L-100-3b	1	Fatigue_1	5	0.6	3	6.83	1	2.34		5.66	3.70	-0.14	5.00	-3.74	1.00	6.32	11.57
5L-100-4b	1	Fatigue_1	5	0.6	4	4.88	1	2.67		6.38	3.70	-0.14	5.00	-3.74	1.00	6.17	-3.31
5L-100-5b	1	Fatigue_1	5	0.6	5	4.10	1	2.99		6.66	3.70	-0.14	5.00	-3.74	1.00	6.66	0.02

Appendix A.3 Parameters of empirical equation of shear distribution factors as function of (L) span length at ULS

Bridge type	# of Trucks	# of lanes (n)	Span length (L)	R _L	Number of Box (N)	Center to center girder spacing (S)	Result from FEA			Parameters of empirical equation			Empirical equation	Variance	
							μ	Fv inner	Fv outer	e	a	b			
2 Lanes															
2L-20-2b	2	Full Load	2	20	0.9	2	5.00	1.00	1.21		1.8	14.5	-0.01	1.22	0.23
2L-20-3b	2	Full Load	2	20	0.9	3	3.33	1.00	1.68		1.8	14.5	-0.01	1.68	0.30
2L-40-2b	2	Full Load	2	40	0.9	2	5.00	1.00	1.22		1.8	14.5	-0.01	1.23	1.10
2L-40-3b	2	Full Load	2	40	0.9	3	3.33	1.00	1.68		1.8	14.5	-0.01	1.71	1.86
2L-60-2b	2	Full Load	2	60	0.9	2	5.00	1.00	1.23		1.8	14.5	-0.01	1.25	1.87
2L-60-3b	2	Full Load	2	60	0.9	3	3.33	1.00	1.71		1.8	14.5	-0.01	1.73	1.50
2L-80-2b	2	Full Load	2	80	0.9	2	5.00	1.00	1.26		1.8	14.5	-0.01	1.27	1.25
2L-80-3b	2	Full Load	2	80	0.9	3	3.33	1.00	1.74		1.8	14.5	-0.01	1.76	1.15
2L-100-2b	2	Full Load	2	100	0.9	2	5.00	1.00	1.27		1.8	14.5	-0.01	1.29	1.39
2L-100-3b	2	Full Load	2	100	0.9	3	3.33	1.00	1.75		1.8	14.5	-0.01	1.78	1.88
2 Lanes															
2L-20-2b	2	Full Load	2	20	0.9	2	5.00	1.00		1.15	1.72	14.5	-0.01	1.15	-0.27
2L-20-3b	2	Full Load	2	20	0.9	3	3.33	1.00		1.55	1.72	14.5	-0.01	1.54	-0.27
2L-40-2b	2	Full Load	2	40	0.9	2	5.00	1.00		1.17	1.72	14.5	-0.01	1.17	-0.46
2L-40-3b	2	Full Load	2	40	0.9	3	3.33	1.00		1.57	1.72	14.5	-0.01	1.56	-0.08
2L-60-2b	2	Full Load	2	60	0.9	2	5.00	1.00		1.20	1.72	14.5	-0.01	1.19	-1.04
2L-60-3b	2	Full Load	2	60	0.9	3	3.33	1.00		1.60	1.72	14.5	-0.01	1.59	-0.86
2L-80-2b	2	Full Load	2	80	0.9	2	5.00	1.00		1.20	1.72	14.5	-0.01	1.20	-0.19
2L-80-3b	2	Full Load	2	80	0.9	3	3.33	1.00		1.62	1.72	14.5	-0.01	1.61	-0.61
2L-100-2b	2	Full Load	2	100	0.9	2	5.00	1.00		1.21	1.72	14.5	-0.01	1.22	0.79
2L-100-3b	2	Full Load	2	100	0.9	3	3.33	1.00		1.64	1.72	14.5	-0.01	1.63	-0.48
3 Lanes															
3L-20-2b	3	Full Load	3	20	0.8	2	6.75	1.00	1.23		1.45	15.8	-0.01	1.18	-3.80
3L-20-3b	3	Full Load	3	20	0.8	3	4.50	1.00	1.32		1.45	15.8	-0.01	1.42	7.56
3L-20-4b	3	Full Load	3	20	0.8	4	3.38	1.00	1.67		1.45	15.8	-0.01	1.61	-3.42
3L-40-2b	3	Full Load	3	40	0.8	2	6.75	1.00	1.22		1.45	15.8	-0.01	1.20	-1.67
3L-40-3b	3	Full Load	3	40	0.8	3	4.50	1.00	1.35		1.45	15.8	-0.01	1.44	6.24
3L-40-4b	3	Full Load	3	40	0.8	4	3.38	1.00	1.65		1.45	15.8	-0.01	1.64	-0.74
3L-60-2b	3	Full Load	3	60	0.8	2	6.75	1.00	1.23		1.45	15.8	-0.01	1.21	-1.72
3L-60-3b	3	Full Load	3	60	0.8	3	4.50	1.00	1.35		1.45	15.8	-0.01	1.46	7.56
3L-60-4b	3	Full Load	3	60	0.8	4	3.38	1.00	1.66		1.45	15.8	-0.01	1.66	-0.44
3L-80-2b	3	Full Load	3	80	0.8	2	6.75	1.00	1.27		1.45	15.8	-0.01	1.23	-3.01
3L-80-3b	3	Full Load	3	80	0.8	3	4.50	1.00	1.36		1.45	15.8	-0.01	1.48	8.28
3L-80-4b	3	Full Load	3	80	0.8	4	3.38	1.00	1.69		1.45	15.8	-0.01	1.68	-0.76
3L-100-2b	3	Full Load	3	100	0.8	2	6.75	1.00	1.30		1.45	15.8	-0.01	1.25	-4.12
3L-100-3b	3	Full Load	3	100	0.8	3	4.50	1.00	1.37		1.45	15.8	-0.01	1.50	8.84
3L-100-4b	3	Full Load	3	100	0.8	4	3.38	1.00	1.73		1.45	15.8	-0.01	1.70	-1.39

Cont.

Bridge type	# of Trucks	# of lanes (n)	Span length (L)	R _L	Number of Box (N)	Center to center girder spacing (S)	Result from FEA			Parameters of empirical equation			Empirical equation	Variance	
							μ	Fv inner	Fv outer	e	a	b			
3 Lanes															
3L-20-2b	3	Full Load	3	20	0.8	2	6.75	1.00		1.14	1.4	15.8	-0.01	1.14	0.16
3L-20-3b	3	Full Load	3	20	0.8	3	4.50	1.00		1.25	1.4	15.8	-0.01	1.34	7.47
3L-20-4b	3	Full Load	3	20	0.8	4	3.38	1.00		1.52	1.4	15.8	-0.01	1.51	-1.05
3L-40-2b	3	Full Load	3	40	0.8	2	6.75	1.00		1.18	1.4	15.8	-0.01	1.16	-1.66
3L-40-3b	3	Full Load	3	40	0.8	3	4.50	1.00		1.26	1.4	15.8	-0.01	1.36	7.61
3L-40-4b	3	Full Load	3	40	0.8	4	3.38	1.00		1.53	1.4	15.8	-0.01	1.53	-0.54
3L-60-2b	3	Full Load	3	60	0.8	2	6.75	1.00		1.21	1.4	15.8	-0.01	1.17	-3.12
3L-60-3b	3	Full Load	3	60	0.8	3	4.50	1.00		1.29	1.4	15.8	-0.01	1.38	6.91
3L-60-4b	3	Full Load	3	60	0.8	4	3.38	1.00		1.57	1.4	15.8	-0.01	1.55	-1.30
3L-80-2b	3	Full Load	3	80	0.8	2	6.75	1.00		1.22	1.4	15.8	-0.01	1.19	-2.56
3L-80-3b	3	Full Load	3	80	0.8	3	4.50	1.00		1.30	1.4	15.8	-0.01	1.40	7.48
3L-80-4b	3	Full Load	3	80	0.8	4	3.38	1.00		1.59	1.4	15.8	-0.01	1.57	-1.28
3L-100-2b	3	Full Load	3	100	0.8	2	6.75	1.00		1.24	1.4	15.8	-0.01	1.20	-2.65
3L-100-3b	3	Full Load	3	100	0.8	3	4.50	1.00		1.31	1.4	15.8	-0.01	1.42	7.72
3L-100-4b	3	Full Load	3	100	0.8	4	3.38	1.00		1.62	1.4	15.8	-0.01	1.59	-1.91

4 Lanes															
4L-20-3b	4	Full Load	4	20	0.7	3	5.67	1.00	1.48		1.4	18.5	-0.01	1.44	-2.83
4L-20-4b	4	Full Load	4	20	0.7	4	4.25	1.00	1.47		1.4	18.5	-0.01	1.62	9.79
4L-20-5b	4	Full Load	4	20	0.7	5	3.40	1.00	1.84		1.4	18.5	-0.01	1.77	-4.05
4L-40-3b	4	Full Load	4	40	0.7	3	5.67	1.00	1.49		1.4	18.5	-0.01	1.46	-2.37
4L-40-4b	4	Full Load	4	40	0.7	4	4.25	1.00	1.48		1.4	18.5	-0.01	1.64	10.19
4L-40-5b	4	Full Load	4	40	0.7	5	3.40	1.00	1.81		1.4	18.5	-0.01	1.79	-1.38
4L-60-3b	4	Full Load	4	60	0.7	3	5.67	1.00	1.52		1.4	18.5	-0.01	1.47	-3.12
4L-60-4b	4	Full Load	4	60	0.7	4	4.25	1.00	1.48		1.4	18.5	-0.01	1.65	11.65
4L-60-5b	4	Full Load	4	60	0.7	5	3.40	1.00	1.83		1.4	18.5	-0.01	1.81	-1.34
4L-80-3b	4	Full Load	4	80	0.7	3	5.67	1.00	1.56		1.4	18.5	-0.01	1.49	-4.28
4L-80-4b	4	Full Load	4	80	0.7	4	4.25	1.00	1.50		1.4	18.5	-0.01	1.67	11.48
4L-80-5b	4	Full Load	4	80	0.7	5	3.40	1.00	1.88		1.4	18.5	-0.01	1.83	-2.80
4L-100-3b	4	Full Load	4	100	0.7	3	5.67	1.00	1.60		1.4	18.5	-0.01	1.51	-5.65
4L-100-4b	4	Full Load	4	100	0.7	4	4.25	1.00	1.51		1.4	18.5	-0.01	1.69	11.85
4L-100-5b	4	Full Load	4	100	0.7	5	3.40	1.00	1.91		1.4	18.5	-0.01	1.85	-3.27

4 Lanes															
4L-20-3b	4	Full Load	4	20	0.7	3	5.67	1.00		1.33	1.33	18.5	-0.01	1.33	0.71
4L-20-4b	4	Full Load	4	20	0.7	4	4.25	1.00		1.37	1.33	18.5	-0.01	1.47	7.17
4L-20-5b	4	Full Load	4	20	0.7	5	3.40	1.00		1.65	1.33	18.5	-0.01	1.58	-4.03
4L-40-3b	4	Full Load	4	40	0.7	3	5.67	1.00		1.38	1.33	18.5	-0.01	1.35	-1.99
4L-40-4b	4	Full Load	4	40	0.7	4	4.25	1.00		1.36	1.33	18.5	-0.01	1.48	9.51
4L-40-5b	4	Full Load	4	40	0.7	5	3.40	1.00		1.62	1.33	18.5	-0.01	1.60	-1.19
4L-60-3b	4	Full Load	4	60	0.7	3	5.67	1.00		1.42	1.33	18.5	-0.01	1.36	-4.06
4L-60-4b	4	Full Load	4	60	0.7	4	4.25	1.00		1.37	1.33	18.5	-0.01	1.50	9.79
4L-60-5b	4	Full Load	4	60	0.7	5	3.40	1.00		1.66	1.33	18.5	-0.01	1.62	-2.57
4L-80-3b	4	Full Load	4	80	0.7	3	5.67	1.00		1.45	1.33	18.5	-0.01	1.38	-4.90
4L-80-4b	4	Full Load	4	80	0.7	4	4.25	1.00		1.39	1.33	18.5	-0.01	1.52	9.18
4L-80-5b	4	Full Load	4	80	0.7	5	3.40	1.00		1.70	1.33	18.5	-0.01	1.63	-3.81
4L-100-3b	4	Full Load	4	100	0.7	3	5.67	1.00		1.47	1.33	18.5	-0.01	1.40	-5.29
4L-100-4b	4	Full Load	4	100	0.7	4	4.25	1.00		1.41	1.33	18.5	-0.01	1.53	9.11
4L-100-5b	4	Full Load	4	100	0.7	5	3.40	1.00		1.73	1.33	18.5	-0.01	1.65	-4.75

Cont.

Bridge type	# of Trucks	# of lanes (n)	Span length (L)	R _L	Number of Box (N)	Center to center girder spacing (S)	Result from FEA			Parameters of empirical equation			Empirical equation	Variance	
							μ	Fv inner	Fv outer	e	a	b			
5 Lanes															
5L-20-3b	5	Full Load	5	20	0.6	3	6.83	1.00	1.61		1.1	13.6	-0.01	1.71	5.99
5L-20-4b	5	Full Load	5	20	0.6	4	4.88	1.00	1.73		1.1	13.6	-0.01	1.67	-3.42
5L-20-5b	5	Full Load	5	20	0.6	5	4.10	1.00	1.67		1.1	13.6	-0.01	1.80	7.30
5L-40-3b	5	Full Load	5	40	0.6	3	6.83	1.00	1.61		1.1	13.6	-0.01	1.73	7.66
5L-40-4b	5	Full Load	5	40	0.6	4	4.88	1.00	1.77		1.1	13.6	-0.01	1.70	-4.31
5L-40-5b	5	Full Load	5	40	0.6	5	4.10	1.00	1.71		1.1	13.6	-0.01	1.82	6.59
5L-60-3b	5	Full Load	5	60	0.6	3	6.83	1.00	1.61		1.1	13.6	-0.01	1.76	9.58
5L-60-4b	5	Full Load	5	60	0.6	4	4.88	1.00	1.79		1.1	13.6	-0.01	1.72	-4.00
5L-60-5b	5	Full Load	5	60	0.6	5	4.10	1.00	1.70		1.1	13.6	-0.01	1.85	8.67
5L-80-3b	5	Full Load	5	80	0.6	3	6.83	1.00	1.64		1.1	13.6	-0.01	1.79	8.91
5L-80-4b	5	Full Load	5	80	0.6	4	4.88	1.00	1.82		1.1	13.6	-0.01	1.75	-4.06
5L-80-5b	5	Full Load	5	80	0.6	5	4.10	1.00	1.72		1.1	13.6	-0.01	1.88	9.16
5L-100-3b	5	Full Load	5	100	0.6	3	6.83	1.00	1.67		1.1	13.6	-0.01	1.82	8.57
5L-100-4b	5	Full Load	5	100	0.6	4	4.88	1.00	1.86		1.1	13.6	-0.01	1.78	-4.28
5L-100-5b	5	Full Load	5	100	0.6	5	4.10	1.00	1.74		1.1	13.6	-0.01	1.91	9.94

5 Lanes															
5L-20-3b	5	Full Load	5	20	0.6	3	6.83	1.00		1.46	1.1	15	-0.01	1.55	5.99
5L-20-4b	5	Full Load	5	20	0.6	4	4.88	1.00		1.56	1.1	15	-0.01	1.51	-3.18
5L-20-5b	5	Full Load	5	20	0.6	5	4.10	1.00		1.54	1.1	15	-0.01	1.63	5.36
5L-40-3b	5	Full Load	5	40	0.6	3	6.83	1.00		1.48	1.1	15	-0.01	1.57	5.54
5L-40-4b	5	Full Load	5	40	0.6	4	4.88	1.00		1.61	1.1	15	-0.01	1.53	-4.52
5L-40-5b	5	Full Load	5	40	0.6	5	4.10	1.00		1.54	1.1	15	-0.01	1.65	7.11
5L-60-3b	5	Full Load	5	60	0.6	3	6.83	1.00		1.51	1.1	15	-0.01	1.59	5.49
5L-60-4b	5	Full Load	5	60	0.6	4	4.88	1.00		1.64	1.1	15	-0.01	1.56	-5.38
5L-60-5b	5	Full Load	5	60	0.6	5	4.10	1.00		1.55	1.1	15	-0.01	1.67	7.80
5L-80-3b	5	Full Load	5	80	0.6	3	6.83	1.00		1.51	1.1	15	-0.01	1.61	6.44
5L-80-4b	5	Full Load	5	80	0.6	4	4.88	1.00		1.67	1.1	15	-0.01	1.58	-5.45
5L-80-5b	5	Full Load	5	80	0.6	5	4.10	1.00		1.58	1.1	15	-0.01	1.70	7.63
5L-100-3b	5	Full Load	5	100	0.6	3	6.83	1.00		1.53	1.1	15	-0.01	1.63	7.13
5L-100-4b	5	Full Load	5	100	0.6	4	4.88	1.00		1.70	1.1	15	-0.01	1.60	-5.63
5L-100-5b	5	Full Load	5	100	0.6	5	4.10	1.00		1.60	1.1	15	-0.01	1.72	7.43

Appendix A.4 Parameters of empirical equation of shear distribution factors as function of (L) span length at FLS

Bridge type	# of Trucks	# of lanes (n)	Span Length (L)	R _L	Number of Box (N)	Center to center girder spacing (S)	μ	Result from FEA		Parameters of empirical equation			Empirical equation	Variance	
								F _{V inner}	F _{V outer}	e	a	b			
2 Lanes															
2L-20-2b	1	Fatigue_1	2	20	0.9	2	5.00	1	1.80		1.67	9	0	1.77	-1.81
2L-20-3b	1	Fatigue_1	2	20	0.9	3	3.33	1	2.37		1.67	9	0	2.32	-1.93
2L-40-2b	1	Fatigue_1	2	40	0.9	2	5.00	1	1.76		1.67	9	0	1.77	0.23
2L-40-3b	1	Fatigue_1	2	40	0.9	3	3.33	1	2.28		1.67	9	0	2.32	1.68
2L-60-2b	1	Fatigue_1	2	60	0.9	2	5.00	1	1.73		1.67	9	0	1.77	2.31
2L-60-3b	1	Fatigue_1	2	60	0.9	3	3.33	1	2.29		1.67	9	0	2.32	1.27
2L-80-2b	1	Fatigue_1	2	80	0.9	2	5.00	1	1.77		1.67	9	0	1.77	-0.04
2L-80-3b	1	Fatigue_1	2	80	0.9	3	3.33	1	2.31		1.67	9	0	2.32	0.51
2L-100-2b	1	Fatigue_1	2	100	0.9	2	5.00	1	1.79		1.67	9	0	1.77	-1.14
2L-100-3b	1	Fatigue_1	2	100	0.9	3	3.33	1	2.36		1.67	9	0	2.32	-1.85

2 Lanes															
2L-20-2b	1	Fatigue_1	2	20	0.9	2	5.00	1		1.66	1.6	9.3	0	1.63	-1.93
2L-20-3b	1	Fatigue_1	2	20	0.9	3	3.33	1		2.15	1.6	9.3	0	2.08	-3.17
2L-40-2b	1	Fatigue_1	2	40	0.9	2	5.00	1		1.63	1.6	9.3	0	1.63	-0.11
2L-40-3b	1	Fatigue_1	2	40	0.9	3	3.33	1		2.05	1.6	9.3	0	2.08	1.62
2L-60-2b	1	Fatigue_1	2	60	0.9	2	5.00	1		1.64	1.6	9.3	0	1.63	-0.50
2L-60-3b	1	Fatigue_1	2	60	0.9	3	3.33	1		2.10	1.6	9.3	0	2.08	-1.15
2L-80-2b	1	Fatigue_1	2	80	0.9	2	5.00	1		1.65	1.6	9.3	0	1.63	-1.09
2L-80-3b	1	Fatigue_1	2	80	0.9	3	3.33	1		2.12	1.6	9.3	0	2.08	-1.95
2L-100-2b	1	Fatigue_1	2	100	0.9	2	5.00	1		1.66	1.6	9.3	0	1.63	-1.56
2L-100-3b	1	Fatigue_1	2	100	0.9	3	3.33	1		2.15	1.6	9.3	0	2.08	-3.48

3 Lanes															
3L-20-2b	1	Fatigue_1	3	20	0.8	2	6.75	1	1.88		1.8	12.6	0	1.87	-0.80
3L-20-3b	1	Fatigue_1	3	20	0.8	3	4.50	1	2.68		1.8	12.6	0	2.58	-3.58
3L-20-4b	1	Fatigue_1	3	20	0.8	4	3.38	1	3.41		1.8	12.6	0	3.25	-4.70
3L-40-2b	1	Fatigue_1	3	40	0.8	2	6.75	1	1.84		1.8	12.6	0	1.87	1.20
3L-40-3b	1	Fatigue_1	3	40	0.8	3	4.50	1	2.59		1.8	12.6	0	2.58	-0.27
3L-40-4b	1	Fatigue_1	3	40	0.8	4	3.38	1	3.18		1.8	12.6	0	3.25	1.98
3L-60-2b	1	Fatigue_1	3	60	0.8	2	6.75	1	1.83		1.8	12.6	0	1.87	2.03
3L-60-3b	1	Fatigue_1	3	60	0.8	3	4.50	1	2.55		1.8	12.6	0	2.58	1.01
3L-60-4b	1	Fatigue_1	3	60	0.8	4	3.38	1	3.16		1.8	12.6	0	3.25	2.87
3L-80-2b	1	Fatigue_1	3	80	0.8	2	6.75	1	1.84		1.8	12.6	0	1.87	1.23
3L-80-3b	1	Fatigue_1	3	80	0.8	3	4.50	1	2.57		1.8	12.6	0	2.58	0.41
3L-80-4b	1	Fatigue_1	3	80	0.8	4	3.38	1	3.17		1.8	12.6	0	3.25	2.44
3L-100-2b	1	Fatigue_1	3	100	0.8	2	6.75	1	1.88		1.8	12.6	0	1.87	-0.64
3L-100-3b	1	Fatigue_1	3	100	0.8	3	4.50	1	2.61		1.8	12.6	0	2.58	-1.24
3L-100-4b	1	Fatigue_1	3	100	0.8	4	3.38	1	3.22		1.8	12.6	0	3.25	0.76

Cont.

Bridge type	# of Trucks	# of lanes (n)	Span Length (L)	R _L	Number of Box (N)	Center to center girder spacing (S)	μ	Result from FEA		Parameters of empirical equation			Empirical equation	Variance	
								F _{V inner}	F _{V outer}	e	a	b			
3 Lanes															
3L-20-2b	1	Fatigue_1	3	20	0.8	2	6.75	1		1.74	1.74	13	0	1.73	-0.32
3L-20-3b	1	Fatigue_1	3	20	0.8	3	4.50	1		2.43	1.74	13	0	2.34	-3.53
3L-20-4b	1	Fatigue_1	3	20	0.8	4	3.38	1		3.05	1.74	13	0	2.90	-4.95
3L-40-2b	1	Fatigue_1	3	40	0.8	2	6.75	1		1.73	1.74	13	0	1.73	0.54
3L-40-3b	1	Fatigue_1	3	40	0.8	3	4.50	1		2.34	1.74	13	0	2.34	0.24
3L-40-4b	1	Fatigue_1	3	40	0.8	4	3.38	1		2.82	1.74	13	0	2.90	2.79
3L-60-2b	1	Fatigue_1	3	60	0.8	2	6.75	1		1.73	1.74	13	0	1.73	0.23
3L-60-3b	1	Fatigue_1	3	60	0.8	3	4.50	1		2.34	1.74	13	0	2.34	0.20
3L-60-4b	1	Fatigue_1	3	60	0.8	4	3.38	1		2.84	1.74	13	0	2.90	2.12
3L-80-2b	1	Fatigue_1	3	80	0.8	2	6.75	1		1.71	1.74	13	0	1.73	1.14
3L-80-3b	1	Fatigue_1	3	80	0.8	3	4.50	1		2.35	1.74	13	0	2.34	-0.44
3L-80-4b	1	Fatigue_1	3	80	0.8	4	3.38	1		2.87	1.74	13	0	2.90	1.00
3L-100-2b	1	Fatigue_1	3	100	0.8	2	6.75	1		1.73	1.74	13	0	1.73	0.24
3L-100-3b	1	Fatigue_1	3	100	0.8	3	4.50	1		2.38	1.74	13	0	2.34	-1.74
3L-100-4b	1	Fatigue_1	3	100	0.8	4	3.38	1		2.93	1.74	13	0	2.90	-1.22
4 Lanes															
4L-20-3b	1	Fatigue_1	4	20	0.7	3	5.67	1	2.77		1.78	14.7	0	2.72	-1.81
4L-20-4b	1	Fatigue_1	4	20	0.7	4	4.25	1	3.54		1.78	14.7	0	3.41	-3.60
4L-20-5b	1	Fatigue_1	4	20	0.7	5	3.40	1	4.13		1.78	14.7	0	4.06	-1.72
4L-40-3b	1	Fatigue_1	4	40	0.7	3	5.67	1	2.69		1.78	14.7	0	2.72	1.10
4L-40-4b	1	Fatigue_1	4	40	0.7	4	4.25	1	3.44		1.78	14.7	0	3.41	-0.75
4L-40-5b	1	Fatigue_1	4	40	0.7	5	3.40	1	4.02		1.78	14.7	0	4.06	1.02
4L-60-3b	1	Fatigue_1	4	60	0.7	3	5.67	1	2.65		1.78	14.7	0	2.72	2.74
4L-60-4b	1	Fatigue_1	4	60	0.7	4	4.25	1	3.37		1.78	14.7	0	3.41	1.08
4L-60-5b	1	Fatigue_1	4	60	0.7	5	3.40	1	3.98		1.78	14.7	0	4.06	1.90
4L-80-3b	1	Fatigue_1	4	80	0.7	3	5.67	1	2.69		1.78	14.7	0	2.72	1.09
4L-80-4b	1	Fatigue_1	4	80	0.7	4	4.25	1	3.39		1.78	14.7	0	3.41	0.44
4L-80-5b	1	Fatigue_1	4	80	0.7	5	3.40	1	4.02		1.78	14.7	0	4.06	0.90
4L-100-3b	1	Fatigue_1	4	100	0.7	3	5.67	1	2.74		1.78	14.7	0	2.72	-0.41
4L-100-4b	1	Fatigue_1	4	100	0.7	4	4.25	1	3.47		1.78	14.7	0	3.41	-1.65
4L-100-5b	1	Fatigue_1	4	100	0.7	5	3.40	1	4.08		1.78	14.7	0	4.06	-0.63
4 Lanes															
4L-20-3b	1	Fatigue_1	4	20	0.7	3	5.67	1		2.53	1.74	15.45	0	2.48	-1.78
4L-20-4b	1	Fatigue_1	4	20	0.7	4	4.25	1		3.19	1.74	15.45	0	3.07	-3.73
4L-20-5b	1	Fatigue_1	4	20	0.7	5	3.40	1		3.70	1.74	15.45	0	3.62	-2.04
4L-40-3b	1	Fatigue_1	4	40	0.7	3	5.67	1		2.45	1.74	15.45	0	2.48	1.12
4L-40-4b	1	Fatigue_1	4	40	0.7	4	4.25	1		3.05	1.74	15.45	0	3.07	0.48
4L-40-5b	1	Fatigue_1	4	40	0.7	5	3.40	1		3.52	1.74	15.45	0	3.62	2.78
4L-60-3b	1	Fatigue_1	4	60	0.7	3	5.67	1		2.45	1.74	15.45	0	2.48	1.29
4L-60-4b	1	Fatigue_1	4	60	0.7	4	4.25	1		3.04	1.74	15.45	0	3.07	0.82
4L-60-5b	1	Fatigue_1	4	60	0.7	5	3.40	1		3.55	1.74	15.45	0	3.62	2.11
4L-80-3b	1	Fatigue_1	4	80	0.7	3	5.67	1		2.45	1.74	15.45	0	2.48	1.21
4L-80-4b	1	Fatigue_1	4	80	0.7	4	4.25	1		3.06	1.74	15.45	0	3.07	0.15
4L-80-5b	1	Fatigue_1	4	80	0.7	5	3.40	1		3.61	1.74	15.45	0	3.62	0.41
4L-100-3b	1	Fatigue_1	4	100	0.7	3	5.67	1		2.47	1.74	15.45	0	2.48	0.37
4L-100-4b	1	Fatigue_1	4	100	0.7	4	4.25	1		3.12	1.74	15.45	0	3.07	-1.65
4L-100-5b	1	Fatigue_1	4	100	0.7	5	3.40	1		3.68	1.74	15.45	0	3.62	-1.69

Cont.

Bridge type	# of Trucks	# of lanes (n)	Span Length (L)	R _L	Number of Box (N)	Center to center girder spacing (S)	μ	Result from FEA		Parameters of empirical equation			Empirical equation	Variance	
								F _{V inner}	F _{V outer}	e	a	b			
5 Lanes															
5L-20-3b	1	Fatigue_1	5	20	0.6	3	6.83	1	2.84		1.8	17.23	0	2.87	0.96
5L-20-4b	1	Fatigue_1	5	20	0.6	4	4.88	1	3.57		1.8	17.23	0	3.43	-3.90
5L-20-5b	1	Fatigue_1	5	20	0.6	5	4.10	1	4.34		1.8	17.23	0	4.31	-0.66
5L-40-3b	1	Fatigue_1	5	40	0.6	3	6.83	1	2.78		1.8	17.23	0	2.87	3.11
5L-40-4b	1	Fatigue_1	5	40	0.6	4	4.88	1	3.55		1.8	17.23	0	3.43	-3.43
5L-40-5b	1	Fatigue_1	5	40	0.6	5	4.10	1	4.20		1.8	17.23	0	4.31	2.56
5L-60-3b	1	Fatigue_1	5	60	0.6	3	6.83	1	2.76		1.8	17.23	0	2.87	3.92
5L-60-4b	1	Fatigue_1	5	60	0.6	4	4.88	1	3.50		1.8	17.23	0	3.43	-1.94
5L-60-5b	1	Fatigue_1	5	60	0.6	5	4.10	1	4.20		1.8	17.23	0	4.31	2.66
5L-80-3b	1	Fatigue_1	5	80	0.6	3	6.83	1	2.79		1.8	17.23	0	2.87	2.58
5L-80-4b	1	Fatigue_1	5	80	0.6	4	4.88	1	3.55		1.8	17.23	0	3.43	-3.36
5L-80-5b	1	Fatigue_1	5	80	0.6	5	4.10	1	4.24		1.8	17.23	0	4.31	1.61
5L-100-3b	1	Fatigue_1	5	100	0.6	3	6.83	1	2.83		1.8	17.23	0	2.87	1.27
5L-100-4b	1	Fatigue_1	5	100	0.6	4	4.88	1	3.57		1.8	17.23	0	3.43	-3.90
5L-100-5b	1	Fatigue_1	5	100	0.6	5	4.10	1	4.33		1.8	17.23	0	4.31	-0.34

5 Lanes															
5L-20-3b	1	Fatigue_1	5	20	0.6	3	6.83	1		2.59	1.77	18	0	2.65	2.28
5L-20-4b	1	Fatigue_1	5	20	0.6	4	4.88	1		3.30	1.77	18	0	3.15	-4.54
5L-20-5b	1	Fatigue_1	5	20	0.6	5	4.10	1		3.90	1.77	18	0	3.93	0.88
5L-40-3b	1	Fatigue_1	5	40	0.6	3	6.83	1		2.55	1.77	18	0	2.65	3.90
5L-40-4b	1	Fatigue_1	5	40	0.6	4	4.88	1		3.19	1.77	18	0	3.15	-1.25
5L-40-5b	1	Fatigue_1	5	40	0.6	5	4.10	1		3.76	1.77	18	0	3.93	4.65
5L-60-3b	1	Fatigue_1	5	60	0.6	3	6.83	1		2.55	1.77	18	0	2.65	3.91
5L-60-4b	1	Fatigue_1	5	60	0.6	4	4.88	1		3.19	1.77	18	0	3.15	-1.32
5L-60-5b	1	Fatigue_1	5	60	0.6	5	4.10	1		3.76	1.77	18	0	3.93	4.54
5L-80-3b	1	Fatigue_1	5	80	0.6	3	6.83	1		2.55	1.77	18	0	2.65	3.97
5L-80-4b	1	Fatigue_1	5	80	0.6	4	4.88	1		3.21	1.77	18	0	3.15	-1.71
5L-80-5b	1	Fatigue_1	5	80	0.6	5	4.10	1		3.81	1.77	18	0	3.93	3.12
5L-100-3b	1	Fatigue_1	5	100	0.6	3	6.83	1		2.56	1.77	18	0	2.65	3.52
5L-100-4b	1	Fatigue_1	5	100	0.6	4	4.88	1		3.24	1.77	18	0	3.15	-2.75
5L-100-5b	1	Fatigue_1	5	100	0.6	5	4.10	1		3.88	1.77	18	0	3.93	1.44

Appendix A.5: Parameters of empirical equation of shear distribution factors as function of (β) at ULS

Bridge type	# of Trucks	# of lanes (n)	R_L	Number of Box (N)	Center to center girder spacing (S)	μ	Result from FEA			Parameters of Empirical equation			Empirical Equation	Variance	
							(β) of F_{m-}	$F_{v \text{ inner}}$	$F_{v \text{ outer}}$	e	a	b			
2 Lanes															
2L-20-2b	2	Full Load	2	0.9	2	5.00	1.0	2.35	1.21		1.80	13.60	0.30	1.22	0.19
2L-20-3b	2	Full Load	2	0.9	3	3.33	1.0	2.59	1.68		1.80	13.60	0.30	1.67	-0.24
2L-40-2b	2	Full Load	2	0.9	2	5.00	1.0	1.52	1.22		1.80	13.60	0.30	1.24	1.41
2L-40-3b	2	Full Load	2	0.9	3	3.33	1.0	1.77	1.68		1.80	13.60	0.30	1.70	1.65
2L-60-2b	2	Full Load	2	0.9	2	5.00	1.0	1.11	1.23		1.80	13.60	0.30	1.25	1.62
2L-60-3b	2	Full Load	2	0.9	3	3.33	1.0	1.33	1.71		1.80	13.60	0.30	1.72	0.79
2L-80-2b	2	Full Load	2	0.9	2	5.00	1.0	0.93	1.26		1.80	13.60	0.30	1.25	-0.06
2L-80-3b	2	Full Load	2	0.9	3	3.33	1.0	1.14	1.74		1.80	13.60	0.30	1.73	-0.60
2L-100-2b	2	Full Load	2	0.9	2	5.00	1.0	0.82	1.27		1.80	13.60	0.30	1.26	-1.16
2L-100-3b	2	Full Load	2	0.9	3	3.33	1.0	1.02	1.75		1.80	13.60	0.30	1.73	-1.10
2 Lanes (β) of F_{m-}															
2L-20-2b	2	Full Load	2	0.9	2	5.00	1.0	3.77		1.15	1.80	14.00	0.30	1.15	-0.37
2L-20-3b	2	Full Load	2	0.9	3	3.33	1.0	4.15		1.55	1.80	14.00	0.30	1.58	2.15
2L-40-2b	2	Full Load	2	0.9	2	5.00	1.0	2.44		1.17	1.80	14.00	0.30	1.18	0.71
2L-40-3b	2	Full Load	2	0.9	3	3.33	1.0	2.82		1.57	1.80	14.00	0.30	1.62	3.60
2L-60-2b	2	Full Load	2	0.9	2	5.00	1.0	1.78		1.20	1.80	14.00	0.30	1.20	0.05
2L-60-3b	2	Full Load	2	0.9	3	3.33	1.0	2.12		1.60	1.80	14.00	0.30	1.65	2.80
2L-80-2b	2	Full Load	2	0.9	2	5.00	1.0	1.49		1.20	1.80	14.00	0.30	1.21	0.04
2L-80-3b	2	Full Load	2	0.9	3	3.33	1.0	1.82		1.62	1.80	14.00	0.30	1.66	2.21
2L-100-2b	2	Full Load	2	0.9	2	5.00	1.0	1.32		1.21	1.80	14.00	0.30	1.21	-0.09
2L-100-3b	2	Full Load	2	0.9	3	3.33	1.0	1.63		1.64	1.80	14.00	0.30	1.66	1.24
3 Lanes (β) of F_{m+}															
3L-20-2b	3	Full Load	3	0.8	2	6.75	1.0	3.01	1.23		1.45	15.00	0.20	1.18	-3.81
3L-20-3b	3	Full Load	3	0.8	3	4.50	1.0	3.25	1.32		1.45	15.00	0.20	1.41	7.22
3L-20-4b	3	Full Load	3	0.8	4	3.38	1.0	3.85	1.67		1.45	15.00	0.20	1.60	-4.46
3L-40-2b	3	Full Load	3	0.8	2	6.75	1.0	1.81	1.22		1.45	15.00	0.20	1.20	-1.43
3L-40-3b	3	Full Load	3	0.8	3	4.50	1.0	1.82	1.35		1.45	15.00	0.20	1.44	6.49
3L-40-4b	3	Full Load	3	0.8	4	3.38	1.0	2.28	1.65		1.45	15.00	0.20	1.63	-1.10
3L-60-2b	3	Full Load	3	0.8	2	6.75	1.0	1.30	1.23		1.45	15.00	0.20	1.21	-2.11
3L-60-3b	3	Full Load	3	0.8	3	4.50	1.0	1.57	1.35		1.45	15.00	0.20	1.45	6.77
3L-60-4b	3	Full Load	3	0.8	4	3.38	1.0	1.78	1.66		1.45	15.00	0.20	1.64	-1.46
3L-80-2b	3	Full Load	3	0.8	2	6.75	1.0	1.11	1.27		1.45	15.00	0.20	1.21	-4.42
3L-80-3b	3	Full Load	3	0.8	3	4.50	1.0	1.32	1.36		1.45	15.00	0.20	1.45	6.40
3L-80-4b	3	Full Load	3	0.8	4	3.38	1.0	1.53	1.69		1.45	15.00	0.20	1.65	-2.74
3L-100-2b	3	Full Load	3	0.8	2	6.75	1.0	0.97	1.27		1.45	15.00	0.20	1.21	-4.43
3L-100-3b	3	Full Load	3	0.8	3	4.50	1.0	1.17	1.37		1.45	15.00	0.20	1.45	5.73
3L-100-4b	3	Full Load	3	0.8	4	3.38	1.0	1.37	1.73		1.45	15.00	0.20	1.65	-4.45

Cont.

Bridge type	# of Trucks	# of lanes (n)	R _L	Number of Box (N)	Center to center girder spacing (S)	μ	Result from FEA			Parameters of Empirical equation			Empirical Equation	Variance
							(β) of Fm+	Fv inner	Fv outer	e	a	b		

3 Lanes (β) of Fm-															
3L-20-2b	3	Full Load	3	0.8	2	6.75	1.0	4.81		1.14	1.42	15.00	0.20	1.13	-0.75
3L-20-3b	3	Full Load	3	0.8	3	4.50	1.0	5.20		1.25	1.42	15.00	0.20	1.34	6.84
3L-20-4b	3	Full Load	3	0.8	4	3.38	1.0	6.16		1.52	1.42	15.00	0.20	1.49	-2.22
3L-40-2b	3	Full Load	3	0.8	2	6.75	1.0	2.90		1.18	1.42	15.00	0.20	1.16	-1.43
3L-40-3b	3	Full Load	3	0.8	3	4.50	1.0	2.91		1.26	1.42	15.00	0.20	1.37	8.72
3L-40-4b	3	Full Load	3	0.8	4	3.38	1.0	3.65		1.53	1.42	15.00	0.20	1.54	0.11
3L-60-2b	3	Full Load	3	0.8	2	6.75	1.0	2.08		1.21	1.42	15.00	0.20	1.17	-3.14
3L-60-3b	3	Full Load	3	0.8	3	4.50	1.0	2.51		1.29	1.42	15.00	0.20	1.38	7.16
3L-60-4b	3	Full Load	3	0.8	4	3.38	1.0	2.85		1.57	1.42	15.00	0.20	1.55	-0.93
3L-80-2b	3	Full Load	3	0.8	2	6.75	1.0	1.77		1.22	1.42	15.00	0.20	1.18	-3.49
3L-80-3b	3	Full Load	3	0.8	3	4.50	1.0	2.12		1.30	1.42	15.00	0.20	1.39	6.85
3L-80-4b	3	Full Load	3	0.8	4	3.38	1.0	2.44		1.59	1.42	15.00	0.20	1.56	-1.71
3L-100-2b	3	Full Load	3	0.8	2	6.75	1.0	1.55		1.24	1.42	15.00	0.20	1.18	-4.58
3L-100-3b	3	Full Load	3	0.8	3	4.50	1.0	1.88		1.31	1.42	15.00	0.20	1.39	6.00
3L-100-4b	3	Full Load	3	0.8	4	3.38	1.0	2.19		1.62	1.42	15.00	0.20	1.57	-3.32

4 Lanes (β) of Fm+															
4L-20-3b	4	Full Load	4	0.7	3	5.67	1.0	3.90	1.48		1.40	17.40	0.24	1.44	-3.03
4L-20-4b	4	Full Load	4	0.7	4	4.25	1.0	4.14	1.47		1.40	17.40	0.24	1.61	9.23
4L-20-5b	4	Full Load	4	0.7	5	3.40	1.0	4.38	1.84		1.40	17.40	0.24	1.75	-4.83
4L-40-3b	4	Full Load	4	0.7	3	5.67	1.0	2.40	1.49		1.40	17.40	0.24	1.47	-1.69
4L-40-4b	4	Full Load	4	0.7	4	4.25	1.0	2.64	1.48		1.40	17.40	0.24	1.64	10.60
4L-40-5b	4	Full Load	4	0.7	5	3.40	1.0	2.87	1.81		1.40	17.40	0.24	1.79	-1.31
4L-60-3b	4	Full Load	4	0.7	3	5.67	1.0	1.80	1.52		1.40	17.40	0.24	1.48	-2.75
4L-60-4b	4	Full Load	4	0.7	4	4.25	1.0	2.02	1.48		1.40	17.40	0.24	1.65	11.74
4L-60-5b	4	Full Load	4	0.7	5	3.40	1.0	2.24	1.83		1.40	17.40	0.24	1.80	-1.54
4L-80-3b	4	Full Load	4	0.7	3	5.67	1.0	1.50	1.56		1.40	17.40	0.24	1.49	-4.61
4L-80-4b	4	Full Load	4	0.7	4	4.25	1.0	1.71	1.50		1.40	17.40	0.24	1.66	10.79
4L-80-5b	4	Full Load	4	0.7	5	3.40	1.0	1.92	1.88		1.40	17.40	0.24	1.81	-3.67
4L-100-3b	4	Full Load	4	0.7	3	5.67	1.0	1.32	1.56		1.40	17.40	0.24	1.49	-4.56
4L-100-4b	4	Full Load	4	0.7	4	4.25	1.0	1.52	1.51		1.40	17.40	0.24	1.67	10.18
4L-100-5b	4	Full Load	4	0.7	5	3.40	1.0	1.72	1.91		1.40	17.40	0.24	1.82	-4.97

4 Lanes (β) of Fm-															
4L-20-3b	4	Full Load	4	0.7	3	5.67	1.0	6.24		1.33	1.40	18.50	0.24	1.32	-0.48
4L-20-4b	4	Full Load	4	0.7	4	4.25	1.0	6.63		1.37	1.40	18.50	0.24	1.47	7.57
4L-20-5b	4	Full Load	4	0.7	5	3.40	1.0	7.00		1.65	1.40	18.50	0.24	1.60	-2.59
4L-40-3b	4	Full Load	4	0.7	3	5.67	1.0	3.84		1.38	1.40	18.50	0.24	1.36	-1.36
4L-40-4b	4	Full Load	4	0.7	4	4.25	1.0	4.22		1.36	1.40	18.50	0.24	1.52	11.93
4L-40-5b	4	Full Load	4	0.7	5	3.40	1.0	4.59		1.62	1.40	18.50	0.24	1.65	2.13
4L-60-3b	4	Full Load	4	0.7	3	5.67	1.0	2.88		1.42	1.40	18.50	0.24	1.37	-3.36
4L-60-4b	4	Full Load	4	0.7	4	4.25	1.0	3.23		1.37	1.40	18.50	0.24	1.54	12.34
4L-60-5b	4	Full Load	4	0.7	5	3.40	1.0	3.58		1.66	1.40	18.50	0.24	1.67	0.83
4L-80-3b	4	Full Load	4	0.7	3	5.67	1.0	2.40		1.45	1.40	18.50	0.24	1.38	-4.70
4L-80-4b	4	Full Load	4	0.7	4	4.25	1.0	2.74		1.39	1.40	18.50	0.24	1.55	11.15
4L-80-5b	4	Full Load	4	0.7	5	3.40	1.0	3.06		1.70	1.40	18.50	0.24	1.68	-0.93
4L-100-3b	4	Full Load	4	0.7	3	5.67	1.0	2.11		1.46	1.40	18.50	0.24	1.39	-4.94
4L-100-4b	4	Full Load	4	0.7	4	4.25	1.0	2.44		1.41	1.40	18.50	0.24	1.55	10.25
4L-100-5b	4	Full Load	4	0.7	5	3.40	1.0	2.75		1.73	1.40	18.50	0.24	1.69	-2.63

Cont.

Bridge type	# of Trucks	# of lanes (n)	R _L	Number of Box (N)	Center to center girder spacing (S)	μ	Result from FEA			Parameters of Empirical equation			Empirical Equation	Variance	
							(β) of Fm+	Fv inner	Fv outer	e	a	b			
5 Lanes (β) of Fm+															
5L-20-3b	5	Full Load	5	0.6	3	6.83	1.0	4.58	1.61		1.12	13.00	0.14	1.71	6.44
5L-20-4b	5	Full Load	5	0.6	4	4.88	1.0	4.99	1.73		1.12	13.00	0.14	1.68	-2.86
5L-20-5b	5	Full Load	5	0.6	5	4.10	1.0	5.08	1.67		1.12	13.00	0.14	1.81	8.29
5L-40-3b	5	Full Load	5	0.6	3	6.83	1.0	2.74	1.61		1.12	13.00	0.14	1.75	8.54
5L-40-4b	5	Full Load	5	0.6	4	4.88	1.0	2.98	1.77		1.12	13.00	0.14	1.72	-3.21
5L-40-5b	5	Full Load	5	0.6	5	4.10	1.0	3.22	1.71		1.12	13.00	0.14	1.85	8.03
5L-60-3b	5	Full Load	5	0.6	3	6.83	1.0	2.03	1.61		1.12	13.00	0.14	1.76	9.62
5L-60-4b	5	Full Load	5	0.6	4	4.88	1.0	2.26	1.79		1.12	13.00	0.14	1.73	-3.64
5L-60-5b	5	Full Load	5	0.6	5	4.10	1.0	2.48	1.70		1.12	13.00	0.14	1.86	9.31
5L-80-3b	5	Full Load	5	0.6	3	6.83	1.0	1.68	1.64		1.12	13.00	0.14	1.77	7.67
5L-80-4b	5	Full Load	5	0.6	4	4.88	1.0	1.89	1.82		1.12	13.00	0.14	1.74	-4.81
5L-80-5b	5	Full Load	5	0.6	5	4.10	1.0	2.10	1.72		1.12	13.00	0.14	1.87	8.55
5L-100-3b	5	Full Load	5	0.6	3	6.83	1.0	1.46	1.67		1.12	13.00	0.14	1.77	5.90
5L-100-4b	5	Full Load	5	0.6	4	4.88	1.0	1.67	1.83		1.12	13.00	0.14	1.74	-4.91
5L-100-5b	5	Full Load	5	0.6	5	4.10	1.0	1.87	1.74		1.12	13.00	0.14	1.88	7.87

5 Lanes (β) of Fm-															
5L-20-3b	5	Full Load	5	0.6	3	6.83	1.0	7.32		1.46	1.12	14.00	0.14	1.56	6.72
5L-20-4b	5	Full Load	5	0.6	4	4.88	1.0	7.98		1.56	1.12	14.00	0.14	1.52	-2.55
5L-20-5b	5	Full Load	5	0.6	5	4.10	1.0	8.12		1.54	1.12	14.00	0.14	1.64	6.38
5L-40-3b	5	Full Load	5	0.6	3	6.83	1.0	4.39		1.48	1.12	14.00	0.14	1.60	7.78
5L-40-4b	5	Full Load	5	0.6	4	4.88	1.0	4.77		1.61	1.12	14.00	0.14	1.57	-2.29
5L-40-5b	5	Full Load	5	0.6	5	4.10	1.0	5.15		1.54	1.12	14.00	0.14	1.69	9.71
5L-60-3b	5	Full Load	5	0.6	3	6.83	1.0	3.25		1.51	1.12	14.00	0.14	1.62	7.42
5L-60-4b	5	Full Load	5	0.6	4	4.88	1.0	3.61		1.64	1.12	14.00	0.14	1.59	-3.42
5L-60-5b	5	Full Load	5	0.6	5	4.10	1.0	3.96		1.55	1.12	14.00	0.14	1.71	10.14
5L-80-3b	5	Full Load	5	0.6	3	6.83	1.0	2.68		1.51	1.12	14.00	0.14	1.63	7.48
5L-80-4b	5	Full Load	5	0.6	4	4.88	1.0	3.03		1.67	1.12	14.00	0.14	1.60	-4.30
5L-80-5b	5	Full Load	5	0.6	5	4.10	1.0	3.36		1.58	1.12	14.00	0.14	1.72	9.07
5L-100-3b	5	Full Load	5	0.6	3	6.83	1.0	2.34		1.53	1.12	14.00	0.14	1.63	7.01
5L-100-4b	5	Full Load	5	0.6	4	4.88	1.0	2.67		1.68	1.12	14.00	0.14	1.60	-4.63
5L-100-5b	5	Full Load	5	0.6	5	4.10	1.0	2.99		1.60	1.12	14.00	0.14	1.72	7.72

Appendix A.6: Parameters of empirical equation of shear distribution factors as function of (β) at FLS

Bridge type	# of Trucks	# of lanes (n)	R_L	Number of Box (N)	Center to center girder spacing (S)	μ	(β) of F_{m+}	Result from FEA		Parameters of empirical equation			Empirical Equation	Variance	
								$F_{V_{inner}}$	$F_{V_{outer}}$	e	a	b			
2 Lanes															
2L-20-2b	1	Fatigue_1	2	0.9	2	5.00	1	2.35	1.80		1.66	9	0	1.76	-2.49
2L-20-3b	1	Fatigue_1	2	0.9	3	3.33	1	2.59	2.37		1.66	9	0	2.29	-3.01
2L-40-2b	1	Fatigue_1	2	0.9	2	5.00	1	1.52	1.76		1.66	9	0	1.76	-0.46
2L-40-3b	1	Fatigue_1	2	0.9	3	3.33	1	1.77	2.28		1.66	9	0	2.29	0.57
2L-60-2b	1	Fatigue_1	2	0.9	2	5.00	1	1.11	1.73		1.66	9	0	1.76	1.60
2L-60-3b	1	Fatigue_1	2	0.9	3	3.33	1	1.33	2.29		1.66	9	0	2.29	0.16
2L-80-2b	1	Fatigue_1	2	0.9	2	5.00	1	0.93	1.77		1.66	9	0	1.76	-0.73
2L-80-3b	1	Fatigue_1	2	0.9	3	3.33	1	1.14	2.31		1.66	9	0	2.29	-0.59
2L-100-2b	1	Fatigue_1	2	0.9	2	5.00	1	0.82	1.79		1.66	9	0	1.76	-1.82
2L-100-3b	1	Fatigue_1	2	0.9	3	3.33	1	1.02	2.36		1.66	9	0	2.29	-2.92
2 Lanes (β) of F_{m-}															
2L-20-2b	1	Fatigue_1	2	0.9	2	5.00	1	3.77		1.66	1.6	9	0	1.68	1.34
2L-20-3b	1	Fatigue_1	2	0.9	3	3.33	1	4.15		2.15	1.6	9	0	2.15	0.06
2L-40-2b	1	Fatigue_1	2	0.9	2	5.00	1	2.44		1.63	1.6	9	0	1.68	3.22
2L-40-3b	1	Fatigue_1	2	0.9	3	3.33	1	2.82		2.05	1.6	9	0	2.15	5.00
2L-60-2b	1	Fatigue_1	2	0.9	2	5.00	1	1.78		1.64	1.6	9	0	1.68	2.82
2L-60-3b	1	Fatigue_1	2	0.9	3	3.33	1	2.12		2.10	1.6	9	0	2.15	2.15
2L-80-2b	1	Fatigue_1	2	0.9	2	5.00	1	1.49		1.65	1.6	9	0	1.68	2.21
2L-80-3b	1	Fatigue_1	2	0.9	3	3.33	1	1.82		2.12	1.6	9	0	2.15	1.31
2L-100-2b	1	Fatigue_1	2	0.9	2	5.00	1	1.32		1.66	1.6	9	0	1.68	1.72
2L-100-3b	1	Fatigue_1	2	0.9	3	3.33	1	1.63		2.15	1.6	9	0	2.15	-0.27
3 Lanes (β) of F_{m+}															
3L-20-2b	1	Fatigue_1	3	0.8	2	6.75	1	3.01	1.88		1.78	12.80	-0.27	1.93	2.83
3L-20-3b	1	Fatigue_1	3	0.8	3	4.50	1	3.25	2.68		1.78	12.8	-0.27	2.67	-0.31
3L-20-4b	1	Fatigue_1	3	0.8	4	3.38	1	3.85	3.41		1.78	12.8	-0.27	3.38	-0.69
3L-40-2b	1	Fatigue_1	3	0.8	2	6.75	1	1.81	1.84		1.78	12.8	-0.27	1.88	2.15
3L-40-3b	1	Fatigue_1	3	0.8	3	4.50	1	1.82	2.59		1.78	12.8	-0.27	2.58	-0.13
3L-40-4b	1	Fatigue_1	3	0.8	4	3.38	1	2.28	3.18		1.78	12.8	-0.27	3.27	2.58
3L-60-2b	1	Fatigue_1	3	0.8	2	6.75	1	1.30	1.83		1.78	12.8	-0.27	1.86	1.84
3L-60-3b	1	Fatigue_1	3	0.8	3	4.50	1	1.57	2.55		1.78	12.8	-0.27	2.57	0.59
3L-60-4b	1	Fatigue_1	3	0.8	4	3.38	1	1.78	3.16		1.78	12.8	-0.27	3.23	2.34
3L-80-2b	1	Fatigue_1	3	0.8	2	6.75	1	1.11	1.84		1.78	12.8	-0.27	1.85	0.63
3L-80-3b	1	Fatigue_1	3	0.8	3	4.50	1	1.32	2.57		1.78	12.8	-0.27	2.56	-0.53
3L-80-4b	1	Fatigue_1	3	0.8	4	3.38	1	1.53	3.17		1.78	12.8	-0.27	3.21	1.35
3L-100-2b	1	Fatigue_1	3	0.8	2	6.75	1	0.97	1.88		1.78	12.8	-0.27	1.85	-1.52
3L-100-3b	1	Fatigue_1	3	0.8	3	4.50	1	1.17	2.61		1.78	12.8	-0.27	2.55	-2.48
3L-100-4b	1	Fatigue_1	3	0.8	4	3.38	1	1.37	3.22		1.78	12.8	-0.27	3.20	-0.66

Cont.

Bridge type	# of Trucks	# of lanes (n)	R _L	Number of Box (N)	Center to center girder spacing (S)	μ	(β) of Fm+	Result from FEA		Parameters of empirical equation			Empirical Equation	Variance	
								F _{V inner}	F _{V outer}	e	a	b			
3 Lanes								(β) of Fm-							
3L-20-2b	1	Fatigue_1	3	0.8	2	6.75	1	4.81		1.74	1.73	13.25	-0.14	1.78	2.33
3L-20-3b	1	Fatigue_1	3	0.8	3	4.50	1	5.20		2.43	1.73	13.25	-0.14	2.40	-0.94
3L-20-4b	1	Fatigue_1	3	0.8	4	3.38	1	6.16		3.05	1.73	13.25	-0.14	3.00	-1.63
3L-40-2b	1	Fatigue_1	3	0.8	2	6.75	1	2.90		1.73	1.73	13.25	-0.14	1.74	1.06
3L-40-3b	1	Fatigue_1	3	0.8	3	4.50	1	2.91		2.34	1.73	13.25	-0.14	2.34	0.35
3L-40-4b	1	Fatigue_1	3	0.8	4	3.38	1	3.65		2.82	1.73	13.25	-0.14	2.92	3.46
3L-60-2b	1	Fatigue_1	3	0.8	2	6.75	1	2.08		1.73	1.73	13.25	-0.14	1.73	-0.15
3L-60-3b	1	Fatigue_1	3	0.8	3	4.50	1	2.51		2.34	1.73	13.25	-0.14	2.33	-0.12
3L-60-4b	1	Fatigue_1	3	0.8	4	3.38	1	2.85		2.84	1.73	13.25	-0.14	2.89	1.88
3L-80-2b	1	Fatigue_1	3	0.8	2	6.75	1	1.77		1.71	1.73	13.25	-0.14	1.72	0.43
3L-80-3b	1	Fatigue_1	3	0.8	3	4.50	1	2.12		2.35	1.73	13.25	-0.14	2.32	-1.17
3L-80-4b	1	Fatigue_1	3	0.8	4	3.38	1	2.44		2.87	1.73	13.25	-0.14	2.88	0.32
3L-100-2b	1	Fatigue_1	3	0.8	2	6.75	1	1.55		1.73	1.73	13.25	-0.14	1.72	-0.70
3L-100-3b	1	Fatigue_1	3	0.8	3	4.50	1	1.88		2.38	1.73	13.25	-0.14	2.32	-2.72
3L-100-4b	1	Fatigue_1	3	0.8	4	3.38	1	2.19		2.93	1.73	13.25	-0.14	2.87	-2.15
4 Lanes								(β) of Fm+							
4L-20-3b	1	Fatigue_1	4	0.7	3	5.67	1	3.90	2.77		1.77	14.9	-0.15	2.77	-0.27
4L-20-4b	1	Fatigue_1	4	0.7	4	4.25	1	4.14	3.54		1.77	14.9	-0.15	3.46	-2.13
4L-20-5b	1	Fatigue_1	4	0.7	5	3.40	1	4.38	4.13		1.77	14.9	-0.15	4.12	-0.19
4L-40-3b	1	Fatigue_1	4	0.7	3	5.67	1	2.40	2.69		1.77	14.9	-0.15	2.72	1.09
4L-40-4b	1	Fatigue_1	4	0.7	4	4.25	1	2.64	3.44		1.77	14.9	-0.15	3.41	-0.80
4L-40-5b	1	Fatigue_1	4	0.7	5	3.40	1	2.87	4.02		1.77	14.9	-0.15	4.06	0.99
4L-60-3b	1	Fatigue_1	4	0.7	3	5.67	1	1.80	2.65		1.77	14.9	-0.15	2.71	2.10
4L-60-4b	1	Fatigue_1	4	0.7	4	4.25	1	2.02	3.37		1.77	14.9	-0.15	3.39	0.39
4L-60-5b	1	Fatigue_1	4	0.7	5	3.40	1	2.24	3.98		1.77	14.9	-0.15	4.03	1.21
4L-80-3b	1	Fatigue_1	4	0.7	3	5.67	1	1.50	2.69		1.77	14.9	-0.15	2.70	0.16
4L-80-4b	1	Fatigue_1	4	0.7	4	4.25	1	1.71	3.39		1.77	14.9	-0.15	3.38	-0.56
4L-80-5b	1	Fatigue_1	4	0.7	5	3.40	1	1.92	4.02		1.77	14.9	-0.15	4.02	-0.12
4L-100-3b	1	Fatigue_1	4	0.7	3	5.67	1	1.32	2.74		1.77	14.9	-0.15	2.69	-1.51
4L-100-4b	1	Fatigue_1	4	0.7	4	4.25	1	1.52	3.47		1.77	14.9	-0.15	3.37	-2.81
4L-100-5b	1	Fatigue_1	4	0.7	5	3.40	1	1.72	4.08		1.77	14.9	-0.15	4.01	-1.83
4 Lanes								1 (β) of Fm-							
4L-20-3b	1	Fatigue_1	4	0.7	3	5.67	1	6.24		2.53	1.73	15.60	-0.08	2.51	-0.60
4L-20-4b	1	Fatigue_1	4	0.7	4	4.25	1	6.63		3.19	1.73	15.6	-0.08	3.10	-2.66
4L-20-5b	1	Fatigue_1	4	0.7	5	3.40	1	7.00		3.70	1.73	15.6	-0.08	3.66	-0.97
4L-40-3b	1	Fatigue_1	4	0.7	3	5.67	1	3.84		2.45	1.73	15.6	-0.08	2.48	1.04
4L-40-4b	1	Fatigue_1	4	0.7	4	4.25	1	4.22		3.05	1.73	15.6	-0.08	3.06	0.31
4L-40-5b	1	Fatigue_1	4	0.7	5	3.40	1	4.59		3.52	1.73	15.6	-0.08	3.61	2.58
4L-60-3b	1	Fatigue_1	4	0.7	3	5.67	1	2.88		2.45	1.73	15.6	-0.08	2.47	0.70
4L-60-4b	1	Fatigue_1	4	0.7	4	4.25	1	3.23		3.04	1.73	15.6	-0.08	3.05	0.14
4L-60-5b	1	Fatigue_1	4	0.7	5	3.40	1	3.58		3.55	1.73	15.6	-0.08	3.59	1.37
4L-80-3b	1	Fatigue_1	4	0.7	3	5.67	1	2.40		2.45	1.73	15.6	-0.08	2.46	0.38
4L-80-4b	1	Fatigue_1	4	0.7	4	4.25	1	2.74		3.06	1.73	15.6	-0.08	3.04	-0.78
4L-80-5b	1	Fatigue_1	4	0.7	5	3.40	1	3.06		3.61	1.73	15.6	-0.08	3.58	-0.58
4L-100-3b	1	Fatigue_1	4	0.7	3	5.67	1	2.11		2.47	1.73	15.6	-0.08	2.46	-0.61
4L-100-4b	1	Fatigue_1	4	0.7	4	4.25	1	2.44		3.12	1.73	15.6	-0.08	3.04	-2.72
4L-100-5b	1	Fatigue_1	4	0.7	5	3.40	1	2.75		3.68	1.73	15.6	-0.08	3.58	-2.82

Cont.

Bridge type	# of Trucks	# of lanes (n)	R _L	Number of Box (N)	Center to center girder spacing (S)	μ	(β) of Fm+	Result from FEA		Parameters of empirical equation			Empirical Equation	Variance
								F _{V inner}	F _{V outer}	e	a	b		

5 Lanes															
(β) of Fm+															
5L-20-3b	1	Fatigue_1	5	0.6	3	6.83	1	4.58	2.84		1.80	17.45	-0.06	2.88	1.33
5L-20-4b	1	Fatigue_1	5	0.6	4	4.88	1	4.99	3.57		1.8	17.45	-0.06	3.45	-3.41
5L-20-5b	1	Fatigue_1	5	0.6	5	4.10	1	5.08	4.34		1.8	17.45	-0.06	4.34	-0.12
5L-40-3b	1	Fatigue_1	5	0.6	3	6.83	1	2.74	2.78		1.8	17.45	-0.06	2.86	2.81
5L-40-4b	1	Fatigue_1	5	0.6	4	4.88	1	2.98	3.55		1.8	17.45	-0.06	3.42	-3.63
5L-40-5b	1	Fatigue_1	5	0.6	5	4.10	1	3.22	4.20		1.8	17.45	-0.06	4.31	2.44
5L-60-3b	1	Fatigue_1	5	0.6	3	6.83	1	2.03	2.76		1.8	17.45	-0.06	2.85	3.36
5L-60-4b	1	Fatigue_1	5	0.6	4	4.88	1	2.26	3.50		1.8	17.45	-0.06	3.41	-2.40
5L-60-5b	1	Fatigue_1	5	0.6	5	4.10	1	2.48	4.20		1.8	17.45	-0.06	4.29	2.26
5L-80-3b	1	Fatigue_1	5	0.6	3	6.83	1	1.68	2.79		1.8	17.45	-0.06	2.85	1.89
5L-80-4b	1	Fatigue_1	5	0.6	4	4.88	1	1.89	3.55		1.8	17.45	-0.06	3.41	-3.93
5L-80-5b	1	Fatigue_1	5	0.6	5	4.10	1	2.10	4.24		1.8	17.45	-0.06	4.29	1.08
5L-100-3b	1	Fatigue_1	5	0.6	3	6.83	1	1.46	2.83		1.8	17.45	-0.06	2.84	0.52
5L-100-4b	1	Fatigue_1	5	0.6	4	4.88	1	1.67	3.57		1.8	17.45	-0.06	3.41	-4.55
5L-100-5b	1	Fatigue_1	5	0.6	5	4.10	1	1.87	4.33		1.8	17.45	-0.06	4.29	-0.94

5 Lanes															
(β) of Fm-															
5L-20-3b	1	Fatigue_1	5	0.6	3	6.83	1	7.32		2.59	1.76	18.20	-0.07	2.67	2.95
5L-20-4b	1	Fatigue_1	5	0.6	4	4.88	1	7.98		3.30	1.76	18.2	-0.07	3.17	-3.94
5L-20-5b	1	Fatigue_1	5	0.6	5	4.10	1	8.12		3.90	1.76	18.2	-0.07	3.95	1.34
5L-40-3b	1	Fatigue_1	5	0.6	3	6.83	1	4.39		2.55	1.76	18.2	-0.07	2.64	3.38
5L-40-4b	1	Fatigue_1	5	0.6	4	4.88	1	4.77		3.19	1.76	18.2	-0.07	3.13	-1.88
5L-40-5b	1	Fatigue_1	5	0.6	5	4.10	1	5.15		3.76	1.76	18.2	-0.07	3.90	3.91
5L-60-3b	1	Fatigue_1	5	0.6	3	6.83	1	3.25		2.55	1.76	18.2	-0.07	2.63	2.93
5L-60-4b	1	Fatigue_1	5	0.6	4	4.88	1	3.61		3.19	1.76	18.2	-0.07	3.12	-2.40
5L-60-5b	1	Fatigue_1	5	0.6	5	4.10	1	3.96		3.76	1.76	18.2	-0.07	3.89	3.32
5L-80-3b	1	Fatigue_1	5	0.6	3	6.83	1	2.68		2.55	1.76	18.2	-0.07	2.62	2.76
5L-80-4b	1	Fatigue_1	5	0.6	4	4.88	1	3.03		3.21	1.76	18.2	-0.07	3.11	-3.00
5L-80-5b	1	Fatigue_1	5	0.6	5	4.10	1	3.36		3.81	1.76	18.2	-0.07	3.88	1.67
5L-100-3b	1	Fatigue_1	5	0.6	3	6.83	1	2.34		2.56	1.76	18.2	-0.07	2.62	2.18
5L-100-4b	1	Fatigue_1	5	0.6	4	4.88	1	2.67		3.24	1.76	18.2	-0.07	3.10	-4.16
5L-100-5b	1	Fatigue_1	5	0.6	5	4.10	1	2.99		3.88	1.76	18.2	-0.07	3.87	-0.13

Appendix A.7: Parameters of empirical equation of shear distribution factors as function of (β^2) at ULS

Bridge type	# of Trucks	# of lanes (n)	R_L	Number of Box (N)	Center to center girder spacing (S)	Result from FEA			Parameters of empirical equation				Empirical Equation	Variance	
						(β) of F_{m+}	$F_{v \text{ inner}}$	$F_{v \text{ outer}}$	a	b	c	e			
2 Lanes															
2L-20-2b	2	Full Load	2	0.9	2	5.00	2.35	1.21		12.6	2	-0.46	1.8	1.18	-2.89
2L-20-3b	2	Full Load	2	0.9	3	3.33	2.59	1.68		12.6	2	-0.46	1.8	1.64	-2.38
2L-40-2b	2	Full Load	2	0.9	2	5.00	1.52	1.22		12.6	2	-0.46	1.8	1.19	-2.23
2L-40-3b	2	Full Load	2	0.9	3	3.33	1.77	1.68		12.6	2	-0.46	1.8	1.64	-2.28
2L-60-2b	2	Full Load	2	0.9	2	5.00	1.11	1.23		12.6	2	-0.46	1.8	1.22	-0.67
2L-60-3b	2	Full Load	2	0.9	3	3.33	1.33	1.71		12.6	2	-0.46	1.8	1.67	-2.32
2L-80-2b	2	Full Load	2	0.9	2	5.00	0.93	1.26		12.6	2	-0.46	1.8	1.24	-1.38
2L-80-3b	2	Full Load	2	0.9	3	3.33	1.14	1.74		12.6	2	-0.46	1.8	1.69	-2.96
2L-100-2b	2	Full Load	2	0.9	2	5.00	0.82	1.27		12.6	2	-0.46	1.8	1.25	-1.79
2L-100-3b	2	Full Load	2	0.9	3	3.33	1.02	1.75		12.6	2	-0.46	1.8	1.70	-2.89
2 Lanes (β)of F_{m-}															
2L-20-2b	2	Full Load	2	0.9	2	5.00	3.77		1.15	12	0.86	-0.01	1.75	1.11	-3.56
2L-20-3b	2	Full Load	2	0.9	3	3.33	4.15		1.55	12	0.86	-0.01	1.75	1.48	-4.26
2L-40-2b	2	Full Load	2	0.9	2	5.00	2.44		1.17	12	0.86	-0.01	1.75	1.20	2.09
2L-40-3b	2	Full Load	2	0.9	3	3.33	2.82		1.57	12	0.86	-0.01	1.75	1.59	1.47
2L-60-2b	2	Full Load	2	0.9	2	5.00	1.78		1.20	12	0.86	-0.01	1.75	1.25	4.05
2L-60-3b	2	Full Load	2	0.9	3	3.33	2.12		1.60	12	0.86	-0.01	1.75	1.65	3.35
2L-80-2b	2	Full Load	2	0.9	2	5.00	1.49		1.20	12	0.86	-0.01	1.75	1.27	5.28
2L-80-3b	2	Full Load	2	0.9	3	3.33	1.82		1.62	12	0.86	-0.01	1.75	1.68	4.00
2L-100-2b	2	Full Load	2	0.9	2	5.00	1.32		1.21	12	0.86	-0.01	1.75	1.28	5.91
2L-100-3b	2	Full Load	2	0.9	3	3.33	1.63		1.64	12	0.86	-0.01	1.75	1.70	3.80
3 Lanes (β)of F_{m+}															
3L-20-2b	3	Full Load	3	0.8	2	6.75	3.01	1.23		13.4	1.9	-0.36	1.46	1.17	-4.70
3L-20-3b	3	Full Load	3	0.8	3	4.50	3.25	1.32		13.4	1.9	-0.36	1.46	1.42	7.56
3L-20-4b	3	Full Load	3	0.8	4	3.38	3.85	1.67		13.4	1.9	-0.36	1.46	1.66	-0.68
3L-40-2b	3	Full Load	3	0.8	2	6.75	1.81	1.22		13.4	1.9	-0.36	1.46	1.19	-2.63
3L-40-3b	3	Full Load	3	0.8	3	4.50	1.82	1.35		13.4	1.9	-0.36	1.46	1.43	5.61
3L-40-4b	3	Full Load	3	0.8	4	3.38	2.28	1.65		13.4	1.9	-0.36	1.46	1.61	-2.28
3L-60-2b	3	Full Load	3	0.8	2	6.75	1.30	1.23		13.4	1.9	-0.36	1.46	1.22	-1.42
3L-60-3b	3	Full Load	3	0.8	3	4.50	1.57	1.35		13.4	1.9	-0.36	1.46	1.44	6.69
3L-60-4b	3	Full Load	3	0.8	4	3.38	1.78	1.66		13.4	1.9	-0.36	1.46	1.63	-1.91
3L-80-2b	3	Full Load	3	0.8	2	6.75	1.11	1.27		13.4	1.9	-0.36	1.46	1.23	-2.75
3L-80-3b	3	Full Load	3	0.8	3	4.50	1.32	1.36		13.4	1.9	-0.36	1.46	1.46	7.45
3L-80-4b	3	Full Load	3	0.8	4	3.38	1.53	1.69		13.4	1.9	-0.36	1.46	1.65	-2.38
3L-100-2b	3	Full Load	3	0.8	2	6.75	0.97	1.30		13.4	1.9	-0.36	1.46	1.25	-4.11
3L-100-3b	3	Full Load	3	0.8	3	4.50	1.17	1.37		13.4	1.9	-0.36	1.46	1.48	7.61
3L-100-4b	3	Full Load	3	0.8	4	3.38	1.37	1.73		13.4	1.9	-0.36	1.46	1.67	-3.45

Cont.

Bridge type	# of Trucks	# of lanes (n)	R _L	Number of Box (N)	Center to center girder spacing (S)	Result from FEA			Parameters of empirical equation				Empirical Equation	Variance	
						(β)of Fm+	Fv inner	Fv outer	a	b	c	e			
3 Lanes															
(β)of Fm-															
3L-20-2b	3	Full Load	3	0.8	2	6.75	4.81		1.14	13.4	1.18	-0.13	1.4	1.11	-2.76
3L-20-3b	3	Full Load	3	0.8	3	4.50	5.20		1.25	13.4	1.18	-0.13	1.4	1.31	4.65
3L-20-4b	3	Full Load	3	0.8	4	3.38	6.16		1.52	13.4	1.18	-0.13	1.4	1.49	-1.91
3L-40-2b	3	Full Load	3	0.8	2	6.75	2.90		1.18	13.4	1.18	-0.13	1.4	1.13	-3.71
3L-40-3b	3	Full Load	3	0.8	3	4.50	2.91		1.26	13.4	1.18	-0.13	1.4	1.33	5.34
3L-40-4b	3	Full Load	3	0.8	4	3.38	3.65		1.53	13.4	1.18	-0.13	1.4	1.47	-4.13
3L-60-2b	3	Full Load	3	0.8	2	6.75	2.08		1.21	13.4	1.18	-0.13	1.4	1.17	-3.69
3L-60-3b	3	Full Load	3	0.8	3	4.50	2.51		1.29	13.4	1.18	-0.13	1.4	1.35	4.57
3L-60-4b	3	Full Load	3	0.8	4	3.38	2.85		1.57	13.4	1.18	-0.13	1.4	1.50	-4.49
3L-80-2b	3	Full Load	3	0.8	2	6.75	1.77		1.22	13.4	1.18	-0.13	1.4	1.18	-3.11
3L-80-3b	3	Full Load	3	0.8	3	4.50	2.12		1.30	13.4	1.18	-0.13	1.4	1.37	5.27
3L-80-4b	3	Full Load	3	0.8	4	3.38	2.44		1.59	13.4	1.18	-0.13	1.4	1.52	-4.51
3L-100-2b	3	Full Load	3	0.8	2	6.75	1.55		1.24	13.4	1.18	-0.13	1.4	1.19	-3.40
3L-100-3b	3	Full Load	3	0.8	3	4.50	1.88		1.31	13.4	1.18	-0.13	1.4	1.38	5.19
3L-100-4b	3	Full Load	3	0.8	4	3.38	2.19		1.61	13.4	1.18	-0.13	1.4	1.53	-4.97
4 Lanes															
(β)of Fm+															
4L-20-3b	4	Full Load	4	0.7	3	5.67	3.90	1.48		15	2.33	-0.36	1.4	1.42	-4.46
4L-20-4b	4	Full Load	4	0.7	4	4.25	4.14	1.47		15	2.33	-0.36	1.4	1.60	8.75
4L-20-5b	4	Full Load	4	0.7	5	3.40	4.38	1.84		15	2.33	-0.36	1.4	1.77	-4.06
4L-40-3b	4	Full Load	4	0.7	3	5.67	2.40	1.49		15	2.33	-0.36	1.4	1.42	-4.57
4L-40-4b	4	Full Load	4	0.7	4	4.25	2.64	1.48		15	2.33	-0.36	1.4	1.59	7.00
4L-40-5b	4	Full Load	4	0.7	5	3.40	2.87	1.81		15	2.33	-0.36	1.4	1.73	-4.65
4L-60-3b	4	Full Load	4	0.7	3	5.67	1.80	1.52		15	2.33	-0.36	1.4	1.46	-3.81
4L-60-4b	4	Full Load	4	0.7	4	4.25	2.02	1.48		15	2.33	-0.36	1.4	1.62	9.57
4L-60-5b	4	Full Load	4	0.7	5	3.40	2.24	1.83		15	2.33	-0.36	1.4	1.76	-4.07
4L-80-3b	4	Full Load	4	0.7	3	5.67	1.50	1.56		15	2.33	-0.36	1.4	1.49	-4.21
4L-80-4b	4	Full Load	4	0.7	4	4.25	1.71	1.50		15	2.33	-0.36	1.4	1.65	10.03
4L-80-5b	4	Full Load	4	0.7	5	3.40	1.92	1.88		15	2.33	-0.36	1.4	1.78	-5.16
4L-100-3b	4	Full Load	4	0.7	3	5.67	1.32	1.60		15	2.33	-0.36	1.4	1.51	-5.36
4L-100-4b	4	Full Load	4	0.7	4	4.25	1.52	1.51		15	2.33	-0.36	1.4	1.67	10.51
4L-100-5b	4	Full Load	4	0.7	5	3.40	1.72	1.91		15	2.33	-0.36	1.4	1.80	-5.65
4 Lanes															
(β)of Fm-															
4L-20-3b	4	Full Load	4	0.7	3	5.67	6.24		1.33	15	1.85	-0.17	1.4	1.32	-0.11
4L-20-4b	4	Full Load	4	0.7	4	4.25	6.63		1.37	15	1.85	-0.17	1.4	1.50	9.18
4L-20-5b	4	Full Load	4	0.7	5	3.40	7.00		1.65	15	1.85	-0.17	1.4	1.65	0.20
4L-40-3b	4	Full Load	4	0.7	3	5.67	3.84		1.38	15	1.85	-0.17	1.4	1.35	-2.24
4L-40-4b	4	Full Load	4	0.7	4	4.25	4.22		1.36	15	1.85	-0.17	1.4	1.50	10.43
4L-40-5b	4	Full Load	4	0.7	5	3.40	4.59		1.62	15	1.85	-0.17	1.4	1.63	0.55
4L-60-3b	4	Full Load	4	0.7	3	5.67	2.88		1.42	15	1.85	-0.17	1.4	1.39	-1.97
4L-60-4b	4	Full Load	4	0.7	4	4.25	3.23		1.37	15	1.85	-0.17	1.4	1.54	12.76
4L-60-5b	4	Full Load	4	0.7	5	3.40	3.58		1.66	15	1.85	-0.17	1.4	1.66	0.39
4L-80-3b	4	Full Load	4	0.7	3	5.67	2.40		1.45	15	1.85	-0.17	1.4	1.43	-1.53
4L-80-4b	4	Full Load	4	0.7	4	4.25	2.74		1.39	15	1.85	-0.17	1.4	1.58	13.32
4L-80-5b	4	Full Load	4	0.7	5	3.40	3.06		1.70	15	1.85	-0.17	1.4	1.70	-0.08
4L-100-3b	4	Full Load	4	0.7	3	5.67	2.11		1.47	15	1.85	-0.17	1.4	1.45	-1.37
4L-100-4b	4	Full Load	4	0.7	4	4.25	2.44		1.41	15	1.85	-0.17	1.4	1.60	13.75
4L-100-5b	4	Full Load	4	0.7	5	3.40	2.75		1.73	15	1.85	-0.17	1.4	1.72	-0.77

Cont.

Bridge type	# of Trucks	# of lanes (n)	R_L	Number of Box (N)	Center to center girder spacing (S)	Result from FEA			Parameters of empirical equation				Empirical Equation	Variance	
						(β)of Fm+	Fv inner	Fv outer	a	b	c	e			
5 Lanes															
(β)of Fm+															
5L-20-3b	5	Full Load	5	0.6	3	6.83	4.58	1.61		12.3	0.7	-0.1	1.12	1.74	8.28
5L-20-4b	5	Full Load	5	0.6	4	4.88	4.99	1.73		12.3	0.7	-0.1	1.12	1.73	0.02
5L-20-5b	5	Full Load	5	0.6	5	4.10	5.08	1.67		12.3	0.7	-0.1	1.12	1.87	11.84
5L-40-3b	5	Full Load	5	0.6	3	6.83	2.74	1.61		12.3	0.7	-0.1	1.12	1.74	7.87
5L-40-4b	5	Full Load	5	0.6	4	4.88	2.98	1.77		12.3	0.7	-0.1	1.12	1.71	-3.79
5L-40-5b	5	Full Load	5	0.6	5	4.10	3.22	1.71		12.3	0.7	-0.1	1.12	1.84	7.50
5L-60-3b	5	Full Load	5	0.6	3	6.83	2.03	1.61		12.3	0.7	-0.1	1.12	1.76	9.42
5L-60-4b	5	Full Load	5	0.6	4	4.88	2.26	1.79		12.3	0.7	-0.1	1.12	1.72	-4.03
5L-60-5b	5	Full Load	5	0.6	5	4.10	2.48	1.70		12.3	0.7	-0.1	1.12	1.85	8.71
5L-80-3b	5	Full Load	5	0.6	3	6.83	1.68	1.64		12.3	0.7	-0.1	1.12	1.77	8.02
5L-80-4b	5	Full Load	5	0.6	4	4.88	1.89	1.82		12.3	0.7	-0.1	1.12	1.74	-4.82
5L-80-5b	5	Full Load	5	0.6	5	4.10	2.10	1.72		12.3	0.7	-0.1	1.12	1.87	8.26
5L-100-3b	5	Full Load	5	0.6	3	6.83	1.46	1.67		12.3	0.7	-0.1	1.12	1.78	6.66
5L-100-4b	5	Full Load	5	0.6	4	4.88	1.67	1.83		12.3	0.7	-0.1	1.12	1.75	-4.59
5L-100-5b	5	Full Load	5	0.6	5	4.10	1.87	1.74		12.3	0.7	-0.1	1.12	1.88	7.89
5 Lanes															
(β)of Fm-															
5L-20-3b	5	Full Load	5	0.6	3	6.83	7.32		1.46	12.8	0.7	-0.05	1.12	1.53	5.19
5L-20-4b	5	Full Load	5	0.6	4	4.88	7.98		1.56	12.8	0.7	-0.05	1.12	1.51	-3.09
5L-20-5b	5	Full Load	5	0.6	5	4.10	8.12		1.54	12.8	0.7	-0.05	1.12	1.64	6.04
5L-40-3b	5	Full Load	5	0.6	3	6.83	4.39		1.48	12.8	0.7	-0.05	1.12	1.57	5.65
5L-40-4b	5	Full Load	5	0.6	4	4.88	4.77		1.61	12.8	0.7	-0.05	1.12	1.54	-4.46
5L-40-5b	5	Full Load	5	0.6	5	4.10	5.15		1.54	12.8	0.7	-0.05	1.12	1.65	7.10
5L-60-3b	5	Full Load	5	0.6	3	6.83	3.25		1.51	12.8	0.7	-0.05	1.12	1.61	6.74
5L-60-4b	5	Full Load	5	0.6	4	4.88	3.61		1.64	12.8	0.7	-0.05	1.12	1.57	-4.54
5L-60-5b	5	Full Load	5	0.6	5	4.10	3.96		1.55	12.8	0.7	-0.05	1.12	1.68	8.40
5L-80-3b	5	Full Load	5	0.6	3	6.83	2.68		1.51	12.8	0.7	-0.05	1.12	1.63	7.91
5L-80-4b	5	Full Load	5	0.6	4	4.88	3.03		1.67	12.8	0.7	-0.05	1.12	1.59	-4.54
5L-80-5b	5	Full Load	5	0.6	5	4.10	3.36		1.58	12.8	0.7	-0.05	1.12	1.70	8.19
5L-100-3b	5	Full Load	5	0.6	3	6.83	2.34		1.53	12.8	0.7	-0.05	1.12	1.65	8.25
5L-100-4b	5	Full Load	5	0.6	4	4.88	2.67		1.70	12.8	0.7	-0.05	1.12	1.61	-5.09
5L-100-5b	5	Full Load	5	0.6	5	4.10	2.99		1.60	12.8	0.7	-0.05	1.12	1.72	7.51

Appendix A.8: Parameters of empirical equation of shear distribution factors as function of (β^2) at FLS

Bridge type	# of Trucks	# of lanes (n)	R_L	Number of Box (N)	center to center girder spacing (S)	μ	(β) of F_{m+}	Result from FEA		Parameters of empirical equation				Empirical Equation	Variance		
								$F_{V_{inner}}$	$F_{V_{outer}}$	a	b	c	e				
2 Lanes																	
2L-20-2b	1	Fatigue	1	2	0.9	2	5.00	1	2.35	1.80		8.00	1.18	-0.36	1.65	1.79	-0.76
2L-20-3b	1	Fatigue	1	2	0.9	3	3.33	1	2.59	2.37		8.00	1.18	-0.36	1.65	2.36	-0.06
2L-40-2b	1	Fatigue	1	2	0.9	2	5.00	1	1.52	1.76		8.00	1.18	-0.36	1.65	1.75	-0.73
2L-40-3b	1	Fatigue	1	2	0.9	3	3.33	1	1.77	2.28		8.00	1.18	-0.36	1.65	2.28	-0.10
2L-60-2b	1	Fatigue	1	2	0.9	2	5.00	1	1.11	1.73		8.00	1.18	-0.36	1.65	1.77	2.41
2L-60-3b	1	Fatigue	1	2	0.9	3	3.33	1	1.33	2.29		8.00	1.18	-0.36	1.65	2.29	-0.17
2L-80-2b	1	Fatigue	1	2	0.9	2	5.00	1	0.93	1.77		8.00	1.18	-0.36	1.65	1.79	0.97
2L-80-3b	1	Fatigue	1	2	0.9	3	3.33	1	1.14	2.31		8.00	1.18	-0.36	1.65	2.30	-0.30
2L-100-2b	1	Fatigue	1	2	0.9	2	5.00	1	0.82	1.79		8.00	1.18	-0.36	1.65	1.80	0.54
2L-100-3b	1	Fatigue	1	2	0.9	3	3.33	1	1.02	2.36		8.00	1.18	-0.36	1.65	2.31	-2.13

2 Lanes																	
(β) of F_{m-}																	
Bridge type	# of Trucks	# of lanes (n)	R_L	Number of Box (N)	center to center girder spacing (S)	μ	(β) of F_{m+}	$F_{V_{inner}}$	$F_{V_{outer}}$	a	b	c	e	Empirical Equation	Variance		
2L-20-2b	1	Fatigue	1	2	0.9	2	5.00	1	3.77		1.66	8.30	0.90	-0.17	1.63	1.67	0.37
2L-20-3b	1	Fatigue	1	2	0.9	3	3.33	1	4.15		2.15	8.30	0.90	-0.17	1.63	2.19	2.18
2L-40-2b	1	Fatigue	1	2	0.9	2	5.00	1	2.44		1.63	8.30	0.90	-0.17	1.63	1.63	0.01
2L-40-3b	1	Fatigue	1	2	0.9	3	3.33	1	2.82		2.05	8.30	0.90	-0.17	1.63	2.11	2.97
2L-60-2b	1	Fatigue	1	2	0.9	2	5.00	1	1.78		1.64	8.30	0.90	-0.17	1.63	1.65	0.91
2L-60-3b	1	Fatigue	1	2	0.9	3	3.33	1	2.12		2.10	8.30	0.90	-0.17	1.63	2.12	0.60
2L-80-2b	1	Fatigue	1	2	0.9	2	5.00	1	1.49		1.65	8.30	0.90	-0.17	1.63	1.67	1.38
2L-80-3b	1	Fatigue	1	2	0.9	3	3.33	1	1.82		2.12	8.30	0.90	-0.17	1.63	2.13	0.52
2L-100-2b	1	Fatigue	1	2	0.9	2	5.00	1	1.32		1.66	8.30	0.90	-0.17	1.63	1.68	1.69
2L-100-3b	1	Fatigue	1	2	0.9	3	3.33	1	1.63		2.15	8.30	0.90	-0.17	1.63	2.14	-0.43

3 Lanes																	
(β) of F_{m+}																	
Bridge type	# of Trucks	# of lanes (n)	R_L	Number of Box (N)	center to center girder spacing (S)	μ	(β) of F_{m+}	$F_{V_{inner}}$	$F_{V_{outer}}$	a	b	c	e	Empirical Equation	Variance		
3L-20-2b	1	Fatigue	1	3	0.8	2	6.75	1	3.01	1.88		11.77	0.84	-0.22	1.79	1.89	0.70
3L-20-3b	1	Fatigue	1	3	0.8	3	4.50	1	3.25	2.68		11.77	0.84	-0.22	1.79	2.63	-1.64
3L-20-4b	1	Fatigue	1	3	0.8	4	3.38	1	3.85	3.41		11.77	0.84	-0.22	1.79	3.42	0.45
3L-40-2b	1	Fatigue	1	3	0.8	2	6.75	1	1.81	1.84		11.77	0.84	-0.22	1.79	1.85	0.46
3L-40-3b	1	Fatigue	1	3	0.8	3	4.50	1	1.82	2.59		11.77	0.84	-0.22	1.79	2.55	-1.59
3L-40-4b	1	Fatigue	1	3	0.8	4	3.38	1	2.28	3.18		11.77	0.84	-0.22	1.79	3.20	0.46
3L-60-2b	1	Fatigue	1	3	0.8	2	6.75	1	1.30	1.83		11.77	0.84	-0.22	1.79	1.86	1.91
3L-60-3b	1	Fatigue	1	3	0.8	3	4.50	1	1.57	2.55		11.77	0.84	-0.22	1.79	2.55	-0.16
3L-60-4b	1	Fatigue	1	3	0.8	4	3.38	1	1.78	3.16		11.77	0.84	-0.22	1.79	3.19	1.08
3L-80-2b	1	Fatigue	1	3	0.8	2	6.75	1	1.11	1.84		11.77	0.84	-0.22	1.79	1.87	1.58
3L-80-3b	1	Fatigue	1	3	0.8	3	4.50	1	1.32	2.57		11.77	0.84	-0.22	1.79	2.56	-0.36
3L-80-4b	1	Fatigue	1	3	0.8	4	3.38	1	1.53	3.17		11.77	0.84	-0.22	1.79	3.20	0.87
3L-100-2b	1	Fatigue	1	3	0.8	2	6.75	1	0.97	1.88		11.77	0.84	-0.22	1.79	1.88	0.13
3L-100-3b	1	Fatigue	1	3	0.8	3	4.50	1	1.17	2.61		11.77	0.84	-0.22	1.79	2.57	-1.67
3L-100-4b	1	Fatigue	1	3	0.8	4	3.38	1	1.37	3.22		11.77	0.84	-0.22	1.79	3.21	-0.54

Cont.

Bridge type	# of Trucks	# of lanes (n)	R _L	Number of Box (N)	center to center girder spacing (S)	μ	(β)of Fm+	Result from FEA		Parameters of empirical equation				Empirical Equation	Variance		
								F _{V inner}	F _{V outer}	a	b	c	e				
3 Lanes								(β)of Fm-									
3L-20-2b	1	Fatigue	1	3	0.8	2	6.75	1	4.81		1.74	11.90	0.74	-0.11	1.74	1.75	0.31
3L-20-3b	1	Fatigue	1	3	0.8	3	4.50	1	5.20		2.43	11.90	0.74	-0.11	1.74	2.38	-1.89
3L-20-4b	1	Fatigue	1	3	0.8	4	3.38	1	6.16		3.05	11.90	0.74	-0.11	1.74	3.06	0.48
3L-40-2b	1	Fatigue	1	3	0.8	2	6.75	1	2.90		1.73	11.90	0.74	-0.11	1.74	1.72	-0.43
3L-40-3b	1	Fatigue	1	3	0.8	3	4.50	1	2.91		2.34	11.90	0.74	-0.11	1.74	2.32	-0.77
3L-40-4b	1	Fatigue	1	3	0.8	4	3.38	1	3.65		2.82	11.90	0.74	-0.11	1.74	2.86	1.64
3L-60-2b	1	Fatigue	1	3	0.8	2	6.75	1	2.08		1.73	11.90	0.74	-0.11	1.74	1.74	0.47
3L-60-3b	1	Fatigue	1	3	0.8	3	4.50	1	2.51		2.34	11.90	0.74	-0.11	1.74	2.33	-0.36
3L-60-4b	1	Fatigue	1	3	0.8	4	3.38	1	2.85		2.84	11.90	0.74	-0.11	1.74	2.87	1.12
3L-80-2b	1	Fatigue	1	3	0.8	2	6.75	1	1.77		1.71	11.90	0.74	-0.11	1.74	1.75	2.14
3L-80-3b	1	Fatigue	1	3	0.8	3	4.50	1	2.12		2.35	11.90	0.74	-0.11	1.74	2.34	-0.31
3L-80-4b	1	Fatigue	1	3	0.8	4	3.38	1	2.44		2.87	11.90	0.74	-0.11	1.74	2.88	0.51
3L-100-2b	1	Fatigue	1	3	0.8	2	6.75	1	1.55		1.73	11.90	0.74	-0.11	1.74	1.76	1.90
3L-100-3b	1	Fatigue	1	3	0.8	3	4.50	1	1.88		2.38	11.90	0.74	-0.11	1.74	2.36	-1.07
3L-100-4b	1	Fatigue	1	3	0.8	4	3.38	1	2.19		2.93	11.90	0.74	-0.11	1.74	2.90	-1.27
4 Lanes								(β)of Fm+									
4L-20-3b	1	Fatigue	1	4	0.7	3	5.67	1	3.90	2.77		13.94	0.70	-0.15	1.78	2.78	0.32
4L-20-4b	1	Fatigue	1	4	0.7	4	4.25	1	4.14	3.54		13.94	0.70	-0.15	1.78	3.51	-0.67
4L-20-5b	1	Fatigue	1	4	0.7	5	3.40	1	4.38	4.13		13.94	0.70	-0.15	1.78	4.22	2.24
4L-40-3b	1	Fatigue	1	4	0.7	3	5.67	1	2.40	2.69		13.94	0.70	-0.15	1.78	2.71	0.71
4L-40-4b	1	Fatigue	1	4	0.7	4	4.25	1	2.64	3.44		13.94	0.70	-0.15	1.78	3.40	-1.04
4L-40-5b	1	Fatigue	1	4	0.7	5	3.40	1	2.87	4.02		13.94	0.70	-0.15	1.78	4.05	0.92
4L-60-3b	1	Fatigue	1	4	0.7	3	5.67	1	1.80	2.65		13.94	0.70	-0.15	1.78	2.72	2.64
4L-60-4b	1	Fatigue	1	4	0.7	4	4.25	1	2.02	3.37		13.94	0.70	-0.15	1.78	3.40	0.79
4L-60-5b	1	Fatigue	1	4	0.7	5	3.40	1	2.24	3.98		13.94	0.70	-0.15	1.78	4.04	1.52
4L-80-3b	1	Fatigue	1	4	0.7	3	5.67	1	1.50	2.69		13.94	0.70	-0.15	1.78	2.73	1.42
4L-80-4b	1	Fatigue	1	4	0.7	4	4.25	1	1.71	3.39		13.94	0.70	-0.15	1.78	3.41	0.45
4L-80-5b	1	Fatigue	1	4	0.7	5	3.40	1	1.92	4.02		13.94	0.70	-0.15	1.78	4.05	0.69
4L-100-3b	1	Fatigue	1	4	0.7	3	5.67	1	1.32	2.74		13.94	0.70	-0.15	1.78	2.74	0.26
4L-100-4b	1	Fatigue	1	4	0.7	4	4.25	1	1.52	3.47		13.94	0.70	-0.15	1.78	3.42	-1.36
4L-100-5b	1	Fatigue	1	4	0.7	5	3.40	1	1.72	4.08		13.94	0.70	-0.15	1.78	4.06	-0.63
4 Lanes								(β)of Fm-									
4L-20-3b	1	Fatigue	1	4	0.7	3	5.67	1	6.24		2.53	14.00	0.80	-0.09	1.74	2.47	-2.01
4L-20-4b	1	Fatigue	1	4	0.7	4	4.25	1	6.63		3.19	14.00	0.80	-0.09	1.74	3.09	-3.09
4L-20-5b	1	Fatigue	1	4	0.7	5	3.40	1	7.00		3.70	14.00	0.80	-0.09	1.74	3.68	-0.35
4L-40-3b	1	Fatigue	1	4	0.7	3	5.67	1	3.84		2.45	14.00	0.80	-0.09	1.74	2.43	-0.77
4L-40-4b	1	Fatigue	1	4	0.7	4	4.25	1	4.22		3.05	14.00	0.80	-0.09	1.74	3.01	-1.58
4L-40-5b	1	Fatigue	1	4	0.7	5	3.40	1	4.59		3.52	14.00	0.80	-0.09	1.74	3.55	0.66
4L-60-3b	1	Fatigue	1	4	0.7	3	5.67	1	2.88		2.45	14.00	0.80	-0.09	1.74	2.46	0.59
4L-60-4b	1	Fatigue	1	4	0.7	4	4.25	1	3.23		3.04	14.00	0.80	-0.09	1.74	3.03	-0.44
4L-60-5b	1	Fatigue	1	4	0.7	5	3.40	1	3.58		3.55	14.00	0.80	-0.09	1.74	3.56	0.42
4L-80-3b	1	Fatigue	1	4	0.7	3	5.67	1	2.40		2.45	14.00	0.80	-0.09	1.74	2.49	1.53
4L-80-4b	1	Fatigue	1	4	0.7	4	4.25	1	2.74		3.06	14.00	0.80	-0.09	1.74	3.06	-0.27
4L-80-5b	1	Fatigue	1	4	0.7	5	3.40	1	3.06		3.61	14.00	0.80	-0.09	1.74	3.58	-0.59
4L-100-3b	1	Fatigue	1	4	0.7	3	5.67	1	2.11		2.47	14.00	0.80	-0.09	1.74	2.51	1.43
4L-100-4b	1	Fatigue	1	4	0.7	4	4.25	1	2.44		3.12	14.00	0.80	-0.09	1.74	3.08	-1.42
4L-100-5b	1	Fatigue	1	4	0.7	5	3.40	1	2.75		3.68	14.00	0.80	-0.09	1.74	3.60	-2.13

Cont.

Bridge type	# of Trucks	# of lanes (n)	R _L	Number of Box (N)	center to center girder spacing (S)	μ	(β) of Fm+	Result from FEA		Parameters of empirical equation				Empirical Equation	Variance	
								F _{V inner}	F _{V outer}	a	b	c	e			
5 Lanes																
(β) of Fm+																
5L-20-3b	1	Fatigue	1	5	0.6	3	6.83	1	4.58	2.84	16.00	0.94	-0.15	1.80	2.88	1.37
5L-20-4b	1	Fatigue	1	5	0.6	4	4.88	1	4.99	3.57	16.00	0.94	-0.15	1.80	3.49	-2.35
5L-20-5b	1	Fatigue	1	5	0.6	5	4.10	1	5.08	4.34	16.00	0.94	-0.15	1.80	4.39	1.25
5L-40-3b	1	Fatigue	1	5	0.6	3	6.83	1	2.74	2.78	16.00	0.94	-0.15	1.80	2.83	1.82
5L-40-4b	1	Fatigue	1	5	0.6	4	4.88	1	2.98	3.55	16.00	0.94	-0.15	1.80	3.38	-4.76
5L-40-5b	1	Fatigue	1	5	0.6	5	4.10	1	3.22	4.20	16.00	0.94	-0.15	1.80	4.25	1.14
5L-60-3b	1	Fatigue	1	5	0.6	3	6.83	1	2.03	2.76	16.00	0.94	-0.15	1.80	2.86	3.56
5L-60-4b	1	Fatigue	1	5	0.6	4	4.88	1	2.26	3.50	16.00	0.94	-0.15	1.80	3.41	-2.66
5L-60-5b	1	Fatigue	1	5	0.6	5	4.10	1	2.48	4.20	16.00	0.94	-0.15	1.80	4.27	1.61
5L-80-3b	1	Fatigue	1	5	0.6	3	6.83	1	1.68	2.79	16.00	0.94	-0.15	1.80	2.88	3.03
5L-80-4b	1	Fatigue	1	5	0.6	4	4.88	1	1.89	3.55	16.00	0.94	-0.15	1.80	3.43	-3.42
5L-80-5b	1	Fatigue	1	5	0.6	5	4.10	1	2.10	4.24	16.00	0.94	-0.15	1.80	4.29	1.13
5L-100-3b	1	Fatigue	1	5	0.6	3	6.83	1	1.46	2.83	16.00	0.94	-0.15	1.80	2.89	2.32
5L-100-4b	1	Fatigue	1	5	0.6	4	4.88	1	1.67	3.57	16.00	0.94	-0.15	1.80	3.45	-3.46
5L-100-5b	1	Fatigue	1	5	0.6	5	4.10	1	1.87	4.33	16.00	0.94	-0.15	1.80	4.31	-0.36

5 Lanes																	
(β) of Fm-																	
5L-20-3b	1	Fatigue	1	5	0.6	3	6.83	1	7.32		2.59	16.80	0.66	-0.07	1.77	2.64	1.70
5L-20-4b	1	Fatigue	1	5	0.6	4	4.88	1	7.98		3.30	16.80	0.66	-0.07	1.77	3.17	-3.88
5L-20-5b	1	Fatigue	1	5	0.6	5	4.10	1	8.12		3.90	16.80	0.66	-0.07	1.77	3.97	1.85
5L-40-3b	1	Fatigue	1	5	0.6	3	6.83	1	4.39		2.55	16.80	0.66	-0.07	1.77	2.59	1.28
5L-40-4b	1	Fatigue	1	5	0.6	4	4.88	1	4.77		3.19	16.80	0.66	-0.07	1.77	3.07	-3.91
5L-40-5b	1	Fatigue	1	5	0.6	5	4.10	1	5.15		3.76	16.80	0.66	-0.07	1.77	3.82	1.78
5L-60-3b	1	Fatigue	1	5	0.6	3	6.83	1	3.25		2.55	16.80	0.66	-0.07	1.77	2.61	2.24
5L-60-4b	1	Fatigue	1	5	0.6	4	4.88	1	3.61		3.19	16.80	0.66	-0.07	1.77	3.08	-3.38
5L-60-5b	1	Fatigue	1	5	0.6	5	4.10	1	3.96		3.76	16.80	0.66	-0.07	1.77	3.84	2.00
5L-80-3b	1	Fatigue	1	5	0.6	3	6.83	1	2.68		2.55	16.80	0.66	-0.07	1.77	2.63	3.14
5L-80-4b	1	Fatigue	1	5	0.6	4	4.88	1	3.03		3.21	16.80	0.66	-0.07	1.77	3.11	-3.09
5L-80-5b	1	Fatigue	1	5	0.6	5	4.10	1	3.36		3.81	16.80	0.66	-0.07	1.77	3.86	1.18
5L-100-3b	1	Fatigue	1	5	0.6	3	6.83	1	2.34		2.56	16.80	0.66	-0.07	1.77	2.65	3.33
5L-100-4b	1	Fatigue	1	5	0.6	4	4.88	1	2.67		3.24	16.80	0.66	-0.07	1.77	3.12	-3.58
5L-100-5b	1	Fatigue	1	5	0.6	5	4.10	1	2.99		3.88	16.80	0.66	-0.07	1.77	3.88	0.00

APPENDIX A.9 Comparison between the load distribution factor from the FEA and CHBDC equation in ULS

Bridge type	# of Trucks		# of lanes (n)	R _L	Number of Box (N)	RESULT (FEA)				CHBDC CODE			
						F _{M+}	F _{M-}	F _{V inner}	F _{V outer}	F _{M+}	F _{M-}	F _{V inner}	F _{V outer}
2L-20-2b	2	Full Load	2	0.9	2	1.77	3.14	1.21	1.15	1.15	1.25	1.39	1.39
2L-20-3b	2	Full Load	2	0.9	3	1.75	2.82	1.68	1.55	1.17	1.28	1.39	1.39
2L-40-2b	2	Full Load	2	0.9	2	1.27	2.38	1.22	1.17	1.10	1.16	1.39	1.39
2L-40-3b	2	Full Load	2	0.9	3	1.28	2.71	1.68	1.57	1.12	1.18	1.39	1.39
2L-60-2b	2	Full Load	2	0.9	2	1.15	2.26	1.23	1.20	1.08	1.12	1.39	1.39
2L-60-3b	2	Full Load	2	0.9	3	1.19	2.41	1.71	1.60	1.09	1.14	1.39	1.39
2L-80-2b	2	Full Load	2	0.9	2	1.18	2.00	1.26	1.20	1.07	1.10	1.39	1.39
2L-80-3b	2	Full Load	2	0.9	3	1.16	2.15	1.74	1.62	1.08	1.12	1.39	1.39
2L-100-2b	2	Full Load	2	0.9	2	1.12	1.88	1.27	1.21	1.06	1.09	1.39	1.39
2L-100-3b	2	Full Load	2	0.9	3	1.11	2.51	1.75	1.64	1.07	1.11	1.39	1.39
3L-20-2b	3	Full Load	3	0.8	2	1.59	3.29	1.23	1.14	1.23	1.40	1.41	1.41
3L-20-3b	3	Full Load	3	0.8	3	1.53	2.87	1.32	1.25	1.25	1.44	1.41	1.41
3L-20-4b	3	Full Load	3	0.8	4	1.73	3.36	1.67	1.52	1.30	1.55	1.41	1.41
3L-40-2b	3	Full Load	3	0.8	2	1.31	2.65	1.22	1.18	1.13	1.22	1.41	1.41
3L-40-3b	3	Full Load	3	0.8	3	1.30	2.54	1.35	1.26	1.13	1.22	1.41	1.41
3L-40-4b	3	Full Load	3	0.8	4	1.30	2.56	1.65	1.53	1.17	1.28	1.41	1.41
3L-60-2b	3	Full Load	3	0.8	2	1.14	2.12	1.23	1.21	1.10	1.15	1.41	1.41
3L-60-3b	3	Full Load	3	0.8	3	1.16	2.19	1.35	1.29	1.12	1.19	1.41	1.41
3L-60-4b	3	Full Load	3	0.8	4	1.17	2.26	1.66	1.57	1.13	1.21	1.41	1.41
3L-80-2b	3	Full Load	3	0.8	2	1.14	2.15	1.27	1.22	1.08	1.13	1.41	1.41
3L-80-3b	3	Full Load	3	0.8	3	1.12	2.20	1.36	1.30	1.10	1.16	1.41	1.41
3L-80-4b	3	Full Load	3	0.8	4	1.16	2.41	1.69	1.59	1.11	1.18	1.41	1.41
3L-100-2b	3	Full Load	3	0.8	2	1.12	2.16	1.30	1.24	1.07	1.11	1.41	1.41
3L-100-3b	3	Full Load	3	0.8	3	1.11	2.34	1.37	1.31	1.09	1.14	1.41	1.41
3L-100-4b	3	Full Load	3	0.8	4	1.13	2.45	1.73	1.62	1.10	1.16	1.41	1.41
4L-20-3b	4	Full Load	4	0.7	3	1.94	3.64	1.48	1.33	1.33	1.62	1.52	1.52
4L-20-4b	4	Full Load	4	0.7	4	1.65	3.00	1.47	1.37	1.36	1.68	1.52	1.52
4L-20-5b	4	Full Load	4	0.7	5	1.61	2.72	1.84	1.65	1.39	1.74	1.52	1.52

Cont.

Bridge type	# of Trucks		# of lanes (n)	R _L	Number of Box (N)	RESULT (FEA)				CHBDC CODE			
						F _{M+}	F _{M-}	F _{V inner}	F _{V outer}	F _{M+}	F _{M-}	F _{V inner}	F _{V outer}
4L-40-3b	4	Full Load	4	0.7	3	1.44	3.25	1.49	1.38	1.19	1.33	1.52	1.52
4L-40-4b	4	Full Load	4	0.7	4	1.44	3.08	1.48	1.36	1.21	1.37	1.52	1.52
4L-40-5b	4	Full Load	4	0.7	5	1.44	2.94	1.81	1.62	1.23	1.41	1.52	1.52
4L-60-3b	4	Full Load	4	0.7	3	1.27	2.93	1.52	1.42	1.14	1.24	1.52	1.52
4L-60-4b	4	Full Load	4	0.7	4	1.25	2.80	1.48	1.37	1.16	1.27	1.52	1.52
4L-60-5b	4	Full Load	4	0.7	5	1.26	2.91	1.83	1.66	1.18	1.30	1.52	1.52
4L-80-3b	4	Full Load	4	0.7	3	1.19	2.68	1.56	1.45	1.12	1.19	1.52	1.52
4L-80-4b	4	Full Load	4	0.7	4	1.17	2.49	1.42	1.33	1.14	1.22	1.52	1.52
4L-80-5b	4	Full Load	4	0.7	5	1.20	2.74	1.88	1.70	1.15	1.25	1.52	1.52
4L-100-3b	4	Full Load	4	0.7	3	1.17	2.69	1.60	1.47	1.10	1.17	1.52	1.52
4L-100-4b	4	Full Load	4	0.7	4	1.15	2.65	1.51	1.41	1.12	1.20	1.52	1.52
4L-100-5b	4	Full Load	4	0.7	5	1.18	2.80	1.91	1.73	1.14	1.22	1.52	1.52
5L-20-3b	5	Full Load	5	0.8	3	2.21	4.28	1.61	1.46	1.59	2.01	1.71	1.71
5L-20-4b	5	Full Load	5	0.8	4	2.18	3.68	1.73	1.56	1.56	2.04	1.63	1.63
5L-20-5b	5	Full Load	5	0.8	5	2.13	3.55	1.67	1.54	1.65	2.18	1.71	1.71
5L-40-3b	5	Full Load	5	0.8	3	1.57	4.12	1.61	1.48	1.38	1.56	1.71	1.71
5L-40-4b	5	Full Load	5	0.8	4	1.58	3.61	1.77	1.61	1.40	1.61	1.71	1.71
5L-40-5b	5	Full Load	5	0.8	5	1.43	3.20	1.71	1.54	1.43	1.66	1.71	1.71
5L-60-3b	5	Full Load	5	0.8	3	1.35	3.71	1.61	1.51	1.31	1.43	1.71	1.71
5L-60-4b	5	Full Load	5	0.8	4	1.35	3.38	1.79	1.64	1.33	1.47	1.71	1.71
5L-60-5b	5	Full Load	5	0.8	5	1.34	3.23	1.70	1.55	1.35	1.51	1.71	1.71
5L-80-3b	5	Full Load	5	0.8	3	1.27	3.54	1.64	1.51	1.17	1.26	1.57	1.57
5L-80-4b	5	Full Load	5	0.8	4	1.24	3.30	1.82	1.67	1.29	1.41	1.71	1.71
5L-80-5b	5	Full Load	5	0.8	5	1.20	2.94	1.72	1.58	1.31	1.44	1.71	1.71
5L-100-3b	5	Full Load	5	0.8	3	1.22	3.31	1.67	1.53	1.26	1.34	1.71	1.71
5L-100-4b	5	Full Load	5	0.8	4	1.22	3.13	1.86	1.70	1.27	1.37	1.71	1.71
5L-100-5b	5	Full Load	5	0.8	5	1.17	3.01	1.74	1.60	1.29	1.40	1.71	1.71

APPENDIX A.10 Comparison between the load distribution factor from the FEA and CHBDC equation in FLS

Bridge type	# of Trucks	# of lanes (n)	R _L	Number of Box (N)	Result (FEA)				Result (CHBDC)				
					F _{M+}	F _{M-}	F _{V inner}	F _{V outer}	F _{M+}	F _{M-}	F _{V inner}	F _{V outer}	
2L-20-2b	1	Fatigue_1	2	0.9	2	2.97	4.67	1.80	1.66	1.41	1.80	2.35	2.35
2L-20-3b	1	Fatigue_1	2	0.9	3	3.00	4.34	2.37	2.15	1.46	1.95	2.35	2.35
2L-40-2b	1	Fatigue_1	2	0.9	2	1.64	2.92	1.76	1.63	1.24	1.43	2.35	2.35
2L-40-3b	1	Fatigue_1	2	0.9	3	1.79	3.54	2.28	2.05	1.29	1.52	2.35	2.35
2L-60-2b	1	Fatigue_1	2	0.9	2	1.67	3.32	2.08	1.96	1.17	1.29	2.35	2.35
2L-60-3b	1	Fatigue_1	2	0.9	3	1.60	3.30	2.29	2.10	1.21	1.36	2.35	2.35
2L-80-2b	1	Fatigue_1	2	0.9	2	1.42	2.46	1.77	1.65	1.14	1.24	2.35	2.35
2L-80-3b	1	Fatigue_1	2	0.9	3	1.50	2.92	2.31	2.12	1.18	1.30	2.36	2.36
2L-100-2b	1	Fatigue_1	2	0.9	2	1.33	2.33	1.79	1.66	1.13	1.21	2.35	2.35
2L-100-3b	1	Fatigue_1	2	0.9	3	1.41	3.73	2.36	2.15	1.16	1.26	2.36	2.36
3L-20-2b	1	Fatigue_1	3	0.8	2	3.46	6.50	1.88	1.74	2.12	3.04	3.18	3.18
3L-20-3b	1	Fatigue_1	3	0.8	3	3.50	5.98	2.68	2.43	2.21	3.35	3.18	3.18
3L-20-4b	1	Fatigue_1	3	0.8	4	4.14	7.60	3.46	3.05	2.47	4.40	3.18	3.18
3L-40-2b	1	Fatigue_1	3	0.8	2	2.19	3.96	1.84	1.73	1.75	2.08	3.18	3.18
3L-40-3b	1	Fatigue_1	3	0.8	3	2.30	4.37	2.59	2.34	1.75	2.08	3.18	3.18
3L-40-4b	1	Fatigue_1	3	0.8	4	2.38	4.78	3.18	2.82	1.88	2.38	3.18	3.18
3L-60-2b	1	Fatigue_1	3	0.8	2	1.64	2.84	1.83	1.73	1.62	1.82	3.18	3.18
3L-60-3b	1	Fatigue_1	3	0.8	3	1.79	3.64	2.55	2.34	1.69	1.95	3.18	3.18
3L-60-4b	1	Fatigue_1	3	0.8	4	1.94	4.19	3.16	2.84	1.74	2.06	3.18	3.18
3L-80-2b	1	Fatigue_1	3	0.8	2	1.52	2.92	1.84	1.71	1.58	1.74	3.18	3.18
3L-80-3b	1	Fatigue_1	3	0.8	3	1.66	3.65	2.57	2.35	1.63	1.83	3.18	3.18
3L-80-4b	1	Fatigue_1	3	0.8	4	1.82	4.31	3.17	2.87	1.68	1.93	3.18	3.18
3L-100-2b	1	Fatigue_1	3	0.8	2	1.45	2.95	1.88	1.73	1.55	1.68	3.18	3.18
3L-100-3b	1	Fatigue_1	3	0.8	3	1.61	3.83	2.61	2.38	1.60	1.77	3.18	3.18
3L-100-4b	1	Fatigue_1	3	0.8	4	1.71	4.31	3.22	2.93	1.64	1.85	3.18	3.18
4L-20-3b	1	Fatigue_1	4	0.7	3	4.96	8.94	2.77	2.53	3.15	5.70	4.00	4.00
4L-20-4b	1	Fatigue_1	4	0.7	4	4.39	7.67	3.54	3.19	3.31	6.53	4.00	4.00
4L-20-5b	1	Fatigue_1	4	0.7	5	4.31	7.00	4.13	3.70	3.48	7.59	4.00	4.00

Cont.

Bridge type	# of Trucks		# of lanes (n)	R _L	Number of Box (N)	Result (FEA)				Result (CHBDC)			
						F _{M+}	F _{M-}	F _{V inner}	F _{V outer}	F _{M+}	F _{M-}	F _{V inner}	F _{V outer}
4L-40-3b	1	Fatigue_1	4	0.7	3	2.96	5.87	2.69	2.45	2.41	3.11	4.00	4.00
4L-40-4b	1	Fatigue_1	4	0.7	4	3.08	6.44	3.44	3.05	2.51	3.36	4.00	4.00
4L-40-5b	1	Fatigue_1	4	0.7	5	3.16	6.74	4.02	3.52	2.60	3.64	4.00	4.00
4L-60-3b	1	Fatigue_1	4	0.7	3	2.22	5.17	2.65	2.45	2.20	2.61	4.00	4.00
4L-60-4b	1	Fatigue_1	4	0.7	4	2.35	5.68	3.37	3.04	2.27	2.78	4.00	4.00
4L-60-5b	1	Fatigue_1	4	0.7	5	2.52	6.36	3.98	3.55	2.35	2.96	4.00	4.00
4L-80-3b	1	Fatigue_1	4	0.7	3	1.97	4.74	2.69	2.45	2.10	2.41	4.00	4.00
4L-80-4b	1	Fatigue_1	4	0.7	4	2.10	5.13	3.39	3.06	2.17	2.55	4.00	4.00
4L-80-5b	1	Fatigue_1	4	0.7	5	2.25	5.92	4.02	3.61	2.24	2.69	4.00	4.00
4L-100-3b	1	Fatigue_1	4	0.7	3	1.83	4.69	2.74	2.47	2.05	2.30	4.00	4.00
4L-100-4b	1	Fatigue_1	4	0.7	4	1.95	5.20	3.47	3.12	2.11	2.42	4.00	4.00
4L-100-5b	1	Fatigue_1	4	0.7	5	2.09	5.94	4.08	3.68	2.17	2.55	4.00	4.00
5L-20-3b	1	Fatigue_1	5	0.6	3	5.90	10.75	2.84	2.59	4.38	10.60	4.82	4.82
5L-20-4b	1	Fatigue_1	5	0.6	4	6.01	9.91	3.65	3.30	4.59	14.81	4.59	4.59
5L-20-5b	1	Fatigue_1	5	0.6	5	5.97	9.82	4.34	3.90	4.93	17.30	4.82	4.82
5L-40-3b	1	Fatigue_1	5	0.6	3	3.39	7.55	2.78	2.55	3.07	4.20	4.82	4.82
5L-40-4b	1	Fatigue_1	5	0.6	4	3.58	7.58	3.55	3.19	3.20	4.58	4.82	4.82
5L-40-5b	1	Fatigue_1	5	0.6	5	3.37	7.68	4.20	3.76	3.20	5.02	4.82	4.82
5L-60-3b	1	Fatigue_1	5	0.6	3	2.50	6.28	2.76	2.55	2.74	3.36	4.82	4.82
5L-60-4b	1	Fatigue_1	5	0.6	4	2.72	7.05	3.50	3.19	2.84	3.59	4.82	4.82
5L-60-5b	1	Fatigue_1	5	0.6	5	2.84	7.42	4.20	3.76	2.94	3.84	4.82	4.82
5L-80-3b	1	Fatigue_1	5	0.6	3	2.21	6.02	2.79	2.55	2.40	2.80	4.44	4.44
5L-80-4b	1	Fatigue_1	5	0.6	4	2.39	6.77	3.55	3.21	2.69	3.23	4.82	4.82
5L-80-5b	1	Fatigue_1	5	0.6	5	2.41	6.64	4.24	3.81	2.77	3.43	4.82	4.82
5L-100-3b	1	Fatigue_1	5	0.6	3	2.03	5.66	2.83	2.56	2.52	2.88	4.82	4.82
5L-100-4b	1	Fatigue_1	5	0.6	4	2.18	6.38	3.61	3.24	2.60	3.04	4.82	4.82
5L-100-5b	1	Fatigue_1	5	0.6	5	2.24	6.66	4.33	3.88	2.68	3.21	4.82	4.82

APPENDIX A.11 Comparison between the load distribution factor from the FEA and AASHTO-LRFD equation in ULS

Bridge type	# of Trucks		# of lanes (n)	R _L	Number of Box (N)	RESULT (FEA)				AASHTO CODE $W_L = .1 + 1.7(N_L/N_B) + .85/N_L$
						F _{M+}	F _{M-}	F _{V inner}	F _{V outer}	
2L-20-2b	2	Full Load	2	0.9	2	1.77	3.14	1.21	1.15	2.23
2L-20-3b	2	Full Load	2	0.9	3	1.75	2.82	1.68	1.55	1.66
2L-40-2b	2	Full Load	2	0.9	2	1.27	2.38	1.22	1.17	2.23
2L-40-3b	2	Full Load	2	0.9	3	1.28	2.71	1.68	1.57	1.66
2L-60-2b	2	Full Load	2	0.9	2	1.15	2.26	1.23	1.20	2.23
2L-60-3b	2	Full Load	2	0.9	3	1.19	2.41	1.71	1.60	1.66
2L-80-2b	2	Full Load	2	0.9	2	1.18	2.00	1.26	1.20	2.23
2L-80-3b	2	Full Load	2	0.9	3	1.16	2.15	1.74	1.62	1.66
2L-100-2b	2	Full Load	2	0.9	2	1.12	1.88	1.27	1.21	2.23
2L-100-3b	2	Full Load	2	0.9	3	1.11	2.51	1.75	1.64	1.66
3L-20-2b	3	Full Load	3	0.8	2	1.59	3.29	1.23	1.14	2.93
3L-20-3b	3	Full Load	3	0.8	3	1.53	2.87	1.32	1.25	2.08
3L-20-4b	3	Full Load	3	0.8	4	1.73	3.36	1.67	1.52	1.66
3L-40-2b	3	Full Load	3	0.8	2	1.31	2.65	1.22	1.18	2.93
3L-40-3b	3	Full Load	3	0.8	3	1.30	2.54	1.35	1.26	2.08
3L-40-4b	3	Full Load	3	0.8	4	1.30	2.56	1.65	1.53	1.66
3L-60-2b	3	Full Load	3	0.8	2	1.14	2.12	1.23	1.21	2.93
3L-60-3b	3	Full Load	3	0.8	3	1.16	2.19	1.35	1.29	2.08
3L-60-4b	3	Full Load	3	0.8	4	1.17	2.26	1.66	1.57	1.66
3L-80-2b	3	Full Load	3	0.8	2	1.14	2.15	1.27	1.22	2.93
3L-80-3b	3	Full Load	3	0.8	3	1.12	2.20	1.36	1.30	2.08
3L-80-4b	3	Full Load	3	0.8	4	1.16	2.41	1.69	1.59	1.66
3L-100-2b	3	Full Load	3	0.8	2	1.12	2.16	1.30	1.24	2.93
3L-100-3b	3	Full Load	3	0.8	3	1.11	2.34	1.37	1.31	2.08
3L-100-4b	3	Full Load	3	0.8	4	1.13	2.45	1.73	1.62	1.66
4L-20-3b	4	Full Load	4	0.7	3	1.94	3.64	1.48	1.33	2.68
4L-20-4b	4	Full Load	4	0.7	4	1.65	3.00	1.47	1.37	2.01
4L-20-5b	4	Full Load	4	0.7	5	1.61	2.72	1.84	1.65	1.67
4L-40-3b	4	Full Load	4	0.7	3	1.44	3.25	1.49	1.38	2.68

Cont.

Bridge type	# of Trucks		# of lanes (n)	R _L	Number of Box (N)	RESULT (FEA)				AASHTO CODE $W_L = .1 + 1.7(N_L/N_B) + .85/N_L$
						F _{M+}	F _{M-}	F _{V inner}	F _{V outer}	
4L-40-4b	4	Full Load	4	0.7	4	1.44	3.08	1.48	1.36	2.01
4L-40-5b	4	Full Load	4	0.7	5	1.44	2.94	1.81	1.62	1.87
4L-60-3b	4	Full Load	4	0.7	3	1.27	2.93	1.52	1.42	2.58
4L-60-4b	4	Full Load	4	0.7	4	1.25	2.80	1.48	1.37	2.01
4L-60-5b	4	Full Load	4	0.7	5	1.26	2.91	1.83	1.66	1.87
4L-80-3b	4	Full Load	4	0.7	3	1.19	2.68	1.56	1.45	2.58
4L-80-4b	4	Full Load	4	0.7	4	1.17	2.49	1.42	1.33	2.01
4L-80-5b	4	Full Load	4	0.7	5	1.20	2.74	1.88	1.70	1.87
4L-100-3b	4	Full Load	4	0.7	3	1.17	2.69	1.60	1.47	2.58
4L-100-4b	4	Full Load	4	0.7	4	1.15	2.65	1.51	1.41	2.01
4L-100-5b	4	Full Load	4	0.7	5	1.18	2.80	1.91	1.73	1.87
5L-20-3b	5	Full Load	5	0.6	3	2.21	4.28	1.61	1.46	3.10
5L-20-4b	5	Full Load	5	0.6	4	2.18	3.68	1.73	1.56	2.40
5L-20-5b	5	Full Load	5	0.6	5	2.13	3.55	1.67	1.54	1.97
5L-40-3b	5	Full Load	5	0.6	3	1.57	4.12	1.61	1.48	3.10
5L-40-4b	5	Full Load	5	0.6	4	1.58	3.61	1.77	1.61	2.40
5L-40-5b	5	Full Load	5	0.6	5	1.43	3.20	1.71	1.54	1.97
5L-60-3b	5	Full Load	5	0.6	3	1.35	3.71	1.61	1.51	3.10
5L-60-4b	5	Full Load	5	0.6	4	1.35	3.38	1.79	1.64	2.40
5L-60-5b	5	Full Load	5	0.6	5	1.34	3.23	1.70	1.55	1.97
5L-80-3b	5	Full Load	5	0.6	3	1.27	3.54	1.64	1.51	3.10
5L-80-4b	5	Full Load	5	0.6	4	1.24	3.30	1.82	1.67	2.40
5L-80-5b	5	Full Load	5	0.6	5	1.20	2.94	1.72	1.58	1.97
5L-100-3b	5	Full Load	5	0.6	3	1.22	3.31	1.67	1.53	3.10
5L-100-4b	5	Full Load	5	0.6	4	1.22	3.13	1.86	1.70	2.40
5L-100-5b	5	Full Load	5	0.6	5	1.17	3.01	1.74	1.60	1.97

APPENDIX A.12 Comparison between the load distribution factor from the FEA and AASHTO-LRFD equation in FLS

Bridge type	# of Trucks		# of lanes (n)	R _L	Number of Box (N)	Result (FEA)				Result (AASHTO)
						F _{M+}	F _{M-}	F _{V inner}	F _{V outer}	$W_L = .1 + 1.7(N_L/N_B) + .85/N_L$
2L-20-2b	1	Fatigue _1	2	0.9	2	2.97	4.67	1.80	1.66	2.23
2L-20-3b	1	Fatigue _1	2	0.9	3	3.00	4.34	2.37	2.15	1.66
2L-40-2b	1	Fatigue _1	2	0.9	2	1.64	2.92	1.76	1.63	2.23
2L-40-3b	1	Fatigue _1	2	0.9	3	1.79	3.54	2.28	2.05	1.66
2L-60-2b	1	Fatigue _1	2	0.9	2	1.67	3.32	2.08	1.96	2.23
2L-60-3b	1	Fatigue _1	2	0.9	3	1.60	3.30	2.29	2.10	1.66
2L-80-2b	1	Fatigue _1	2	0.9	2	1.42	2.46	1.77	1.65	2.23
2L-80-3b	1	Fatigue _1	2	0.9	3	1.50	2.92	2.31	2.12	1.66
2L-100-2b	1	Fatigue _1	2	0.9	2	1.33	2.33	1.79	1.66	2.23
2L-100-3b	1	Fatigue _1	2	0.9	3	1.41	3.73	2.36	2.15	1.66
3L-20-2b	1	Fatigue _1	3	0.8	2	3.46	6.50	1.88	1.74	2.93
3L-20-3b	1	Fatigue _1	3	0.8	3	3.50	5.98	2.68	2.43	2.08
3L-20-4b	1	Fatigue _1	3	0.8	4	4.14	7.60	3.46	3.05	1.66
3L-40-2b	1	Fatigue _1	3	0.8	2	2.19	3.96	1.84	1.73	2.93
3L-40-3b	1	Fatigue _1	3	0.8	3	2.30	4.37	2.59	2.34	2.08
3L-40-4b	1	Fatigue _1	3	0.8	4	2.38	4.78	3.18	2.82	1.66
3L-60-2b	1	Fatigue _1	3	0.8	2	1.64	2.84	1.83	1.73	2.93
3L-60-3b	1	Fatigue _1	3	0.8	3	1.79	3.64	2.55	2.34	2.08
3L-60-4b	1	Fatigue _1	3	0.8	4	1.94	4.19	3.16	2.84	1.66
3L-80-2b	1	Fatigue _1	3	0.8	2	1.52	2.92	1.84	1.71	2.93
3L-80-3b	1	Fatigue _1	3	0.8	3	1.66	3.65	2.57	2.35	2.08
3L-80-4b	1	Fatigue _1	3	0.8	4	1.82	4.31	3.17	2.87	1.66
3L-100-2b	1	Fatigue _1	3	0.8	2	1.45	2.95	1.88	1.73	2.93
3L-100-3b	1	Fatigue _1	3	0.8	3	1.61	3.83	2.61	2.38	2.08
3L-100-4b	1	Fatigue _1	3	0.8	4	1.71	4.31	3.22	2.93	1.66
4L-20-3b	1	Fatigue _1	4	0.7	3	4.96	8.94	2.77	2.53	2.58
4L-20-4b	1	Fatigue _1	4	0.7	4	4.39	7.67	3.54	3.19	2.01
4L-20-5b	1	Fatigue _1	4	0.7	5	4.31	7.00	4.13	3.70	1.67
4L-40-3b	1	Fatigue _1	4	0.7	3	2.96	5.87	2.69	2.45	2.58
4L-40-4b	1	Fatigue _1	4	0.7	4	3.08	6.44	3.44	3.05	2.01

Cont.

Bridge type	# of Trucks		# of lanes (n)	R _L	Number of Box (N)	Result (FEA)				Result (AASHTO)
						F _{M+}	F _{M-}	F _{V inner}	F _{V outer}	$W_L = .1 + 1.7(N_L/N_B) + .85/N_L$
4L-40-5b	1	Fatigue_1	4	0.7	5	3.16	6.74	4.02	3.52	1.67
4L-60-3b	1	Fatigue_1	4	0.7	3	2.22	5.17	2.65	2.45	2.58
4L-60-4b	1	Fatigue_1	4	0.7	4	2.35	5.68	3.37	3.04	2.01
4L-60-5b	1	Fatigue_1	4	0.7	5	2.52	6.36	3.98	3.55	1.67
4L-80-3b	1	Fatigue_1	4	0.7	3	1.97	4.74	2.69	2.45	2.58
4L-80-4b	1	Fatigue_1	4	0.7	4	2.10	5.13	3.39	3.06	2.01
4L-80-5b	1	Fatigue_1	4	0.7	5	2.25	5.92	4.02	3.61	1.67
4L-100-3b	1	Fatigue_1	4	0.7	3	1.83	4.69	2.74	2.47	2.58
4L-100-4b	1	Fatigue_1	4	0.7	4	1.95	5.20	3.47	3.12	2.01
4L-100-5b	1	Fatigue_1	4	0.7	5	2.09	5.94	4.08	3.68	1.67
5L-20-3b	1	Fatigue_1	5	0.6	3	5.90	10.75	2.84	2.59	3.10
5L-20-4b	1	Fatigue_1	5	0.6	4	6.01	9.91	3.65	3.30	2.40
5L-20-5b	1	Fatigue_1	5	0.6	5	5.97	9.82	4.34	3.90	1.97
5L-40-3b	1	Fatigue_1	5	0.6	3	3.39	7.55	2.78	2.55	3.10
5L-40-4b	1	Fatigue_1	5	0.6	4	3.58	7.58	3.55	3.19	2.40
5L-40-5b	1	Fatigue_1	5	0.6	5	3.37	7.68	4.20	3.76	1.97
5L-60-3b	1	Fatigue_1	5	0.6	3	2.50	6.28	2.76	2.55	3.10
5L-60-4b	1	Fatigue_1	5	0.6	4	2.72	7.05	3.50	3.19	2.40
5L-60-5b	1	Fatigue_1	5	0.6	5	2.84	7.42	4.20	3.76	1.97
5L-80-3b	1	Fatigue_1	5	0.6	3	2.21	6.02	2.79	2.55	3.10
5L-80-4b	1	Fatigue_1	5	0.6	4	2.39	6.77	3.55	3.21	2.40
5L-80-5b	1	Fatigue_1	5	0.6	5	2.41	6.64	4.24	3.81	1.97
5L-100-3b	1	Fatigue_1	5	0.6	3	2.03	5.66	2.83	2.56	3.10
5L-100-4b	1	Fatigue_1	5	0.6	4	2.18	6.38	3.61	3.24	2.40
5L-100-5b	1	Fatigue_1	5	0.6	5	2.24	6.66	4.33	3.88	1.97

References

- AASHTO. (1980). **Guide specifications for horizontally curved highway bridges**, Washington, D.C.
- AASHTO. (2003). **Guide specifications for horizontally curved highway bridges**, Washington, D.C.
- AASHTO Standard (1996). **Guide specifications for horizontally curved highway bridges**, Washington, D.C.
- AASHTO-LRFD. (2007). *LRFD bridge design specifications*, 3rd Ed., Washington, DC.
- Androus A. (2003). **Experimental and theoretical studies of composite multiple-box girder bridges**. M.Sc. Thesis, Department of Civil Engineering, Ryerson University, Ontario, Canada.
- American Association of State Highway and Transportation Officials, AASHTO. 1996. Standard Specifications for Highway Bridges. Washington, D.C.
- Baker, T. H. (1991). **Plate stiffness constants for concrete filled steel grid decks: Static and fatigue strength determination of design properties for grid decks**. Vol. 1, Research Rep. ST-9, Dept of Civil Engineering, Univ. of Pittsburgh, Pittsburgh.
- Bazant, Z.P. and El Nimeiri, M. (1974). **Stiffness method for curved box girders**. ASCE Journal. of the Structural Division, 100 (ST10): 2071-2090.
- Canadian Standards Association, (2006). **Canadian highway bridge design code, CHBDC**. Etobicoke, Ontario, Canada.
- Chang, S. T., and Zheng, F.Z. (1987). **Negative shear lag in cantilever box girder with constant depth** Journal Struct. Eng., 113(1); 20-35.

- Cheung, Y. K. 1968. **Finite strip method analysis of elastic slabs**. Journal of the Engineering Mechanics Division, ASCE, 94 EM6: 1365-1378.
- Cheung, M. S. and Cheung, Y. K. (1971). **Analysis of curved box girder bridges by the finite- strip method**. International Association of Bridges and Structural Engineering, IABSE, 31(I):1-8.
- Cheung, Y.K. and Cheung, M. S. (1972). **Free vibration of curved and straight beam- slab or box-girder bridges**. International Association of Bridges and Structural Engineering, 32 (2): 41-52.
- Cheung, M. S. and Cheung, Y. K. (1978). **Finite- strip evaluation of effective flange width of bridge girders**. Canadian Journal of Civil Engineering, 5(2): 174-185.
- Cheung, M. S. (1984). **Analysis of continuous curved box girder bridges by the finite-strip method**. Japanese Association of Civil Engineering, 1-10.
- Cheung, Y.k. (1969). **The analysis of cylindrical orthotropic curved bridge deck**. IABSE Publications, Vol. 29, part II, 41-52.
- Chu, H. and Pinjarkar, S.G. (1971). **Analysis of horizontally curved box girder bridges**. ASCE Journal of the Structural Division, 97 (ST10): 2481-2501.
- Dabrowski, R. (1968). **Curved thin-walled girders, theory and analysis**, Springer, New York.
- El-Azab, M.A. 1999. Static and dynamic analysis of thin walled box girder bridges by exact beam finite elements. Ph.D. Department of Civil Engineering Al Azhar University, Cairo, Egypt.
- Elbadry, M. M., and Debaiky, A. S. (1998). **Time-dependant stresses and deformations in segmentally erected curved concrete box-girder bridges**. Proc., Canadian Society of Civil Engineering, Calgary, Canada, 1: 399-412.
- Fam, A. R. and Turkstra, C.J. (1975). **A finite element scheme for box bridge analysis**. Computers and Structures Journal, Pergamon Press, 5: 179-186.

- Fam, A. R. and Turkstra, C.J. (1976). **Model study of horizontally curved box girder.** ASCE J. of the Structural Division, 102(ST5): 1097-1108.
- Fam, A. R. M. (1973). **Static and free-vibration analysis of curved box bridges.** structural Dynamic Series No. 73-2, Department of Civil Engineering and Applied Mechanics, McGill University, Montreal, Quebec, Canada.
- Fang-LI, Pei-wu, Jian-sun, Xiao-wu (2009) **Application of 3D finite element software in web cracking analysis of concrete box-girder bridges.** Second international conference on informational computing science.
- Goldberg, J. R. and Leve, H. L.,(1975) **Theory of prismatic folded plate structures, Publications, IABSE, Vol. 17.**
- Gangarao, H. V. S., Raju, P. R., and Koppula, N. R. (1992). **Behavior of concrete-filled steel grid decks.** *Transportation Research Record, 1371*, Transportation Research Board, Washington, D.C., 1-7.
- Galuta, E. M. and Cheung, M.S. 1995. Combined boundary element and finite element analysis of composite box girder bridges. *Computers and Structures Journal*, Pergamon Press, 57(3):427-437.
- Hassan, W. (2005). **Shear distribution in curved composite multiple-box girder bridges.** M.Sc. Thesis, Department of Civil Engineering, Ryerson University, Ontario, Canada.
- Heins, C. P. 1978. Box girder bridge design-state-of-the-Art. *AISC Engineering Journal*, 2: 126-142.
- Heins, C. P. and Lee, W. H. 1981. Curved box-girder bridge: field test. *ASCE Journal of the Structural Division*, 107(2): 317-327
- Heins, C. P., and Jin, J. O. (1984). **Live load distribution on braced curved I- girders.** *ASCE Journal of Structural Engineering*, 110(3): 523-530.
- Higgins, C. (2003). **LRFD orthotropic plate model for live load moment in filled grid decks.** *J. Bridge Eng.*,

- Higgins, C. (2004). **Orthotropic plate model for estimating deflections in filled grid decks**. *J. Bridge Eng.*, 9(6): 599–605.
- Ho, S., Cheung, M. S., Ng, S. F., and Yu, T. (1989). **Longitudinal girder moments in simply supported bridges by the finite strip method**. *Canadian Journal of Civil Engineering*, 16(5): 698-703.
- Huang, H., Chajes, M. J., Mertz, D. R., Shenton, H. W., and Kaliakin, V. N. (2002). **Behavior of open steel grid decks for bridges**. *J. Constr. Steel Res.*, 58(5–8); 819–842.
- Huang, H., Kaliakin, V. N., Chajes, M. J., Mertz, D. R., and Shenton, H. W. (2007). **Application of orthotropic thin plate theory to filled steel grid decks for bridges**. *J. Bridge Eng.*, 12(6): 807–810.
- Kabir, A. F. and Scordelis, A. C. (1974). **Computer programs for curved bridges on flexible bents**. Structural Engineering and Structural Mechanics Report No. UC/SESM 74-10, University of California, Berkeley, CA.
- Li, H. G. (1992). **Thin-walled box beam finite elements for static analysis of curved haunched and skew multi-cell girder bridges**. Ph.D. Thesis, Dept. of Civil Engineering, Carleton Univ., Ottawa, Ontario, Canada.
- Logan D., **A first course in the finite-element method, 3rd Edition, Text Book**, 2002 Ministry of Transportation Ontario, MTO. 2002. Structural Manual. St. Catharines, Ontario, Canada.
- Maisel, B. I. (1985). **Analysis of concrete box beams using small computer capacity**. *Can. J. Civ. Eng.*, 12 (2): 265-278.
- Mangelsdorf, C. P., Baker, T. H., and Swanson, J. A. (2002). **Predicting deflections in concrete-filled grid deck panels**. *Transportation Research Record 1814*, Transportation Research Board, Washington, DC, 17–24.

- Meyer, C. and Scordelis, A. C. (1971). **Analysis of curved folded plate structures**. ASCE J. of the Structural Division, 97: 2459-2480.
- Moffatt, K.R., Lim, P.T.K. (1976). **Finite element analysis of composite box girder bridges having complete or incomplete interaction** *Proceedings of the Institution of Civil Engineers (London). Part 1 - Design & Construction*, v 61(2): 1-22.
- Newmark, N. M., Siess, C. P. and Beckham, R. R. (1948). **Studies of Slab on Beam Highway Bridges. Part I: Test of Simple-Span Right I-Beam Bridges**. Eng. Experiment Station, University of Illinois, Urbana, III, Bulletin Series No. 375.
- Ng, S. F., Cheung, M. S., and Hachem, H. M. (1993). **Study of a curved continuous composite box girder bridge**. Canadian Journal of Civil Engineering, 20(1): 107-119.
- Ng, S. F., Cheung, M. S., and Hachem, H. M. (1993). **Study of a curved continuous composite box girder bridge**. Can. J. Civ. Eng., 20(1):107-119.
- Nour, S. (2003). **Load distribution in curved composite concrete deck-steel multiple-spine box girder bridges**. M.Sc. Thesis, Department of Civil Engineering, Windsor University, Windsor, Ontario, Canada.
- Nutt, R. V., Schamber, R. A., and Zokaie, T. (1988). **Distribution of wheel loads on highway bridges**. Transportation Research Board, National Cooperative Highway Research Council, Imbsen & Associates Inc., Sacramento, Calif.
- Ozakca, M. and Taysi, N. and Kolcu, F. (2003). **Buckling optimization of variable thickness prismatic folded plates**. Department of Civil Engineering University of Gaziantep, 41: 711-730
- Razaqpur, A. G., and Li, H. G. (1997). **Analysis of curved multi-cell box girder assemblages**. Struct. Eng. Mech., 5(1): 33-49.

- Razaqpur, A., Abbas, H., El-Samny, K., and Azab, M. (2000). Free vibration analysis of box girder bridges by thin-walled beam model. Proc., Bridge Engineering Conf., Egyptian Society of Engineers, Egypt, (1): 621-632.
- Samaan, M. (2004). **Dynamic and static analyses of continuous curved composite multiple-box girder bridges**. Ph.D. Dissertation Faculty of Graduate Studies and Research University of Windsor, Windsor, Ontario, Canada.
- Sennah, K. M. (1998). **Load distribution factors and dynamic characteristics of curved composite concrete deck- steel cellular bridges**. Ph.D. Thesis, Department of civil Engineering, university of Windsor, Ontario, Canada.
- Sennah, K. M. and Kennedy, J.B. (1998). **Shear distribution in simply-supported curved composite cellular bridges**. Journal of Bridge Engineering, ASCE, 3(2): 47-55.
- Sennah, K. M. and Kennedy, J. B. (1998). **Vibration of horizontally curved continuous composite cellular bridges**. Canadian Journal of Civil Engineering, 25: 139-150.
- Sennah, K. M., and Kennedy, J.B. (2002). **Literature Review in Analysis of Box Girder Bridge**. J. of Bridge Engineering , ASCE, 7(2):134-143.
- Sennah, K. M., Samaan, M. and Kennedy, J. (2007). **Dynamic analysis of curved continuous multiple-box girder bridges**. Journal of Bridge Engineering, ASCE, 12(2): 184-194.
- Shushkewich, K. W. (1988). **Approximate analysis of concrete box girder bridge**. J. Struct. Eng. 114(7): 1644-1657.
- Topkaya, C. Williamson, E.B (2003). **Development of computational software for analysis of curved girders under construction loads**. *Computers & Structures*, 81(21): 2087-98.
- Vlasov, V. Z. (1965). **Thin-walled elastic beams**. OTS61-11400, National Science Foundation, Washington, D. C.

- Willam, K. J. and Scordelis, A. C. (1972). **Cellular structures of arbitrary plan geometry**. ASCE Journal. of the Structural Division, 98(ST7): 1377-1394.
- Wilson, E. L., and Habibullah, A. 2010. Structural Analysis Program SAP2000, Computers & Structures.
- Yousif, Z. and Hindi, R. (2007). **AASHTO-LRFD Live Load Distribution for Beam-and-Slab Bridges: Limitations and Applicability**. Journal of Bridge Engineering , 12(6): 1084-0702.
- Zokaie, T., Imbsen, R. A., and Osterkamp, T. A. (1991). **Distribution of wheel loads on highway bridges**. Transportation Research Record. CA, 1290: 119-126.
- Zokaie, T., and Imbsen, R. A. (1993) . **Distribution of wheel loads on highway bridges**. National Cooperative Highway Research Program (NCHRP)12-26 Project Report, Transportation Research Board, Washington, D. C.
- Zokaie, T. (2000). **AASHTO-LRFD live load distribution specifications**. Journal of Bridge Eng., 5(2), 131-138.